# Functional xylem anatomy: intra and interspecific variation in stems of herbaceous and woody species

Chacon Dória, L.

# FUNCTIONAL XYLEM ANATOMY

## intra and interspecific variation in stems of herbaceous and woody species

Larissa Chacon Dória

2019

Larissa Chacon Dória. 2019. *Functional xylem anatomy: intra and interspecific variation in stems of herbaceous and woody species.*

PhD thesis at the University of Leiden, The Netherlands.

ISBN: 978-94-6332-549-3

*This PhD research was financially supported by:*

Conselho Nacional de Desenvolvimento Científico e Tecnológico, CNPq, Brazil.

Alberta Mennega Stichting, The Netherlands.

*This PhD research was carried out at:*

Naturalis Biodiversity Center, The Netherlands.

University of Bordeaux, France.

University of La Laguna, Canary Islands, Spain.

Universidade Estadual Paulista, Brazil.

Universidade Federal da Paraíba, Brazil.

*Editorial layout and cover design*

Fabio Nucci and Larissa Chacon Dória

Cover image: *artwork based on a stem cross section of the insular woody Argyranthemum adauctum collected on Tenerife, Canary Islands, in November 2015.*

# Functional xylem anatomy
## intra and interspecific variation in stems of herbaceous and woody species

Proefschrift

ter verkrijging van
de graad van Doctor aan de Universiteit Leiden,
op gezag van Rector Magnificus prof.mr. C.J.J.M. Stolker,
volgens besluit van het College voor Promoties
te verdedigen op woensdag 9 oktober 2019
klokke 11:15 uur

door

**Larissa Chacon Dória**
geboren te João Pessoa, Brazil
in 1988

| | |
|---|---|
| *Promotor:* | Prof. Dr. Erik Smets<br>*Naturalis Biodiversity Center, Leiden University & KU Leuven* |
| *Copromotor:* | Dr. Frederic Lens<br>*Naturalis Biodiversity Center & Leiden University* |
| *Promotiecommissie:* | Prof. Dr. Gilles van Wezel (voorzitter)<br>*Leiden University, The Netherlands* |
| | Prof. Dr. Peter van Welzen (secretaris)<br>*Naturalis Biodiversity Center & Leiden University, The Netherlands* |
| *Overige commissieleden:* | Prof. Dr. Steven Jansen<br>*Ulm University, Germany* |
| | Prof. Dr. Remko Offringa<br>*Leiden University, The Netherlands* |
| | Dr. Carmen Regina Marcati<br>*Universidade Estadual Paulista, Brazil* |
| | Dr. Sylvain Delzon<br>*University of Bordeaux, France* |

*What you get by achieving your goals is not as important as what you become by achieving your goals.*

*Henry David Thoreau*

# TABLE OF CONTENTS

*Chapter 1*

# GENERAL INTRODUCTION AND THESIS OUTLINE

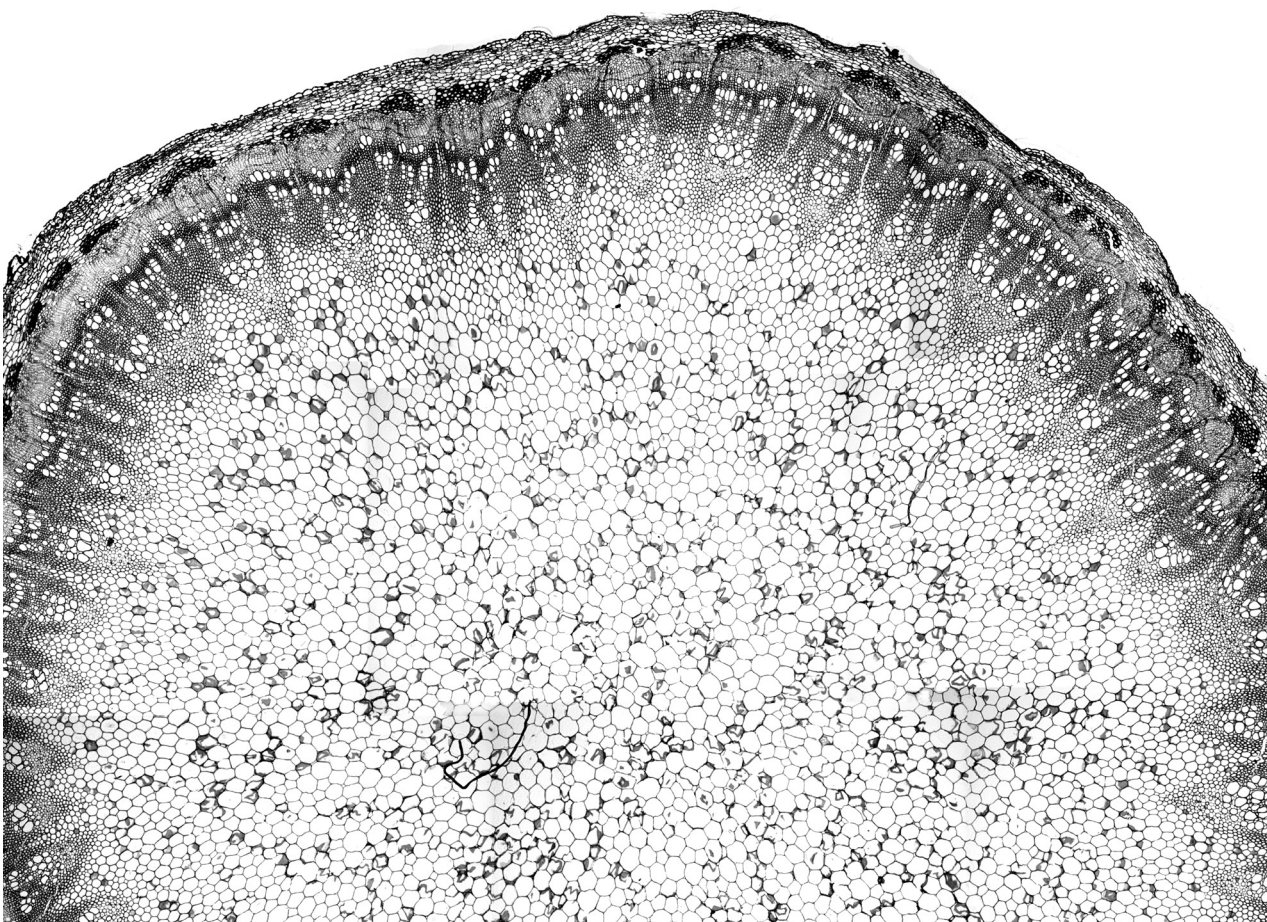

The evolution of a specialized, axially-arranged tissue enabling long-distance transport of sugar and water throughout the plant body, allowed the earliest woody land plants to become successful in terrestrial ecosystems since their evolution around 400 million years ago (Hartmann 2011; Ligrone *et al.* 2012). The vascular system includes xylem, that allows trees to conduct water from the soil to more than 100 m, favoring woody plants to colonize diverse environments, compete, and coexist (Koch *et al.* 2004). The physiology of water transport defines many aspects of the daily functioning of plants and it has been considered the "backbone" of the plant terrestrial ecosystems since it defines a physical limit to plant productivity and survival (Brodribb 2009). Therefore, xylem anatomy plays a central role in plant hydraulic strategies due to the interaction with the whole hydraulic continuum: from the root-rhizosphere interface to the water-air interface in the leaves (Barnard *et al.* 2011). Additionally, wood anatomy has its inherent trade-offs associated with the division of labour between water conduction and structural support functions (Chave *et al.* 2009).

This thesis is entirely dedicated to the functional aspects of xylem anatomy in woody and herbaceous species based on in-depth observations with different microscopy techniques (light, scanning and transmission electron microscopy) coupled with experimental measurements of water transport in stems as a proxy for drought stress resistance. In the two first chapters we assess the variation of the main wood anatomical characters in two co-occurring woody species in the two main seasonally dry biomes in Brazil, cerrado and caatinga, to infer wood functional roles and sampling height-related anatomical adaptations to deal with abiotic factors. In the following two last chapters, we combine hydraulic measurements with detailed stem anatomical observations to assess plant resistance to drought in woody and herbaceous species occurring in Tenerife, Canary Islands. Before going into detail of the findings of my studies, I will introduce some topics on basic xylem anatomy and long distance water transport in plants, along with a historical background of both fields. I will also give an overview about the relationship between xylem anatomy and physiology, and its relevance for ecosystems ecology.

## General introduction to xylem anatomy

### *Starting from the basics*

The vascular tissues of plants, including xylem and phloem, form a continuous system extending throughout the plant body carrying out two essential functions: delivering of resources (water, essential minerals, sugars and amino acids) to different parts of the plant body, and providing of mechanical support (Evert 2006; Lucas *et al.* 2013).

The term xylem is derived from the Greek word xylon, which means wood, and it is the principal water-conducting and supporting tissue of plants. The primary xylem is formed very early in the primary plant body (seedling stage) before the onset of secondary growth, and is developed from procambium strands that develop close to the stem and root apical meristems (Esau 1965; Evert 2006) (Fig. 1 A, I). Wood or secondary xylem is developed by a (secondary) meristem, called cambium, which produces wood cells towards the inside of the stem in typical radial files using pericline divisions, while secondary phloem is produced towards the outside (Fig. 1 A, II - V). In contrast to the primary xylem, it consists of an axial and a radial system composed of three different cell types: vessel elements (and/or tracheids), fibers and parenchyma (Evert 2006) (Fig. 1 B). The primary xylem often remains functional in herbaceous species that do not undergo secondary growth (Fig. 1 A, I). However, most of the eudicot herbaceous species show a certain degree of wood formation (Schweingruber 2007; Schweingruber *et al.* 2011). It is normally confined to the base of the stems, either limited to the vascular bundle regions or somewhat expanded by a complete vascular cambium into a tiny wood cylinder (Lens *et al.* 2012a) (Fig. 1 A, III - IV). Consequently, all herbaceous non-monocot angiosperms have a limited amount of wood formation in their stems, especially at the stem base, which can continuously vary amongst these herbaceous species emphasizing that there is a fuzzy boundary between 'herbaceousness' and 'woodiness'. This makes it sometimes complex in some lineages to decide at which woodiness level a species can be considered truly woody (Lens *et al.* 2012a). Therefore, Kidner *et al.* (2016) proposed the following definition for a woody species: species that produce a distinct wood cylinder extending towards the upper parts of the stem.

Wood consists of a number of different cell types: water conducting tracheary elements (vessel elements and tracheids), non-tracheary elements (fibers) and parenchyma cells (axial parenchyma and ray parenchyma) (Fig. 1 B). Vessel elements and tracheids are both axially elongated, non-living at maturity, and have lignified secondary walls. Tracheids are generally present in the wood of gymnosperms, exerting both the function of conducting water and providing mechanical support. They are single cells ranging in size from about 0.5 - 4 mm in length and 8-80 µm in diameter connected to each other via lateral cavities in the secondary cell wall, the bordered pits (Pittermann & Sperry 2003; Choat *et al.* 2008; Pittermann 2010). On the other hand, vessel elements are the main water-conducting cells of angiosperms and are stacked one on top of the other forming an elongated, hollow tube, called vessel, that might be up to 0.5 mm in diameter and several meters (up to 16m in some lianas; Ewers 1990) in length. They differ from tracheids by the occurrence of perforation plates, which are wide openings in the cell wall that are positioned at both end walls and axially connect the vessel elements within a single vessel.

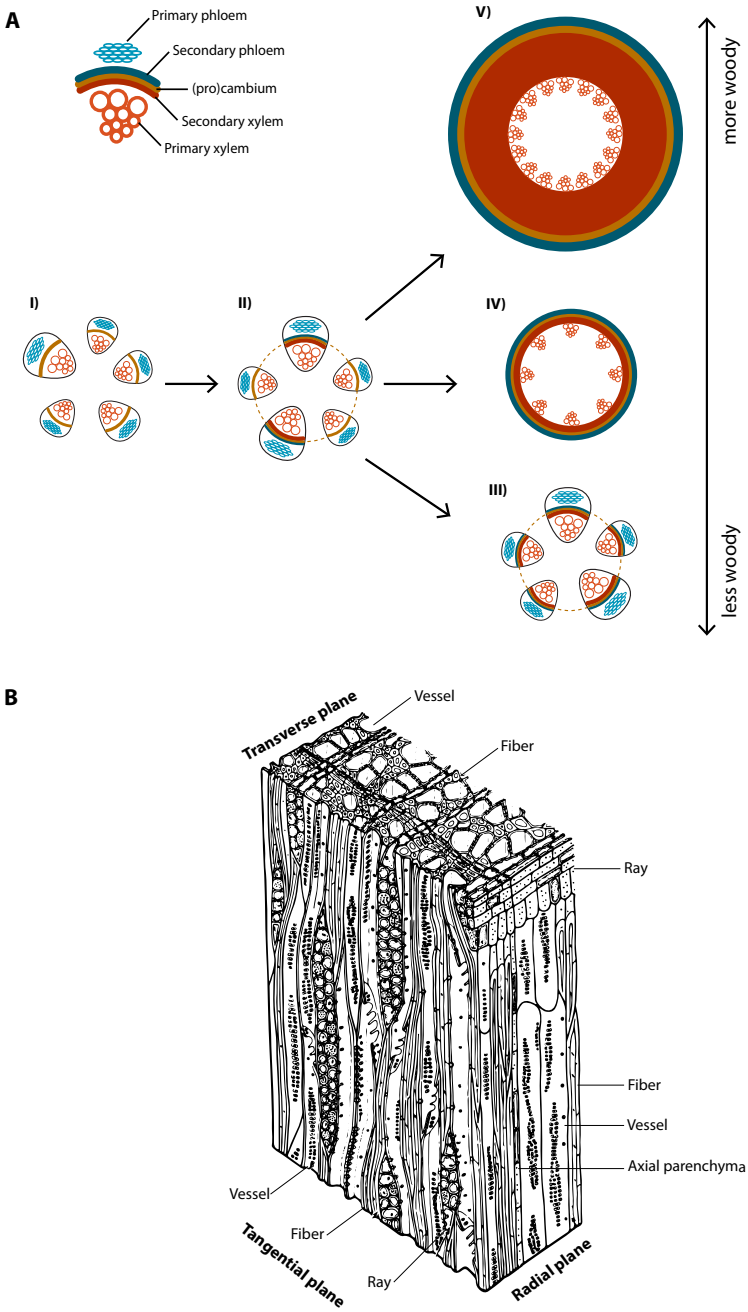


**Figure 1** • Transition from primary to secondary growth and wood anatomy. A – Production of secondary xylem and phloem via the division and differentiation of cambium cells. The isolated procambium within each vascular bundles – referred to as the intrafascicular cambium – (I) gradually extends towards adjacent vascular bundles into a closed vascular cambim (II), which produces secondary phloem to the outside and secondary xylem (wood) to the inside in a continuous range of variation (III – V). B – 3D view of angiosperm wood with its respective cells. *Adapted from Spicer (2016) and Evert (2006).*

Intervessel pits are small cavities in the secondary cell wall between adjacent vessels, surrounded by overarching parts of the secondary cell wall, forming the so-called pit borders (Fig. 2 A). The intervessel pits have a crucial role in water transport, since the water movement from roots to leaves has to cross millions of pits in tall trees. Intervessel pits retain a modified porous layer derived from hydrolysis of the middle lamella and of the primary walls, called intervessel pit membrane. In angiosperms, the intervessel pit membranes consist of homogeneous microlayers of cellulose microfibrils and other partly unknown molecules, forming the nano-sized pores which allow the movement of water molecules from one vessel to another, thereby determining the flow resistance accounting for more than 50% of the total xylem hydraulic resistance in many species (Sperry *et al.* 2005; Wheeler *et al.* 2005; Choat *et al.* 2006). Therefore, there should be a trade-off between hydraulic efficiency and safety at the intervessel pit level (Choat *et al.* 2008; Jansen *et al.* 2009).

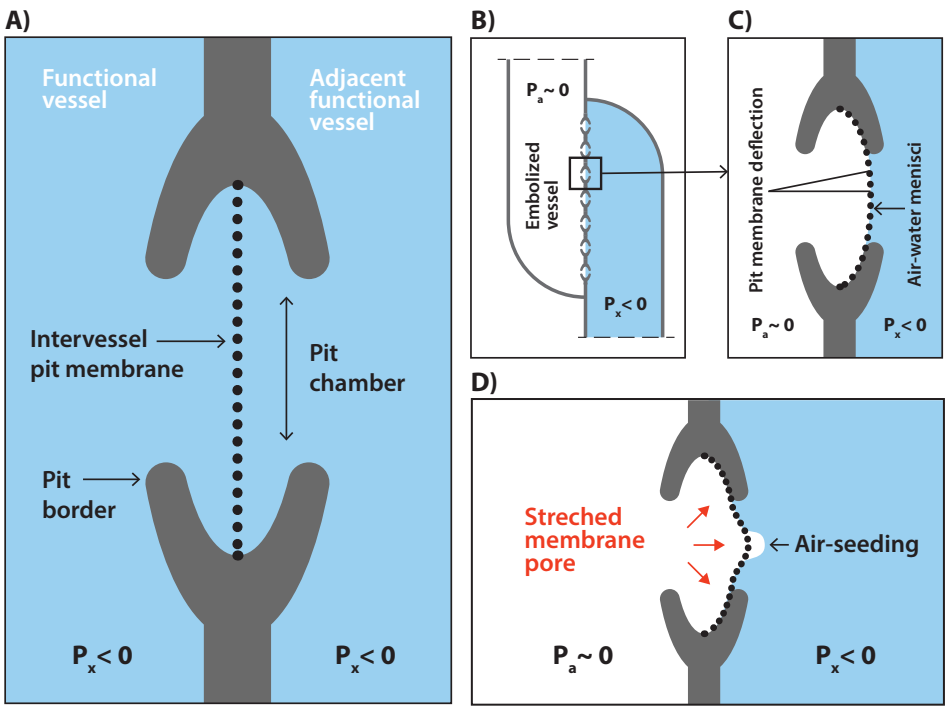


**Figure 2** • Intervessel pit in angiosperms and the role of intervessel pit membrane in the air-seeding. A – View of an intervessel pit with its membrane in a relaxed state, between two adjacent functional vessels. B – Embolized vessel leading to an increase in xylem pressure (atmospheric pressure). C – The difference in pressure between adjacent vessels deflects the pit membrane. D – Increasing pressure difference might stretch the pit membrane pores leading to the spread of air bubbels inside the functional vessel via a process called air-seeding. *Adapted from Venturas et al. (2017).*

Surrounding the vessels, there is often a matrix of fibers which often have thin-to-thick secondary walls (Fig. 1 B). This functional division in labour between vessel and fibers reflects the optimized vascular strategy of angiosperms compared to gymnosperms, allowing efficient movement of water through vessels, while mechanical requirements are met by fibers (Pittermann 2010). The parenchyma cells represent the living cells in wood and are axially and radially arranged, depending on the fusiform or ray initial cell types in the vascular cambium. Both types of parenchyma have functions ranging from storage and transport of nonstructural carbohydrates and mineral inclusions (Salleo *et al.* 2004; O'Brien *et al.* 2014; Plavcová & Jansen 2015), to water storage and xylem hydraulic capacitance (Holbrook 1995; Pfautsch *et al.* 2015a), and into a lesser extent, mechanical contributions (Burgert & Eckstein 2001; Reiterer *et al.* 2002; Martinez-Cabrera *et al.* 2009).



*The pioneering wood anatomists*

Plant anatomy goes back to the 17th century with Hooke's microscopic observation of cell walls in the outer bark of oak trees. Hooke coined the term "cells" for what he observed and reported seeing similar structures in the wood of other plants. Almost 300 years later, Solereder published the first comparative wood anatomical study, entitled *Systematic Anatomy of the Dicotyledons* (Solereder 1908), which was mainly based on observations of twigs found in herbaria. Solereder's master piece formed the basis for the wood anatomy bible by Metcalfe & Chalk (1950): Anatomy of the Dicotyledons. This work is still considered as an important source of information, and was triggered at that time by the growing need for timber identification, fueled by the increasing number of unfamiliar timbers that were introduced to the market, especially from tropical countries (Metcalfe 1973).

In the field of evolutionary wood anatomy, the prominent study of Bailey & Tupper (1918), introduced evolutionary hypotheses of tracheary elements in vascular plants, now known as the Baileyan Trends. The Baileyan Trends state that lineages with vessels have evolved from tracheid bearing (i.e. vesseless) species, and this specialization was associated with evolutionary and irreversible changes in the perforation plate morphology from scalariform to simple plates, along with shorter and wider vessel element lengths, and transitions in the arrangement of interconduits pits from scalariform and opposite to alternate. Despite the importance of Bailey's work to the wood anatomy field – considered as a classical text book example to illustrate the phylogenetic signal of comparative wood anatomy – Olson (2012, 2014) offered valuable critiques about his linear view from "primitive" to "specialized" xylem, and mainly emphasized the absence for the causes behind his trends. These causes began to become more evident in the studies of ecological wood anatomy with the pioneering study of Carlquist (1966) about the environmental factors controlling evolution in wood anatomy of Compositae. The field of ecological wood anatomy was expanded later by many others who shed

more light on the importance of climatic drivers behind evolutionary patterns in wood, and also started speculations about the functional role of different xylem cell types, sizes and arrangements (Carlquist 1975, 1980, 1985; Baas 1976; Baas *et al.* 1983; Baas & Schweingruber 1987; Alves & Angyalossy-Alfonso 2000, 2002; Lens *et al.* 2004).

*The general ecological trends and trade-offs in xylem anatomy*

The literature in ecological wood anatomy has generated a number of global ecological trends. Wood anatomical variation has been assessed in the light of different abiotic drivers, such as latitude and altitude (van den Oever *et al.* 1981; Jansen *et al.* 2004; Lens *et al.* 2004), water availability and temperature (Carlquist 1985, Baas & Carlquist 1985; Alves & Angyalossy-Alfonso 2002; Bosio *et al.* 2010), and soil nutrients (Lupi *et al.* 2012; Dória *et al.* 2016).

A number of ecological trends associated with plants from drier areas and lower latitudes can be summarized as follows: decreasing incidence of scalariform perforations plates (Baas & Schweingruber 1987; Alves & Angyalossy-Alfonso 2000), higher incidence of vestured pits (Jansen *et al.* 2004), higher occurrence of vessels with different size classes, shorter vessel elements (Carlquist 1966, 1977) and narrower vessels (Carlquist 1966; Bosio *et al.* 2010), higher vessel density, and more and larger vessel grouping patterns in association with non-conducting fibers (Baas *et al.* 1983; Carlquist & Hoekman 1985), and thicker fiber walls (Alves & Angyalossy-Alfonso 2002).

Because wood performs different functions - water transport, mechanical support and storage of water and nutrients - there are conflicting demands. This would require proficiency at one function, leading to a poorer performance at another function, which may give rise to trade-offs (Baas *et al.* 2004; Sperry *et al.* 2006) (Fig. 3). These different demands may shift depending upon the environment, and therefore, the ecological trends in wood anatomy generally support these trade-offs. A dominant hypothesis regarding the hydraulic safety versus efficiency trade-off has long been proposed (Zimmermann & Brown 1977; Carlquist 1988). Higher efficiency in conduction is linked to larger vessels and allows a more efficient photosynthesis, faster plant growth and lower xylem construction costs, i.e., less xylem tissue for a given amount of leaf area (Poorter *et al.* 2010; Gleason *et al.* 2012). However, across aridity gradients, species should develop corresponding adaptive strategies to water availability. In other words, efficient hydraulic strategy may not allow plants to operate at higher xylem tensions during high transpiration or in soils with low water potential. On the other hand, increasing safety from hydraulic failure corresponds to increased investment in conduit wall area per conduit volume and greater fiber wall thickness to withstand greater negative pressure, which would involve higher carbon construction cost (Hacke *et al.* 2001a, 2004; Jacobsen *et al.* 2007). The conflict is whether we might expect an increased cavita-

tion safety leading to decreased hydraulic efficiency. Some findings indeed support the safety x efficiency trade-off (Tyree *et al.* 1994; Hacke *et al.* 2006; Sperry *et al.* 2008; Meinzer *et al.* 2010), while others, including global meta analyses, show that many species have low efficiency and low safety, which cannot be understood by reference to a trade-off (Choat *et al.* 2005; Gleason *et al.* 2016a).

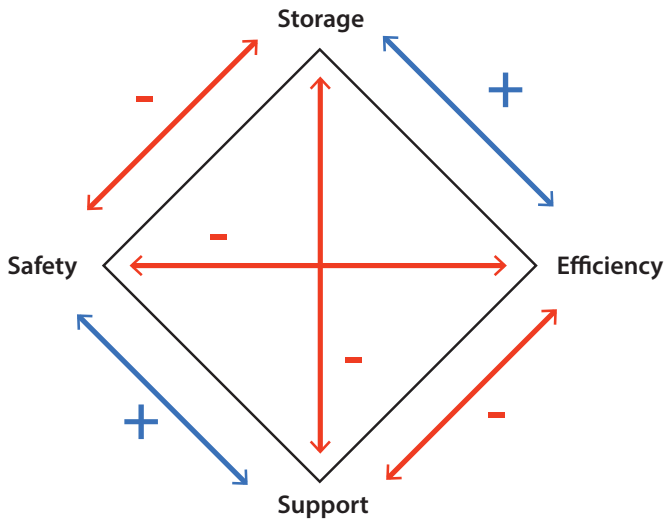


**Figure 3** • Relationships (trade-offs) amongst xylem functions. Storage refers to water storage (capacitance) and carbohydrate storage; efficiency refers to the conductive efficiency (Ks in $m^2MPa^{-1}s^{-1}$); support refers to mechanical strength (vessels $t/b^2$ and fiber wall thickness) and safety refers to resistance to embolism (MPa). Red lines express a negative association between two functions and blue lines a positive one. *Adapted from Pratt & Jacobsen (2017).*

### *The xylem trade-off at the individual whole tree level*

The majority of wood anatomical studies deal either with interspecific variation, assessing variation in floras of specific regions, or intraspecific variation evaluating individuals of the same species occurring in contrasting environments. Nevertheless, the intra-individual variation in wood anatomical characters is substantial, but often overlooked. A wide range of wood anatomical characters exhibit strong axial variation from the base towards the tip of the stem. In the literature, most of this variation is focusing on vessel widening from top to bottom in order to deal with the more negative water potentials in the upper parts of the trees and to maintain hydraulic integrity (McCulloh & Sperry 2005; Pfautsch *et al.* 2011; Olson *et al.* 2018). Indeed, the water resistance increases with longer conduits pathways as stated by the Hagen-Poiseuille's law, as well as the flow rate increases proportionally to the fourth power of the vessel diameter (Tyree & Zimmerman 2002). To overcome the higher flow resistance, the vessels need to widen basipetally as explained by the West, Brown and Enquist model (WBE model, West *et al.* 1999).

Additionally, vessel density is expected to increase upwards, as has been predicted by hydraulic models and shown by anatomical studies, in order to increase hydraulic conductance with the narrowing of vessels upwards (Höltta *et al.* 2011). In the context of hydraulic safety - efficiency trade-off, intervessel pits constitute a major proportion, roughly half, of the hydraulic resistance (Sperry *et al.* 2006; Choat *et al.* 2008), and, therefore, it is also expected to vary along the main axis of a tree. The few studies dealing with intra-individual variation at the pit level showed different results to pit aperture diameter, which either decrease (Domec *et al.* 2008) or increase (Lazzarin *et al.* 2008) with increasing tree height. Variation in the ultrastructure of intervessel pits in the angiosperm Eucalyptus grandis was found to be more variable across vertical gradients (Pfautsch *et al.* 2018).

## General introduction to plant hydraulics

### *The ascent of sap and the vulnerability of xylem to cavitation*

The groundbreaking publication dealing with the Cohesion Tension Theory (CTT) by Dixon and Joly (1894) explains that long distance water transport in plants is performed under tension (subatmospheric pressure), which implies that xylem sap is transported in a metastable state. The driving force is generated by evaporative demand at the leaf surfaces and is transmitted by tension in water menisci through a continuous water column that is pulled up by a difference in negative xylem pressure (Tyree & Zimmermann 2002). This mechanism is now widely accepted as the basis of xylem water transport. Under this metastable condition, if pressure drops below the minimum pressure that a water meniscus can support, capillary failure can occur, generating cavitation. This phenomenon could ultimately result in embolism (formation of air bubbles), which reduces the ability of plants to deliver water to leaves (Zimmermann 1983). The two main environmental factors that lead to xylem embolism are freeze-thaw cycles and drought. As sap freezes, dissolved gasses are forced out to the solution, forming gas bubbles in the conduits. When sap thaws, these bubbles can be dissolved or can nucleate in an embolism event (Sperry & Sullivan 1992). During drought events, as the water available in the soil decreases, the xylem tension needed to pull up water from soil to leaves increases. This increase in xylem tension will increase the probability of drought-induced embolism formation (Brodribb & Hill 2000). All the chapters of my thesis deal with drought stress, so I will pay greater attention in explaining the mechanism behind drought-induced embolism formation. The spread of embolism through conduits is explained by the air-seeding mechanism (Fig. 2 B - D) (Tyree & Sperry 1989; Tyree & Zimmermann 2002). It states that a functional xylem conduit becomes air-seeded when a gas bubble from an adjacent gas filled conduit penetrates the shared intervessel pit membrane (Brodersen *et al.* 2013). It is hypothesized that air-seeding

occurs through the largest pore of the intervessel pit membrane, which may even further enlarge when the membrane deflects due to the increasing drought-induced pressure difference between both conduits (Pockman *et al.* 1995; Choat *et al.* 2008; Jansen *et al.* 2009) (Fig. 2 B – D).

*Measuring embolism resistance in plants*

A vulnerability curve (VC) is a plot of the percentage loss of hydraulic conductivity (PLC) versus the xylem water potential (measured in MPa) (Fig. 4). In other words, it quantifies the plant resistance to xylem embolism (Tyree & Zimmermann 2002). There are key features in a VC that plant physiologists use as proxies for comparing species resistance to embolism: $P_{12}$, $P_{50}$ and $P_{88}$. They refer, respectively, to the pressures inducing 12%, 50% and 88% loss of hydraulic conductivity. Physiologically, they indicate the pressure of the starting entry of air in the 3D vessel network, and the potential lethal level of hydraulic failure in conifers and in angiosperms, respectively (Brodribb & Cochard 2009; Urli *et al.* 2013). Nevertheless, $P_{50}$ is the most common proxy used in the literature to compare levels of embolism resistance amongst species of gymnosperms and angiosperms.

There are different possible techniques to construct a VC, differing on how embolism is induced and how it is quantified (Cochard 2006; Cochard *et al.* 2013; Venturas *et al.* 2017). The methods to induce embolism are 1) bench drying, where large excised branches are put to dehydration in air and thereby best mimicking the actual plant drought-stress (Tyree *et al.* 1992); 2) air injection, where positive air pressure induces embolism (Sperry & Tyree 1988); and 3) the centrifuge-based methods that generate negative xylem pressures in the center of the sample due to centrifugal force (Pockman *et al.* 1995; Cochard *et al.* 2010). In order to quantify the relative change in hydraulic conductivity, scientists are using the conductivity apparatus where the flow is measured using a balance (Sperry *et al.* 1988) or the xyl'em apparatus (Cochard *et al.* 2013). In the high-throughput, custum built centrifuge called Cavitron, the hydraulic conductance is measured during sample centrifugation, which greatly accelerates the measurement (Cochard *et al.* 2005, 2013). Additionally, it requires less plant material than the bench drying method, reducing sample variability since several pressures can be evaluated on the same segment (Martin-St Paul *et al.* 2014; Venturas *et al.* 2017). More recently, two methods to measure embolism formation were proposed, the optical vulnerability method (Brodribb *et al.* 2016) which allows the visualization of dynamic leaf (and stem and root) embolism during water stress, and the pneumatic method (Pereira *et al.* 2016) which calculates the amount of air flow out of branches under different water potentials.

The challenges of assessing plant hydraulic conductivity is mainly related to the fact that sap is under a metastable state and small perturbations can trigger cavitation. Therefore, methodological issues have always been under debate in the plant

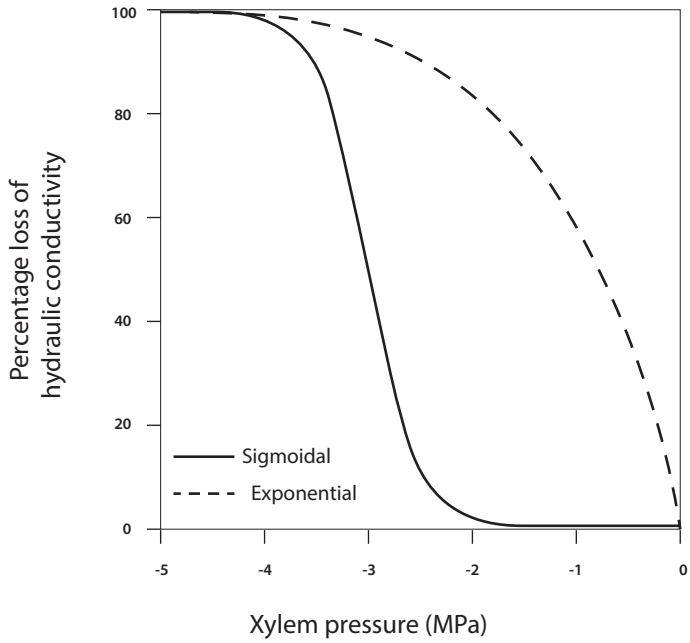


**Figure 4** • Xylem vulnerability curve showing the relationship between the loss of hydraulic conductivity and xylem pressure. The sigmoidal and exponential curves are represented, showing the difference in the decline of conductivity at low xylem pressures. *Adapted from Cochard et al. (2013).*

hydraulic field due to the risk of artefacts (Cochard *et al.* 2013). One of the most debated artefacts is the biological value of the "exponential" shape of the vulnerability curves (Delzon & Cochard 2014; Martin-St Paul *et al.* 2014; Torres-Ruiz *et al.* 2014). Vulnerability curves constructed with the Cavitron technique to species with long vessels have been shown to overestimate vulnerability to embolism (Choat *et al.* 2010; Cochard *et al.* 2010; Wang *et al.* 2014). These so-called "r" shaped curves have been attributed to the "open vessel" artefact, when vessels are long enough to extend from the cut end of the sample to its middle, which results in pre-existing embolisms caused by the open vessel end, and thereby, showing a rapid decline in conductivity at mild xylem pressures that generates the 'r' shape of the VC (Fig. 4). This highlights the importance of using cross-validation methods for curves having an 'exponential' shape (Cochard *et al.* 2013).

### *The functional significance of $P_{50}$ in plants*

Understanding how conductivity declines in a vessel network has become ecological relevant in the light of increasing drought episodes under a changing climate. The accumulated embolism, as a consequence of severe water stress, may lead to plant death (Brodribb *et al.* 2010), a relationship emphasized by experimental results demonstrating the link between embolism resistance ($P_{50}$ and $P_{88}$) and plant mortality (Brodribb & Cochard 2009; Urli *et al.* 2013). In this line, xylem

vulnerability to embolism has been identified as one of the major physiological factors driving reductions in forest productivity and drought-induced mortality in trees (Anderegg *et al.* 2012; Adams *et al.* 2017). In a recent commentary paper, $P_{50}$ has been regarded as a super trait, with the capacity to globally predict species distribution and drought sensitivity (Brodribb 2017).

The importance of hydraulic failure in determining the survival of plants is exacerbated in recent meta-analyses showing that the majority of woody plants across forest biomes operate close to their hydraulic safety margins, i.e., margins observed between the minimum xylem water potential that a plant experiences in the field and the level of water stress that is likely to induce hydraulic failure (Choat *et al.* 2012). In accordance, $P_{50}$ has been shown to be strongly correlated with species distribution in terms of water availability across a wide variety of species (Blackman *et al.* 2012; Anderegg *et al.* 2016; Larter *et al.* 2017; Trueba *et al.* 2017), making $P_{50}$ relevant for modeling of forest die-off under climate change.

There is a vast body of literature focusing on embolism resistance for stems of hundreds of woody species (Choat *et al.* 2012). Contrastingly, stem embolism resistance remains poorly investigated for herbaceous species: it is recorded in the literature for around 30 herbaceous species, of which a minority are eudicots; most herbaceous species investigated are grasses (e.g. Rosenthal *et al.* 2010; Lens *et al.* 2013a, 2016; Nolf *et al.* 2014, 2016; Skelton *et al.* 2017; Dória *et al.* 2018; Volaire *et al.* 2018). Based on the current limited data set, most herbaceous species are considered sensitive to embolism formation. However, more recent studies have shown that some grass species ($P_{50}$ up to - 7.5 MPa; Lens *et al.* 2016) as well as some herbaceous eudicot species belonging to Brassicaceae ($P_{50}$ up to -4. MPa; Dória *et al.* 2019) are remarkably resistant to embolism formation, implying that both herbs and trees share the ability to support very negative water potentials during drought stress.

While the vast majority of studies examines inter-species differences in stem $P_{50}$, the intra-species variation is less understood. Even though, the degree of hydraulic variation in a single species could have impact on population responses to changes in climate extremes, being, therefore, also important for modeling climate impacts on vegetation (Anderegg *et al.* 2013, 2015).

### *Linking xylem anatomy with plant hydraulics: looking for structure-function relationships*

Wood anatomy plays a central role in plant hydraulic strategies due to the inherent trade-offs associated with wood, namely water transport, mechanical support and food/water storage. Aside from the immediate physiological responses to differences in water availability, plants can adjust their hydraulic architecture over long-term responses (Hacke *et al.* 2017; Tng *et al.* in press). The degree of wood

plasticity at the individual level serves as a suitable proxy for understanding a species' ability to maintain the integrity of xylem water transport under extreme levels of xylem tension (Anderegg & Meinzer 2015).

There is a variety of wood traits that correlate with embolism resistance. Wood density, for instance, is expected to impact the long distance water transport in plants, since it is correlated with the amount of areas dedicated to conduit lumina, suggesting the presence of a mechanical-function trade-off (Pratt *et al.* 2007; Chave *et al.* 2009). The correlation between wood density and embolism resistance is often regarded as indirect and it is explained by the need to resist vessel collapse under drought-induced tension (Hacke *et al.* 2001a; Fichot *et al.* 2010; Ogasa *et al.* 2013). Additionally, increased wood density has also been shown to correlate with decreased sapwood capacitance (Scholz *et al.* 2011) and with minimum leaf water potential (Meinzer *et al.* 2008). At the tissue level, the total vessel wall thickness, as well as the fiber matrix surrounding the vessels also appear to be important in resisting vessel wall collapse under negative pressures (Hacke *et al.* 2001a; Jacobsen *et al.* 2005, 2007; Pratt *et al.* 2007; Dória *et al.* 2018). Likewise, also in herbaceous species, more lignified stems, which theoretically lead to higher stem densities, are linked with hydraulic safety in angiosperms (Lens *et al.* 2013a, 2016; Dória *et al.* 2018; Dória *et al.* 2019). The link between wood density, total degree of lignification and embolism resistance might be also explained by the ability of more lignified cells in avoiding the occurrence of microcracks or ruptures in the conduit walls, potentially nucleating embolisms (Li *et al.* 2016; Dória *et al.* 2018).

*The hydraulic relevance of intervessel pit membranes in embolism resistance*

Xylem conduits are much shorter than the maximum plant height, and therefore, the long distance water transport has to cross millions of intervessel pits to reach tree canopies. Hence, intervessel pits are essential in regulating hydraulic conductance. Accordingly, the air-seeding hypothesis theoretically provides a link between the ultrastructure of pit membranes and their function in limiting the spread of embolism (Sperry & Tyree 1988; Tyree & Zimmermann 2002). It states that vulnerability to drought stress-induced embolism should be dependent on the ultrastructure, thickness and chemical composition of intervessel pit membranes, since the air-seeding mechanism will depend mostly on the size of the nanometer-sized pit membrane pores (Sperry & Tyree 1988; Choat *et al.* 2008; Lens *et al.* 2011, 2013; Li *et al.* 2016). This is consistent with the fact that the hydraulic resistance of individual pits is imposed by both the average porosity and the thickness of intervessel pit membranes (Choat *et al.* 2006, 2008). The number of microfibril layers and therefore the thickness of intervessel pit membranes are likely to affect the length of the irregularly shaped pores that air-water menisci need to cross before embolism formation may occur in a neighbouring vessel (Choat et al 2008; Jansen *et al.* 2009; Lens *et al.* 2011; Li *et al.* 2016). The thickness of pit membrane

($T_{PM}$) ranges in between 70 - 1180 nm (Meyra *et al.* 2007; Jansen *et al.* 2009) and it has been considered the strongest predictor of drought-induced embolism resistance ($P_{50}$) in angiosperms across a broad taxonomic range of species when the samples are properly fixated (Jansen *et al.* 2009; Lens *et al.* 2011; Li *et al.* 2016).

Positive correlations between $T_{PM}$ and lignification characters, such as the thickness of the vessel wall (Jansen *et al.* 2009; Lens *et al.* 2011) and the proportion of lignified area per total stem area (Dória *et al.* 2018) suggest that there could be developmental coordination between $T_{PM}$ and lignification characters in wood. This provides a functional explanation for the indirect and positive relationship between wood density/lignification and embolism resistance (Hacke *et al.* 2001a; Lens *et al.* 2013a; Dória *et al.* 2018).



### *An unappreciated structure-function link: increased woodiness vs embolism resistance in otherwise herbaceous lineages*

In many predominantly herbaceous families of eudicots, an evolutionary life form shift from herbaceousness towards woody life forms has occurred (Carlquist 1974). Yet, it is still not completely known why and how many times these shifts happened during the evolutionary history of flowering plants. This process is called derived woodiness and it is considered a derived phenomenon because it arises from herbaceousness, which is in turn derived from woodiness that is the ancestral character state in angiosperms (Baldwin & Sanderson 1998; Givnish 1998). The phenomenon of derived woodiness was firstly described on islands relying on the observation that several plant families with predominantly herbaceous species in the continents have woody relatives on islands (Whittaker & Fernández-Palacios 2007). For that reason, it was also referred to as insular woodiness, which is still considered as the most conspicuous aspect of (sub)tropical floras (Carlquist 1974; Lens *et al.* 2013b).

Several hypotheses have been proposed to explain why this shift from herbaceousness toward woodiness occur: 1) the competition hypothesis, proposed by Darwin (1859), states that herbaceous species reaching islands grow in denser populations, forcing plants to grow taller to capture more sunlight; one way to grow taller is to reinforce the stems and thus become woody; 2) the longevity & promotion of outcrossing hypothesis defends the idea that the development of wood would allow these plants to extend their lifespans and flower longer in insular areas that often have few polinators (Wallace 1878; Böhle *et al.* 1996); 3) the moderate insular climate hypothesis suggests that the mild climate of islands, especially the absence of freezing, would allow these plants to grow continuously throughout the year, promoting the development of woody shrubs (Carlquist 1974); and finally, 4) the absence of large native herbivores hypothesis states that the absence of these herbivores would allow plants to continue develop and grow during their life cycle,

and thereby becoming woodier (Carlquist 1974). However, all of these hypotheses tried to explain the evolution towards derived woodiness on islands (insular woodiness). An ongoing research shows that the majority of shifts from herbs towards woody shrubs in flowering plants took place on continents (305 continental genera vs. 151 insular genera; F. Lens, ongoing review). Interestingly, these continental habit shifts are most abundant in areas with at least a few consecutive dry months per year, such as coastal mediterranean regions (55 genera), steppes (75 genera) and (semi) deserts (80 genera) (F. Lens, ongoing review). This relationship between drought and insular woodiness has also been demonstrated on the Canary Islands, where ca. 65% of the 220 insular woody species grow in markedly dry regions resistance (Lens *et al.* 2013b). Consequently, there seems to be a strong correlation between increased woodiness and increased drought. However, woody shrubs derived from herbaceous relatives do also occur in wet environments throughout the world's islands and continents (47 genera found so far; F. Lens, ongoing review), implying that drought stress is not involved in triggering woodiness in all the derived woody lineages identified so far.

# Thesis outline

The aim of my thesis is to investigate the relationship and coordination amongst xylem anatomical traits, giving functional roles in relation to hydraulic conductivity, as well as the influence of abiotic factors in xylem anatomy variation. Additionally, it also brings knowledge about which xylem anatomical characters of stems of woody and herbaceous species explain differences in embolism resistance between species. Therefore, I investigated stem anatomy of woody species occurring in two seasonally dry biomes in Brazil, the cerrado and the caatinga, and of woody and herbaceous species on Tenerife (Canary Islands, Spain). The thesis contains in total 6 chapters, with the first chapter providing the general introduction and outline of the thesis, and the last chapter giving an overall summary and conclusion of my results, which are presented in 4 papers (chapters 2-5), each with their specific objectives:

## Chapter 2

Based on the knowledge that embolism is a strong selective pressure and that plants need to balance between hydraulic efficiency and the risk of vulnerability to embolism, it is essential to understand the different xylem anatomical strategies that species use to deal with abiotic environmental constraints. In this chapter, I investigated xylem anatomical adaptations of two co-occurring species in the two

main seasonally dry biomes in Brazil, the cerrado and the caatinga. I tested the significance of the abiotic characters in the variation of xylem anatomical traits of both species, and the particular wood anatomical adaptations of individuals of the same species occurring in both sites.

## Chapter 3

Several wood traits exhibit strong axial variation to deal with increasing height constraints, especially the increase in water resistance. In this chapter I assessed the same populations of the two species from the previous chapter, occurring in both sites. We tested how wood traits (co)vary along the main trunk of an individual tree and into what extent the differences between both sites would explain the axial variation observed in wood traits.



## Chapter 4

Insular woodiness refers to the evolutionary transition from herbaceousness toward derived woodiness in island plant species. Despite several proposed hypotheses, it is still not completely known why plants have become woody. Although it is still considered an island phenomenon, these life form transitions towards derived woodiness are also common in continents where they thrive in areas with a few consecutive dry months per year. Additionally, most of the derived woody Canary Island species are native to the dry coastal regions, which points to a potential link between increased wood formation and increased drought resistance. In this chapter, I tested this drought stress hypothesis in a daisy clade, using species of the insular woody *Argyranthemum* and their herbaceous relatives native to the European continent.

## Chapter 5

Hydraulic failure is one of the main physiological mechanisms associated with reductions in forest productivity and drought-induced tree mortality. Despite the ecological and economic importance of herbaceous species, knowledge about the resistance to embolism formation in herbaceous species remains negligible compared to woody species. Moreover, recent findings in embolism resistance of herbaceous monocots show that these species have a $P_{50}$ range that is almost as extensive as the $P_{50}$ range in woody trees, contradicting the previously idea that all herbaceous species vulnerable to embolism formation. Here, I investigated whether this is also true for a group of eudicot species belonging to Brassicaceae and Asteraceae, occurring in different vegetation zones of the Canary Islands. I also tested whether the difference in mean annual precipitation amongst the vegetation zones would explain the difference in $P_{50}$ for populations collected in different zones.

*Chapter 2*

# Do woody plants of the Caatinga show a higher degree of xeromorphism than in the Cerrado?

*Larissa C. Dória[1*], Diego S. Podadera[2], Marco A. Batalha[3], Rivete S. Lima[4], Carmen R. Marcati[5]*

*Adapted from*
**Flora** 224 (2016): 244 – 251. DOI: *10.1016/j.flora.2016.09.00*

[1] Naturalis Biodiversity Center, Vondellaan 55, 2332 AA Leiden, The Netherlands.

[2] Programa de Pós-Graduação em Ecologia, UNICAMP, Campinas, SP, Brazil.

[3] Univ. Federal de São Carlos, Centro de Ciências Biológicas e da Saúde, Departamento de Botânica, 13565905, São Carlos, São Paulo, Brazil.

[4] Univ. Federal da Paraíba, Centro de Ciências Exatas e da Natureza, Departamento de Sistemática e Ecologia, 58059900, João Pessoa, Paraíba, Brazil.

[5] Univ. Estadual Paulista, UNESP, Faculdade de Ciências Agronômicas, Departamento de Ciência Florestal, Rua José Barbosa de Barros, nº 1780, 18.610-307, Botucatu, SP, Brazil.

*Corresponding author: larissachacondoria@gmail.com

[1] This work is part of the Master's Degree thesis of the first author, Programa de Pós-Graduação em Ciências Biológicas (Botânica), Instituto de Biociências de Botucatu, Univ. Estadual Paulista, UNESP, 18618970, Botucatu, São Paulo, Brazil.

# Abstract

The maintenance and success of plants in different environments is tied to water availability, to the capacities in water transport and to the development of strategies to deal with water deficit. Here, we conducted a study in two seasonally dry Brazilian phytogeographic domains: the cerrado and the caatinga to evaluate whether the adaptive wood anatomy strategies to deal with water deficit would be the same for two species that occur in both domains, and which variables would best explain the variation in wood anatomy variables. Qualitative and quantitative wood anatomy, Student's t-tests, permutational multivariate analyses of variance (PERMANOVA) and pair-contrast analyses were done for 20 specimens of *Tabebuia aurea* and *Tocoyena formosa* from both environments. Our results showed that the species was the strongest variable to explain the variation in the data. But, the environment also appeared as an important variable. Even the caatinga being drier than the Cerrado, this did not result in a higher degree of xeromorphism for both species in the caatinga. Each species, in each environment showed different strategies to deal with the water availability: while vessel diameter and intervessel pit morphology indicate a higher xeromorphic degree for *T. aurea* from the caatinga, vessel grouping index, vessel density, and vessel-ray pit morphology indicate a higher xeromorphic degree of *T. formosa* from the Cerrado. We suggest that the oligotrophic soil and the presence of aluminum in soil may influence the degree of xeromorphism in wood anatomy structure.


Keywords: *Tabebuia aurea*; *Tocoyena formosa*; water availability; wood anatomy strategies; xylem embolism.

# Introduction

Water is a primary limiting factor in many terrestrial ecosystems. The plants require water to maintain a variety of physiological process, such as stomatal conductance and CO2 uptake during photosynthesis (Woodruff *et al.* 2016). Inside the plant body, the water is conducted through a complex network of dead cells, and the hydraulic conductance has been linked with transpiration, carbon gain and growth rate (Tyree 2003; Brodribb 2009).

The assumption that water in the xylem is conducted under negative pressure (the Cohesion Tension Theory) was proposed by Dixon in 1914. From that on, studies have shown that the xylem network is prone to become filled with gas (embolism), and its subsequent spread can substantially decrease the hydraulic conductivity, which can result in tissue damage, decreases in gas exchange, and ultimately plant death (Tyree & Zimmermann 2002; Brodersen & McElrone 2013). Thus, hydraulic dysfunction by embolism is a strong selective pressure, and it is imperative for plants to balance the risk of suffering embolism and improving efficiency in water conduction. This balance has led to the development of a variety of hydraulic architecture and mechanisms to maximize efficiency and reduce vulnerability (increasing safety), reflecting differences in species distribution and in ecological and evolutionary aspects (Pockman and Sperry 2000; Sperry 2003; Baas *et al.* 2004).

In this context, there is a general trade-off between safety and efficiency in water conduction taking into account vessels characteristics. Vessels play a key role for angiosperm hydraulic performance. As wider they are, the more efficient conductors of water and more vulnerable to cavitation they will be. On the other hand, as narrower the vessels are the less efficient conductors of water and safer in hydraulic conductance they will be. As a result, safety on water conduction may be adaptive to xeric conditions while efficiency may be adaptive to mesic conditions (Zimmermann 1983; Hacke *et al.* 2006). Although the trade-off safety – efficiency of water transport is true, it is not always observed across species (Tyree *et al.* 1994). For some species, the most common examined wood anatomy traits associated with embolism resistance, for instance vessel diameter, are not correlated with embolism resistance (Schreiber *et al.* 2015). Other species might show both, low efficiency and low safety, which cannot be understood under a trade-off approach (Maherali *et al.* 2004). Furthermore, recent evidences suggest that the vessel diameter – plant size relationship is predictable across species (Olson & Rosell 2013; Olson *et al.* 2013, 2014). The vessel diameter is proportional to stem diameter, and the latter proportional to stem length, suggesting that taper in relation to stem length gives rise to the vessel diameter – stem diameter relationship.

Because xylem anatomy is largely responsible for the cavitation resistance (Johnson *et al.* 2012), it is clear that many xylem network traits could contribute to the safety – efficiency trade-off, and that these traits would interact in different ways, and at different multiple scales (Gleason *et al.* 2015). For instance, vessel length and diameter (Loepfe *et al.* 2007) and the degree of vessel grouping (Carlquist 1984; Lens *et al.* 2011) are important determinant components of this trade-off safety – efficiency in angiosperms, influencing the continuity of water flow. In addition, there are general ecological trends in wood anatomy supporting the dominant safety – efficiency trade-off. Species from drier environments tend to have narrow vessels (Carlquist 1966; Bosio *et al.* 2010), short vessel elements (Carlquist 1982), and high values of vessel density and vessel grouping (Baas *et al.* 1983; Carlquist & Hoekman 1985; Sonsin *et al.* 2012). Moreover, these species tend to have low values for vulnerability (V = vessel element diameter/vessel density) and mesomorphy (M = V × vessel element length) indices (Carlquist 1977; Sonsin *et al.* 2012), and show thicker fiber walls (Alves & Angyalossy-Alfonso 2002) necessary to support negative xylem pressures (Hacke & Sperry 2001).



Successful colonization of xeric habitats by both angiosperms and gymnosperms has been linked to xylem highly resistant to embolism formation (Brodribb *et al.* 2012). Different levels of safety and efficiency are expected in different environments because xylem operates at widely different water potentials (Choat *et al.* 2012), and in seasonally dry environments the higher negative pressure in the vessels of plants can increase the risk of cavitation and embolisms (Sperry & Hacke 2002). The cerrado and the caatinga are two examples of seasonally dry environments in Brazil (Pennington *et al.* 2000) with at least five consecutive dry months (Nimer 1972; Silva *et al.* 2008), although climatic conditions are harsher in the latter. The Cerrado, a savanna-like ecosystem, is located in the Brazilian Central Plateau, with annual mean temperatures around 22–23 °C and average annual rainfall around 1,500 mm (Silva *et al.* 2008). Soils are usually deep, nutrient-poor and aluminum-rich, the latter toxic to some plant species (Coutinho 2002). The caatinga is a tropical dry forest ecosystem of the semiarid region of northeast Brazil, with annual mean temperatures around 26–27 °C (Andrade-Lima1981) and average annual rainfall between 300 and 800 mm (Nimer 1972).

In the light of these considerations, we aimed to test if woody species occurring in the cerrado and in the caatinga would show different wood anatomy strategies, and different degree of xeromorphism, to deal with the absence of water during the months of drought. Moreover, we tested the differences between sites and which variables could best explain the variation in the anatomy variables.

# Material and Methods

## Plant material and study site

We selected two species common to both the Cerrado (Ratter *et al.* 2003) and the caatinga (Moro *et al.* 2014): *Tabebuia aurea* (Silva Manso) Benth. & Hook. f. ex S. Moore and *Tocoyena formosa* (Cham. & Schltdl.) K. Schum.

In the Cerrado, we sampled individuals of both species in the "Palmeira da Serra" Private Reserve, in the municipality of Pratânia, in the state of São Paulo (Fig. 1), southeastern Brazil (22° 48' 35" S 48° 39' 57" W). In the caatinga, we sampled individuals of *Tabebuia aurea* in the municipality of São João do Cariri (7° 23' 27" S, 36° 32' 2" W) and individuals of *Tocoyena formosa* in the municipality of Serra Branca (7° 29' 14" S, 36 ° 39' 51" W), both in the state of Paraíba (Fig. 1), northeastern Brazil.

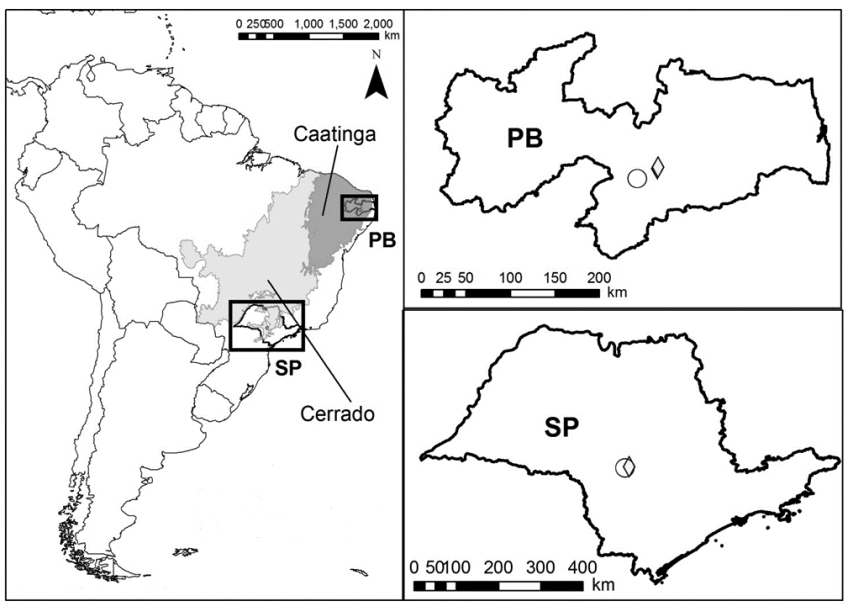


**Figure 1** • Study sites in the cerrado and in the caatinga. The circle (O) indicates the study site sampling of *Tocoyena formosa* and the diamond (◊) the study site sampling of *Tabebuia aurea*.

A dataset of 12 years (2000 – 2012) was used to estimate the mean monthly rainfall and temperature in that period. The climatic data were provided by the Estação Experimental of the Faculdade de Ciências Agronômicas, Universidade Estadual Paulista (UNESP), Botucatu Campus, for the Cerrado and by the Estação

Experimental of São João do Cariri, for the caatinga. The Cerrado has a milder climate than caatinga, with mean temperature below 25 °C throughout the year. The precipitation in this domain is higher, with maximum monthly rainfall of 350 mm during the wet season. Even though, the Cerrado shows a remarkable dry season from June to September when precipitation reaches less than 50 mm in a month (Fig. 2). The caatinga is a hotter environment, with temperatures above 25 °C throughout the year. This domain also has longer dry season than the Cerrado, extending from July to December, when the precipitation reaches zero. During the rainy season the maximum monthly rainfall does not exceed 100 mm (Fig. 2).

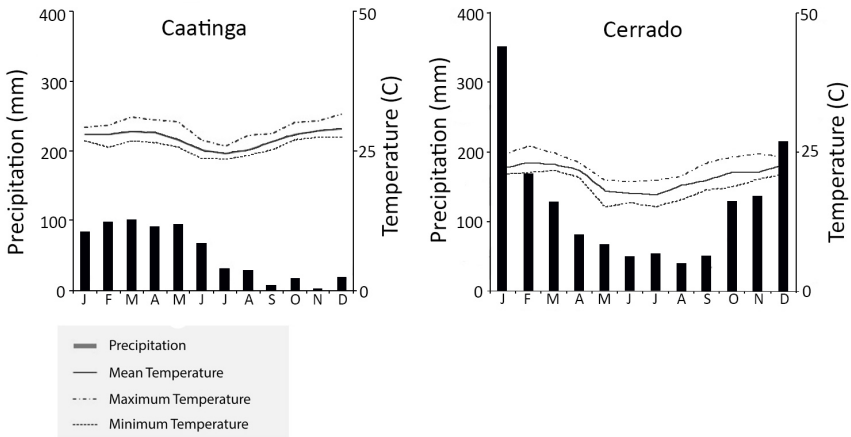


**Figure 2** • Climate graphs with mean precipitation and temperature from 2000 to 2012.

## Sampling and anatomical study

We standardized the number of individuals studied taking into account the individuals of *Tabebuia aurea* available at the study site in the cerrado area (population size = 5). So, for both species, we collected 5 different individuals, in both areas, amounting 20 individuals studied.

We collected samples from the basal region of the thicker branches of the shrub *Tocoyena formosa* and from the main stem at breast height of the tree *Tabebuia aurea*. In the field we measured the stem circumference at the height at which the samples were taken, and the plant height. The wood samples were fixed in FAA 70% (Formaldehyde 37%, acid acetic, ethanol 70% – 1:1:18) and thereafter stored in 70% alcohol. We cut tangential longitudinal, radial longitudinal and cross sections of 15–20 µm thickness of each sample with a sliding microtome. To prepare permanent histological slides, we followed Johansen (1940) and Sass (1951).

Sections were double-stained with aqueous 1% safranin and aqueous 1% astra blue (1:9). Histological slides were mounted permanently in synthetic resin (Entellan®). For maceration, we followed Franklin's (1945) method modified by Kraus & Arduin (1997). The cells were dissociated in acetic acid and hydrogen peroxide (1:1), stained with aqueous 1% safranin and mounted in a 1:1 glycerin-water solution. The wood anatomy slides were analysed using an Olympus DP70, equipped with Axio Cam MRC and Axiovision software. We followed the suggestions of the International Association of Wood Anatomists Hardwood List (IAWA Committee 1989) to determine the wood anatomy features, and the suggestions of Scholz *et al.* (2013) and Carlquist (1977, 2001) for measurements of the wood anatomy variables. The qualitative data for wood anatomy are given in Supplementary Information.

We collected soil samples from both regions at a depth of 0–20 cm and of 20–40 cm (ten replicates each), close to the sites of species occurrence. Soil samples were sent to the Departamento de Solos of the Faculdade Ciências Agronômicas, Universidade Estadual Paulista (UNESP), Botucatu, São Paulo state, for physical and chemical analysis. Soil analysis was carried out as per the procedures described by Raij *et al.* (2001). Air-dried soil samples were analyzed for the available contents of phosphorus (P); aluminum (Al); potential acidity (H+Al); the basic cations, including potassium (K), calcium (Ca), and magnesium (Mg); sum of the bases Ca, Mg and K (SB); pH; base saturation (V%); micronutrients boron (B), copper (Cu), iron (Fe), manganese (Mn) and zinc (Zn). The cation exchange capacity (CEC) was analyzed using buffered SMP solution (pH = 7) (Shoemaker *et al.* 1961). The total organic carbon (O.M.) was analyzed using the Colorimetric Method (Walkley & Black 1934, modified).

## Statistical analyses

The quantitative analysis was based on 30 individual measurements per specimen to achieve mean values within 90% confidence limits, following Freese (1967) and Eckblad (1991).

To test for differences between sites, we conducted a permutational multivariate analyses of variance (PERMANOVA) with anatomical variables (rank transformed) as dependent variables; the interaction between site and species as independent variable; and plant height and stem diameter as covariates. To avoid collinearity, we selected the variables based on biological knowledge (for variables biologically correlated we choose one of them, e.g. ray height in µm and ray height in number of cells, we selected ray height in µm and deleted ray height in number of cells) , correlation coefficients (values below 0.6), and visual analyses of pairwise scatter-plots (Zuur *et al.* 2010). PERMANOVA was performed using the adonis function in the vegan package (Oksanen *et al.* 2015) in R (R Core Team 2014), based on

Euclidian distances and 999 permutations. To detect specific differences between sites for each species, pair-contrast analyses were done using the contrasts function in the stats package (R Core Team 2014) and the adonis function in the vegan package (Oksanen *et al.* 2015) in R (R Core Team 2014).

To test for anatomical differences within each species between the two sites, we performed Student's t-test for each wood anatomical variable with normal distribution (fiber length, fiber lumen diameter, ray width in µm and in number of cells, ray frequency, intervessel pit diameter and aperture, vessel-ray pit diameter and aperture). Because vessel element length, vessel diameter, vessel density, vessel grouping, fiber diameter, fiber wall thickness, ray height in µm and in number of cells, vulnerability and mesomophy indexes did not present normal distribution (graphical tools analyses as proposed by Zuur *et al.* 2010), we performed Kruskal-Wallis Rank Sum test.



# Results

### *Wood anatomy differences*

The wood anatomy description of *Tabebuia aurea* and *Tocoyena formosa* is given in Supplementary Information (Fig. S1, Fig. S2).

To avoid collinearity, we selected five wood anatomy variables, out of 19, to be tested in the permutational multivariate analyses. The five variables selected were: vessel element length, vessel grouping index, fiber lumen diameter, ray width in µm, and intervessel pit diameter (Table 1). The covariates plant height and stem diameter were not included in the final model because they were not significant. According to PERMANOVA results (Table 1), site, species and the interaction site × species explained 50% of the variation in the group of anatomical variables analyzed. Species was the strongest explanatory variable (28%). The contrast analysis testing the differences between sites within each species showed significant differences only for *T. aurea*.

*Tabebuia aurea* from caatinga differed from those of the Cerrado in eight out 19 wood anatomy features analyzed, which were: vessel diameter, fiber wall thickness, ray height in µm, ray width in µm and in number of cells, ray frequency, intervessel pit diameter, vessel-ray pit diameter (Table 2). Narrower vessels, narrower intervessel pits diameter and vessel-ray pits diameter, thinner fiber wall thickness, shorter and narrower rays, and higher frequency of rays were observed in individuals from caatinga.

Table 1: Summary of PERMANOVA, results based on 999 permutations, with anatomical variables (rank transformed) as dependent variables; the interaction between site and species as independent variable; and plant height and stem diameter as covariates.

| **Parameters** | ***df*** | **SS** | **MS** | ***F* Model** | $R^2$ | ***P*(>*F*)** |
|---|---|---|---|---|---|---|
| Site | 1 | 0.965 | 0.965 | 4.249 | 0.132 | 0.005 |
| Species | 1 | 2.066 | 2.066 | 9.098 | 0.282 | 0.001 |
| Site : species | 1 | 0.654 | 0.654 | 2.878 | 0.089 | 0.031 |
| Plant height | --- | --- | --- | --- | --- | --- |
| Stem diameter | --- | --- | --- | --- | --- | --- |
| Residuals | 16 | 3.634 | 0.227 | | 0.497 | |
| TOTAL | 19 | 7.319 | | | 1.000 | |
| | | | | | | |
| Contrast analysis | | | | | | |
| *T. aurea* in the caatinga and in the cerrado | 1 | 1.407 | 1.407 | 4.196 | 0.192 | 0.008 |
| *T. formosa* in the caatinga and in the cerrado | 1 | 0.212 | 0.212 | 0.632 | 0.029 | 0.620 |
| Residuals | 17 | 5.700 | 0.335 | | 0.779 | |
| TOTAL | 19 | 7.319 | | | 1.000 | |

SS, sum-of-squares; MS, mean squares; and *P*(>*F*) are *P*-values. ---: non-significant. We used Euclidian distance to measure dissimilarity between samples.

*Tocoyena formosa* from caatinga differed from those of the Cerrado in five out 19 wood anatomy features analyzed, which were: vessel density, vessel grouping index, vessel-ray pit diameter, vulnerability index and mesomorphy index (Table 2). Lower density of vessels and vessel group index, and higher values for mesomorphy and vulnerability indexes were observed in the individuals from caatinga. Moreover, as well as *T. aurea*, narrower vessel-ray pit diameter were observed for *T. formosa* in caatinga.

### *Soil characterization*

The soils in both domains were sandy (Table 3). The cerrado soils were more acid, with higher aluminum and H saturation of soil cation exchange capacity (Table 3) and lower concentration of macronutrients (P, K, Ca, Mg) and micronutrients, such as manganese (Table 3). In addition, the cerrado soils showed a higher proportion of copper and iron than the caatinga soils (Table 3).

# Discussion

In this study we investigated whether two species occurring both in the caatinga and in the cerrado, two seasonally dry environments in Brazil, would show different wood anatomy strategies to deal with the drought period. We also tested if the sites would be differentiated by the wood anatomy variables and which variables, such as the species-specific characteristics, and the environmental influence could explain the variation in the wood anatomy data variables.

The plant height and the stem diameter were not significant to explain the variation in the wood anatomical data using the PERMANOVA model (Table 1). Rather than plant height and stem diameter, site, species and site × species interaction explained half of the variation (Table 1). Most of the variation was explained by the variable species, emphasizing the importance of the phylogenetic traits. However, the site also appeared as an important source of variation, but not as a universal trend, because the site did not explain the variation for *Tocoyena formosa* (contrast analyses Table 1). Nevertheless, the influence of the site is supported by the differences in the Students t-test, which showed nine different anatomical variables for *Tabebuia aurea* and five different variables for *T. formosa* (Table 2). These results seem to point out *T. aurea* as more sensitive to the environmental conditions (higher phenotypic plasticity) than *T. formosa*. The differences in wood anatomy variables within species in different environments, can be seen as different wood anatomical strategies in drought resistance for each species in both environments.

Worldwide, forest species operate with narrow margins of hydraulic safety (Choat *et al.* 2012), frequently leading to embolism formation. Therefore, strategies to prevent or reverse embolisms are required to increase plant survival. Plants in drier sites frequently present narrower vessels than plants in moister sites (Carlquist 1966; Carlquist & Hoekman 1985; Alves & Angyalossy-Alfonso 2000; Lens *et al.* 2004; Bosio *et al.* 2010). Indeed, we found narrower vessels in *T. aurea* from caatinga that is a drier environment than cerrado. This characteristic could be explained in terms of increased safety on sap flow. Based on the Hagen–Poiseuille law the diameter scales to the fourth power of the conductance, so, a narrow vessel is associated with lower hydraulic efficiency (or high hydraulic resistance) (Ewers *et al.* 1990), being less vulnerable to the impact of drought induced cavitation than wider conduits (Lens *et al.* 2004; Schreiber *et al.* 2015). In addition to narrower vessels, we also found narrower intervessel pit diameter in *T. aurea* from caatinga. A decrease in the membrane area of the intervessel pit is correlated with an increase in resistance to drought-induced cavitation (Hacke *et al.* 2006). Vessel and intervessel pits diameter directly influence the resistance in hydraulic conductivity, each accounting for about half of the total resistance (Sperry *et al.* 2005). Our data

Table 2: Quantitative wood anatomy characters of *Tabebuia aurea* and *Tocoyena formosa* from the cerrado and the caatinga. t-test was performed for variables with normal distribution, and the others with Kruskal-Wallis Rank Sum test. The values are means with the corresponding standard error.

| **Wood anatomy features** | ***T. aurea*** **caatinga** | ***T. aurea*** **cerrado** | **t test (p value)** | **Kruskal-Wallis Rank Sum test** | ***T. formosa*** **caatinga** | ***T. formosa*** **cerrado** | **t test (p value)** | **Kruskal-Wallis Rank Sum test** |
|---|---|---|---|---|---|---|---|---|
| Vessel element length (µm) | 259.0 ± 3.4 | 271.0 ± 14.7 | | 0.6015 | 557.7 ± 48.7 | 466.1 ± 25.8 | | 0.1745 |
| Vessel diameter (µm) | 89.6± 4.1 | 106.9 ± 5.7 | | 0.0472 | 48.4 ± 0.9 | 44.4 ± 1.5 | | 0.0758 |
| Vessel density (nº $mm^{-2}$) | 8.9 ± 1.4 | 10.9 ± 1.3 | | 0.6015 | 52.6 ± 4.3 | 81.3 ± 7.7 | | 0.0163 |
| Vessel grouping index (nº of vessels per group) | 1.5 ± 0.0 | 1.9 ± 0.2 | | 0.1172 | 1.2 ± 0.0 | 1.5 ± 0.0 | | 0.0090 |
| Fiber length (µm) | 799.8 ± 33.9 | 839.9 ± 32.3 | 0.4160 | | 1146.9 ± 56.0 | 1052.6 ± 39.2 | 0.2092 | |
| Fiber diameter (µm) | 16.3 ± 0.2 | 17.2 ± 0.5 | | 0.2506 | 21.4 ± 0.9 | 22.3 ± 0.3 | | 0.6015 |
| Fiber lumen diameter (µm) | 8.5 ± 0.2 | 8.4 ± 0.5 | 0.8863 | | 7.9 ± 0.4 | 8.3 ± 0.5 | 0.5755 | |
| Fiber wall thickness (µm) | 3.9 ± 0.1 | 4.4 ± 0.2 | | 0.0090 | 6.7 ± 0.3 | 7.0 ± 0.1 | | 0.4647 |
| Ray height (µm) | 139.7 ± 7.2 | 200.3 ± 12.6 | | 0.0090 | 549.9 ± 29.0 | 575.0 ± 6.8 | | 0.1745 |
| Ray height (number of cells) | 6.8 ± 0.3 | 7.9 ± 0.7 | | 0.1745 | 11.8 ± 0.7 | 13.0 ± 0.8 | | 0.2506 |
| Ray width (µm) | 20.6 ± 2.9 | 29.8 ± 1.8 | 0.0326 | | 22.9 ± 1.2 | 23.5 ± 3.6 | 0.8933 | |
| Ray width (number of cells) | 1.4 ± 0.1 | 1.7 ± 0.1 | 0.0215 | | 1.3 ± 0.0 | 1.5 ± 0.1 | 0.1212 | |
| Ray frequency (nº $mm^{-1}$) | 13.9 ± 0.9 | 10.3 ± 0.5 | 0.0092 | | 19.4 ± 0.6 | 17.8 ± 0.3 | 0.0741 | |
| Intervessel pit diameter (µm) | 4.6 ± 0.2 | 5.9 ± 0.2 | 0.0035 | | 4.5 ± 0.3 | 4.5 ± 0.1 | 0.9464 | |
| Intervessel pit aperture (µm) | 2.4 ± 0.1 | 2.6 ± 0.1 | 0.3668 | | 1.7 ± 0.1 | 1.5 ± 0.1 | 0.2252 | |
| Vessel-ray pit diameter (µm) | 4.0 ± 0.1 | 4.5 ± 0.1 | 0.0155 | | 4.1 ± 0.1 | 4.4 ± 0.0 | 0.0169 | |
| Vessel-ray pit aperture (µm) | 2.5 ± 0.1 | 2.9 ± 0.2 | 0.0765 | | 1.6 ± 0.0 | 1.8 ± 0.1 | 0.1104 | |
| Vulnerability index | 12.1 ± 3.4 | 10.3 ± 1.3 | | 0.9168 | 0.9 ± 0.1 | 0.6 ± 0.1 | | 0.0163 |
| Mesomorphy index | 3124.8 ± 865.6 | 2809.9 ± 430.7 | | 0.9168 | 528.7 ± 63.6 | 259.9 ± 19.1 | | 0.0090 |

Table 3: Soil analysis of collection sites, from the Private Cerrado Reserve "Palmeira da Serra" in the cerrado and from the municipality of Serra Branca, in the caatinga.

**Physical analyses**

| Domains | Sandy | | | Clay | Silt | Texture |
|---|---|---|---|---|---|---|
| | Coarse | Fine | Total | | | |
| | g/kg | | | | | |
| cerrado | ---- | ---- | 861 | 99 | 40 | sandy |
| caatinga | ---- | ---- | 921 | 36 | 43 | sandy |

**Micronutrients**

| Domains | Boron | Copper | Iron | Manganese | Zinc |
|---|---|---|---|---|---|
| | mg/dm$^3$ | | | | |
| cerrado | 0.21 | 0.7 | 115 | 1.2 | 0.2 |
| caatinga | 0.13 | 0.2 | 65 | 8.0 | 0.3 |

**Fertility**

| Domains | pH $CaCl_2$ | O.M. | $P_{resin}$ | H + Al | K | Ca | Mg | SB | CEC | V% | S |
|---|---|---|---|---|---|---|---|---|---|---|---|
| | | g/dm$^3$ | mg/dm$^3$ | mmol/dm$^3$ | | | | | | | |
| cerrado | 4.0 | 6.0 | 2.0 | 36.0 | 0.3 | 1.0 | 0 | 2.0 | 38.0 | 5.0 | --- |
| caatinga | 4.7 | 8.0 | 5.0 | 15.0 | 1.1 | 7.0 | 3.0 | 11.0 | 26.0 | 42.0 | 5.0 |

pH $CaCl_2$ = hydrogen ion concentration; O.M. = organic matter; $P_{resin}$= phosphor; H+Al = potential acidity; K = potassium; Mg = magnesium; SB = sum of basis; CEC = cation exchange capacity; V% = saturation/base; S = sulfur; $CaCl_2$ = calcium chloride; g/dm$^3$ = gram/decimeter cubic; mg/dm$^3$ = miligram/decimeter cubic; mmol/dm$^3$ = milimoles charge/decimeter cubic; g/kg = gram/kilogram.

on vessel and intervessel pit morphology in *T. aurea* indicate a higher xeromorphic degree of plants in the caatinga. A similar relationship has been observed in other Brazilian species from dryer environments (Marcati *et al.* 2001; Sonsin *et al.* 2012), confirming its significance for hydraulic safety on this species.

*Tabebuia aurea* from the cerrado seems to have a different strategy to avoid air-seeding and embolism formation. Our data showed taller and wider rays for these individuals, which could be interpreted as an evidence of drought resistance mechanism played by the parenchyma tissue (Brodersen *et al.* 2010; Nardini *et al.* 2011). The parenchyma cells have already been shown to be correlated with drought mechanisms such as xylem capacitance and refilling of embolised vessels (Trifiló *et al.* 2014). It has been speculated that this tissue not only stores water, but could also provide symplastic connections with bark and pith, both important water reservoirs (Scholz *et al.* 2007). Additionally, it has been suggested that vessel-associated radial and axial parenchyma may be involved in the embolism refilling process by releasing sugars and water into embolised vessels (Salleo *et al.* 2008; Brodersen & McElrone 2013). The rays work, in this case, as an efficient radial pathway from the phloem carrying water, needed to raise the water potential for refilling. Moreover, the rays could also play the role of carrying ions (being the phloem as the source), to be loaded into xylem, responsible to create the osmotic force to the refilling process (Metzner *et al.* 2010; Nardini *et al.* 2011).

The large diameter of vessel-ray pits in the two cerrado species indicates an investment in a more efficient sugar transport into embolized vessels. The vessel-ray pits are effective in the transport of osmotically active sugar (from starch hydrolysis; Bucci *et al.* 2003) from these parenchyma cells into embolized vessels, providing an osmotic mechanism for embolism reversal (Salleo *et al.* 2006, 2008; Nardini *et al.* 2011). A higher concentration of solutes and, therefore, a lower osmotic potential in the embolized vessels, increases the water transport into these vessels reestablishing the flow with a possible reversal mechanism of embolisms (Hacke & Sperry 2003). A decrease in starch concentration in parenchyma cells would turn these cells into sinks for the phloem. As a response, the phloem would unload sugars and water into these cells, via their rays, generating the necessary driving force for refilling the xylem, and potentially reversing embolism (Salleo *et al.* 2009; Nardini *et al.* 2011).

Different from *T. aurea*, the higher values for the vessel density and vessel grouping index, and lower values for vulnerability and mesomorphy indices of *T. formosa* seem to be good predictors of strategies to deal with water deficit of this species from the cerrado. The relationship of these predictors with hydraulic safety and conductivity has already been reported (Carlquist 2001, 2012; Bosio *et al.* 2010; Sonsin *et al.* 2012;) . A higher vessel grouping index allows the continuity of

water transport if one or several vessels in a group are incapacitated by air embolisms (Carlquist 1984, 2012), therefore improving the hydraulic efficiency.

In spite of the remarkable dry season, the cerrado is not considered a xerophytic vegetation type as the caatinga is (Oliveira & Marquis 2002). For instance, most of cerrado 's plants develop large green leaves in the body plant throughout the year (Morretes & Ferri 1959). Moreover, some plants also flourish during the dry period (Rivera *et al.* 2002), and develop deep root system enabling plants to access water stored deeply in the soil during the periods of drought, maintaining transpiration and carbon fixation (Oliveira *et al.* 2005). Taking these general characteristics of cerrado plants into account, we believe that the drought resistance adaptations discussed here for both cerrado species are not an adaptive response to water availability. We suggest that this can be a response for the chronic low availability of edaphic mineral nutrients (oligotrophism) and the high aluminum concentration (aluminum toxicity) in the cerrado soils (Table 3). The oligotrophic and aluminum toxic soils have been reported as the main cause of xeromorphic features in the cerrado plants, such as sclerophylly in leaves (Coutinho 1983; Salatino 1993), being conceptualizedas the theory of Oligotrophic Scleromorphism (Arens 1958; Arens *et al.* 1958; described in English in Salatino 1993), or peinomorphism (sensu Walter 1973). In the same way, by the higher sclerophylly commonly found in the leaves of the cerrado species (Oliveira *et al.* 2003; Souza *et al.* 2015), we would expect higher sclerophylly for wood characters as well, which was shown by the thicker fiber walls found in individuals of *T. aurea* from the cerrado. Moreover, the individuals of *T. formosa* from the cerrado are shorter (Table S1, Supplementary Information) than those from the caatinga. This reduced size can also be explained by the higher aluminum concentration (Table 3) as well as the lower concentration of essential micronutrients, such as manganese (Table 3) in the cerrado soils. Aluminum is a strong plant growth reducing element in acid soils (Kochian 1995), and the deficiency of any essential micronutrient can cause disorders in physiological and biochemical processes, resulting in reduced plant growth (Kozlowski *et al.* 1991). These results point to mention that the Oligotrophic Scleromorphism Theory can also be applied to wood anatomical features in this particular case, supporting our hypotheses of high aluminum concentration and oligotrophism as a cause of the presence of xeromorphic features in wood of *T. formosa* from the cerrado.

When we compare in general the anatomical adaptation of the two species, on each environment, we notice particular adaptations for each species. In other words, each species has its own trade-off to deal with the environment adversities both in the cerrado and in the caatinga. For instance, while *T. aurea* ranged on vessel diameter (wider in the cerrado), and *T. formosa* ranged in the vessel density and vessel index grouping (both higher in the cerrado), maintaining relatively steady the vessel diameter. Moreover, *T. aurea* showed a huge variation in the rays (wider and higher in the cerrado), while the same did not occurr for *T. formosa*,

which preserved constant size of the rays. This constancy in ray size could be probably compensated by the higher number of vessels/mm² in *T. formosa* compared with *T. aurea*. It seems that the lower number of vessels/mm² in *T. aurea* can be offset by the variation in ray size, which in some way, interact with the sparse vessels via the vessel-ray pits connections.

In summary, the environment has a noteworthy influence in wood anatomy characters, even if it is not a universal key to explain the variation. Its influence is noticed on the particular adaptation within species for each environment. Woody plants of the caatinga did not necessarily show a higher degree of xeromorphism than in the cerrado. Despite the fact that both environments show a period of water deficit, the difference in the rainfall is different for each environment. In the caatinga the irregularity in the rainfall is remarkable during the years and the mean precipitation is less and concentrated in three months. In the cerrado the rainy and drought period is well-defined during the years, but, on the other hand, the plants have to deal with the edaphic adversities. These particular characteristics of both environments is reflected in the particular wood anatomy strategies within species in both environments. It is important to point that the drought adaptation strategies are not restricted to the xylem. The characteristics of leaves (density of stomata, stomatal conductance, epicuticular waxes), rooting depth, and physiological processes (photosynthetic capacity, deciduousness), are also variables that could influence plant responses to water deficit.

# Supplementary information

## Wood anatomy descriptions

*Tabebuia aurea (Silva Manso) Benth. & Hook. f. ex S. Moore*

Growth rings: delimited by axial parenchyma in marginal lines or bands (Fig. 1 A–D) in the wood of individuals from both environments. Vessels: wood diffuse-porous (Fig. 1 A–D); 49% of solitary vessels (Fig. 1 C) in individuals from the cerrado and 54% (Fig. 1 D) in individuals from the caatinga; clusters rare (Fig. 1 C) in both environments, but more frequent in individuals from the cerrado; simple perforation plates (Fig. 1 E) predominant, and foraminate (Fig. 1 E) in a few vessel elements; vessel element tails present; intervessel pits alternate; vessel-ray pits with distinct borders, similar to intervessel pits in size and shape throughout the ray cell. Fibers: simple to minutely bordered pits in both radial and tangential walls. Axial parenchyma: in marginal lines or bands, paratracheal confluent forming irregular bands often, and lozenge-aliform (Fig. 1 A–D); 2–4 cells per parenchyma

strand; amount of 63% of axial parenchyma in both environments; storage starch in axial parenchyma. Rays: 2-seriate (Fig. 1 G) rays predominantly in individuals from the cerrado and uniseriate (Fig. 1 H) predominantly in individuals from the caatinga; all ray cells procumbent (Fig. 1 I–J); storage starch in rays. Storied structure: rays irregularly storied (Fig. 1 G) in individuals from the cerrado and rays, axial parenchyma and vessel elements storied (Fig. 1 H) in individuals from the caatinga. Chrome Azurol-S test: positive.

*Tocoyena formosa (Cham. & Schltdl.) K. Schum.*

Growth rings: delimited by thick-walled and radially flattened latewood fibers (Fig. 2 A–D) in the wood of individuals from both environments. Vessels: wood diffuse-porous (Fig. 2 A–D); 61% of solitary vessels in individuals from the cerrado and 85% in individuals from the caatinga; simple perforation plates (Fig. 2 E, G, I); vessel elements tails present, conspicuous (Fig. 2 E); intervessel pits alternate, vestured (Fig. 2 F); vessel-ray pits with distinct borders, similar to intervessel pits in size and shape throughout the ray cell; deposits in some vessel lumina. Tracheids: vascular tracheids present (Fig. 2 G). Fibers: with distinctly bordered pits in both tangential (Fig. 2 H) and radial (Fig. 2 I) walls. Axial parenchyma: apotracheal diffuse to diffuse-in-aggregates (Fig. 2 C, D); 3–4 cells per parenchyma strand; amount of 5% of axial parenchyma in individuals from the cerrado and 6% of axial parenchyma in individuals from the caatinga; storage starch in axial parenchyma. Rays: 1 to 3 cells wide, with multiseriate portion as wide as uniseriate portion (Fig. 2 H); fused rays (Fig. 2 H); body ray cells procumbent with over 4 rows of upright and/or square marginal cells (Fig. 2 I); perforated ray cells present (Fig. 2 J); storage starch in rays. Chrome Azurol-S test: positive, more pronounced in individuals from the cerrado.

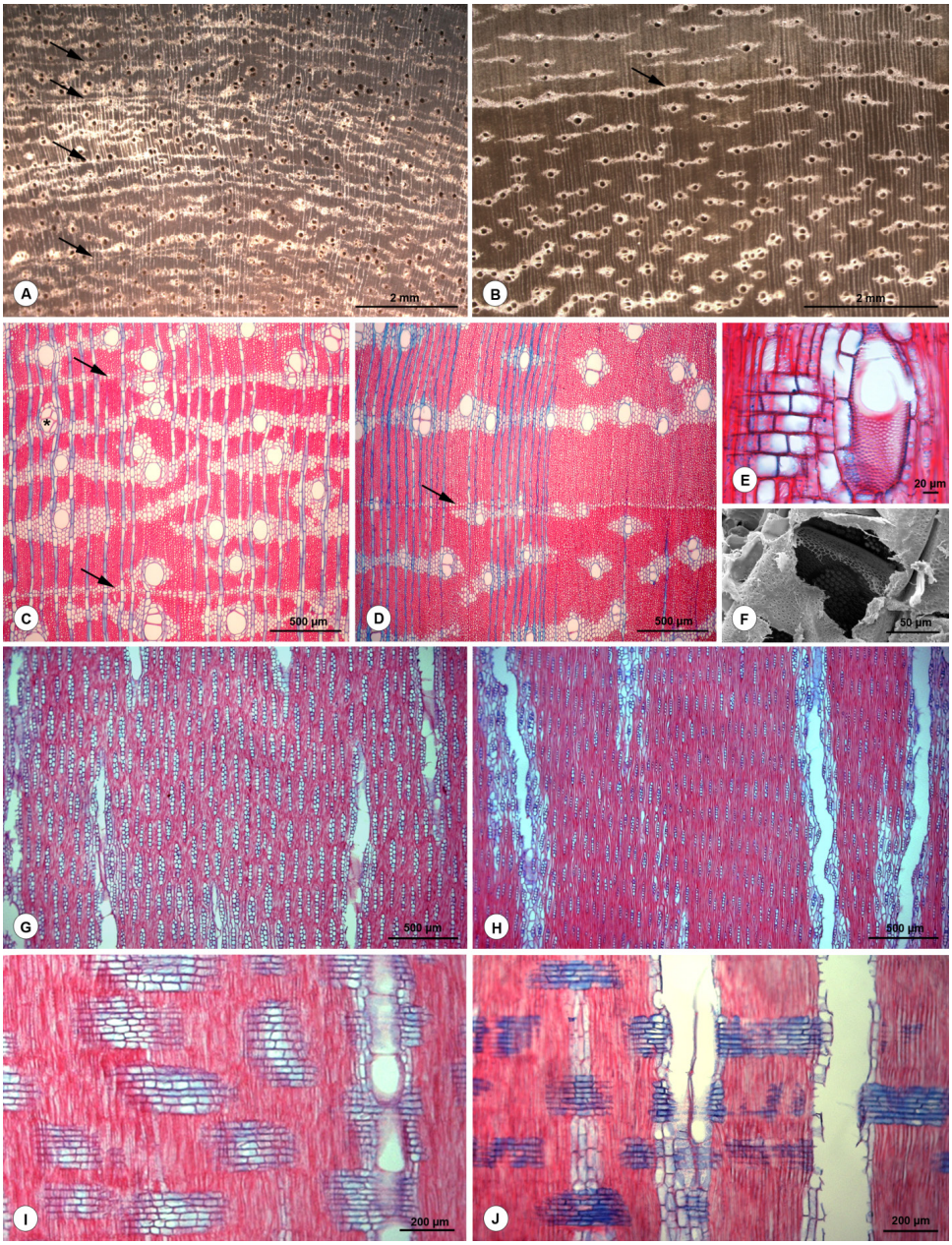


**Figure S1** • Macroscopic and microscopic images of *Tabebuia aurea* secondary xylem. A–D. Cross sections. Growth rings delimited by marginal lines/bands of axial parenchyma (arrows), wood diffuse-porous, and paratracheal axial parenchyma in individuals from the cerrado (A, C) and from the caatinga (B, D). Note narrower growth rings and vessel cluster (*) in individuals from the cerrado (A, C). E. Simple perforation plate in radial longitudinal section. F. Foraminate perforation plate broken by technical artifact in scanning electron microscopic. G–H. Tangential longitudinal sections. G. Two-seriate and irregularly storied rays in individuals from the cerrado. H. Uniseriate regularly storied rays in individuals from the caatinga. I–J. Radial longitudinal section. Ray cells procumbent in individuals from the cerrado (I) and in individuals from the caatinga (J).

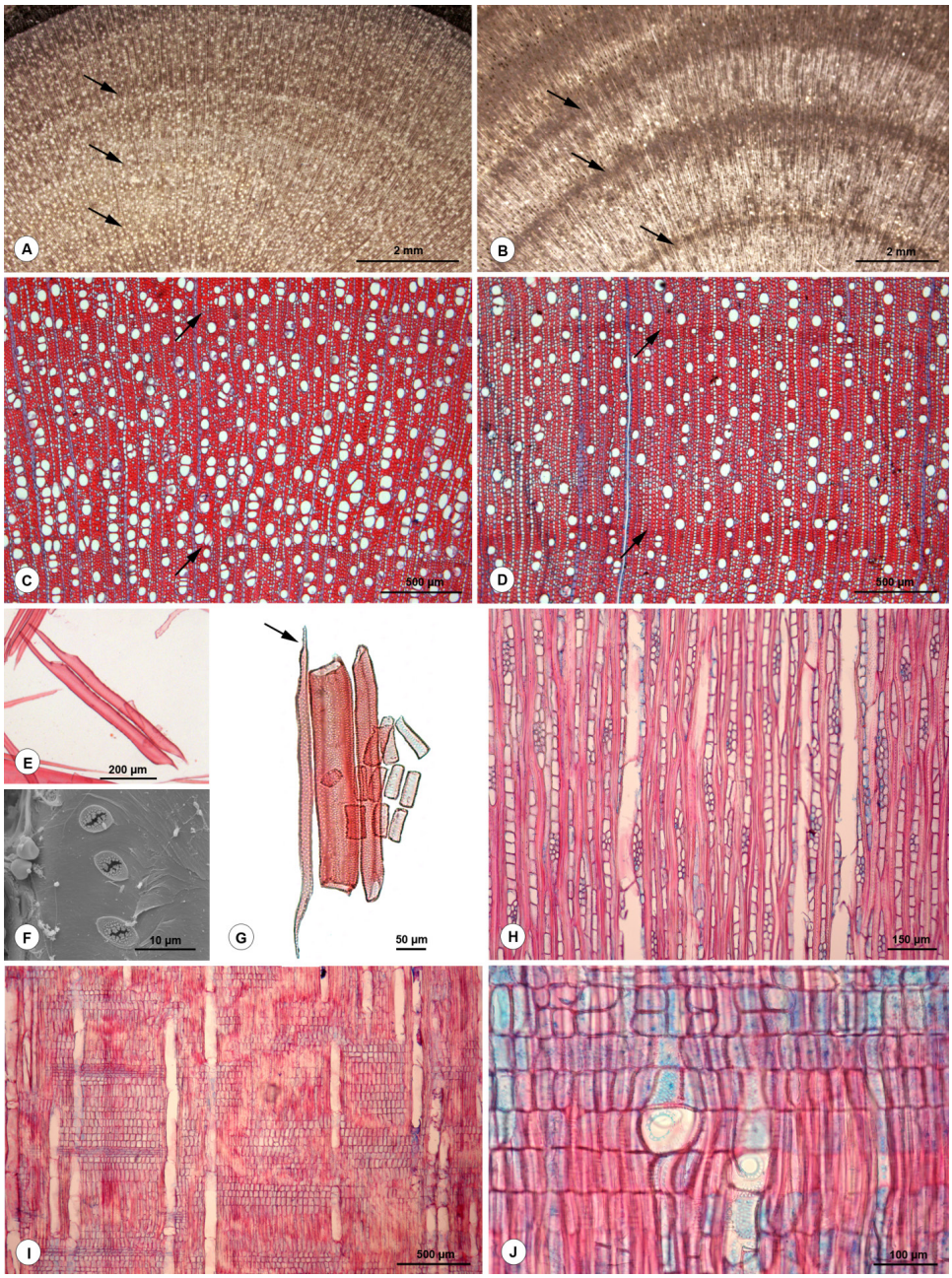


**Figure S2** • Macroscopic and microscopic images of *Tocoyena formosa* secondary xylem. A–D. Cross sections. Growth rings delimited by thick-walled and radially flattened latewood fibers, wood diffuse-porous, and diffuse to diffuse-in-aggregates in individuals from the cerrado (A,C) and from the caatinga (B, D). Note growth markers more pronounced in individuals from the caatinga (B, D). E. Conspicuous tails of vessel elements in macerate. F. Intervessel vestured pits in scanning electron microscopic. G. Vascular tracheid (arrow) and simple perforation plate in macerate. H. Rays 1–3 cells wide with multiseriate portion as wide as uniseriate portion, fused rays in tangencial longitudinal section. I–J. Radial longitudinal sections. I. Heterogeneous rays. J. Perforated ray cells.

*Chapter 3*

# Axial sampling height outperforms site as predictor of wood trait variation

*Larissa C. Dória[1*], Diego S. Podadera[2], Rivete S. Lima[3], Frederic Lens[1] and Carmen R. Marcati[4]*

*Adapted from*
**IAWA Journal** 40 (2019): 191 – 214. DOI: *10.1163/22941932-40190245*

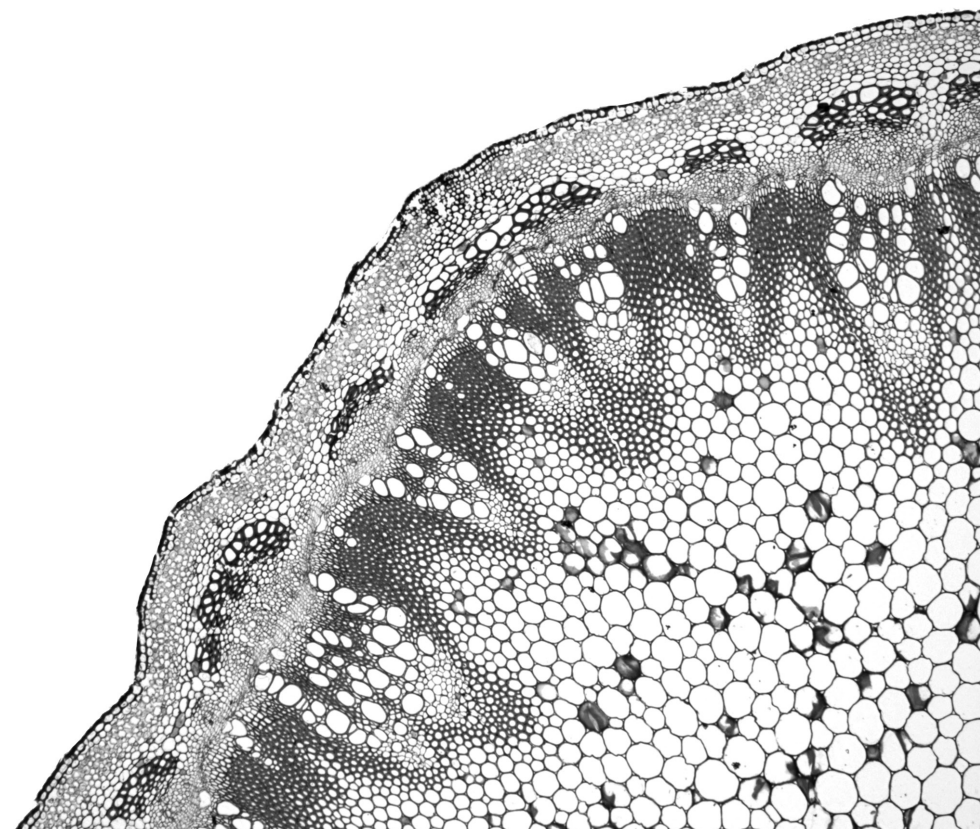

[1] Naturalis Biodiversity Center, Leiden University, P.O. Box 9517, 2300 RA Leiden, The Netherlands.

[2] Programa de Pós-Graduação em Ecologia, UNICAMP, Campinas, São Paulo, Brazil.

[3] Universidade Federal da Paraíba, Centro de Ciências Exatas e da Natureza, Departamento de Sistemática e Ecologia, 58059-900, João Pessoa, Paraíba, Brazil.

[4] Universidade Estadual Paulista, UNESP, Faculdade de Ciências Agronômicas, Departamento de Ciência Florestal, Avenida Universitária, N 3780, 18.610-034, Botucatu, SP, Brazil.

*Corresponding author: larissa.chacondoria@naturalis.nl

# Abstract

Covariation amongst wood traits along the stem axis is important to maintain hydraulic integrity ensuring sufficient sap flow to the canopy. Here, we test how wood traits (co)vary along the trunk and whether two seasonally dry Brazilian habitats (cerrado and caatinga) influence this variation in two co-occurring species *Tocoyena formosa* (Rubiaceae) and *Tabebuia aurea* (Bignoniaceae). The samples were collected at five heights along the main trunk of three individuals per species in both sites. We used light, scanning and transmission electron microscopy to observe the wood traits. Out of 13 wood traits, nine show relationships with sampling height: eight traits predict height in *T. formosa* and five in *T. aurea*. Contrastingly, only three traits show differences between sites and only for *T. formosa*. The intratrunk wood variation is reflected by the hydraulically weighted vessel diameter showing a curvilinear relationship, disagreeing with the prediction of a continuous vessel widening from tip to base. In both species, the largest vessels are linked to the thinnest intervessel pit membranes. Wood density increases basipetally for both species, being site-dependent and correlated with vessel traits in *T. formosa*, and site-independent and determined by fiber wall thickness in *T. aurea*. Furthermore, the functional role of rays was found to be different for each species, and may be related to the marked difference in ray composition. In conclusion, both species shows a unique adaptation to deal with height-related constraints using species-specific co-variation amongst wood traits, while site does not contribute much to the wood variation.


Keywords: caatinga, cerrado, intraspecific variation, *Tabebuia aurea*, thickness of intervessel pit membrane, *Tocoyena formosa*, vessel widening.

# Introduction

There is a vast wood anatomical literature describing an endless variation in anatomical characters between co-occurring species as well as species growing in contrasting environments, emphasizing the ability of plants to develop anatomical strategies to cope with similar or different environmental constraints (Carlquist 1975; Baas & Schweingruber 1987; Hacke & Sperry 2001; Lens *et al.* 2004; Pratt *et al.* 2007; Poorter *et al.* 2010; O'Brien *et al.* 2017). However, studies investigating functional covariation amongst xylem anatomical traits at the individual level remain scarce (Petit *et al.* 2010; Andofillo *et al.* 2013; Olson *et al.* 2018; Pfautsch *et al.* 2018). According to the cohesion-tension theory, maintaining hydraulic integrity becomes more challenging for plants with increasing height due to the more negative pressure inside the water conducting cells of the upper parts of trees, which is required to draw water upwards against gravity in order to reach the leaves (McCulloh & Sperry 2005; Pfautsch *et al.* 2011; Olson *et al.* 2018). Likewise, the increase in hydraulic resistance with stem length predicted by the Hagen-Poiseuille's law states that maximum tree height is limited by the conflicting requirements for water transport efficiency and water column safety (McDowell *et al.* 2002; Koch *et al.* 2004; Domec *et al.* 2008).

There are several xylem anatomical characters that are known to change with tree height. The best studied character is conduit widening from top to bottom, as stated by the West, Brown and Enquist model (WBE model, West *et al.* 1999), implying that the total resistance of water transport will not increase with longer vessel networks (Fan *et al.* 2009; Petit *et al.* 2010; Olson & Rosell 2013; Rosell *et al.* 2017; Olson *et al.* 2018; Pfautsch *et al.* 2018). Also, vessel density will decrease from top to bottom as shown by anatomical studies and predicted by hydraulic models (Höltta *et al.* 2011). The intervessel pits constitute a major proportion, roughly half, of the hydraulic resistance of the xylem (Sperry *et al.* 2006) and are a key feature explaining the variation in embolism resistance amongst tree species (Lens *et al.* 2011; Li *et al.* 2016; Dória *et al.* 2018). The few studies dealing with intraspecific variation at the pit level showed that pit aperture diameter decreased and torus-margo overlap increased significantly with increasing height in the conifers Sequoia sempervirens, Sequoiadendron giganteum, and Pseudotsuga menziesii (Burgess *et al.* 2006; Domec *et al.* 2008; Lazzarin *et al.* 2016), but variation in the ultrastructure of pits in the angiosperm Eucalyptus grandis was found to be more variable across vertical gradients (Pfautsch *et al.* 2018).

In addition to conduits that impact hydraulic conductance, also stem mechanical characters - probably indirectly - impact the long distance water transport in plants, suggesting the presence of a mechanical–functional trade-off. This relation-

ship is often explained by the need to resist vessel collapse under drought-induced tension, either by vessel wall reinforcement (Hacke *et al.* 2001a; Fichot *et al.* 2010) or by thick-walled fibres surrounding the vessels (Jacobsen *et al.* 2005, 2007; Chave *et al.* 2009; Pratt & Jacobsen 2017) that theoretically lead to higher wood densities (Poorter *et al.* 2010; Zanne *et al.* 2010). Likewise, also in herbaceous species, more lignified stems are linked with hydraulic safety in angiosperms (Lens *et al.* 2013a, 2016; Dória *et al.* 2018; Dória *et al.* 2019).

Here, we investigate samples along the vertical axis of the trunk in two woody species (*Tabebuia aurea*, Bignoniaceae; *Tocoyena formosa*, Rubiaceae) that occur both in the distinctive cerrado and caatinga vegetation types experiencing seasonal drought. The cerrado is a savanna-like ecosystem located in the Brazilian Central Plateau, characterized by a strong seasonal climate with distinctive and regular wet and dry periods (Oliveira & Marquis 2002), experiencing a mean annual precipitation of 1500 mm and a mean annual temperature of 22°C (Silva *et al.* 2008). A remarkable characteristic of the cerrado is the deep and nutrient-poor soils with high aluminium content, which is toxic to most plants (Coutinho 2002). The caatinga is a tropical dry forest type located in the semiarid region of the northeast of Brazil, surrounded by the atlantic rain forest and the cerrado domains (Nimer 1972). The caatinga has a mean annual temperature of 27°C and a mean annual precipitation of less than 1000 mm (Andrade-Lima 1981; IBGE 2002), and is defined by a longer and more intense dry season compared to the cerrado (often over five months up to 11 months in some areas), and an irregular precipitation distribution over the years (Moro *et al.* 2016).

An earlier study on *Tabebuia aurea* and *Tocoyena formosa* showed specific wood anatomical strategies to cope with environmental differences between cerrado and caatinga (Dória *et al.* 2016). Here, we sampled individuals from the same population and focus on intraspecific wood trait variation along the vertical axis of the trunk of the same two species and environments (sites). Our study has two major objectives: (1) assess how wood traits vary along the vertical axis of the trunk in the two co-occurring species, and investigate to which extent differences between sites influence the variation in wood traits; (2) assess how wood traits covary amongst them and interpret this co-variation in a functional framework.

# Materials and methods

## Sampling, species and field study

We studied two woody deciduous species, *Tabebuia aurea* (Silva Manso) Benth. & Hook. f. ex S. Moore and *Tocoyena formosa* (Cham. & Schltdl.) K. Schum., both of common occurrence in both caatinga (Moro *et al.* 2014, 2016) and cerrado (Ratter *et al.* 2003). The two species have distinctive wood anatomy, showing different anatomical strategies to deal with the environmental constraints of the two sites (Dória *et al.* 2016). We selected three individuals from both species in each vegetation type, and collected wood samples from the outermost sapwood of the trunk at five different heights (I, at the base to V, at the top of the trunk). Before sampling, we measured the total length of the trunk, collected sample V at the highest point of the trunk, which was 30-50 cm below the branch endings, and subdivided the total trunk height by five in order to collect the remaining samples at equal distances along the main stem. In total, we collected 60 samples derived from the 12 individuals of the two species. The total tree height of the three *T. aurea* individuals varied from 6 m to 8 m and 1.5 m to 5 m for *T. formosa*.

The sampling site for both species in cerrado was in Pratânia municipality, São Paulo state, Brazil (22°48’35’’S, 48°39’57’’W). In caatinga, the sampling was performed at two different sites, 20 km away from each other: for *T. aurea* in São João do Cariri municipality (7°23’27’’S, 36°32’2’’W) and for *T. formosa* in Serra Branca municipality (7°29’14’’S, 36°39’51’’W), both in the state of Paraíba, Brazil. In the cerrado sampling area, the mean temperature is below 25 °C, and the rainiest 5-month period is from October to February with maximum monthly precipitation of 350 mm. The 4-month dry season is from June to September when precipitation reaches less than 50 mm (data from Estação Experimental of the Faculdade de Ciências Agronômicas, UNESP, Botucatu Campus, Brazil). In the caatinga sampling areas, the mean annual temperature is higher (above 25 °C) and the dry season is longer (6 months from July to December) and more intense (precipitation reaching zero) compared to the cerrado. Also, during the irregular rainy season, the maximum monthly rainfall does not exceed 100 mm (data from Estação Experimental of São João do Cariri, Paraíba, Brazil).

## Sapwood density and wood anatomical features

The list of the 13 wood traits assessed is in Supp Table S1.

Wood density was determined for each of the 60 sapwood samples equalling about 1 $cm^3$ in volume, as defined by the ratio of oven-dried mass (at 1000 °C until

constant weight of the sample) to fresh volume (by the weight of water displacement method) (Williamson & Wiemann 2010).

Cross sections (15-20 µm thickness) for light microscopy (LM) were made using a sliding microtome in the Laboratório de Anatomia da Madeira, UNESP, Botucatu Campus, São Paulo State, for the total number of 60 samples for the two species. Sections were double stained with aqueous 1% safranin and aqueous 1% astra blue and mounted in synthetic resin (Entellan®).

The wood anatomical measurements were performed for each of the 60 samples. The diameter of vessels ($D_V$) was calculated based on the lumen area that was considered to be a circle according to the equation:

$$D_V = \sqrt{\frac{4A}{\pi}} \qquad \text{Eqn. 1}$$

where $D_V$ is the vessel diameter and A is the vessel lumen area. The hydraulically weighted vessel diameter ($D_H$) was calculated following the equation:

$$D_H = \frac{\sum D_V^5}{\sum D_V^4} \qquad \text{Eqn. 2}$$

where $D_V$ is the vessel diameter as measured in eqn. (1).

For those samples from the top of the trunk (sampling height V) that included pith we also measured the hydraulically weighted vessel diameter of the first formed secondary xylem vessels close to the pith as a proxy for the diameter of secondary xylem vessels closer to the stem apical meristem. This proxy is referred to as "sampling height VI".

In addition, we measured the vessel density ($V_D$; number of vessel/mm²), vessel grouping index ($V_G$) as proposed by Carlquist (2001) (number of vessels/ number of vessel groups including solitary vessels as vessel groups of one) and the thickness of the vessel wall. Finally, theoretical hydraulic conductivity ($K_{TH}$) was estimated for each sample using the following formula (Fichot *et al.* 2010):

$$Kth = \frac{Dh^4 \pi}{128\eta} \times Vd \qquad \text{Eqn. 3}$$

where η represents viscosity of water at 20 °C (1.002 × 10−9, MPa s), $D_H$ represents the hydraulically weighted vessel diameter as calculated in equation 2 and $V_D$ the vessel density.

For measuring the fractions of each of the xylem cell types (vessels, fibers, rays, and axial parenchyma), we used areas of 1 $mm^2$ in cross section images. We manually painted the area of each group of cell types in different colors using Adobe Photoshop CS6, and calculated the area occupied by each of these groups using Color Counter at ImageJ software (Schindelin *et al.* 2012).

For the ultrastructure of intervessel pits, one individual per site and per species (20 samples in total) was used for scanning electron microscopy (SEM) and transmission electron microscopy (TEM). For SEM, we stored the samples in ethanol 70%, following the lab protocol of Dória *et al.* (2018), and observed the intervessel pits with a field emission SEM (Jeol JSM-7600F, Tokyo, Japan) at a voltage of 5 kV. For transmission electron microscopy (TEM) the samples were fixed for 48h in Karnovsky fixative (Karnovsky 1965) and were subsequently treated according to the protocol described in Dória *et al.* (2018). The relaxed (non-aspirated) intervessel pit membranes were observed using a JEOL JEM 1400-Plus TEM (JEOL, Tokyo, Japan), equipped with a 11 MPixel camera (Quemesa, Olympus); at least 20 intervessel pit membranes per individual were measured.

All the SEM and TEM observations were carried out at Naturalis Biodiversity Center, The Netherlands. For the stem anatomical measurements, we followed the suggestions of the IAWA Committee (1989) and Scholz *et al.* (2013). The measurements were done using ImageJ (National Institutes of Health, Bethesda, USA).

## Statistical analyses

To deal with differences in sampling height amongst individuals, we standardized the sampling height for each individuals to scale in a range between 0 and 1 (min-max scaling).

Generalized mixed-effects models (GLMMs) were used to test the relationship between wood traits, the five sampling heights along the main stem, and the sites (caatinga and cerrado). Individuals were used as the random variable to account for the effect of different samples collected in the same individual. Likewise, GLMMs were used to test for relationships amongst wood traits. We calculated the $R^2$ values based on the method of Nakagawa & Schielzeth (2013), using the function rsquared in the package piecewiseSEM (Lefcheck 2015).

All analyses were performed using R version 3.4.3 (R Core Team 2017) in R Studio version 1.1.414 (R Studio Team 2016) using the package nlme. All the differences were considered significant when $P < 0.05$.

# Results

Regardless of site, the largest fraction of xylem tissues along the trunk in *T. aurea* is represented by fibers (varying from 0.51 to 0.53), followed by rays (varying from 0.19 to 0.24), axial parenchyma (varying from 0.15 to 0.18) and vessels (varying from 0.9 to 0.13) (Fig. 1). For *T. formosa*, the fiber fraction is the largest xylem tissue fraction (varying from 0.37 to 0.40), followed by ray fraction (varying from 0.29 to 0.37), vessel fraction (varying from 0.17 to 0.28) and axial parenchyma fraction (varying from 0.6 to 0.8) (Fig. 2).

There is no difference in pit and aperture size along the different sampling heights (Fig. 1, 2). Likewise, there is no difference in ray morphology from top to bottom in both species, but at the same sampling height there is always a narrow zone of first formed secondary xylem where the rays are composed of more upright ray cells.



### *Relationships between wood traits, sampling height and sites*

Out of 13 wood traits assessed, nine show relationships with the vertical axis and only three show differences between sites (Fig. 3).

The hydraulically weighted vessel diameter shows a similar curvilinear pattern with sampling height for *Tabebuia aurea* and *Tocoyena formosa*. For the former species, there is no significant relationship, but the latter species does show a significant curvilinear relationship with respect to hydraulically weighted vessel diameter (Fig. 3 A; Supp. Table S1) and theoretical hydraulic conductivity (Fig. 3 B; Supp. Table S1). Adding the measurements of secondary xylem vessels closer to the pith in sample height V as a proxy for vessels closer to the stem apical meristem ("sampling height VI"), we do find significant relationship for the two species (Supp. Fig. S1; Supp. Table S2). Vessel fraction is positively correlated with sampling height for both species (Fig. 3 C; Supp. Table S1; see also Fig. 1, 2). Increasing vessel density with increasing sampling height is observed for *T. formosa* (Fig. 3 D; Supp. Table S1; see also Fig. 2), while, increasing vessel grouping with increasing height is observed for *T. aurea* (Fig. 3 E; Supp. Table S1; see also Fig. 1).

The thickness of intervessel pit membranes varies considerably along the vertical trunk axis in both species, but independently from sampling height (Fig. 3 F; Supp. Table S1). For both species, the largest vessels have the thinnest pit membranes (Fig. 3 F).

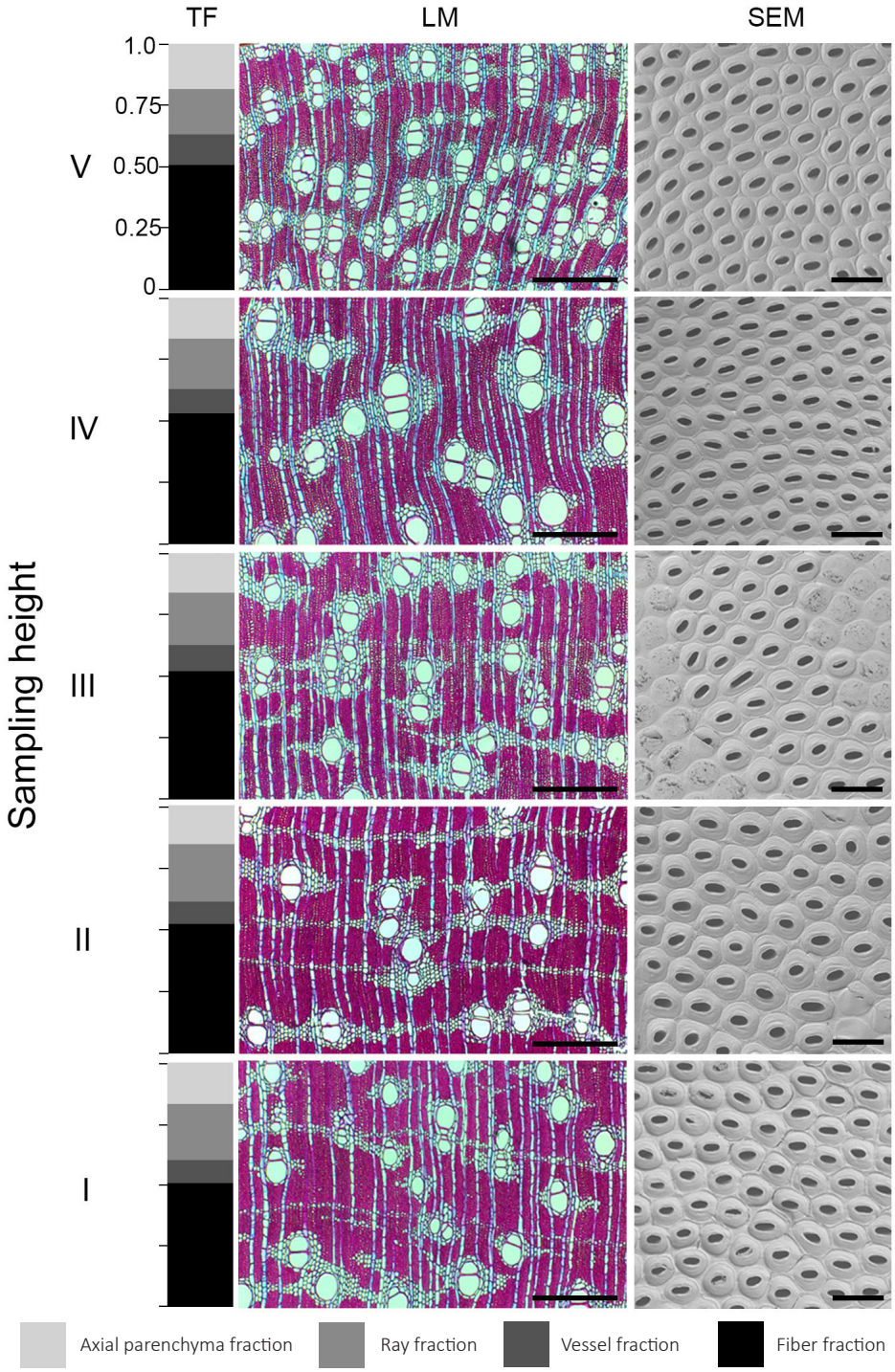


**Figure 1** • Tissue fractions (TF), light microscope cross sections (LM) and scanning electron microscope (SEM) surfaces of *Tabebuia aurea* along the five sampling heights (I: at the basis of trunk, V: at the top of trunk). -- Scale bars = 200 µm (LM), 2 µm (SEM).

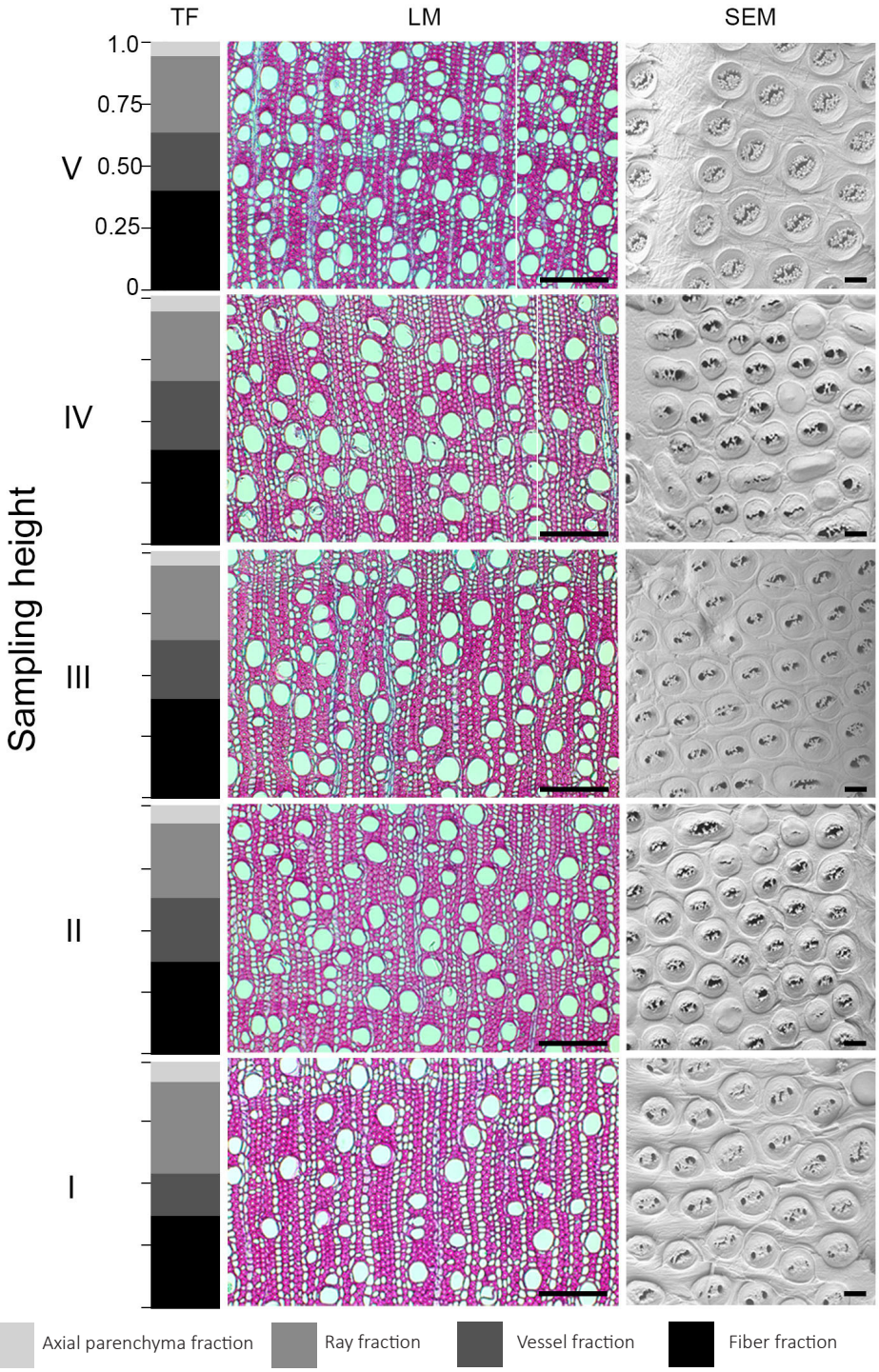


**Figure 2** • Tissue fractions (TF), light microscope cross sections (LM) and scanning electron microscope (SEM) surfaces of *Tocoyena formosa* along the five sampling heights (I: at the basis of trunk, V: at the top of trunk). -- Scale bars = 200 µm (LM), 2 µm (SEM).

Ray fraction shows negative relationship for both species (Fig. 3 G; Supp. Table S1; see also Fig. 1, 2), and it is higher in individuals of *T. formosa* from the caatinga than those of the cerrado (P = 0.012; Fig. 3 G). Likewise, axial parenchyma fraction also shows negative relationship with sampling height, but only for *T. formosa* (Fig. 3 H; Supp. Table S1; see also Fig. 2). Sampling height trends for both species are also observed for wood density (Fig. 3 I; Supp. Table S1) which declines with increasing sampling height. Furthermore, higher wood density is shown by individuals of *T. formosa* from the caatinga (P = 0.008; Fig. 3 I).

For the proportion of fiber wall per fiber, opposite linear trends are observed for each species (Fig. 3 J; Suppl. Table S1): negative for *T. aurea* and positive for *T. formosa*. Fiber fraction and thickness of the intervessel wall are not predicted by sampling height for both species (Fig. 3 K, L), though the latter shows difference between sites for *T. formosa*, with thicker intervessel walls in the individuals from caatinga (P = 0.043, Fig. 3 L).

*Relationships amongst wood traits*

Wood density varies less than 1.5 fold for *T. aurea* (from 0.50 g $cm^{-3}$ to 0.67 g $cm^{-3}$) and two fold for *T. formosa* (from 0.40 g $cm^{-3}$ to 0.77 g $cm^{-3}$) for the 30 samples per species (Fig. 3 I). The variation of wood density in *T. aurea* is positively correlated with the variation of the proportion of fiber wall per fiber (Fig. 4 A; $P < 0.01$, $R^2 = 0.43$). On the other hand, in *T. formosa* it is negatively correlated with vessel fraction (Fig. 4 B; $P = 0.03$, $R^2 = 0.60$), and positively with thickness of the intervessel wall (Fig. 4 C; $P = 0.03$, $R^2 = 0.46$) and ray fraction (Fig. 4 D; $P = 0.04$, $R^2 = 0.54$).

As expected, theoretical hydraulic conductivity ($K_{TH}$) is positively correlated with vessel fraction for both species (Fig. 4 E; $P = 0.03$, $R^2 = 0.51$ for *T. aurea*, and $P < 0.001$, $R^2 = 0.74$ for *T. formosa*). $K_{TH}$ is also correlated with ray fraction (Fig. 4 F), but shows opposite trends for each species: slightly positive for *T. aurea* ($P = 0.05$, $R^2 = 0.42$) and negative for *T. formosa* ($P < 0.001$, $R^2 = 0.74$). Additionally, $K_{TH}$ is negatively correlated with fiber fraction for *T. aurea* (Fig. 4 G; $P < 0.013$, $R^2 = 0.51$). There is no relationship between $K_{TH}$ and wood density for either *T. aurea* or *T. formosa* ($P = 0.57$; $P = 0.24$, respectively, Fig. 4 H).

Thickness of intervessel pit membrane ($T_{PM}$) shows relationships with a different lignification character in the two species: a slightly positive relationship with the thickness of the vessel wall for *T. aurea* (Fig. 5 A - E; $P = 0.05$, $R^2 = 0.38$), and a negative relationship with the proportion of fiber wall per fiber for *T. formosa* (Fig. 6 A - E; $P = 0.01$, $R^2 = 0.57$).

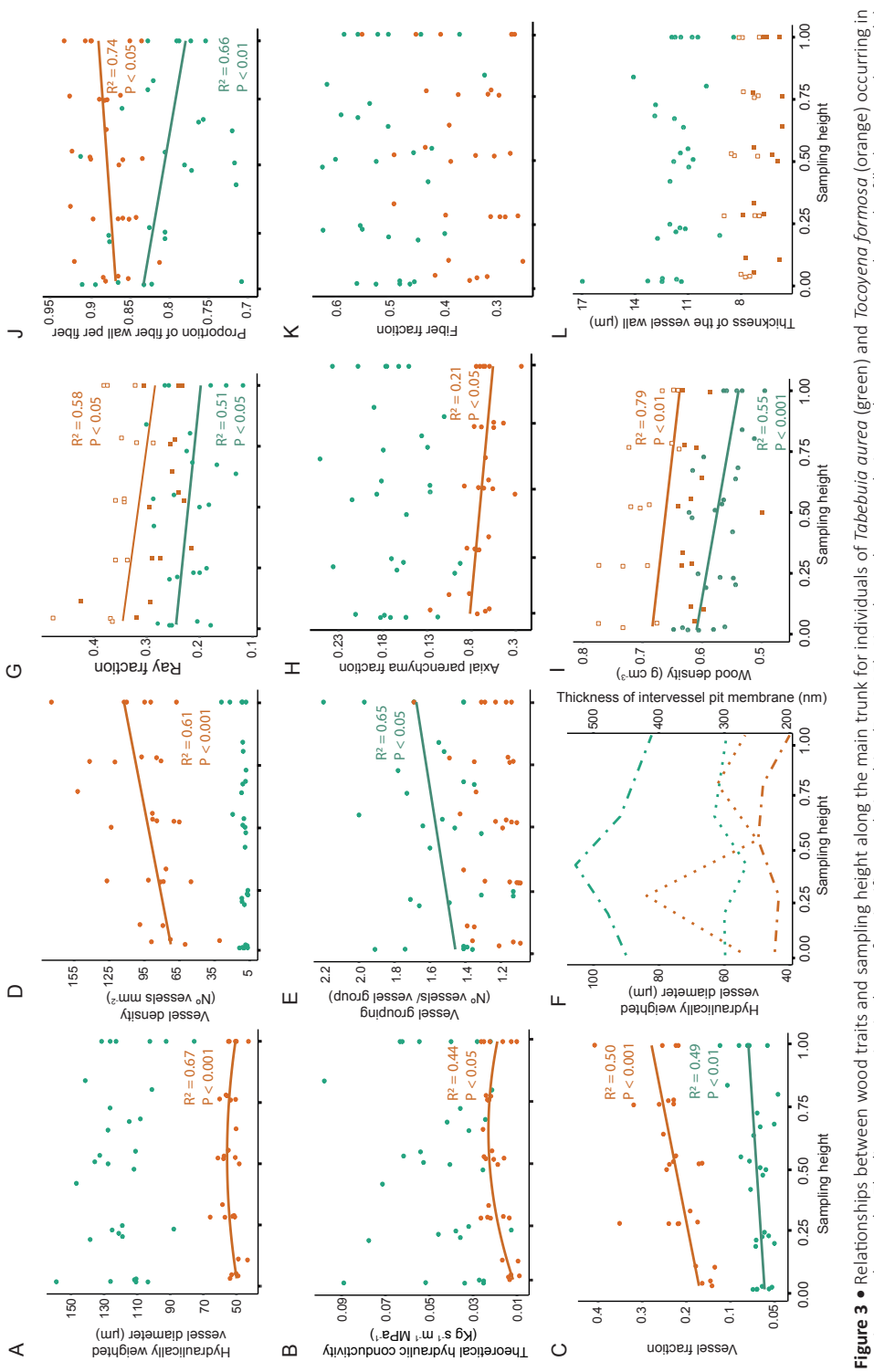


**Figure 3** • Relationships between wood traits and sampling height along the main trunk for individuals of *Tabebuia aurea* (green) and *Tocoyena formosa* (orange) occurring in caatinga and cerrado. The linear regression is shown for significant relationships ($P < 0.05$). Site-dependent correlations, when present, are shown by filled squares (cerrado) and empty squares (caatinga). -- Sampling height 0.00 - 1.00 refers to sampling height I - V. 2F: ·-·-·-· Hydraulically weighted vessel diameter; ····· Thickness of intervessel pit membrane.

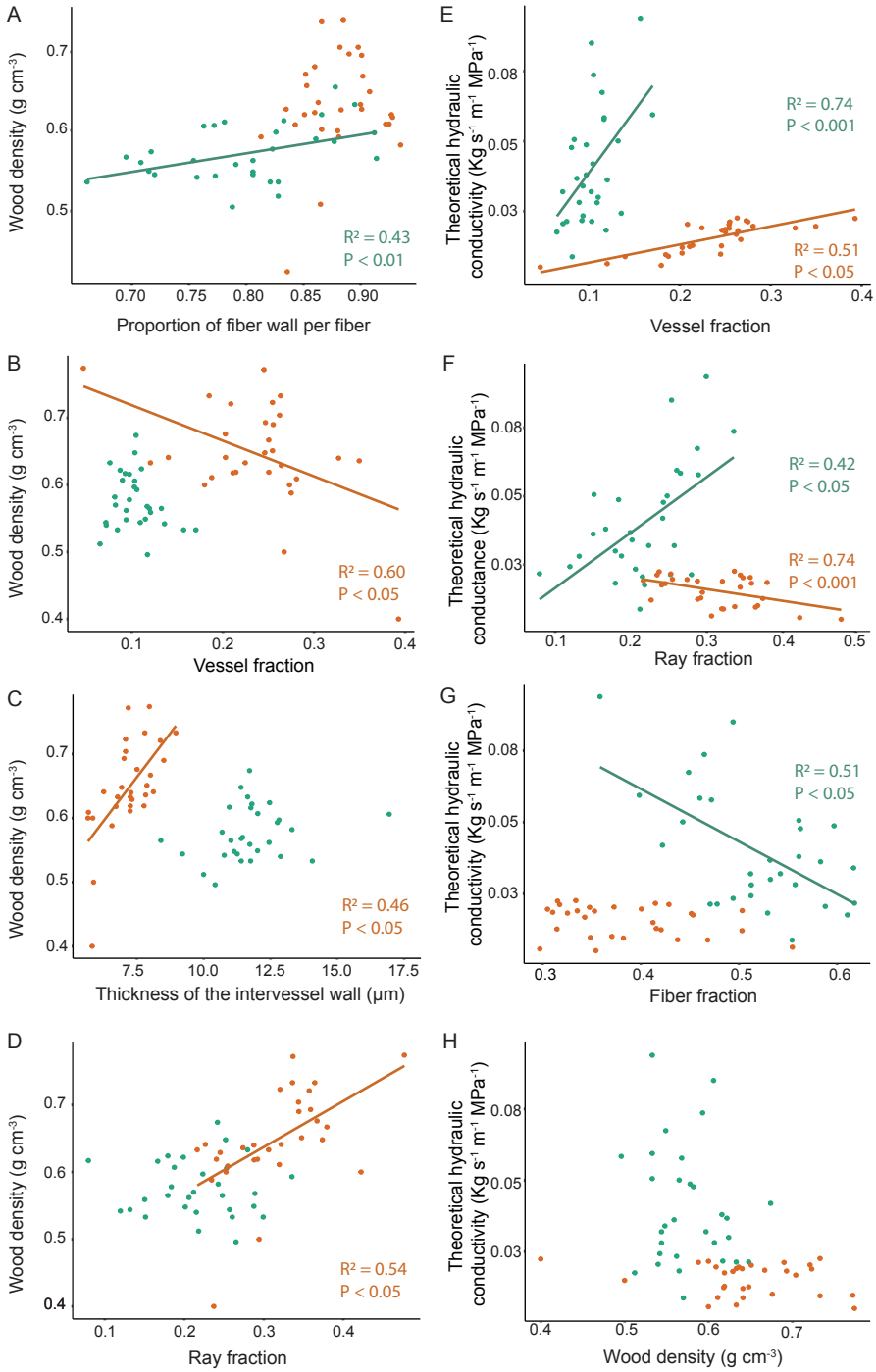


**Figure 4** • Relationships amongst wood density, theoretical hydraulic conductivity and wood anatomical traits for individuals of *Tabebuia aurea* (green) and *Tocoyena formosa* (orange) occurring in caatinga and cerrado. The linear regression is shown for significant relationships (P < 0.05). No site correlations are detected.

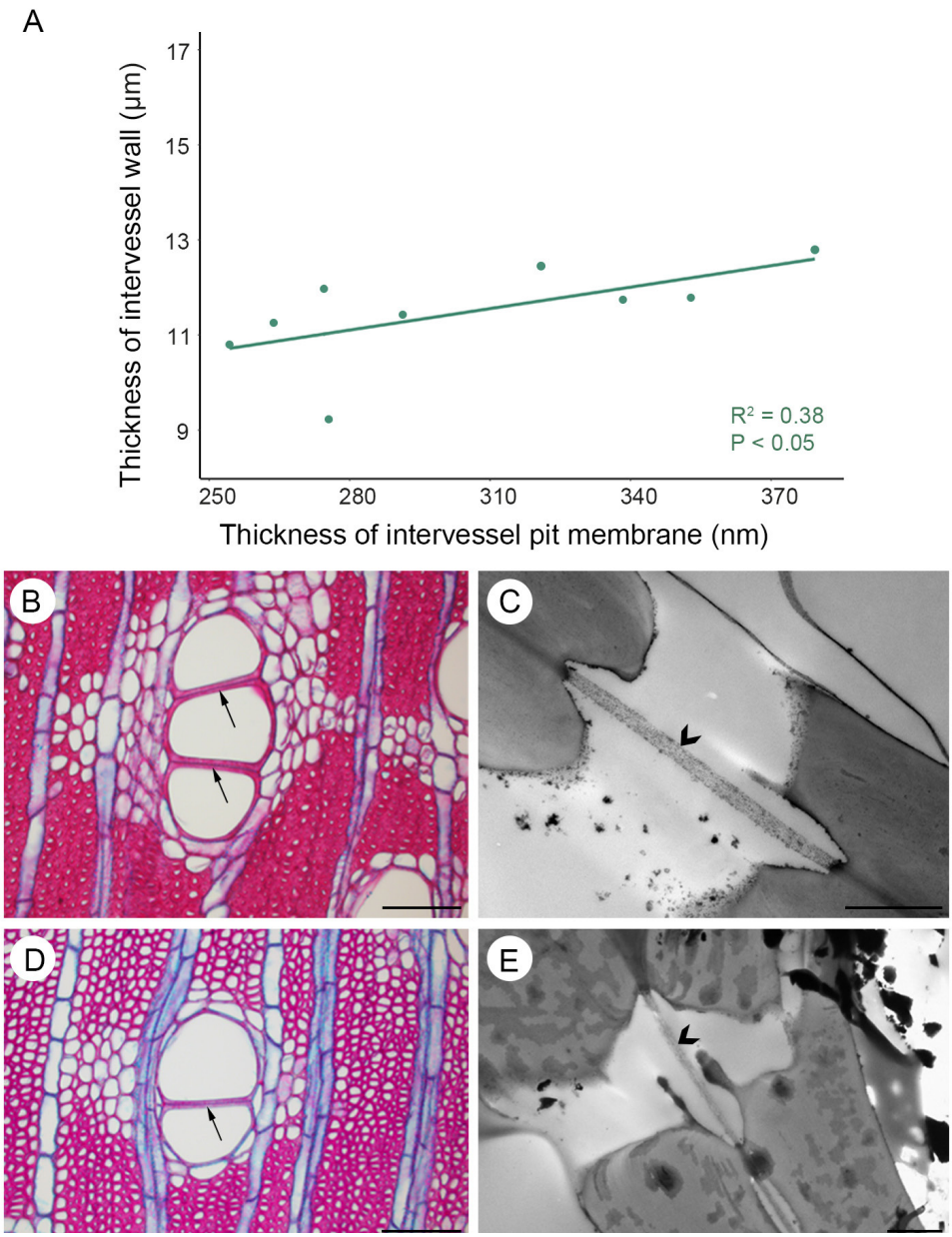


**Figure 5** • Relationships between the thickness of intervessel pit membrane ($T_{PM}$) and vessel wall thickness in *Tabebuia aurea*. (A) Slightly positive relationship between $T_{PM}$ and the thickness of intervessel wall. (B, D) Light microscopy cross sections showing vessel walls. (C,E) Transmission electron microscopy illustrating intervessel pit membranes. The thickness of intervessel walls (arrows) matching with the thickness of pit membrane (arrowheads). Scale bars = 100 µm (B, D); 2 µm (C, E).

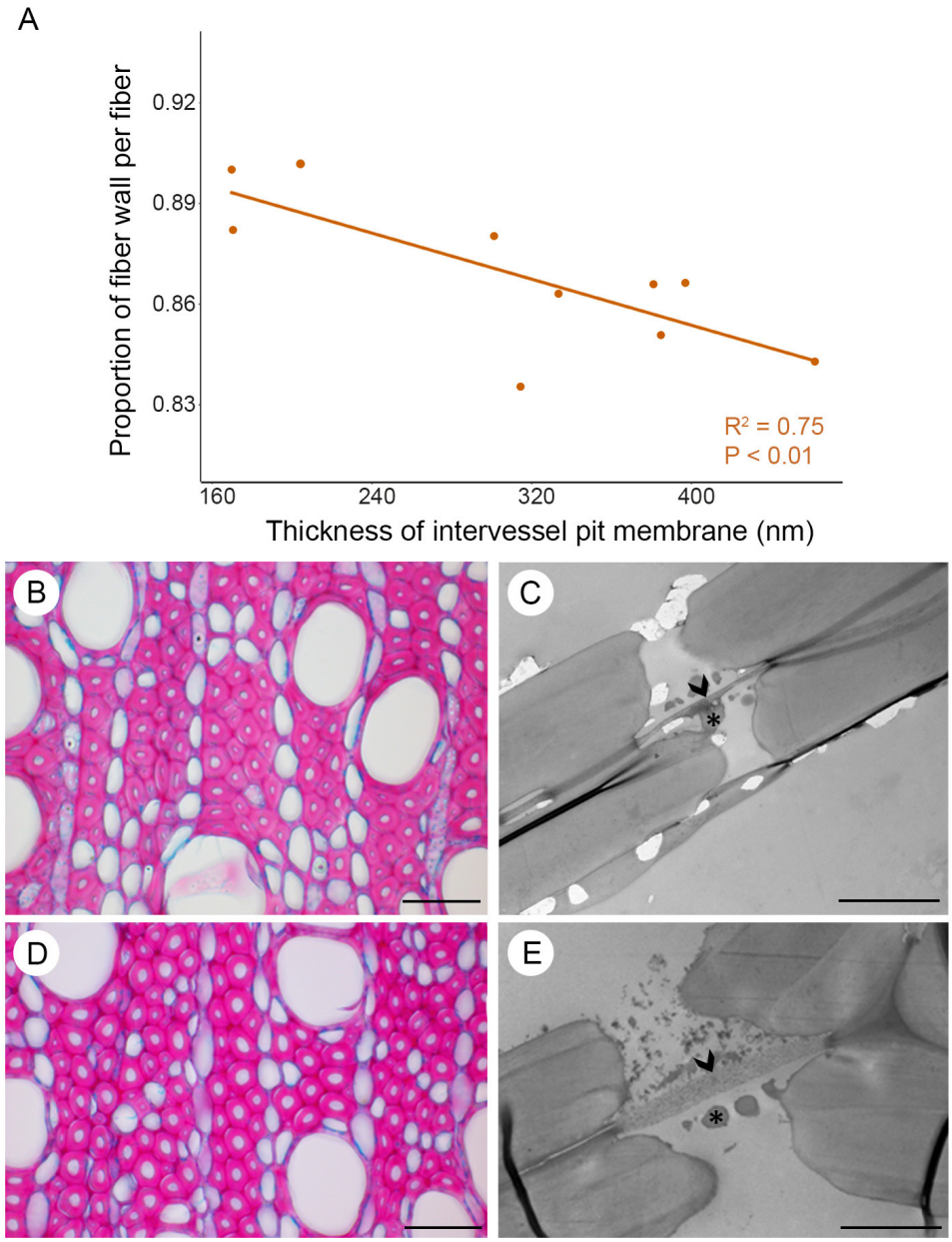


**Figure 6** • Relationships between the thickness of intervessel pit membrane ($T_{PM}$) and fiber wall thickness in *Tocoyena formosa*. (A) Negative relationship between $T_{PM}$ and the proportion of fiber wall per fiber. (B, D) Light microscopy cross sections showing xylem fiber walls. (C,E) Transmission electron microscopy illustrating intervessel pit membranes. The thickness of xylem fiber walls matching with the thickness of pit membrane (arrowheads). -- asterisks (*) represents vestures. Scale bars = 50 µm (B, D); 2 µm (C, E)

# Discussion

Our results show that there is considerable anatomical variation along the vertical gradient of individual trunks, which is functionally adapted to meet mechanical and hydraulic height-related constraints, but intraspecific variation between individuals inhabiting the different sites is negligible. This may seem surprising given the clear difference in rain seasonality (less and irregular distribution of rain throughout the years in caatinga vs. more and well-defined periods of rain in cerrado) and especially the marked difference in soil characteristics (deep and nutrient-poor soils with high aluminium content in cerrado). Furthermore, we have demonstrated that the two species occurring in both sites differ markedly in their wood anatomy and show specific adaptations to deal with the specific abiotic variables of the two sites (Dória *et al.* 2016).



### *Relationships between wood traits and sampling height*

Although a continuous widening of vessel diameter from top to bottom is widely accepted as predicted by the WBE model (West *et al.* 1999; Rosell *et al.* 2017), our data show a narrowing of vessels at the base of the trunk for both species (Fig. 3 A). Similar hump-shaped trend has also been reported in other trees such as Cordia alliodora and Anacardium excelsum (James *et al.* 2003) and in Eucalyptus grandis (Petit *et al.* 2010; Pfautsch *et al.* 2018), and thereby disagreeing with the continuous vessel widening pattern from tip to base. The functional significance of vessel narrowing at the lowest portion of the stem remains debatable, however (Pfautsch *et al.* 2018). In our study, sampling height predicts hydraulically weighted vessel diameter in *T. formosa* (Fig. 3 A). However, this relationship becomes significant for both species when including the measurements of vessels closer to pith region in sampling height V as a proxy for the vessel diameter closer to the stem apical meristem (referring to "sampling height VI"; Supp Fig. S1). Additionally, our results corroborate the prediction of a large dataset testing the relationship between basal and tip vessel diameters and stem length, showing that taller plants (*T. aurea* in our study) have wider conduits at both the base and the tip (Fig. 3 A; Supp Fig S1) (Olson *et al.* 2018). Since theoretical hydraulic conductivity ($K_{TH}$) is estimated from the vessel diameter, the relationship between $K_{TH}$ and sampling height shows the same non-curvilinear pattern.

Vessel fraction shows the same vertical pattern in both species with increasing plant height (Fig. 3 C). For the two species, the increase in vessel fraction towards the tip of the trunk is due to the effect of vessel density which also increases with plant height, though only slightly for *T. aurea* (Fig. 3 D). This increase in number of vessels with height is a pattern supported by hydraulic optimal models along with vessel narrowing towards the apex (Höltta *et al.* 2011). In addition, the axi-

al increase in vessel density and fraction compensates for the potential decrease in conductance due to the reduced vessel diameter (Carlquist 2001; Sperry *et al.* 2008). According to Aloni and Zimmermann (1983) and Aloni (2015), the increasing auxin concentration along the vertical axis of plants regulate cell differentiation and cell expansion rates, leading to more and narrower vessels closer to the stem apex.

While there is an increase of vessel grouping towards the upper parts of the trees in *T. aurea*, the same trend does not occur for *T. formosa* (Fig. 3 E). Grouping of vessels can be functionally explained as a way of providing an alternate pathway for water transport within the same vessel multiple when water transport in some of the vessels is disabled by air embolism (Carlquist 1984). This strategy should minimize the number of water filled vessels that are disconnected from the bulk sap stream, leading to a more efficient water transport mechanism in *T. aurea* (Mrad *et al.* 2018; Jacobsen & Pratt 2018). The wood of *T. formosa*, on the other hand, has vascular tracheids at the end of growth rings (Dória *et al.* 2016), which can form a subsidiary conductive system in case too many of the mainly solitary vessels are embolized due to drought (Carlquist 1984, 2001; Spicer 2016).

For both species, the largest vessels are linked to the thinnest intervessel pit membranes (Fig. 3 F). In terms of vessel development, it is expected that larger vessels would have thinner pit membranes than narrower vessels due to the stretching of the cell wall expansion during the vessel maturation stage (Hacke *et al.* 2017). Also from a hydraulic point of view, it makes sense that more efficient, wider (and presumably also longer) vessels towards the trunk base of taller trees have thinner intervessel pit membranes in order to synergistically reduce the resistance to long distance water transport (Hacke *et al.* 2006; Rosell *et al.* 2017; Choat *et al.* 2008). However, in a 20 m tall Eucalyptus grandis tree, Pfautsch *et al.* (2018) has provided clear evidence that wider vessels have the thickest intervessel pit membranes, which may act as protection from drought-induced air bubble spread in the wider and presumably more vulnerable vessels.

Ray fraction decreases with increasing sampling height for the two species (Fig. 3 G), and the same pattern is observed for the fraction of axial parenchyma in *T. formosa* (Fig. 3 H). This reduction of wood parenchyma in smaller sized stems may be a result of a lesser need of both sugar/water storage and radial transport. In addition, the diffuse-in-aggregates parenchyma pattern in *T. formosa* and the confluent parenchyma pattern in *T. aurea* are interconnected with rays and form an effective 3D parenchyma network (Carlquist 2001) that is more pronounced at the base of the trunk, which increases hydraulic capacitance via symplastic transport (van Bell 1990; Holbrook 1995; Borchert & Pockman 2005; Pfautsch *et al.* 2015a).

Our results also show an increase in wood density with decreasing height for both species (Fig. 3 I), a pattern already shown in other studies (Kord *et al.* 2010, Mattos *et al.* 2011). The main explanation for higher wood density in the lower

part of the trunk is related to mechanics: for instance in *T. aurea* the proportion of fiber wall per fiber explains the higher wood density at the base of the trunk, which serves as mechanical reinforcement as a result of the increased weight that impacts this part of the plant. This phenomenon is probably also related to the observation that wood density tends to increase with cambium age (Zobel & Sprague 1998), leading to denser wood at the lower parts of the trunk and lighter wood in the upper stem portions (Iqbal 1995; Zobel & Sprague 1998; Moya *et al.* 2003).

### *Variation in wood density is linked with the proportion of fiber wall per fiber in T. aurea, but with vessel traits and ray fraction in T. formosa*

Surprisingly, the variation in wood density for the two species studied is correlated with different characters. In *T. aurea*, the axial variation in wood density is positively linked with the proportion of fiber wall per fiber ($P_{FW}F$) (Fig. 4 A), which is considered the most important wood anatomical trait influencing wood density across species (Kollmann & Cote 1968; Zieminska *et al.* 2013). However, for *T. formosa*, the variation in wood density is not significantly related to fibers, but instead is linked to decreased vessel fraction (Fig. 4 B) and increased intervessel wall thickness (Fig. 4 C).

The stronger negative relationship between $P_{FW}F$ and sampling height in *T. aurea* compared to the weakly positive relationship in *T. formosa* (Fig. 3 J; Estimate = -0.07; 0.02, respectively) explains why the proportion of fiber wall per fiber does not impact wood density similarly in both species (Fig. 4 A). By the same token, the explanation of vessel fraction in the variation of wood density of *T. formosa* (Fig. 4 B) might be influenced by the relationship between vessel density versus sampling height (Estimate = 42.20; Fig. 3 D) which is absent in *T. aurea* (Fig. 3 D). The considerable increase in vessel density (linked to more vessel fraction and higher vessel lumen area) with sampling height is probably the driver for decreased wood density in the upper parts of the trunk of *T. formosa* (Fig. 3 I), since wood density is negatively related to vessel lumen area and positively related to the allocation of carbon (Poorter *et al.* 2006; Chave *et al.* 2009; Höltta *et al.* 2011).

Wood density is expected to negatively relate to water transport efficiency, since it is negatively linked to vessel lumen area (in this study for *T. formosa* only, Fig. 4 B) and capacitance (Pratt *et al.* 2007; Sperry *et al.* 2008). In addition, wood density is defined by the presence of a stronger fiber matrix support (Jacobsen *et al.* 2005, 2007), as shown by *T. aurea* (Fig. 4 A) or by the presence of vessels with thicker walls (Hacke *et al.* 2001a; Brodribb & Holbrook 2005) as we observe in *T. formosa* (Fig. 4 C). These latter two mechanical characteristics are frequently cited with regards to vessel collapse prevention under increasing drought-induced negative pressures, although vessels never collapse in mature wood because embolism events always occur before the critical point of vessel collapse is reached (Hacke *et*

*al.* 2001a; Sperry *et al.* 2006, Chave *et al.* 2009, Poorter *et al.* 2010). Based on this information, wood density seems to be more related to mechanical properties in *T. aurea*, while the link between wood density and hydraulics appears to be more obvious in *T. formosa*.

Along the main stem axis, higher ray fraction at the base of the trunk coincides with denser wood for both species (Fig. 3 G, I). Additionally, higher ray fraction in *T. formosa* is correlated to higher wood density (Fig. 4 D). This positive relationship between ray fraction and wood density may be surprising at first as rays consist of parenchyma cells enabling radial transport exchange between phloem and xylem (van Bel 1990; Salleo *et al.* 2004; Höltta *et al.* 2006), as well as storage of water and minerals (Morris *et al.* 2018). A first cause for this correlation may be related to the increased size of the lower trunks that require mechanical reinforcement (higher wood densities), but also more developed rays to transport sugars over longer radial distances. Secondly, the mechanical function of rays should not be ignored: ray fraction is found to be positively correlated to modulus of elasticity (stiffness) and radial tensile strength, both mechanical parameters that are positively linked with wood density (Mattheck & Kubler 1995; Burgert *et al.* 1999; Reiterer *et al.* 2002; Woodrum *et al.* 2003; Zheng & Martinez-Cabrera 2013; see next section).

*Rays may serve different functions in both species*

The opposite trends shown by each species regarding to the relationship between ray fraction and $K_{TH}$ (Fig. 4 F), indicate that rays may have different functional roles for each species. It seems to be more related to mechanical reinforcement in *T. formosa* due to the positive relationship with wood density (Fig. 4 D) and the negative correlation with $K_{TH}$ (Fig. 4 F), and more related to hydraulic conductance in *T. aurea* due to the positive $K_{TH}$ link (Fig. 4 F).

The opposite relationships between ray fraction and $K_{TH}$ for the two species is intriguing. Although this difference is difficult to explain from a functional point of view, it may be related to the marked difference in ray composition: *T. aurea* has homocellular rays with only procumbent cells, while *T. formosa* forms heterocellular rays with rows of upright and square cells (Dória *et al.* 2016). It appears that the homocellular rays in *T. aurea* – perhaps in combination with the abundant paratracheal confluent axial parenchyma form a 3D network which positively influence $K_{TH}$ (Fig. 4 F). Contrastingly, the heterocellular rays of *T. formosa* appear to have a role in the mechanical reinforcement as shown by a positive relationship with wood density (Fig. 4 D). A positive link between wood density and rays has been reported in some studies, including one analysing nearly 800 Chinese tree species (Zhang & Martinez-Cabrera 2013). However, the relationship between mechanical strength and ray proportion is speculative, and should involve links with modulus of elasticity and modulus of rupture (Pratt *et al.* 2007) that still remains to be assessed.

### *Thickness of intervessel pit membrane ($T_{PM}$) is linked to lignification, but shows contrasting correlations in the two species*

$T_{PM}$ shows relationships with two different lignification characters: a positive relationship with vessel wall thickness for *T. aurea* (Fig. 5, A - E) and a negative relationship with the proportion of fiber wall per fiber ($P_{FW}F$) for *T. formosa* (Fig. 6 A - E). The positive link between $T_{PM}$ and lignification has already been emphasized via the previously observed $T_{PM}$ - vessel wall and proportion of lignified area in the stem correlations (Jansen *et al.* 2009; Li *et al.* 2016; Dória *et al.* 2018; Dória *et al.* 2019). Moreover, $T_{PM}$ was found to be the functional missing link to explain why the stems of insular woody daisies are more embolism resistant compared to their herbaceous relatives (Dória *et al.* 2018). Although we have not measured embolism resistance in both species, it is possible that *T. formosa* resembles *T. aurea* in their embolism resistance, based on their similar intervessel pit membrane thickness (on average 311.4 nm and 302.5 nm, respectively) that is hypothesised as one of the best characters to explain variation in embolism resistance amongst woody species due to the direct link with air-seeding (Lens *et al.* 2011; Li et al., 2016; Dória *et al.* 2018; Dória *et al.* 2019). The positive link between $T_{PM}$ and vessel wall thickness in *T. aurea* can be interpreted as synergistic co-variation to cope with drought-induced embolism formation. However, the negative relationship between $T_{PM}$ and the proportion of fiber wall per fiber in *T. formosa* seems to contradict each other since a mechanically stronger fiber matrix has been linked to more - not less - embolism resistance (Jacobsen *et al.* 2005, 2007).

### *Site differences only have subtle impact on wood variation in Tocoyena formosa*

The denser wood and higher ray fraction in the individuals of *T. formosa* from caatinga compared to cerrado can be interpreted in different ways. Firstly, there is a difference in the size of individuals: the caatinga trees are taller (3.40 m - 5 m) and have a thicker trunk base (15 cm - 21 cm) compared to the cerrado ones (1.12 m - 2.32 m; 8 cm - 11 cm, respectively), which is probably related to the limited plant growth in the nutrient-poor cerrado soils with high aluminium content. As stated above, taller and wider trunks of the caatinga trees are correlated with denser wood and greater ray fraction. In addition, our results corroborate the general trend that wood density is higher in drier environments (Chave *et al.* 2006; Preston *et al.* 2006; Onoda *et al.* 2010), as evidenced by the mean annual precipitation of caatinga compared to cerrado (up to 800 mm vs 1500 mm, respectively). The *T. formosa* individuals from caatinga also show thicker vessel walls, a character that is linked with wood density in this species, and higher ray fraction. In addition to the arguments given above, increased ray fraction in *T. formosa* trees from the caatinga might be related to increased need of storage, such as starch (Evert 2006) during the harsh dry period (up to nine consecutive months per year).

## Conclusion

In the two species studied, we find that axial sampling height along the trunk - rather than differences between sites - is a better predictor of wood trait variation; site-dependent differences were confined to only three traits (wood density, ray fraction and intervessel wall thickness) in only one species. The pattern of vessel widening does not follow a continuous from tip to base as expected by hydraulic models. In addition, as predicted by hydraulic models, there is an increase in vessel fraction upwards to compensate for the potential decrease in conductance. Interestingly, the largest vessels are associated with the thinnest intervessel pit membranes, which synergistically reduce the hydraulic resistance. In terms of wood density and rays, both characters show interesting co-variation with different characters along the axial trunk in the two species studied. For *T. aurea*, wood density is positively related to the proportion of fiber wall per fiber suggesting a mechanical function, and rays are speculated to interact more with the hydraulic system due to the positive link with theoretical hydraulic conductivity ($K_{TH}$). For *T. formosa*, on the other hand, wood density may counterbalance hydraulics because of its correlation with vessel fraction and intervessel wall thickness, while rays seem to be more related to mechanical reinforcement due to its positive relationship with wood density and negative relationship with $K_{TH}$. This means that - despite the fact that species have developed unique adaptational strategies to deal with environmental constraints (Dória *et al.* 2016) - they also need to deal with species specific height-related constraints in terms of mechanical-hydraulic trade-offs.

## Acknowledgement

We thank CNPq - Conselho Nacional de Desenvolvimento Científico e Tecnológico, Brazil [PROC. N 206433/2014-0)] for granting L. C. Dória, and Fundação de Amparo à Pesquisa do Estado de São Paulo, Brazil (FAPESP, Proc. 2015/14954-1) for the financial support to C. R. Marcati. We also thank Liliane C. Pereira, R. Langelaan, and W. Star for technical assistance in the laboratory. We acknowledge José Roberto Lima, Maria do Ceo Rodrigues Pessoa Barros, and Aparecido Bessa Ramon for the support during the field collection. We also thank Prof. Dr. Pieter Baas for his valuable comments.

# Supplementary information

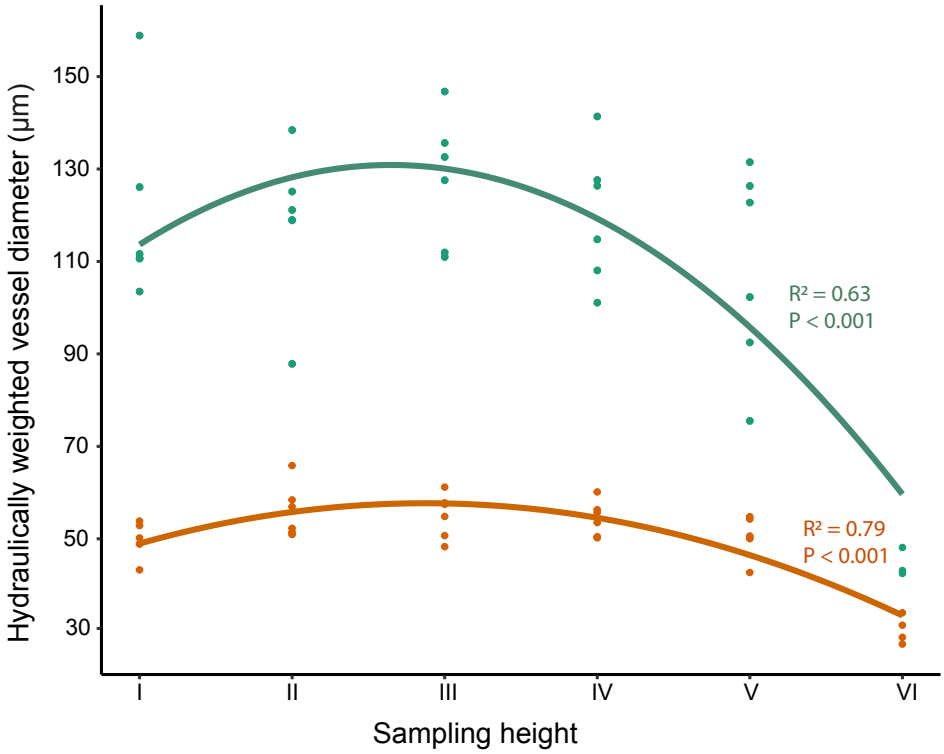


**Figure S1** • Relationship between hydraulically weighted vessel diameter and sampling height along the main trunk for individuals of *Tabebuia aurea* (green) and *Tocoyena formosa* (orange) from caatinga and cerrado. The "sampling height VI" refers to the measurements of the first formed vessels from sampling height V, as a proxy for the vessel diameter closer to the stem apical meristem. The linear regression is shown for significant relationships ($P < 0.05$).

**Table S1** • Relationships between wood anatomical traits, sampling height and site (caatinga and cerrado) for individuals of *Tabebuia aurea* and *Tocoyena formosa*. Regression slopes (β1 = slope for linear models; β2 = slope for quadratic models) and significance levels (*P < 0.05; **P < 0.01; ***P < 0.001) are given. The $R^2$ is the conditional $R^2$ obtained from the function rsquared in the package piecewiseSEM. NS = non-significant relationship; --- = relationship not tested.

| | ***Tabebuia aurea*** | | | | | ***Tocoyena formosa*** | | | | |
|---|---|---|---|---|---|---|---|---|---|---|
| | **Sampling height** | | | **Site** | | **Sampling height** | | | **Site** | |
| **Wood traits** | $R^2$ | $\beta 1$ | $\beta 2$ | $R^2$ | $\beta 1$ | $R^2$ | $\beta 1$ | $\beta 2$ | $R^2$ | $\beta 1$ |
| Hydraulically weighted vessel diameter | NS | NS | NS | NS | NS | *0.67* | 25.93 | *-24.51**** | NS | NS |
| Theoretical hydraulic conductance | NS | NS | NS | NS | NS | 0.44 | 0.040* | -0.031** | NS | NS |
| Vessel fraction | 0.49 | 2.96** | --- | NS | NS | 0.50 | 9.17*** | --- | NS | NS |
| Vessel density | NS | NS | --- | NS | NS | 0.61 | 42.20*** | --- | NS | NS |
| Vessel grouping | 0.65 | 0.22* | --- | NS | NS | NS | NS | --- | NS | NS |
| Thickness of intervessel pit membrane | NS | NS | --- | --- | --- | NS | NS | --- | --- | --- |
| Pit aperture fraction | NS | NS | --- | --- | --- | NS | NS | --- | --- | --- |
| Ray fraction | 0.51 | -5.05* | --- | NS | NS | 0.58 | -6.05* | --- | 0.46 | -8.08 * |
| Axial parenchyma fraction | NS | NS | --- | NS | NS | 0.21 | -2.68* | --- | NS | NS |
| Wood density | 0.55 | -0.072*** | --- | NS | NS | 0.79 | -0.054** | --- | 0.63 | -0.080** |
| Proportion of fiber wall per fiber | 0.66 | -0.067** | --- | NS | NS | 0.74 | 0.020* | --- | NS | NS |
| Fiber fraction | NS | NS | --- | NS | NS | NS | NS | --- | NS | NS |
| Thickness of the intervessel wall | NS | NS | --- | NS | NS | NS | NS | --- | 0.50 | -1.05* |

**Table S2** • Relationships between hydraulically weighted vessel diameter, sampling height and site (caatinga and cerrado) for individuals of *Tabebuia aurea* and *Tocoyena formosa*. The above relationships include the "sampling height VI" vessel diameter measurements. Regression slopes (β1 = slope for linear models; β2 = slope for quadratic models) and significance levels (*P < 0.05; **P < 0.01; ***P < 0.001) are given. The $R^2$ is the conditional $R^2$ obtained from the function rsquared in the package piecewiseSEM. NS = non-significant relationship.

| | ***Tabebuia aurea*** | | | | | ***Tocoyena formosa*** | | | | |
|---|---|---|---|---|---|---|---|---|---|---|
| | **Sampling height** | | | **Site** | | **Sampling height** | | | **Site** | |
| **Wood traits** | $R^2$ | $\beta 1$ | $\beta 2$ | $R^2$ | $\beta 1$ | $R^2$ | $\beta 1$ | $\beta 2$ | $R^2$ | $\beta 1$ |
| Hydraulically weighted vessel diameter | 0.63 | 32.3*** | -6.1*** | NS | NS | *0.79* | 14.49*** | *-2.52**** | NS | NS |

*Chapter 4*

# Insular woody daisies (*Argyranthemum*, Asteraceae) are more resistant to drought-induced hydraulic failure than their herbaceous relatives

*Larissa C. Dória[1], Diego S. Podadera[2], Marcelino del Arco[3], Thibaud Chauvin[4,5], Erik Smets[1], Sylvain Delzon[6] and Frederic Lens[*1]*

*Adapted from*
**Functional Ecology** 32 (2018): 1467 – 1478. DOI: *10.1111/1365-2435.13085*

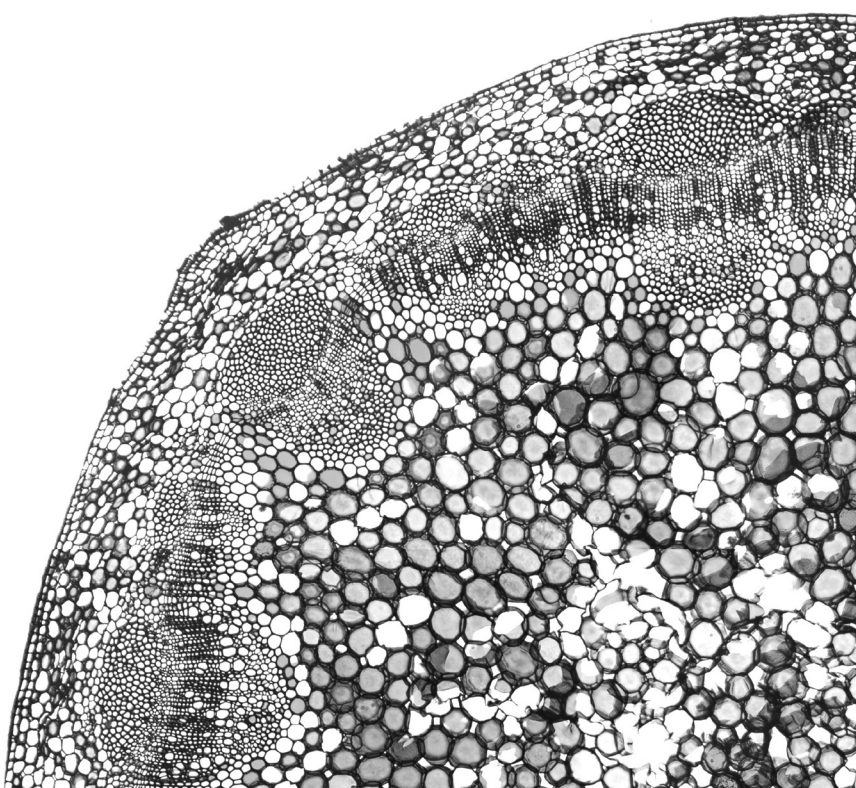

[1] Naturalis Biodiversity Center, Leiden University, P.O. Box 9517, 2300 RA Leiden, The Netherlands.

[2] Programa de Pós-Graduação em Ecologia, UNICAMP, Campinas, São Paulo, Brazil

[3] Department of Plant Biology (Botany), La Laguna University, 38071 La Laguna, Tenerife, Spain.

[4] PIAF, INRA, Univ. Clermont Auvergne, 63100 Clermont-Ferrand, France.

[5] AGPF, INRA Orléans, 45166 Olivet Cedex, France;

[6] BIOGECO INRA, Univ. of Bordeaux, 33610 Cestas, France.

*Corresponding author: frederic.lens@naturalis.nl

# Abstract

Insular woodiness refers to the evolutionary transition from herbaceousness towards derived woodiness on (sub)tropical islands, and leads to island floras that have a higher proportion of woody species compared to floras of nearby continents. Several hypotheses have tried to explain insular woodiness since Darwin's original observations, but experimental evidence why plants became woody on islands is scarce at best. Here, we combine experimental measurements of hydraulic failure in stems (as a proxy for drought stress resistance) with stem anatomical observations in the daisy lineage (Asteraceae), including insular woody *Argyranthemum* species from the Canary Islands and their herbaceous continental relatives. Our results show that stems of insular woody daisies are more resistant to drought-induced hydraulic failure than the stems of their herbaceous counterparts. The anatomical character that best predicts variation in embolism resistance is intervessel pit membrane thickness ($T_{PM}$), which can be functionally linked with air bubble dynamics throughout the 3D vessel network. There is also a strong link between $T_{PM}$ vs degree of woodiness and thickness of the xylem fiber wall vs embolism resistance, resulting in an indirect link between lignification and resistance to embolism formation. Thicker intervessel pit membranes in *Argyranthemum* functionally explain why this insular woody genus is more embolism resistant to drought-induced failure compared to the herbaceous relatives from which it has evolved, but additional data are needed to confirm that palaeoclimatic drought conditions has triggered wood formation in this daisy lineage.

Keywords: Canary Islands, drought, hydraulic failure, insular woodiness, lignification, stem anatomy, thickness of intervessel pit membrane, xylem hydraulics.

# Introduction

It has been known for a long time that island floras have a higher proportion of woody species compared to adjacent continents, and related species on islands are often woodier than their continental relatives (Darwin 1859; Wallace 1878; Carlquist 1974). This phenomenon refers to insular woodiness, and describes the evolutionary transition from herbaceous towards (derived) woody flowering plant species on (sub)tropical oceanic islands (e.g., Carlquist 1974; Lens *et al.* 2013b). Interestingly, woodiness is considered to be ancestral within flowering plants (Doyle 2012), meaning that herbaceous lineages lost woodiness that characterized their ancestrally woody ancestors. This implies that the transition from herbaceousness towards insular woodiness (only on islands) or derived woodiness (on islands and continents) represents an evolutionary reversal back to the woody state (Lens *et al.* 2013b). A number of hypotheses have been put forward to explain insular woodiness, such as (i) increased competition hypothesis (taxon-cycling hypothesis; Darwin 1859; Givnish 1998), (ii) greater longevity hypothesis (promotion-of-outcrossing hypothesis; Wallace 1878; Böhle *et al.* 1996), (iii) moderate climate hypothesis (Carlquist 1974), and (iv) reduced herbivore hypothesis (Carlquist 1974). However, experimental data for these hypotheses are non-existing or based on only a few, small-scale examples. A recent review on insular woodiness of the Canary Islands showed that a majority of the insular woody species grow in dry coastal regions (Lens *et al.* 2013b), and an ongoing global derived woodiness database at the flowering plant level reveals a strong drought signal (F. Lens, unpublished data), suggesting a functional link between wood formation and increased drought stress resistance. Experimental support for this link was found in *Arabidopsis thaliana* (Lens *et al.* 2012b) using xylem physiological measurements in stems, but not a single study has compared drought-induced hydraulic failure with stem anatomy between derived woody plants and their herbaceous relatives growing in nature.

Hydraulic failure has been put forward as one of the prime mechanisms underlying drought-induced mortality in plants (Anderegg *et al.* 2016; Adams *et al.* 2017), and corresponds to the disruption of water transport in embolised xylem conduits when plants face drought (Lens *et al.* 2013a). As the proportion of gas embolism in xylem conduits generally enhances with increasing drought stress, the hydraulic conductivity decreases until a critical threshold, potentially leading to plant death (Brodribb *et al.* 2010; Urli *et al.* 2013; Adams *et al.* 2017). Plant resistance to embolism is estimated using so-called vulnerability curves, from which the $P_{50}$, i.e. the xylem pressure inducing 50% loss of hydraulic conductivity, can be estimated (Cochard *et al.* 2013). $P_{50}$ measurements have been carried out for hundreds of (ancestrally) woody species (Maherali *et al.* 2004; Choat *et al.* 2012; Bouche *et al.* 2014), and show that the species from dry environments are gener-

ally more resistant to embolism (more negative $P_{50}$) than species from wet climates (Choat *et al.* 2012; Lens *et al.* 2013b, 2016; Larter *et al.* 2015). In contrast, vulnerability curves from herbaceous and derived woody stems remain limited to only a few dozen species (Lens *et al.* 2016).

In this paper, we want to assess for the first time the correlation between embolism resistance and insular woodiness by complementing hydraulic stem observations with detailed light microscope and electron microscope observations in the insular woody *Argyranthemum* and its close continental relatives (tribe Anthemideae, family Asteraceae). More specifically, we will address whether this correlation would be functional or rather indirect due to the presence of a vessel feature that is functionally linked with both embolism resistance and increased woodiness in this daisy clade. The woody genus *Argyranthemum*, deeply nested into the predominantly herbaceous lineage including subtribes Leucantheminae, Santolininae and Glebionidinae, is the largest plant genus endemic to the volcanic Macaronesian archipelago and has the Mediterranean herbaceous *Glebionis* and *Ismelia* (Glebionidinae) as closest relatives (Oberprieler *et al.* 2009). *Argyranthemum* encompasses 24 species endemic to the islands of Madeira, Selvagens and the Canaries (Humphries 1976), and predominantly inhabits the dry coastal desert and more humid lowland scrub vegetation, although some species have also invaded the other major habitats of the Canary archipelago (Francisco-Ortega *et al.* 1997).

The main objectives in our study are to investigate (1) whether the insular woody stems of *Argyranthemum* are more resistant to drought-induced hydraulic failure than those of their herbaceous relatives, (2) to find (non-)functional stem anatomical characters that best explain the observed variation in $P_{50}$ between the daisy species observed, and (3) to assess if the woody species native to drier habitats are more resistant to embolism formation compared to *Argyranthemum* species growing in wetter habitats.

# Materials and methods

## Plant material

During different field campaigns (May 2013, January 2014 and November 2015; Supplementary Information Fig. S1), we collected species of the perennial woody *Argyranthemum* (subtribe Glebionidinae) throughout the island of Tenerife, situated near the centre of the Canary Island archipelago in the Atlantic Ocean off the coast of northwestern Africa (del-Arco *et al.* 2006).

We selected the rainy period of Tenerife (November – March) to collect our specimens to avoid high native levels of drought-induced embolism in the stems. For each of the woody individuals studied, we collected at least two 50 cm long stem samples, from the main stem and/or from the proximal branches (depending on the size of the individual), from 10 individuals per species: *A. adauctum*, *A. broussonetii, A. foeniculaceum, A. frutescens,* and *A. gracile* (Fig. S1). All the woody species collected are deciduous, except for the evergreen *A. broussonetti* and *A. adauctum* collected at the laurel forest and humid high altitude zones on Tenerife, respectively.

For comparison with the closely related herbaceous species, we collected *Leucanthemum vulgare* (Leucantheminae subtribe), the only perennial herbaceous species, on the campus of Bordeaux University (France), and performed the measurements during May-June 2013. The other closely related herbaceous species, *Glebionis coronaria*, *G. segetum* (belonging to subtribe Glebionidinae), *Cladanthus mixtus* (Santolininae subtribe), and *Coleostephus myconis* (Leucantheminae subtribe) are all annuals and were collected on the island of Tenerife, Canary Islands (Fig. S1) during their flowering period (March 2016). All the herbaceous species collected on Tenerife are continental species that have invaded the Canaries recently (Arechavaleta *et al.* 2010). Between 10 - 20 individuals of each herbaceous species were harvested.

In the field, we collected straight woody branches of at least 35 cm or 50 cm long for the standard (27 cm diameter) and medium cavitron (42 cm diameter), respectively. The branches were cut in air, immediately wrapped in wet tissues, and sealed in a dark plastic bag. For the herbaceous species, entire individuals were collected, with roots still attached. Afterwards, stems were stored in a cold room (around 5ºC) for a few days in the University of La Laguna, Tenerife, before being shipped by plane to the high-throughput caviplace platform (University of Bordeaux, France).

## Xylem vulnerability to embolism

Prior to measurement, all the branches were cut under water in the lab with a razor blade into a standard length of 27 or 42 cm in order to fit the two cavitron rotors (Cochard 2002; Cochard *et al.* 2013); bark was removed for the woody species. The stems were not flushed prior the measurements to avoid cavitation fatigue as a result of potential damage of intervessel pit membranes (Hacke *et al.* 2001b). First, the maximum conductivity of the stem in its native state (Kmax in $m^2$ $MPa^{-1}$ $s^{-1}$) was calculated under xylem pressure close to zero MPa using a reference ionic solution of 10 mM KCl and 1 mM CaCl2 in deionized ultrapure water. Then, rotation speed of the centrifuge was gradually increased by -0.5 or -1 MPa, to

lower xylem pressure. The percentage loss of conductivity (PLC) of the stem was determined at each pressure step following the equation:

$$PLC = 100 * \left(1 - \frac{K}{K_{max}}\right) \quad \text{Eqn. 1}$$

where Kmax represents the maximum conductance of the stem at the lowest pressure applied (-0.5 MPa), and K represents the conductance associated at each pressure step.

The vulnerability curves, showing the relation between the xylem pressure and the percentage loss of conductivity, were obtained using the Cavisoft software (Cavisoft v1.5, University of Bordeaux, Bordeaux, France). A sigmoid function (Pammenter & Van der Willigen 1998) was fitted to the data from each sample, using the next equation with SAS 9.4 (SAS 9.4, SAS Institute, Cary NC):

$$PLC = \frac{100}{\left[1+exp\left(\frac{s}{25} * (P-P_{50})\right)\right]} \quad \text{Eqn. 2}$$

where S (% $MPa^{-1}$) is the slope of the vulnerability curve at the inflexion point, P is the xylem pressure value used at each step, and $P_{50}$ is the xylem pressure inducing 50% loss of hydraulic conductivity. The parameters S and $P_{50}$ were averaged for each species (n=10).

## Wood anatomy

Light microscopy (LM), scanning electron microscopy (SEM) and transmission electron microscopy (TEM) observations were performed at Naturalis Biodiversity Center based on the samples for which we have obtained suitable vulnerability curves. The samples were taken from at least two individuals per species, from the middle part of the stem segment where the negative pressure caused embolism formation during the cavitron experiment, which reflects the in vivo conditions of a plant experiencing drought stress. All the anatomical measurements (Table 1) were done using ImageJ (National Institutes of Health, Bethesda, USA), following largely the suggestions of Scholz *et al.* (2013) and IAWA Committee (1989).

For LM, the woody species were cut in transverse and tangential sections of 20 µm thickness using a sliding microtome (Reichert, Vienna, Austria). After bleaching with sodium hypochlorite 1-3% and rinsing with water, the sections were briefly stained with a 1:2 mixture of safranin (0.5% in 50% ethanol) and alcian blue (1% in

water), dehydrated in an ethanol series (50%, 70%, 96%), treated with a Parasolve clearing agent (Prosan, Merelbeke, Belgium), and mounted in Euparal (Waldeck GmbH & Co. KG, Germany) (Lens *et al.* 2011). For the herbaceous species, the samples were embedded in LR-White resin following Hamann *et al.* (2011). Transverse sections of 4 µm were made using a rotary microtome (Leica RM 2265), heat fixed to the slide, stained with toluidine blue (0.1% in water), and mounted in Entellan®. The sections were observed using a Leica DM2500 light microscope and photographed with a Leica DFC-425C digital camera (Leica microscopes, Wetzlar, Germany). The diameter of vessels ($D_V$) was calculated based on the lumen area that was considered to be a circle following the equation:

$$D_V = \sqrt{\frac{4A}{\pi}} \qquad \text{Eqn. 3}$$

where $D_V$ is the vessel diameter and A is the vessel lumen area. The hydraulically weighted vessel diameter ($D_H$) was calculated following the equation (Sperry *et al.* 1994):

$$D_H = \frac{\sum D_V^5}{\sum D_V^4} \qquad \text{Eqn. 4}$$

where $D_V$ is the vessel diameter as measured in eqn. (3). We also calculated $D_H$ according to the Tyree & Zimmerman (2002) equation: $D_H = (\sum D_V{}^4/n)^{1/4}$, where n is the number of vessels measured (Table S3), but used Eqn (4) in our statistics analyses since there is no consensus at this point preferring one calculation over the other, and because there is a linear relationship between the $D_H$ values derived from both equations.

For SEM, dried wood specimens from two individuals per species were split in a tangential plane, dehydrated in an ethanol series (50%, 70%, 96%), dried at room temperature, fixed to aluminium stubs with an electron-conductive carbon sticker, platinum-palladium-coated with a sputter coater (Quorum Q150TS Quorum Technologies, Laughton, United Kingdom), and observed with a field emission SEM (Jeol JSM-7600F, Tokyo, Japan) at a voltage of 5 kV to observe the intervessel pits.

For TEM, fresh pieces from the outer part of the xylem were cut into 2 $mm^3$ blocks and immediately fixed 48h in Karnovsky fixative (Karnovsky 1965). Subsequently, the samples were rinsed in 0.1M cacodylate buffer, postfixed with 1% buffered osmium tetroxide for 3h at room temperature, and rinsed again with buffer solution. Subsequently, the samples were stained with 1% uranyl acetate and dehydrated through a graded propanol series (30%, 50%, 70%, 96% and 100%) and acetonitrile, and embedded in Epon 812 n (Electron Microscopy Sciences, Hatfield, England) at 60°C for 48h. After embedding, 2 µm thick cross sections were cut

from the resin blocks with a glass knife to observe areas including adjacent vessels. The cross sectional areas from the resin blocks were then trimmed to maintain only vessel-vessel contact areas, and 90 nm thick cross sections were made with a diamond knife. The sections were dried on 300 mesh copper grids with Formvar coating (Agar Scientific, Stansted, UK). Several grids were prepared for each resin sample and manually counterstained with uranyl acetate and lead citrate. Ultrastructural observations were carried out on intervessel pits with relaxed (non-aspirated) membranes using a JEOL JEM 1400-Plus TEM (JEOL, Tokyo, Japan), equipped with a 11 MPixel camera (Quemesa, Olympus) based on at least 20 observations per individual. Since we only observed intervessel pit membranes from the central stem segment parts where centrifugal force was applied, our measurements provide a relative estimation of intervessel pit membrane thickness.

## Statistical analyses

To test the difference between $P_{50}$, $P_{12}$ (pressure inducing 12% loss of hydraulic conductivity referring to initial air-entry pressure), $P_{88}$ (pressure inducing 88% loss of hydraulic conductivity referring to irreversible death-inducing xylem pressure in angiosperms; Barigah *et al.* 2013; Urli *et al.* 2013), and *S* (slope of vulnerability curve at inflexion point, an indicator for the speed at which embolisms affect the stem) with life form (woodiness vs. herbaceousness), we used generalized least squares (GLS). To deal with heterocedasticity we included a varIdent weights function (Zuur *et al.* 2009). Statistical analyses were done using the gls function from the nlme package (Pinheiro *et al.* 2016) in the R software (R Core Team 2016).

In order to test which stem anatomical characters best explain embolism resistance, we performed a multiple linear regression, with the $P_{50}$ as response variable and the stem anatomical characters as predictive variables. As several of the anatomical features measured were correlated, we selected a priori the predictive variables using the following criteria: biological insights based on previously published studies and a pairwise scatterplot to detect relationship between response variable and predictive variables. To assess high multicollinearity amongst predictive variables we conducted a variance inflation factor (VIF) analysis, keeping only variables with a VIF value lower than 2 (Zuur *et al.* 2010). Subsequently, we performed the stepwise function using the direction method "both" of the "step" function from "stats" package (R Core Team 2016). The regression or differences was considered to be significant if $P < 0.05$. Further, we calculated the hierarchical partitioning (Chevan & Sutherland 1991) for the significant variables retained in the model in order to assess their relative importance to explain the $P_{50}$.

We performed simple linear regression between thickness of intervessel pit membrane ($T_{PM}$) and $P_{50}$ to assess a potential correlation. To deal with heterocedasticity we included a varFixed weights function (Zuur *et al.* 2009). We calculate

**Table 1** • List with the anatomical characters measured, their symbols and units, and the type of microscopy applied.

| Acronym | Definition | Calculation | Units | Technique |
|---|---|---|---|---|
| $D_V$ | Diameter of vessels | Equation 3 | μm | LM |
| $D_H$ | Hydraulically weighted vessel diameter | Equation 4 | μm | LM |
| $DE_V$ | Density of vessels | Number of vessel counted in random selection of 5 zones of 1mm$^2$ wood area | Nº of vessels/mm$^2$ | LM |
| $G_V$ | Vessel grouping index | Total number of vessels divided by the total number of vessel groupings (incl. solitary and grouped vessels) | Nº of vessels/vessel group | LM |
| $T_W$:$D_V$ | Thickness-to-span ratio of vessels | Double intervessel wall thickness divided by maximum vessel diameter in vessel group | - | LM |
| $A_S$ | Total stem area | Total stem area in cross section | μm$^2$ | LM |
| $A_{LIG}$ | Lignified stem area | Total xylem area + fiber caps area in cross section | μm$^2$ | LM |
| $A_{PITH}$ | Pith area | Total pith area in cross section | μm$^2$ | LM |
| $A_F$ | Xylem fiber cell area | Area of single xylem fiber in cross section | μm$^2$ | LM |
| $A_{FL}$ | Xylem fiber lumen area | Area of single xylem fiber lumen in cross section | μm$^2$ | LM |
| $A_{FW}$ | Xylem fiber wall area | $A_F$ minus $A_{FL}$ for the same fiber | μm$^2$ | LM |
| $P_{LIG}$ | Proportion of lignified area per total stem area | $A_{LIG}$ : $A_S$ | - | LM |
| $P_{PITH}$ | Proportion of pith per total stem area | $A_{PITH}$ : $A_S$ | - | LM |
| $P_{FW}F$ | Proportion of xylem fiber wall per fiber | $A_{FW}$ : $A_F$ for the same fiber; measure of xylem fiber wall thickness | - | LM |
| $H_R$ | Height of rays | Measured in tangential section only for woody species | μm | LM |
| $DE_R$ | Density of rays | Total number of rays per mm$^2$ as measured in tangential section (only for woody species) | Nº of rays/mm$^2$ | LM |
| $P_R$ | Proportion of ray area per wood area | Total area of rays per mm$^2$ of tangential section (only for woody species) | - | LM |
| $A_{PB}$ | Intervessel pit border area | Measured in tangential surface | μm$^2$ | SEM |
| $A_{PA}$ | Intervessel pit aperture area | Measured in tangential surface | μm$^2$ | SEM |
| $F_{PA}$ | Intervessel pit aperture fraction | $A_{PA}$ : $A_{PB}$ for the same pit | - | SEM |
| $T_{PM}$ | Thickness of intervessel pit membrane | Thickness of intervessel pit membrane near the center of a relaxed (non-aspirated) membrane | nm | TEM |
| $D_{PC}$ | Depth of intervessel pit chamber | Distance from the pit membrane to the inner pit aperture | nm | TEM |

the $R^2$ values based on the method of Nakagawa & Schielzeth (2013), using the function rsquared in the package piecewiseSEM (Lefcheck 2015). Furthermore, the regression was applied between $P_{50}$ and the proportion of lignified area per total stem area ($P_{LIG}$) for 8 individuals measured of *Cladanthus mixtus* due to the high intraspecific variation in the degree of woodiness for this species.

To assess the correlation between the predictive variables and $P_{50}$ in the general dataset (woody + herbaceous species studied), as well as in the woody and herbaceous dataset separately, we performed Pearson or Spearman correlation analyses depending on the normality of the variable's distribution. $P_{LIG}$ in the general dataset was log-transformed to match the normality. Finally, we performed a Student's t-test to assess the difference in pit membrane thickness between the insular woody and herbaceous group.

# Results



*Xylem vulnerability to embolism in the daisy group*

The insular woody daisy species are more embolism resistant than their herbaceous relatives (Fig. 1; Fig. 2 A-D; Table S1). The vulnerability curves used to construct the average curve were all S-shaped (Fig. S2). $P_{50}$ varied two-fold across species, with significant variation in $P_{50}$ between woody and herbaceous species ($F = 66.45$; $P < 0.0001$). Similar significant variation in $P_{88}$ ($F = 90.03$; $P < 0.0001$) was also observed, but not for $P_{12}$ ($F = 1.61$; $P = 0.20$) (Table S1). The $P_{50}$ ranged from -2.1 MPa for the herbaceous *Glebionis coronaria* up to -5.1 MPa for the woody *A. foeniculaceum* (Fig. 1). Among the woody species, the most vulnerable species is *A. broussonetii* ($P_{50}$ = -3.1 MPa), while *Cladanthus mixtus* is the herbaceous species most resistant to embolism ($P_{50}$ = -2.9 MPa) (Fig. 1). Amongst the herbaceous species, *C. mixtus* shows the largest variation in $P_{50}$, ranging from -1.9 MPa till -4.1 MPa (Fig. 1), but intraspecific variation for most other herbaceous species measured is limited.

The vulnerability curve slopes are significantly higher for the herbaceous species ($F = 67.77$; $P < 0.0001$; Table S1). Slopes of the vulnerability curves varied three-fold across species, with the lowest slope of 16% $MPa^{-1}$ for the woody *A. foeniculaceum*, and the steepest slope of 52% $MPa^{-1}$ for the herbaceous *Glebionis segetum.*

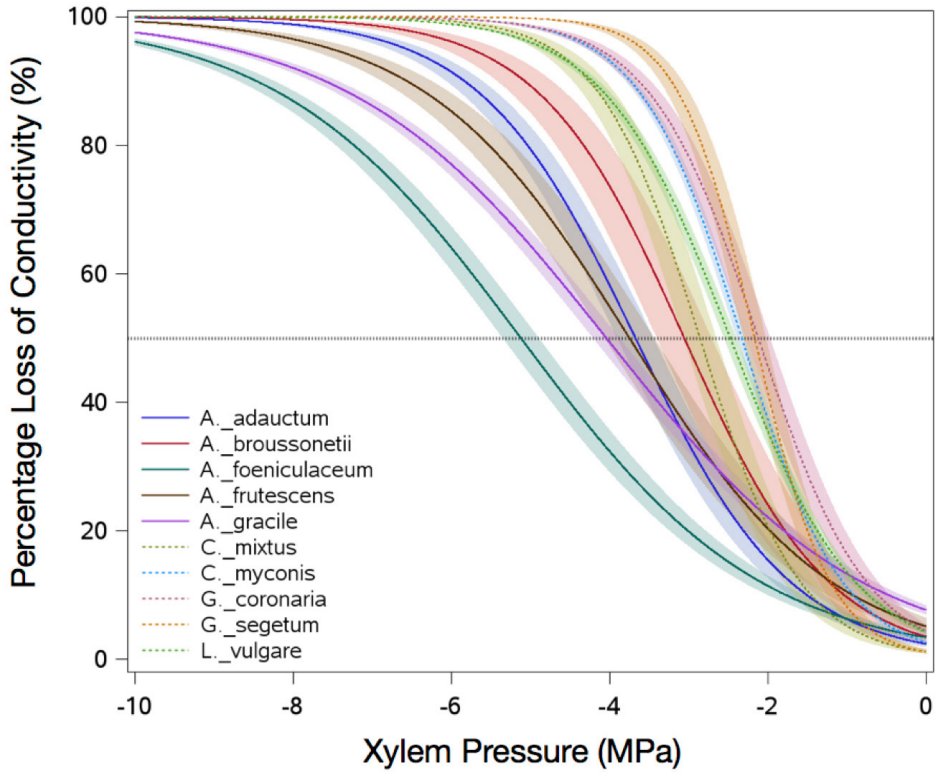


**Figure 1** • Mean vulnerability curve for each of the 10 species studied showing percentage loss of conductivity (%) as a function of xylem pressure (MPa). The plain curves indicate the VCs for the woody species and the dotted VCs represent the herbaceous species. Shaded bands represent standard errors.

### *Relationship between embolism resistance and wood anatomy*

A combined backward and forward multiple regression analysis shows that the thickness of intervessel pit membrane ($T_{PM}$), the proportion of xylem fiber wall per fiber ($P_{FW}F$) and the hydraulically weighted diameter of vessels ($D_H$) best explain the variation in $P_{50}$ (P = 0.0018, $R^2$ = 0.8578; Table 2). However, only $T_{PM}$ and $P_{FW}F$ are significant, with $T_{PM}$ explaining 70% and $P_{FW}F$ 30% of the variation in $P_{50}$ (Table 2).

In the general dataset, the thickness of intervessel pit membrane ($T_{PM}$) correlates with embolism resistance (P = 0.0021, $R^2$ = 0.4425; Fig. 3 A): the more resistant insular woody species (proportion of lignified area per total stem area ranging from 0.70 – 0.84) show thicker intervessel pit membranes than the vulnerable herbaceous species (proportion of lignified area per total stem area ranging from 0.21 – 0.43) (t-test, P = 0.0017; Fig. 2 E, F; Fig. 3 B). $T_{PM}$ is also correlated with vessel grouping index in the general dataset and in the woody dataset (P = 0.0448, r =

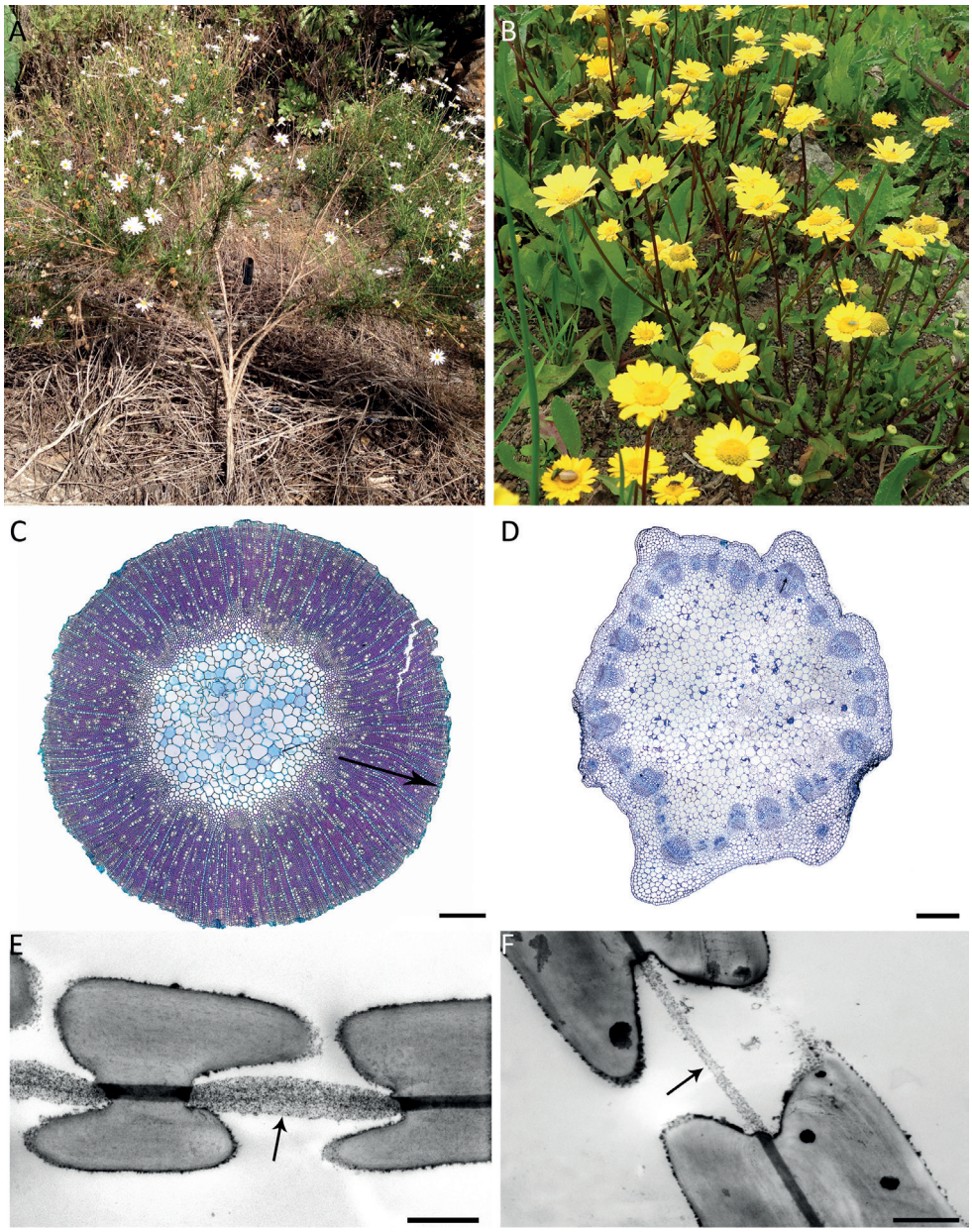


**Figure 2** • Illustration of life form and hydraulically relevant anatomical features of *Argyranthemum gracile* (left) and *Coleostephus myconis* relative (right). (a -b) species in the field; (c - d) light microscope images of stem cross sections, the arrows show the marked difference in xylem area; (e - f) TEM images of intervessel pit membranes (arrows) showing thicker membranes in the woody *A. gracile* (e) compared to the herbaceous *C. myconis* (f). Scale bars represent 500 µm (c - d), 1 µm (e - f).

0.6440; P = 0.0221, r = 0.9297), respectively. Aspirated intervessel pit membranes were very scarce and ignored in our measurements.

In addition to the thickness of intervessel pit membrane (Fig. 3 A), the following anatomical variables in the general dataset (herbaceous and woody species combined, Table S2) are significantly correlated with $P_{50}$: density of vessels (P = 0.0028; r = -0.8317), vessel grouping index (P = 0.0040; r = -0.8151), and the proportion of lignified area per total stem area (P = 0.0060; r = -0.7952) (Fig. 2 C, D). However, when we analyse the woody species separately (Table S2), only vessel grouping index (P = 0.0055; r = -0.9722) and proportion of ray area per wood area (P = 0.04997; r = -0.8784) are significantly correlated with $P_{50}$, whereas all the significant correlations disappear in the herbaceous dataset probably due to the limited variation in $P_{50}$ amongst the herbaceous species studied (Tables S1, S2). The axial parenchyma patterns are very similar between the most resistant and most vulnerable *Argyranthemum* species (scanty paratracheal according to IAWA Committee, 1989).

The simple linear regression for *C. mixtus* individuals shows that the proportion of lignified area per total stem area is highly linked with $P_{50}$ for this population (P = 0.0008; $R^2$=0.84) (Fig. 4 E), which scales with the large intraspecific variation in the degree of woodiness in the stem (Fig. 4 A-D).

# Discussion

### *Stems of insular woody daisies are more embolism resistant than those of their herbaceous relatives*

Our xylem physiological embolism resistance data show one major outcome: stems of the insular woody *Argyranthemum* are more resistant to drought-induced hydraulic failure than those of their herbaceous Anthemideae relatives. Additionally, the difference in slopes of the vulnerability curves between woody and herbaceous species demonstrates that embolism formation occurs slower in the former (Fig. 1; Table S1). The positive link between increased wood formation and embolism resistance within the daisy lineage matches the observation that insular woody species native to the Canary Islands are often distributed in the dry coastal areas (Lens *et al.* 2013a), and agrees with an ongoing global derived woodiness database at the flowering plant level, comprising more than 6000 species of which most of them are native to regions with a marked drought period such as (semi-) deserts, savannas, steppes and Mediterranean-type habitats (F. Lens, unpublished data). Despite the overwhelming evidence for this positive link, it is hard to functionally

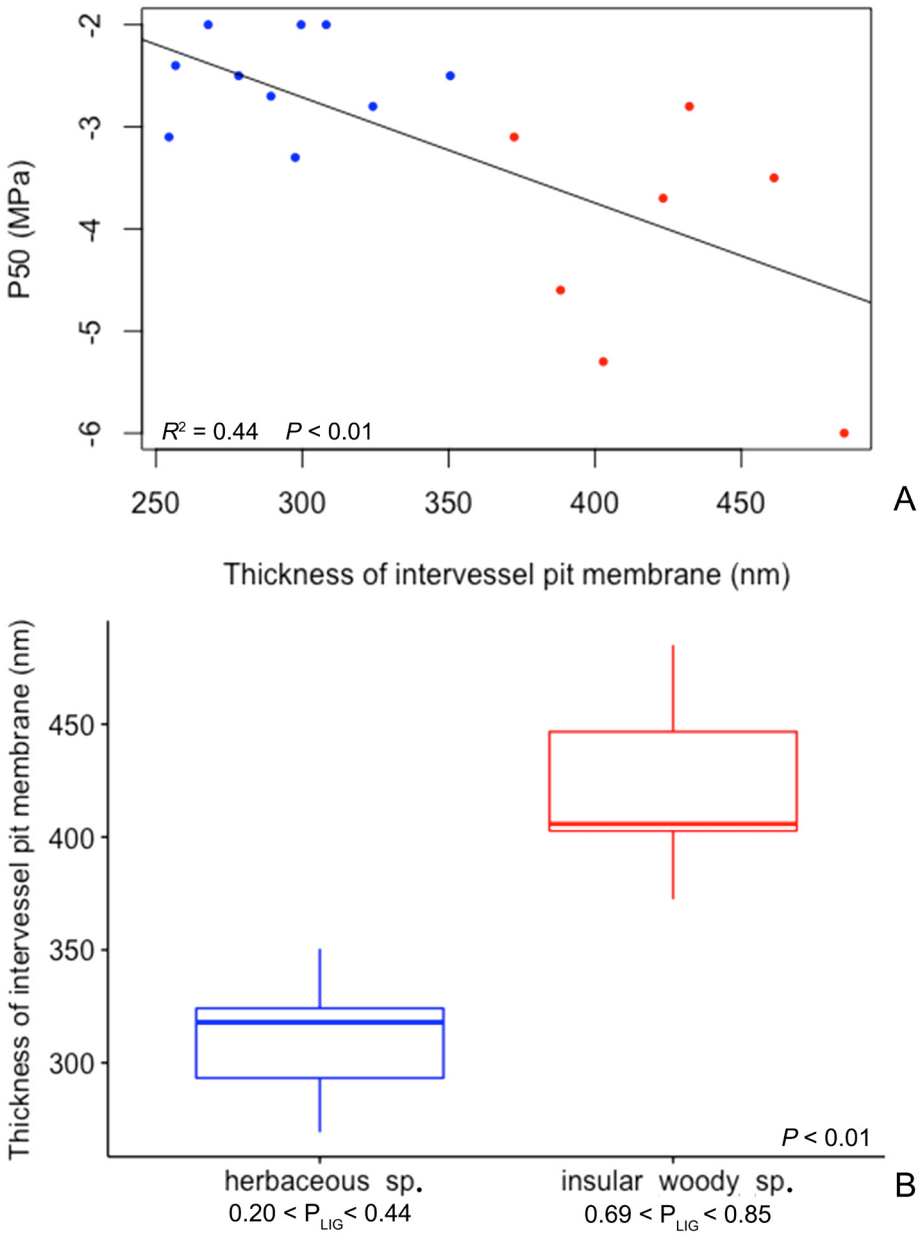


**Figure 3** • Thickness of intervessel pit membrane ($T_{PM}$) and its significant relationship to embolism resistance (a), life form – lignification (b). $P_{LIG}$ = proportion of lignified area per total stem area. Red refers to insular woody species and blue to herbaceous species. Each dot relates to one individual. The bottom, middle and upper lines of the box represent the 25th quartile, the median and the 75th quartile, respectively. Upper and bottom ends of the vertical lines indicate the maximum and minimum values of $T_{PM}$.

**Table 2 •** Multiple regression model of anatomical features explaining the variance in the $P_{50}$ in woody and herbaceous daisies. The values in bold indicate significant correlation (P < 0.05).

| Source of variation | Parameter Estimate | SE | *t*-value | *P*-value | Hierarchical partitioning | VIF values |
|---|---|---|---|---|---|---|
| $T_{PM}$ | -0.0096 | 0.0020 | -4.890 | **0.0027** | 70.30% | 1.2560 |
| $P_{FW}F$ | -4.5862 | 1.8420 | -2.490 | **0.0471** | 29.70% | 1.2453 |
| $D_{HV}$ | -0.0591 | 0.0285 | -2.072 | 0.0836 | | 1.0169 |

$T_{PM}$ = thickness of intervessel pit membrane; $P_{FW}F$ = proportion of xylem fiber wall per fiber; $D_{HV}$ = hydraulically weighted vessel diameter.

explain why derived woody species are better adapted to drought compared to their herbaceous relatives, since at first sight there seems to be no evidence for a direct functional link between increased wood formation and increased drought stress resistance. Obviously, woody species have more reinforced conduit and fibre walls, which indirectly relates to embolism resistance and directly relates to conduit implosion resistance (Hacke *et al.* 2001b; Jacobsen *et al.* 2005), although $P_{50}$ values seem to be well above the implosion limit in angiosperm stem xylem (Sperry 2003). Furthermore, there is a correlation between vessel wall thickness and intervessel pit membrane thickness (Jansen *et al.* 2009; Li *et al.* 2016), meaning that vessel wall thickness is indirectly correlated with embolism resistance via air-seeding. Likewise, it is possible that reinforced vessel and neighbouring fiber walls better avoid micro-cracks through which embolism nucleation may occur or air could be sucked in (Jacobsen *et al.* 2005; see following two sections).

Second, $P_{50}$ seems to behave as an important adaptive trait to survive drought stress within *Argyranthemum*, since the most vulnerable woody species – the evergreen *A. broussonetii* – was sampled in the wet laurel forests, while most other more resistant *Argyranthemum* species are native to drier habitats (Fig. 1; Fig. S1). Similar correlations between $P_{50}$ and precipitation have been identified in many other lineages (Maherali *et al.* 2004; Choat *et al.* 2012; Larter *et al.* 2015; Lens *et al.* 2016; Trueba *et al.* 2017).

### *Variation in intervessel pit membrane thickness ($T_{PM}$) is essential to explain differences in drought-induced hydraulic failure within the daisy lineage*

The anatomical variable that could explain the abovementioned indirect link between insular woodiness and increased embolism resistance must be correlated with both increased wood formation, measured as a higher proportion of lignified area per total stem area ($P_{LIG}$), and with $P_{50}$, and must also functionally explain embolism formation and/or spread within the 3D vessel network. Intervessel pit

membrane thickness ($T_{PM}$) is the ideal candidate to clarify this indirect link, because it matches all criteria: (1) $T_{PM}$ is tightly linked with life form (referring to the proportion of lignified area per total stem area, Fig. 3 B) as well as $P_{50}$ (Fig. 3 A), (2) $T_{PM}$ is the most significant variable in the regression model (explaining 70% of the $P_{50}$ variation, Table 2), highlighting its hydraulic relevance as the best predictor of embolism resistance amongst the daisy species studied (Fig. 2 E, F; Table 2), and (3) the functional aspect of the observed $T_{PM}$ - $P_{50}$ correlation is obvious due to air-seeding, since more embolism resistant daisies have thicker intervessel pit membranes (Fig. 2 E-F; Fig. 3 B; Table S3). The thickness of intervessel pit membrane is likely to affect the length of the tortuous and irregularly shaped pores that air-water menisci need to cross before air-seeding may occur, explaining the spread of embolism through intervessel pit membranes into adjacent conduits, and thereby emphasizing its direct functional link with respect to embolism resistance (Jansen *et al.* 2009; Lens *et al.* 2011, 2013b; Li *et al.* 2016). New findings reveal that the likelihood of bubble snap-off is higher when air passes the longer and more tortuous pore pathway of thicker intervessel pit membranes compared to thinner membranes. It is believed that the lipid-based surfactants molecules in the intervessel pit membrane pores ensure coating of these so-called nanobubbles, while they lower their dynamic, concentration-dependent surface tension and thereby stabilize the bubbles under negative pressure (Schenk *et al.* 2015; Schenk *et al.* 2017).



### *The relationship between increased embolism resistance and increased wood formation/lignification is strong but indirect*

In addition to the observed correlation between the proportion of lignified area per total stem area ($P_{LIG}$) and embolism resistance (Table S2), we have also found another lignification link in our dataset: the proportion of xylem fiber wall per fiber ($P_{FW}F$), which is a measure for fiber wall thickness in the xylem, explains 30% of the variation in $P_{50}$ (Table 2). Since lignification in angiosperm shrubs and trees is mainly defined by wood fibers (Zieminska *et al.* 2013; Zieminska *et al.* 2015), and since wood lignin content is positively linked to embolism resistance in a global dataset (Pereira *et al.* 2017), our observed (indirect) correlation between the proportion of xylem fiber wall per fiber and $P_{50}$ could be expected. Likewise, further support for the strong positive link between lignification and embolism resistance is provided by other sources of data, such as wood density (Jacobsen *et al.* 2005; Hoffman *et al.* 2011; but see meta-analyses by Anderegg *et al.* 2016 and Gleason *et al.* 2016a), conduit wall thickness (Hacke *et al.* 2001a; Cochard *et al.* 2008; Jansen *et al.* 2009) and fiber wall area (Jacobsen *et al.* 2005). Moreover, the link between lignification and embolism resistance has been experimentally demonstrated in grasses (Lens *et al.* 2016), in the wild-type and woody mutant of *Arabidopsis thaliana* (Lens *et al.* 2012b), and in several transgenic poplars modified for lignin metabolism (Awad

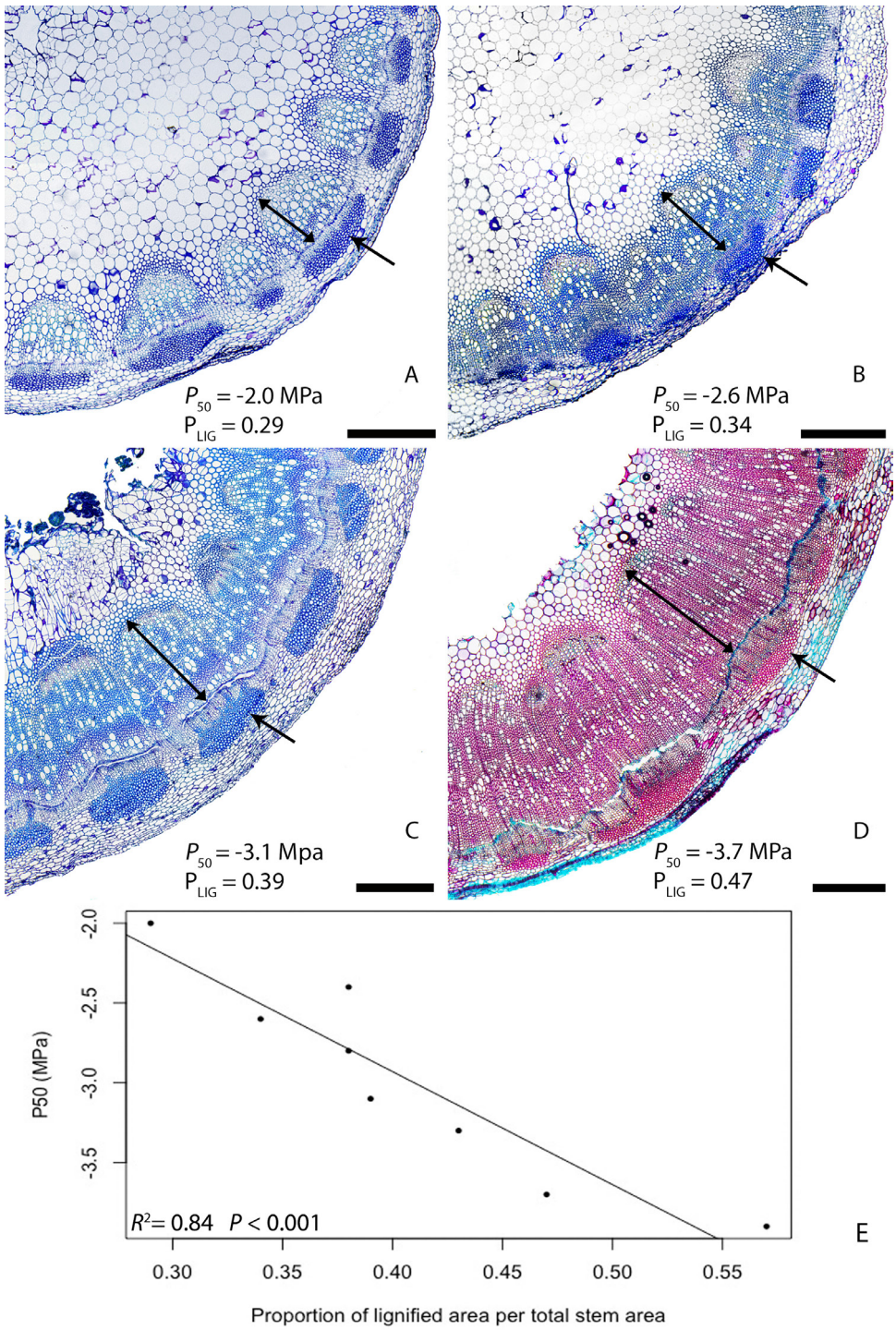


**Figure 4** • The intraspecific variation in the proportion of lignified area per total stem area ($P_{LIG}$) among *Cladanthus mixtus* individuals and its relation with $P_{50}$. (a - d) in ascending order, LM images of cross sections showing the $P_{LIG}$ - $P_{50}$ relationship. (e) fitted linear model between $P_{50}$ and $P_{LIG}$. Double arrow heads indicate the xylem area; single arrow heads point to extraxylary fiber caps. Each dot relates to one individual. Scale bars represent 500 µm.

*et al.* 2012). Based on these observations, it seems that many plant lineages invest much energy to develop a mechanically stronger, embolism resistant stem (Lens *et al.* 2013b, 2016; Pereira *et al.* 2017).

Interestingly, the correlation between the degree of lignification and $P_{50}$ is also confirmed within the herbaceous *Cladanthus mixtus,* where the more embolism resistant individuals ($P_{50}$ ranging from -3.1 MPa to -3.7 MPa) have more lignified stems compared to the more vulnerable individuals ($P_{50}$ ranging from -1.2 MPa to -2.8 MPa; Fig. 4). The large intraspecific variation in *C. mixtus* observed, reflects earlier observations about the fuzzy boundaries between woodiness and herbaceousness (Lens *et al.* 2012a). Indeed, nearly all the herbaceous species in angiosperms that do not belong to the monocots produce wood cells to some extent, but in small quantities and mainly confined to the base of the stem (Dulin & Kirchoff 2010; Schweingruber *et al.* 2011; Lens *et al.* 2012b). This continuous variation in wood formation often leads to intermediate life forms, referred in the literature as 'woody herbs' or 'half shrubs'. Since wood formation in the stems of these intermediate species (including C. mixtus) does not extend into the upper parts of the stem, we consider them not woody enough and thus herbaceous (Kidner *et al.* 2016).



*Relationship between embolism resistance vs vessel grouping index, vessel density and ray abundance*

Our general dataset shows that more embolism resistant species have more vessels per xylem surface area (higher density of vessels - $DE_V$) compared to more vulnerable species. In addition, the general and the woody dataset show that these vessels are grouped in larger multiples (higher vessel grouping index - $G_V$) (Tables S2, S3). Higher vessel grouping patterns allow the continuity of 3D water transport pathway in case one or several vessels in a vessel multiple become embolized (Carlquist 1984; Lens *et al.* 2011). On the other hand, increased vessel-vessel contact areas facilitate the potential spread of air bubbles from one embolised vessel towards an adjacent functional one via air-seeding (Zimmermann 1983). Therefore, the competitive advantage of having higher vessel grouping index may only be valid when the thickness of intervessel pit membrane is large enough to prevent air-seeding within the vessel multiple, which is statistically supported by a tight correlation between the thickness of intervessel pit membrane and vessel grouping index in the general and woody datasets, while the same correlation is not found for the herbaceous dataset with their thinner intervessel pit membranes.

Amongst the insular woody *Argyranthemum* species, there is a weakly significant, positive correlation between the proportion of ray area per wood area ($P_{R'}$ as seen in tangential sections) and embolism resistance ($P = 0.04997$; $r = -0.8784$; Table S2; Fig. S3). We observed in the field that all the leaves of the embolism re-

sistant *Argyranthemum* species native to the drier regions were functionally dead at the end of the dry summer, while new green leaves were starting to flush after the first rains set in (September 2013; Fig. S3 B). In contrast, the most vulnerable (evergreen) *A. broussonetii*, always facing wet conditions throughout the year in its laurel forest habitat, shows less proportion of ray area per wood area (Fig. S3c), although it is a much taller shrub (Fig. S3 A). It is known that ray tissue stores and transports water and carbohydrates via symplastic connections between inner bark and xylem through the vascular cambium (Pfautsch *et al.* 2015a; Pfautsch *et al.* 2015b). Although speculative at this point, the higher proportion of rays in the more resistant species could be interpreted as a water/carbohydrate source that could reactivate meristematic cells at the end of the dormant summer period (Brodersen *et al.* 2010; Nardini *et al.* 2011; Spicer 2014).

## Conclusions

We find that stems of the insular woody species of *Argyranthemum* are more resistant to drought-induced hydraulic failure than those of their herbaceous relatives native to the European mainland. Although this experimental result agrees with a marked drought signal in the ongoing global derived woodiness dataset including over 6000 derived woody flowering plant species representing several hundreds of transitions towards derived woodiness (F. Lens, unpublished data), this does not necessarily mean that drought has triggered wood formation in the common ancestor of *Argyranthemum* after arrival on the Canary Islands. Dated molecular phylogenies estimating the palaeoclimate in which the woody daisies have originated combined with a thorough niche modelling study including additional environmental variables (temperature, precipitation, aridity, potential evapotranspiration, and soil) are likely to shed more light into this fascinating island phenomenon.

We show that intervessel pit membrane thickness best predicts the variation in embolism resistance amongst the daisy species studied, and functionally explains $P_{50}$ via its role in air-seeding. Moreover, the thickness of intervessel pit membrane is the essential missing link to understand the indirect correlation between embolism resistance and increased lignification, a correlation that has also been demonstrated in larger datasets (Hacke *et al.* 2001a; Lens *et al.* 2016; Pereira *et al.* 2017) as well as within species (Lens *et al.* 2013b; this study). Therefore, we argue that lignification characters do not have a direct impact on embolism resistance, but they co-evolve with other anatomical features that are more directly influencing $P_{50}$ in water conducting cells (Lachenbruch & McCulloh 2014; Rosner 2017).

## Acknowledgements

L.C.D. appreciates the Graduate Research Fellowship from CNPq - Conselho Nacional de Desenvolvimento Científico e Tecnológico, Brazil, PROC. Nº 206433/2014-0, and the Alberta Mennega Stichting for funding the collection trips and the visits to the Delzon lab. We also thank the Cabildo de Tenerife (AFF 147/13 Nº Sigma: 2013-00748; AFF 429/13 Nº Sigma: 2013-02030; AFF 149/15 Nº Sigma: 2015-00925; AFF 85/16 Nº Sigma: 2016-00838) and Teide National Park (Nº 152587, REUS 27257, 2013; Nº 536556, REUS 83804, 2013; Res. Nº 222/2015) for the collection permits, and the Cluster of Excellence COTE (ANR-10-LABX-45) and the programme 'Investments for the Future' (ANR-10-EQPX-16, XYLOFOREST) funded by the French National Agency for Research. We also acknowledge the technical support of R. Langelaan, W. Star and G. Capdeville.

The authors declare no conflict of interests.



## Author's contribution

F.L. and S.D. conceived the ideas and designed methodology; L.C.D., M.A., T.C. and F.L. collected the data; L.C.D., D.S.P., S.D., and F.L. analysed the data; L.C.D. and F.L. wrote the manuscript and all authors contributed critically with comments to the draft.

## Data accessibility

Data available from the Dryad Digital Repository:

*https://doi.org/10.5061/dryad.sh546k0*

# Supplementary information

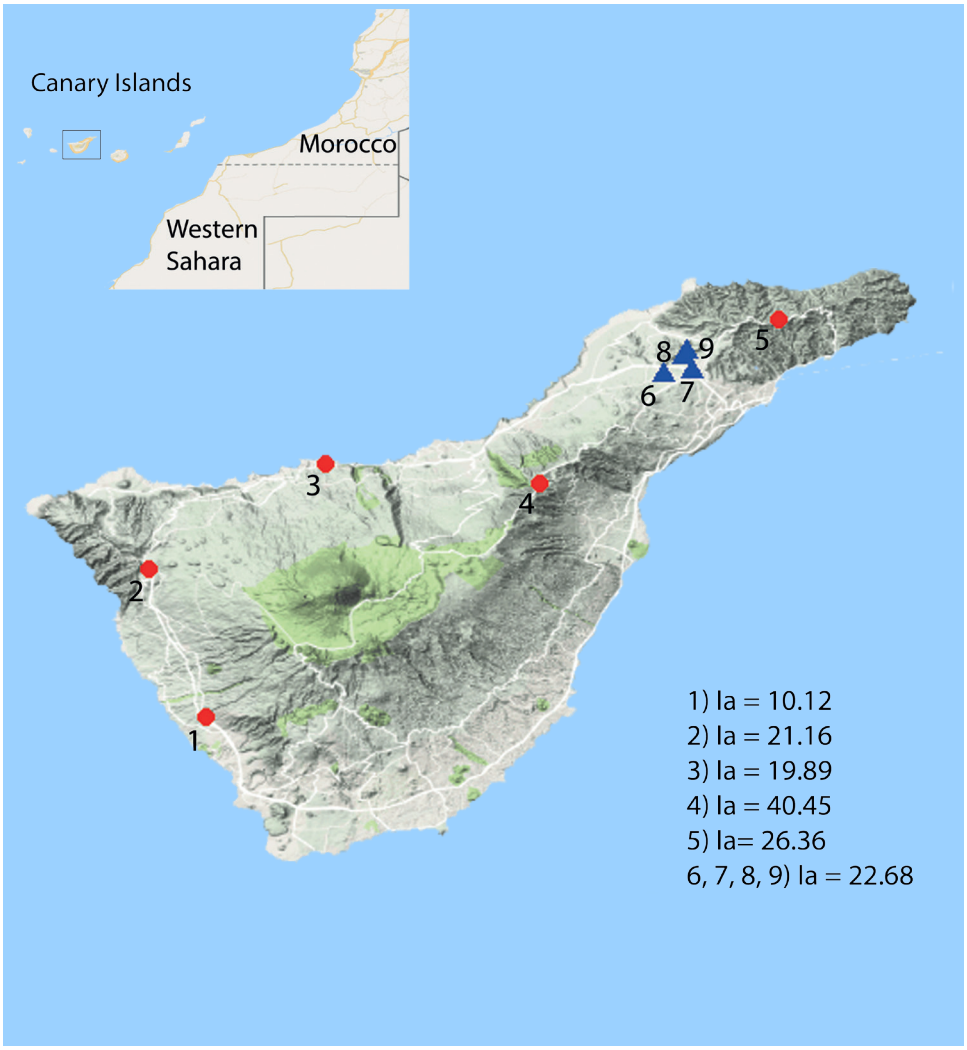


**Figure S1** • Map of Tenerife with the sampling sites and the corresponding aridity indices of Martonne (Ia). The red circles represent the sampling locations of woody *Argyranthemum* species, and the blue triangles refer to the sampling sites of the herbaceous relatives. 1- *A. gracile*; 2- *A. foeniculaceum*; 3- *A. frutescens*; 4- *A. adauctum*; 5- *A. broussonetii*; 6- *Cladanthus mixtus*; 7- *Glebionis coronaria*; 8- *G. segetum*; 9- *Coleostephus myconis*. *Leucanthemum vulgare* (Ia = 41.41) was collected in Bordeaux (France). The green areas represent protected biodiversity parks. For the aridity indices of Martonne (Ia), the smaller the number, the drier the environment.

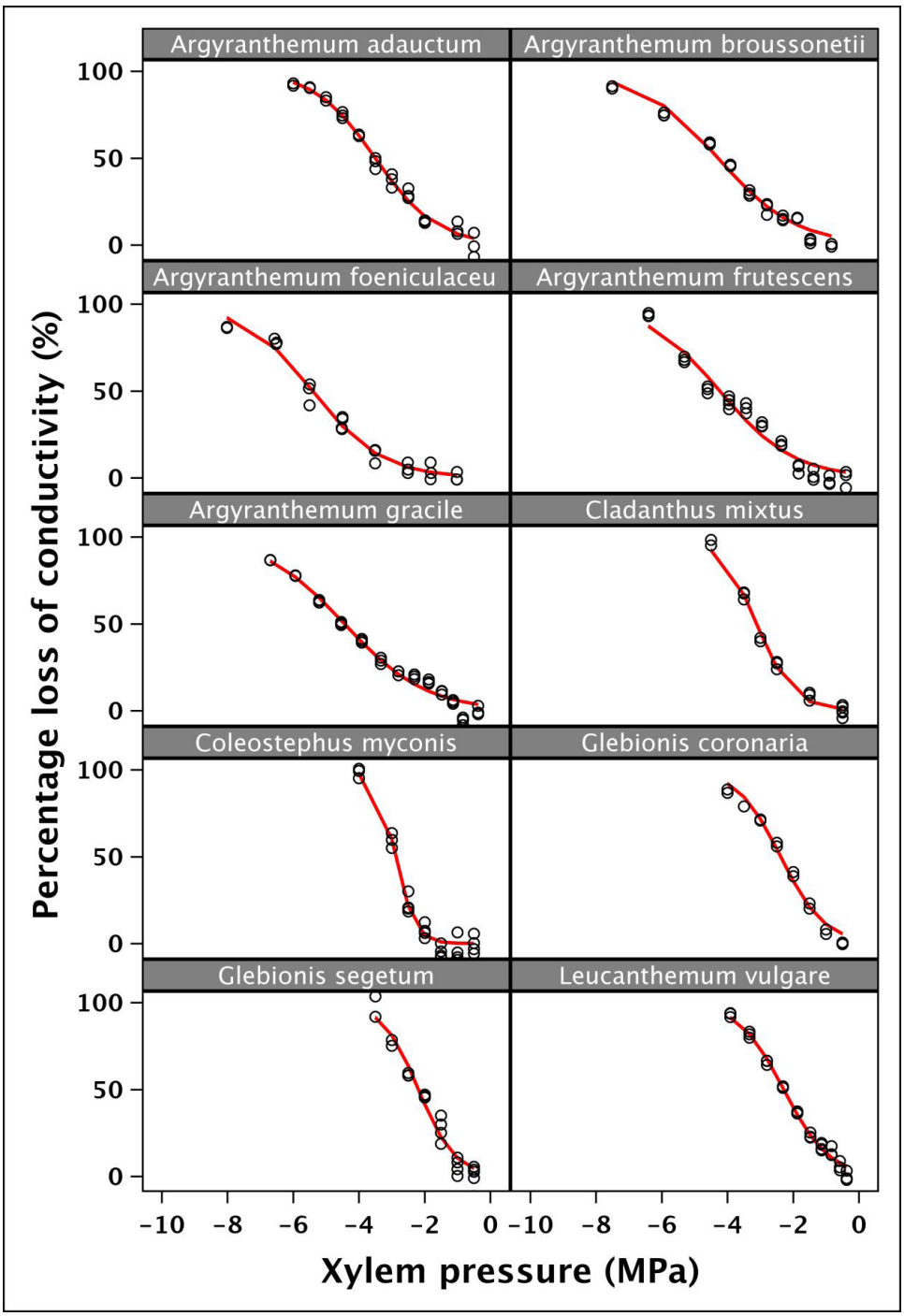


**Figure S2** • Representation of one S-shaped curve based on a single stem referring to the mean $P_{50}$ for all the species studied.

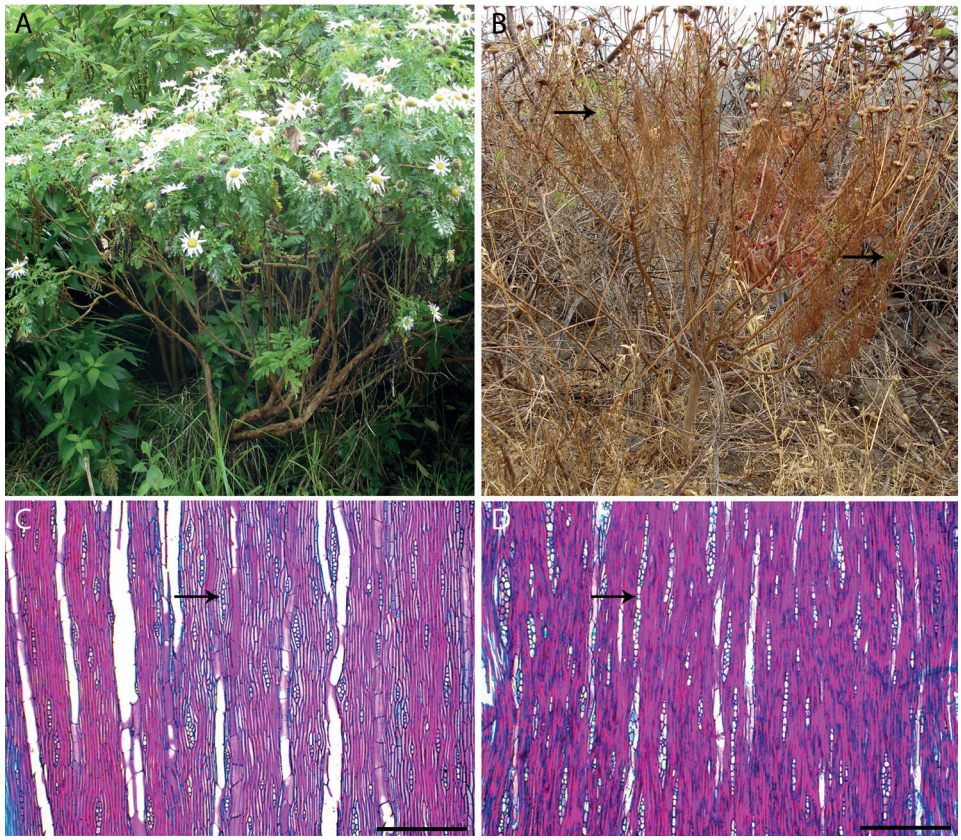


Figure S3. Difference in leaf phenology and ray area in wood between *Argyranthemum* species from contrasting environments on Tenerife, *A. broussonetii* native to the everwet laurel forests (left) and *A. foeniculaceum* growing in the dry southern lowlands (right). (a) - *A. broussonetii* is a tall evergreen shrub (picture taken in May 2011). (b) - *A. foeniculaceum* individual growing in the dry southern coastal regions of Tenerife; picture was taken at the end of the dry summer, 1-2 weeks after the first rains (September 2013), triggering flushing of new leaves (arrows). (c) - Longitudinal tangential wood section of *A. broussonetii* showing short and narrow rays (arrow). (d) - Longitudinal tangential wood section of *A. foeniculaceum* showing taller rays (arrow). Scale bars represent 500 µm.

**Table S1** • Xylem embolism vulnerability parameters of woody and herbaceous daisies. The average and standard error is given for each species. The averages are based on at least 7 individuals per species.

| Species | $P_{50}$ (MPa) | $P_{12}$ (MPa) | $P_{88}$ (MPa) | Slope (%MPa$^{-1}$) |
|---|---|---|---|---|
| *Argyranthemum foeniculaceum* | -5.1 ± 0.23 | -2.0 ± 0.34 | -8.3 ± 0.28 | 16.4 ± 1.33 |
| *Argyranthemum gracile* | -4.0 ± 0.17 | -0.8 ± 0.19 | -7.3 ± 0.25 | 15.4 ± 0.68 |
| *Argyranthemum frutescens* | -3.7 ± 0.32 | -1.0 ± 0.16 | -6.5 ± 0.53 | 19.5 ± 1.55 |
| *Argyranthemum adauctum* | -3.6 ± 0.29 | -1.6 ± 0.26 | -5.6 ± 0.42 | 26.0 ± 2.77 |
| *Argyranthemum broussonetii* | -3.1 ± 0.35 | -0.8 ± 0.25 | -5.3 ± 0.70 | 27.2 ± 4.37 |
| *Cladanthus mixtus* | -2.9 ± 0.21 | -1.4 ± 0.26 | -4.3 ± 0.22 | 39.2 ± 3.78 |
| *Coleostephus myconis* | -2.3 ± 0.06 | -1.0 ± 0.12 | -3.7 ± 0.07 | 39.0 ± 2.33 |
| *Leucanthemum vulgare* | -2.5 ± 0.08 | -0.8 ± 0.12 | -4.2 ± 0.17 | 31.5 ± 2.48 |
| *Glebionis segetum* | -2.2 ± 0.14 | -1.1 ± 0.14 | -3.2 ± 0.18 | 52.0 ± 4.85 |
| *Glebionis coronaria* | -2.1 ± 0.15 | -0.7 ± 0.19 | -3.5 ± 0.13 | 36.4 ± 1.70 |

**Table S2** • Correlations between the wood anatomical traits and $P_{50}$ for the woody and herbaceous daisies combined, as well as for the woody and herbaceous dataset separately. Correlations (r) and levels of significance (P) for each variable are given. The values in bold indicate significant correlation ($P < 0.05$). The correlations are based on the average of at least 2 individuals per species.

| | ***Woody and herbaceous species dataset*** | | ***Woody dataset*** | | ***Herbaceous dataset*** | |
|---|---|---|---|---|---|---|
| **Variables** | ***r*** | ***P*-value** | ***r*** | ***P*-value** | ***r*** | ***P*-value** |
| Density of vessels ($DE_V$) | -0.8317 | **0.0028** | - 0.6519 | 0.2332 | - 0.6926 | 0.1949 |
| Vessel grouping index ($G_V$) | -0.8151 | **0.0040** | - 0.9722 | **0.0055** | -0.0889 | 0.887 |
| Intervessel pit aperture fraction ($F_{PA}$) | -0.4527 | 0.2475 | - 0.3498 | 0.5638 | 0.2346 | 0.7041 |
| Thickness of intervessel pit membrane ($T_{PM}$) | -0.8672 | **0.0011** | - 0.8440 | 0.0722 | 0.3651 | 0.5457 |
| Thickness-to-span ratio of vessels ($T_W$:$D_V$) | -0.4846 | 0.1558 | - 0.5660 | 0.3199 | - 0.038 | 0.9515 |
| Proportion of lignified area per total stem area ($P_{LIG}$) | -0.7952 | **0.0060** | 0.5333 | 0.3547 | - 0.4789 | 0.4144 |
| Proportion of xylem fiber wall per fiber ($P_{FW}F$) | -0.5785 | 0.080 | - 0.5277 | 0.3607 | - 0.2236 | 0.7177 |
| Hydraulically weighted vessel diameter ($D_{HV}$) | -0.3187 | 0.3693 | 0.4999 | 0.391 | - 0.5283 | 0.3601 |
| Density of rays ($DE_R$) | ----- | ----- | 0.3073 | 0.6149 | ----- | ----- |
| Height of rays ($H_R$) | ----- | ----- | -0.7540 | 0.141 | ----- | ----- |
| Proportion of ray area per wood area ($P_R$) | ----- | ----- | -0.8784 | **0.04997** | ----- | ----- |

**Table S3** • Measurements of stem anatomical characters of woody and herbaceous daisies. The average and the standard error is given for each species. For each feature we have measured at least 2 individuals per species, except for *Cladanthus mixtus,* for which we have measured 9 individuals for $P_{LIG}$ (Fig. 4 E) and 4 individuals for $T_{PM}$.

| Species | $P_{50}$ | $D_V$ | $D_{HV1}$ | $D_{HV2}$ | $DE_V$ | $G_V$ | $A_{PB}$ | $A_{PA}$ | $F_{PA}$ | $D_{PC}$ | $T_{PM}$ | $T_W$:$D_V$ |
|---|---|---|---|---|---|---|---|---|---|---|---|---|
| *Argyranthemum foeniculaceum* | -5.1 | 21.91 ± 0.58 | 27.62 ± 1.03 | 23.50 ± 0.79 | 182.6 ± 13.76 | 3.85 ± 0.25 | 11.09 ± 0.19 | 1.81 ± 0.07 | 0.16 ± 0.005 | 690.32 ± 50.36 | 485.10 ± 10.75 | 0.08 ± 0.008 |
| *Argyranthemum gracile* | -4.0 | 23.98 ± 0.81 | 33.93 ± 3.06 | 27.76 ± 1.33 | 170 ± 7.18 | 2.89 ± 0.18 | 11.13 ± 0.34 | 2.16 ± 0.1 | 0.19 ± 0.004 | 706.6 ± 27.63 | 405.73 ± 10.22 | 0.06 ± 0.004 |
| *Argyranthemum frutescens* | -3.7 | 21.51 ± 0.64 | 26.99 ± 3.90 | 23.69 ± 2.92 | 128 ± 7.33 | 2.87 ± 0.17 | 11.52 ± 0.24 | 1.66 ± 0.05 | 0.14 ± 0.003 | 799.69 ± 43.90 | 402.81 ± 9.84 | 0.09 ± 0.008 |
| *Argyranthemum adauctum* | -3.6 | 20.04 ± 0.79 | 29.51 ± 2.71 | 23.83 ± 2.64 | 186.5 ± 11.34 | 2.95 ± 0.17 | 12.05 ± 0.38 | 1.47 ± 0.05 | 0.13 ± 0.004 | 775.9 ± 29.14 | 446.66 ± 11.33 | 0.03 ± 0.002 |
| *Argyranthemum broussonetii* | -3.1 | 23.83 ± 0.95 | 34.29 ± 3.88 | 27.95 ± 4.09 | 108.4 ± 3.28 | 2.48 ± 0.16 | 9.87 ± 0.26 | 1.46 ± 0.06 | 0.15 ± 0.004 | 648.08 ± 33.81 | 372.37 ± 13.52 | 0.04 ± 0.004 |
| *Cladanthus mixtus* | -2.9 | 26.49 ± 0.51 | 32.89 ± 1.23 | 29.00 ± 1.11 | 150.4 ± 12.54 | 2.73 ± 0.12 | 10.49 ± 0.23 | 1.44 ± 0.05 | 0.14 ± 0.003 | 695.21 ± 17.96 | 269.18 ± 6.04 | 0.03 ± 0.002 |
| *Coleostephus myconis* | -2.3 | 19.61 ± 0.52 | 23.64 ± 3.75 | 21.13 ± 2.78 | 66.3 ± 3.09 | 1.94 ± 0.18 | 14.10 ± 0.5 | 1.60 ± 0.08 | 0.11 ± 0.004 | 667.04 ± 27.29 | 324.13 ± 10.19 | 0.05 ± 0.003 |
| *Leucanthemum vulgare* | -2.5 | 19.21 ± 0.50 | 22.80 ± 2.71 | 20.57 ± 2.59 | 65.2 ± 8.71 | 1.95 ± 0.11 | 17.02 ± 0.38 | 1.62 ± 0.06 | 0.09 ± 0.003 | 630.15 ± 38.90 | 350.55 ± 10.46 | 0.08 ± 0.005 |
| *Glebionis segetum* | -2.2 | 24.74 ± 0.65 | 30.26 ± 1.75 | 27.00 ± 0.53 | 89.3 ± 10.54 | 2.8 ± 0.15 | 11.63 ± 0.40 | 1.73 ± 0.14 | 0.13 ± 0.007 | 808.90 ± 25.04 | 317.92 ± 5.99 | 0.04 ± 0.002 |
| *Glebionis coronaria* | -2.1 | 20.43 ± 0.43 | 24.3 ± 0.9 | 21.81 ± 0.46 | 89.57 ± 2.64 | 2.53 ± 0.16 | 9.75 ± 0.23 | 1.65 ± 0.07 | 0.17 ± 0.005 | 658.52 ± 29.79 | 293.24 ± 8.54 | 0.03 ± 0.002 |

$D_V$ = diameter of vessels (μm); $D_{HV1}$ = hydraulically weighted vessel diameter (μm) measured following Sperry *et al*. (1994); $D_{HV2}$ = hydraulically weighted vessel diameter (μm) measured following Tyree & Zimmermann (2002); $DE_V$ = density of vessels; $G_V$ = vessel grouping index; $A_{PB}$ = intervessel pit border area ($\mu m^2$); $A_{PA}$ = intervessel pit aperture area ($\mu m^2$); $F_{PA}$ = intervessel pit aperture fraction; $D_{PC}$ = depth of intervessel pit chamber (nm) ; $T_{PM}$ = thickness of intervessel pit membrane (nm) ; $T_W$:$D_V$ = thickness-to-span ratio of vessels.

**Table S3 •** (continued). Measurements of stem anatomical characters of woody and herbaceous daisies. The average and the standard error is given for each species. For each feature we have measured at least 2 individuals per species, except for *Cladanthus mixtus*, for which we have measured 9 individuals for $P_{LIG}$ (Fig. 4 E) and 4 individuals for $T_{PM}$.

| Species | $P_{50}$ | $A_S$ | $A_{LIG}$ | $P_{LIG}$ | $A_{PITH}$ | $P_{PITH}$ | $A_F$ | $A_{FL}$ | $A_{FW}$ | $P_{FW}F$ | $H_R$ | $DE_R$ | $P_R$ |
|---|---|---|---|---|---|---|---|---|---|---|---|---|---|
| *A. foeniculaceum* | -5.1 | 29397191.2 ± 9475228.5 | 12597133.2 ± 8659116.3 | 0.74 ± 0.04 | 2359010.5 ± 520490.9 | 0.11 ± 0.04 | 204.02 ± 5.65 | 46.60 ± 2.52 | 157.42 ± 5.75 | 0.76 ± 0.1 | 349.26 ± 33.26 | 1.75 ± 0.47 | 0.160 ± 0.004 |
| *A. gracile* | -4.0 | 37673766.9 ± 5056492.2 | 17717336.2 ± 3514301.3 | 0.73 ± 0.02 | 6264299.3 ± 2108346 | 0.15 ± 0.06 | 177.46 ± 5.00 | 61.75 ± 2.85 | 115.71 ± 2.64 | 0.66 ± 0.01 | 348.53 ± 20.78 | 1.17 ± 0.33 | 0.14 ± 0.016 |
| *A. frutescens* | -3.7 | 45642855.9 ± 9139970.8 | 17324632.3 ± 8149853.4 | 0.81 ± 0.02 | 1558422.5 ± 399200.8 | 0.04 ± 0.01 | 205.17 ± 5.77 | 43.20 ± 2.19 | 161.97 ± 4.22 | 0.80 ± 0.01 | 283.04 ± 17.91 | 2.92 ± 0.41 | 0.10 ± 0.011 |
| *A. adauctum* | -3.6 | 16541287.3 ± 1826609.7 | 12962714.6 ± 1380611.3 | 0.78 ± 0.03 | 1220690.5 ± 274095.2 | 0.07 ± 0.009 | 228.01 ± 6.44 | 100.95 ± 4.18 | 127.06 ± 3.67 | 0.57 ± 0.05 | 320.34 ± 20.29 | 4 ± 0.88 | 0.05 ± 0.04 |
| *A. broussonetii* | -3.1 | 53064936.1 ± 7631596.5 | 11114672.4 ± 6961571.3 | 0.77 ± 0.03 | 5427081.2 ± 1072106.1 | 0.10 ± 0.03 | 238.86 ± 7.82 | 96.04 ± 5.22 | 142.82 ± 4.42 | 0.62 ± 0.05 | 186.96 ± 9.08 | 1.83 ± 0.30 | 0.04 ± 0.005 |
| *C. mixtus* | -2.9 | 34396035 ± 5444434.6 | 13273678.5 ± 2947597.8 | 0.37 ± 0.03 | 12673208.7 ± 2339536.1 | 0.38 ± 0.06 | 159.88 ± 3.63 | 59.08 ± 1.96 | 100.80 ± 2.37 | 0.64 ± 0.03 | ----- | ----- | ----- |
| *C. myconis* | -2.3 | 19545030.2 ± 7276406.2 | 3728437.1 ± 2313363.4 | 0.17 ± 0.05 | 10168878.4 ± 3881225.7 | 0.52 ± 0.006 | 155.82 ± 5.40 | 62.02 ± 3.23 | 93.79 ± 2.66 | 0.61 ± 0.008 | ----- | ----- | ----- |
| *L. vulgare* | -2.5 | 20383249.5 ± 5715925 | 8384101.0 ± 988726.3 | 0.22 ± 0.04 | 5066393.6 ± 1702767.8 | 0.24 ± 0.02 | 274.35 ± 10.31 | 106.75 ± 4.83 | 167.60 ± 6.33 | 0.61 ± 0.05 | ----- | ----- | ----- |
| *G. segetum* | -2.2 | 26805310.6 ± 3730745.6 | 7910803.1 ± 1588102.9 | 0.31 ± 0.10 | 13605533.1 ± 5203534.1 | 0.49 ± 0.13 | 243.89 ± 9.44 | 97.12 ± 4.60 | 146.77 ± 5.47 | 0.61 ± 0.01 | ----- | ----- | ----- |
| *G. coronaria* | -2.1 | 17654832.3 ± 2821748.7 | 4811821.3 ± 1011755.4 | 0.27 ± 0.01 | 9667072.0 ± 1115983.6 | 0.55 ± 0.02 | 158.55 ± 4.96 | 62.18 ± 2.94 | 96.37 ± 2.69 | 0.62 ± 0.04 | ----- | ----- | ----- |

$A_S$ = total stem area ($\mu m^2$); $A_{LIG}$ = lignified stem area ($\mu m^2$); $P_{LIG}$ = proportion of lignified area per total stem area; $A_{PITH}$ = pith area ($\mu m^2$); $P_{PITH}$ = proportion of pith per total stem area; $A_F$ = xylem fiber cell area ($\mu m^2$); $A_{FL}$ = xylem fiber lumen area ($\mu m^2$); $A_{FW}$ = xylem fiber wall area ($\mu m^2$); $P_{FW}F$ = proportion of xylem fiber wall per fiber; $H_R$ = height of rays ($\mu m$) ; $DE_R$ = density of rays ; $P_R$ = proportion of ray area per wood area.

*Chapter 5*

# Embolism resistance in stems of herbaceous Brassicaceae and Asteraceae is linked with differences in woodiness and precipitation

*Larissa Chacon Dória[1*], Cynthia Meijs[1], Diego Sotto Podadera[2], Marcelino del Arco[3], Erik Smets[1], Sylvain Delzon[4], Frederic Lens[1]*

*Adapted from*
**Annals of Botany** 124 (2019): 1 – 14. DOI: *10.1093/aob/mcy233.*

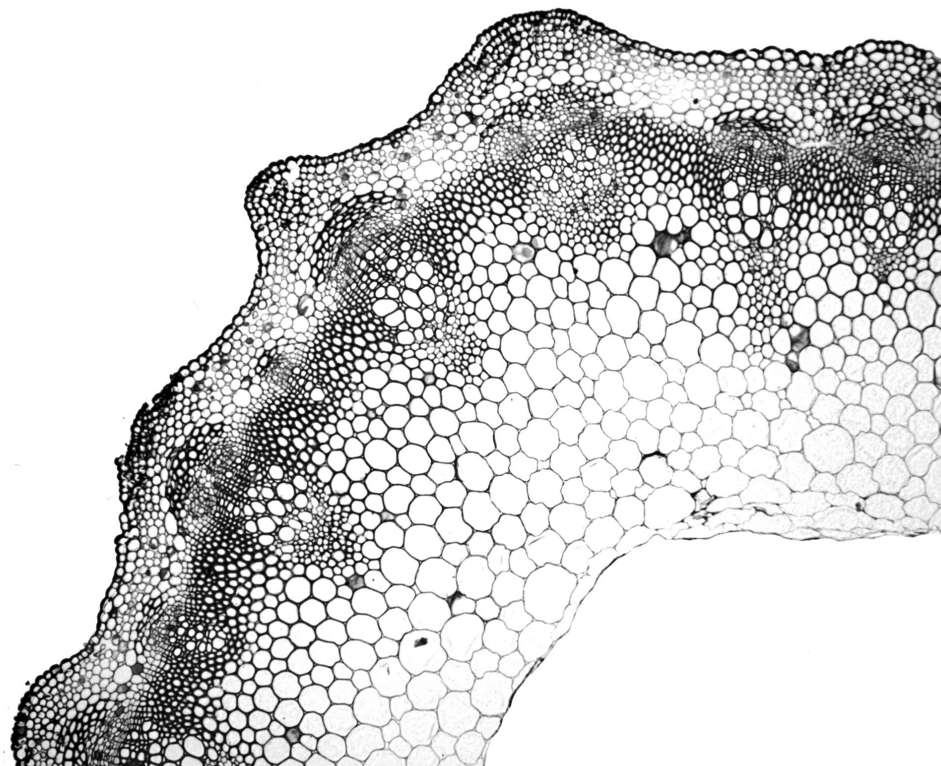

[1] Naturalis Biodiversity Center, Leiden university, P.O. Box 9517, 2300 RA Leiden, The Netherlands.

[2] Programa de Pós-Graduação em Ecologia, UNICAMP, Campinas, São Paulo, Brazil.

[3] Department of Plant Biology (Botany), La Laguna University, 38071 La Laguna, Tenerife, Spain.

[4] BIOGECO INRA, Univ. Bordeaux, 33615 Pessac, France.

*Author for correspondence: larissa.chacondoria@naturalis.nl

# Abstract

Plant survival under extreme drought events has been associated with xylem vulnerability to embolism (the disruption of water transport due to air bubbles in conduits). Despite the ecological and economic importance of herbaceous species, studies focusing on hydraulic failure in herbs remain scarce. Here, we assess the vulnerability to embolism and anatomical adaptations in stems of seven herbaceous Brassicaceae species occurring in different vegetation zones of Tenerife, Canary Islands, and merged them with a similar hydraulic-anatomical dataset for herbaceous Asteraceae from Tenerife. Measurements of vulnerability to xylem embolism using the in situ flow centrifuge technique along with light and transmission electron microscope observations were performed in stems of the herbaceous species. We also assessed the link between embolism resistance versus mean annual precipitation and anatomical stem characters. The herbaceous species show a two-fold variation in stem $P_{50}$ from -2.1 MPa to -4.9 MPa. Within *Hirschfeldia incana* and *Sisymbrium orientale*, there is also a significant stem $P_{50}$ difference between populations growing in contrasting environments. Variation in stem $P_{50}$ is mainly explained by mean annual precipitation as well as by the variation in the degree of woodiness (calculated as the proportion of lignified area per total stem area) and to a lesser extent by the thickness of intervessel pit membranes. Moreover, mean annual precipitation explains the total variance in embolism resistance and stem anatomical traits. The degree of woodiness and thickness of intervessel pit membranes are good predictors of embolism resistance in the herbaceous Brassicaceae and Asteraceae species studied. Differences in mean annual precipitation across the sampling sites affect embolism resistance and stem anatomical characters, being both important characters determining survival and distribution of the herbaceous eudicots.

Keywords: Canary Islands, drought, embolism resistance, herbaceous species, stem anatomy, thickness of intervessel pit membranes, woodiness, xylem hydraulics.

# Introduction

Hydraulic failure is one of the main physiological mechanisms associated with reductions in forest productivity and drought-induced tree mortality (Choat *et al.* 2012; Anderegg *et al.* 2016; Adams *et al.* 2017). Water movement inside the conduits is prone to dysfunction due to negative xylem pressures generating metastable conditions (Tyree & Sperry 1989; Tyree & Zimmermann 2002). With increasing drought stress, embolisms could propagate from a gas-filled conduit to a neighbouring functional conduit through interconduit pit membranes, potentially generating lethal levels of embolisms (Tyree & Zimmermann 2002; Brodribb *et al.* 2010; Brodersen *et al.* 2013). The vulnerability to xylem embolism can be measured by vulnerability curves, in which the percentage loss of hydraulic conductivity is plotted against the xylem pressure (Cochard *et al.* 2010, 2013). The $P_{50}$ value, referring to the negative pressure associated with 50% loss of hydraulic conductivity, is an often-cited proxy for plant drought resistance, although it does not present a critical threshold value for angiosperms (Urli *et al.* 2013; Adams *et al.* 2017).

There is considerable interspecific variation in $P_{50}$ across plant species, from -0.5 MPa up to -19 MPa, and the majority of studies show that species from dry environments are generally more resistant to embolism (more negative $P_{50}$) than species from wet environments (Choat *et al.* 2012; Lens *et al.* 2013a, 2016; Larter *et al.* 2015). Knowledge about intraspecific variation in $P_{50}$ remains scarce and provides contradicting results: it seems to be species-specific, but it can vary either considerable (Kolb & Sperry 1999; Choat *et al.* 2007; Corcuera *et al.* 2011; Nolf *et al.* 2014, 2016; Volaire *et al.* 2018; Cardoso *et al.* 2018), subtle (Holste *et al.* 2006; Martínez-Vilalta *et al.* 2009; Lamy *et al.* 2014; Ahmad *et al.* 2017), or even absent (Maherali *et al.* 2009; Wortemann *et al.* 2011) for woody as well as for herbaceous species.

There is vast body of literature available focusing on hydraulic conductivity and safety for hundreds of woody species (Maherali *et al.* 2004; Pittermann *et al.* 2010; Choat *et al.* 2012; Bouche *et al.* 2014; Gleason *et al.* 2016a,b). Herbs, on the other hand, remain poorly investigated: $P_{50}$ values of stems are available for less than 30 species, of which a minority are eudicots while most species are grasses (e.g. Mencuccini & Comstock 1999; Stiller & Sperry 2002; Kocacinar & Sage 2003; Holste *et al.* 2006; Maherali *et al.* 2009; Rosenthal *et al.* 2010; Lens *et al.* 2013a, 2016; Nolf *et al.* 2014, 2016; Skelton *et al.* 2017; Dória *et al.* 2018; Volaire *et al.* 2018). Based on this limited dataset, most herbaceous species studied so far are sensitive to embolism formation in their stems with a $P_{50}$ around -2.5 MPa. However, some of the grass stems studied are remarkably resistant to embolism formation (up to -7.5 MPa;), implying that both herbs and trees share the ability to support very

negative water potentials without embolism formation during drought stress (Lens *et al.* 2016).

In this study, we focus on the largely neglected research field of xylem hydraulics in herbaceous stems, despite the overwhelming occurrence of economically important herbaceous food crops (Monfreda *et al.* 2008) and the dependency of grazed grasslands for our livestock. The main reason for neglecting herb hydraulics is that their fragile stems and often low hydraulic conductance make vulnerability curves technically more challenging. However, recent fine-tuning of the high-throughput in situ flow centrifuge method (cavitron; Lens *et al.* 2016; Dória *et al.* 2018) and the new optical vulnerability technique (Skelton *et al.* 2017) have yielded stem $P_{50}$ data of herbaceous species, which opens up new opportunities to boost the virtually neglected aspect of herb hydraulics and predict future crop productivity and survival (Challinor *et al.* 2009), especially in a world facing climate change (Rahmstorf & Coumou 2012; Dai 2013).

In addition to the understudied aspect of herb hydraulics, we also investigate stem anatomical characters to assess poorly known structure-function relationships in herbaceous stems. Plant sensitivity to drought-induced embolism is determined by a whole suite of stem anatomical characters in woody trees (Hacke & Jansen 2009; Lens *et al.* 2011; Jacobsen *et al.* 2012; Pivovaroff *et al.* 2016; Pereira *et al.* 2017; O'Brien *et al.* 2017), of which the thickness of intervessel pit membranes is probably one of the most hydraulically relevant anatomical features, altering both water flow efficiency and the spread of potential lethal levels of embolism in the xylem (Jansen *et al.* 2009; Lens *et al.* 2011; Li *et al.* 2016; Gleason *et al.* 2016a; Dória *et al.* 2018). Furthermore, vessel diameter is an informative character determining xylem area-specific conductivity (Ks) (Hacke *et al.* 2016), but also correlates with plant height, environmental constraints and potentially embolism resistance (Davis *et al.* 1999; Olson & Rosell 2013; Schreiber *et al.* 2015; Hacke *et al.* 2016; Olson *et al.* 2018). Mechanical characters such as wood density, total degree of lignification, thickness-to-span ratio of vessels and thickness of the intervessel wall, have also been linked to increasing drought stress resistance (Hacke *et al.* 2001a; Jacobsen *et al.* 2005, 2007; Chave *et al.* 2009; Hoffman *et al.* 2011; Pratt & Jacobsen, 2017). These mechanical characters are often reported as indirectly linked to embolism resistance, since embolism formation and spread occurs at the pit level (Bouche *et al.* 2014; Pereira *et al.* 2017; Dória *et al.* 2018).

In herbaceous eudicots, an increase in embolism resistance is linked with an increase in wood formation, which reflects an increase in the proportion of lignified area per total stem area (Lens *et al.* 2013a, 2016; Tixier *et al.* 2013; Dória *et al.* 2018), and also grasses that are more resistant to embolism formation have more lignified stems compared to the more vulnerable species (Lens *et al.* 2016). Wood formation has been observed in many herbaceous eudicots, especially at the base

of the stem, and several studies show a continuous range in the degree of wood formation between stems of herbaceous eudicot species (Dulin & Kirchoff 2010; Schweingruber *et al.* 2011; Lens *et al.* 2012a; Kidner *et al.* 2016; Dória *et al.* 2018). This highlights the fuzzy boundaries between woodiness and herbaceousness, leading to intermediate life forms such as 'woody herbs' or 'half shrubs' (Lens *et al.* 2012a), but species with these intermediate life forms do not form a wood cylinder that extends towards the upper parts of the stem and are therefore considered as herbaceous (Kidner *et al.* 2016).

In this paper, we combine hydraulic measurements with detailed stem anatomical characteristics and climatic variables (from meteorological stations near the sampling sites) to investigate structure-function relationships in stems of seven herbaceous species belonging to the Brassicaceae family from the island of Tenerife (Canary Islands, Spain), and merged it with a similar dataset for four herbaceous Asteraceae species that were sampled on the same island for a previous publication (Dória *et al.* 2018). The main reason for selecting Tenerife is the huge range of climatic conditions in a small area of 2034 square kilometer, ranging from the humid northern laurel forests of Anaga to the dry southern desert-like region around El Médano, separated by the tall Teide volcano (ca 3700m asl) generating different altitudinal vegetation types (del-Arco *et al.* 2006). We address the following questions: 1) Do herbaceous species growing in drier environments have more embolism resistant stems, both across and within species? 2) What are the stem anatomical characters that explain the variation in embolism resistance amongst the species studied? 3) Is there any relationship between precipitation and both xylem vulnerability to embolism and anatomical characters?

# Materials and methods

## Plant material and climate data

We collected the Brassicaceae specimens throughout the island of Tenerife, in different vegetation zones with different mean annual precipitation and aridity indices. The climatic data of precipitation and temperature for each of the sampling sites were provided by Agencia Estatal de Meteorología (AEMET, Spanish Government), covering a period from 110 to 30 years depending on the meteorological station. We received the data from five different meteorological stations (Anaga San Andrés, Arico Bueno, Arafo, Laguna Instituto and Vilaflor) matching the five sampling sites [Supplementary Information Fig. S1]. We used the mean annual precipitation for each site, and calculated the potential evapotranspiration using the Thornthwaite equation (1948). The aridity indices were calculated as a ratio

of mean annual precipitation by mean annual potential evapotranspiration (UNEP 1997). Since this aridity index is highly correlated with mean annual precipitation ($P < 0.001$, $r = 0.993$) we opted to select the former in the statistical models.

The collection trip was carried out in March 2017, matching with the wet, flowering period of the herbaceous species. We harvested seven annual Brassicaceae species: *Hirschfeldia incana* (L.) Lagr.-Fossat, *Raphanus raphanistrum* L., *Rapistrum rugosum* L. All., *Sinapis alba* L., *Sinapis arvensis* L., *Sisymbrium erysimoides* Desf. and *Sisymbrium orientale* L. The time of germination is similar for all species studied and it is linked with the arrival of the rains in fall and winter. However, there can be small differences between populations, amongst and within species: populations growing on the northern slopes of the island generally germinate earlier than plants growing on the southern slopes due to the moist northeastern trade winds, and populations from higher altitudes usually germinate later than plants from lower altitudes.

The specimens of *H. incana* and *S. orientale* were collected from two different populations occurring in contrasting environments. The northern area of La Laguna (mean annual precipitation= 526.9 mm; aridity index = 0.68) and the southern area of Vilaflor (mean annual precipitation= 396.3 mm; aridity index = 0.53) were the wetter collection sites for *H. incana* and *S. orientale* populations, respectively. The drier sites were the southern areas of Guímar (mean annual precipitation = 311.8 mm; aridity index = 0.39) and the region of Arico Bueno (mean annual precipitation= 264.3 mm; aridity index = 0.34), for *H. incana* and *S. orientale*, respectively [Supplementary Information Fig. S1].

The four annual species of Asteraceae, *Cladanthus mixtus* (L.) Oberpr. & Vogt., *Coleostephus myconis* (L.) Cass., *Glebionis coronaria* (L.) Cass ex Spach and G*lebionis segetum* (L.) Fourr. included in this study were investigated by Dória *et al.* (2018), during the spring of 2016 in Tenerife in the area of La Laguna (mean annual precipitation= 526.9 mm; aridity index = 0.68), following the same methodological procedures described below. For both the Brassicaceae and Asteraceae species we harvested between 10 to 20 individuals per species. All the species studied are annual herbaceous species, but some species (especially *Sinapis alba* and *Sinapis arvensis*) show a tendency to become biannual, which may be a consequence of the release of seasonality compared to the European mainland (Carlquist 1974).

The entire individuals were collected from the soil, with roots still attached, quickly wrapped in wet tissues and sealed with plastic bags. Afterwards, the stems were stored in a cold room (around 5 °C) for maximum five days at the University of La Laguna, Tenerife. The sealed plastic bags were shipped by plane and immediately stored in a fridge for a maximum of two weeks at the caviplace facility to perform the hydraulic measurements (University of Bordeaux, France).

## Xylem vulnerability to embolism

One to three stems per individual from at least 10 individuals per species were used to measure vulnerability to embolism. Prior to measurements, all the stems were cut under water in the lab with a razor blade into a standard length of 27 or 42 cm in order to fit the two cavitron rotors used, and we confirmed that the vessels were shorter than the stem segments using the air pressure technique at 0.2 MPa. The cavitron is a modified centrifuge allowing to lower the negative pressure in the central part of the stem segment by spinning the stems at different speeds while simultaneously measuring the water transport in the vascular system (Cochard 2002; Cochard et al, 2013). First, the maximum hydraulic conductance of the stem in its native state (Kmax in $m^2$ $MPa^{-1}$ $s^{-1}$) was calculated under xylem pressure close to zero MPa using a reference ionic solution of 10 mM KCl and 1 mM CaCl2 in deionized ultrapure water. Then, rotation speed of the centrifuge gradually increased by -0.5 or -1 MPa to lower xylem pressure. The percentage loss of conductivity (PLC) of the stem was determined at each pressure step following the equation:

$$PLC = 100 * \left(1 - \frac{K}{K_{max}}\right) \quad \text{Eqn. 1}$$

where Kmax represents the maximum conductance of the stem and K represents the conductance associated at each pressure step.

The vulnerability curves, showing the change in percentage loss of conductivity according to the xylem pressure, were obtained using the Cavisoft software (Cavisoft v1.5, University of Bordeaux, Bordeaux, France). A sigmoid function (Pammenter and Van der Willigen, 1998) was fitted to the data from each sample, using the following equation with SAS 9.4 (SAS 9.4, SAS Institute, Cary NC):

$$PLC = \frac{100}{\left[1+exp\left(\frac{S}{25} * (P - P_{50})\right)\right]} \quad \text{Eqn. 2}$$

where S (% $MPa^{-1)}$ is the slope of the vulnerability curve at the inflexion point, P is the xylem pressure value used at each step, and $P_{50}$ is the xylem pressure inducing 50% loss of hydraulic conductivity. The parameters *S* and $P_{50}$ were averaged for each species.

## Stem anatomy

Light microscopy (LM), scanning electron microscopy (SEM) and transmission electron microscopy (TEM) were performed at Naturalis Biodiversity Center, the Netherlands, based on the samples for which we had obtained suitable vulnerability curves. The samples were taken from three individuals per species for LM and SEM, and from two individuals per species for TEM, from the middle part of the stem, where the negative pressure caused embolism formation during the cavitron experiment. The lab protocols for LM, SEM and TEM followed Dória *et al.* (2018). All the anatomical measurements were done using ImageJ (National Institutes of Health, Bethesda, USA), following largely the suggestions of Scholz *et al.* (2013) and IAWA Committee (1989).

Amongst the anatomical characters measured using LM, several indicators for lignification were calculated using a cross section, such as the proportion of lignified area per total stem area ($P_{LIG}$, measuring the sum of primary xylem area, secondary xylem (= wood) area and fibre caps area in the cortex and dividing it by the total stem area), the proportion of xylem fiber wall area per fiber area ($P_{FW}F_X$, at the level of a single cell), and the thickness-to-span ratio of vessels ($T_WD_V$). The diameter of vessels ($D_V$) was calculated based on the lumen area that was considered to be a circle according to the equation:

$$D_V = \sqrt{\frac{4A}{\pi}} \qquad \text{Eqn. 3}$$

where $D_V$ is the vessel diameter and A is the vessel lumen area. The hydraulically weighted vessel diameter ($D_H$) was calculated following the equation:

$$D_H = \frac{\sum D_V^5}{\sum D_V^4} \qquad \text{Eqn. 4}$$

where $D_V$ is the vessel diameter as measured in eqn. (3).

The ultrastructure of intervessel pits was observed using a field emission SEM (Jeol JSM-7600F, Tokyo, Japan) and a JEOL JEM 1400-Plus TEM (JEOL, Tokyo, Japan), as described in Dória *et al.* (2018). Since we observed intervessel pit membranes from the central stem segment parts where centrifugal force was applied, our measurements provide a relative estimation of intervessel pit membrane thickness.

## Statistical analyses

We tested the effect of both species and mean annual precipitation on the various hydraulic parameters ($P_{12}$, $P_{50}$, $P_{88}$ and slope) using an ANCOVA. A log transformation, when necessary, was applied to the predictive variables to deal with heteroscedasticity and/or non-normality (Zuur *et al.* 2007). A post-hoc Tukey's HSD test, from the R package Agricolae (Mendiburu 2017), was used to test whether hydraulic parameters differ amongst species. To test the difference in $P_{50}$ between the two Brassicaceae populations growing in contrasting environments (*Hirschfeldia incana* and *Sisymbrium orientale*), we used linear mixed effects model, with the factor species as random effect, from the nlme R package (Pinheiro *et al.* 2018).

We applied simple linear regressions to test for the relationship between $P_{50}$, climate data, and anatomical variables. A log transformation, when necessary, was performed to the predictive variables to deal with heteroscedasticity and/or non-normality (Zuur *et al.* 2007).

In order to evaluate which anatomical variables explain embolism resistance, we performed a multiple linear regression with $P_{50}$ as response variable and stem anatomical characters as predictive variables. We selected a priori the predictive variables using biological knowledge based on previously published studies in combination with a pairwise scatterplot to detect the presence of correlations and collinearities. Then, we conducted a variance inflation factor (VIF) analysis, keeping only variables with a VIF value lower than 2 (Zuur *et al.* 2010). Subsequently, we followed the model simplification removing each time the least significant variable, until all the remaining terms in the model were significant (Crawley 2007). The regression or differences were considered significant if $P < 0.05$. Next, we calculated the hierarchical partitioning (Chevan & Sutherland 1991) for the variables retained in the model in order to assess their relative importance to explain $P_{50}$.

Independent t-tests were used to compare stem anatomical differences between the two populations of Brassicaceae species collected in contrasting environments.

To test whether differences in mean annual precipitation for each sampling site ($P_R$) explained the combined variation of $P_{50}$ and the anatomical characters, including also these characters that were not retained in the multiple regression analysis (the proportion of xylem fiber wall area per fiber area as observed in a cross section, the thickness-to-span ratio of vessels, and the hydraulically weighted vessel diameter), we performed a permutational multivariate analysis of variance (PERMANOVA). The anatomical characters and $P_{50}$ are the response variables (rank transformed) and the mean annual precipitation is the predictive variable. PERMANOVA was performed using the adonis function in the Vegan R package (Oksanen *et al.* 2015), based on Euclidean distances and 999 permutations. Later,

a principal component analysis (PCA) was conducted using the function rda in the package Vegan, to observe simultaneously the relationships amongst the species, the main stem anatomical variables, the physiological variable ($P_{50}$) and the mean annual precipitation ($P_R$). We tested the relationship between some of the stem anatomical variables used in PCA with Pearson's coefficient correlation.

All analyses were performed using R version 3.4.3 (R Core Team 2017) in R Studio version 1.1.414 (R Studio Team 2016). All the differences were considered significant when $P < 0.05$.

# Results

### *Interspecific and intraspecific vulnerability to xylem embolism in the herbaceous stems*

The 11 herbaceous species studied show stem $P_{50}$ values varying two-fold from -2.1 MPa to -4.9 MPa (Fig. 1; Fig. 2 A; see Dória *et al*., 2018 for the vulnerability curves of Asteraceae species) [Supplementary Information Table S1]. The range of stem $P_{50}$ shows significant interspecific variation ($F = 27.161$, $P < 0.001$; Fig. 2 A), with no interaction between species and mean annual precipitation ($F = 2.948$, $P = 0.0901$) [Supplementary Information Table S3]. Species explain 70% of the variance, regardless the variation in mean annual precipitation for the sampling sites, while the mean annual precipitation ($P_R$) explains 30% of the variance, regardless the variation in species ($F = 16.689$, $P < 0.001$; Fig. 2 B) [Supplementary Information Table S3]. Likewise, significant interspecific variations are also observed for $P_{88}$ and $P_{12}$ ($F = 22.507$, $P < 0.001$; $F = 7.868$, $P < 0.001$, respectively) with part of both variations explained by $P_R$ ($F = 6.506$, $P < 0.05$; $F = 4.439$, $P < 0.05$ for $P_{88}$ and $P_{12}$, respectively). Variation in slope amongst the species studied is also significant ($F = 4.940$, $P < 0.001$), but the mean precipitation is not significant for this parameter ($F = 0.138$, $P = 0.712$).

The two Brassicaceae populations of *Hirschfeldia incana* and *Sisymbrium orientale* show significant intraspecific variation in $P_{50}$ ($P < 0.001$, $F = 17.6083$), showing that the contrasting environments are important to explain the intraspecific variation in $P_{50}$ (Fig. 3). For *H. incana*, the drier site receives on average 311.8 mm of mean annual precipitation (aridity index = 0.39), while the more humid site receives on average 526.9 mm (aridity index = 0.68). For *S. orientale*, the drier site has on average 264.3 mm of mean annual precipitation, and the more humid site 396.3 mm for the same period (aridity index = 0.34, 0.53; respectively) [Supplementary Information Fig. S1].

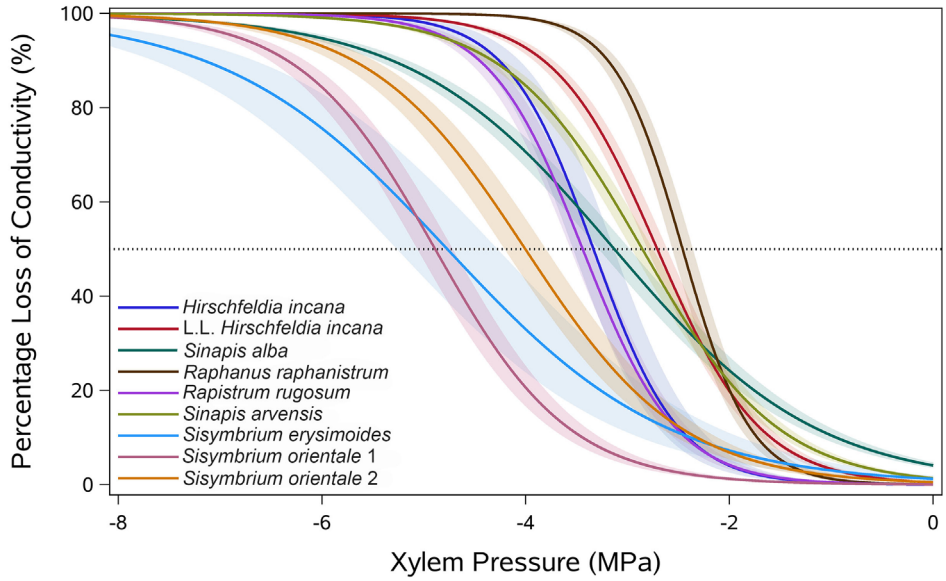


**Figure 1** • Mean vulnerability curves for each of the seven herbaceous Brassicaceae species studied native to different vegetation zones of Tenerife (Canary Islands), with reference to the sampling localities for *Hirschfeldia incana* and *Sisymbrium orientale*. Shaded bands represent $P_{50}$ standard errors, and 50% percentage loss of conductivity (PLC) is indicated by the horizontal dotted line. L.L. refers to the more humid population of *H. incana* collected in the city of La Laguna. The numbers 1 and 2 of *Sisymbrium orientale* refer to the populations collected in drier and more humid sites, respectively. See [Supplementary Information Fig S1].

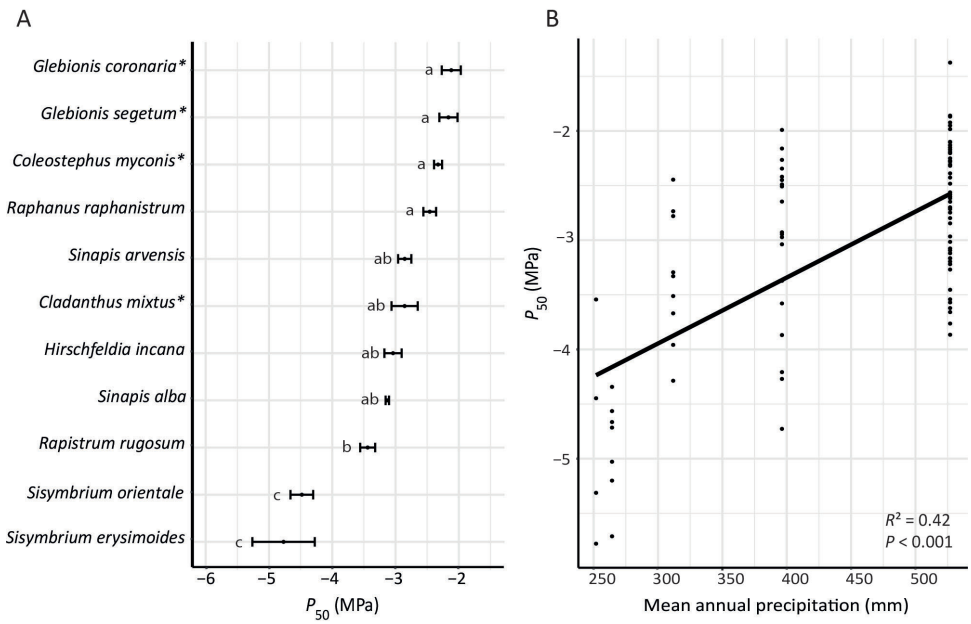


**Figure 2** • Range of stem $P_{50}$ amongst seven herbaceous Brassicaceae and four Asteraceae (represented with an asterix, data from Dória *et al.*, 2018) species from different vegetation zones in Tenerife (Canary Islands, Spain), and its relationship with mean annual precipitation. (A) Mean values of stem $P_{50}$ of the herbaceous Brassicaceae and Asteraceae species studied. Standard errors are represented by bars. Different letters indicate differences between species at $P < 0.05$. (B) Relationship between $P_{50}$ and mean annual precipitation at the individual level (on average six individuals per species). The adjusted $R^2$ and level of significance is given.

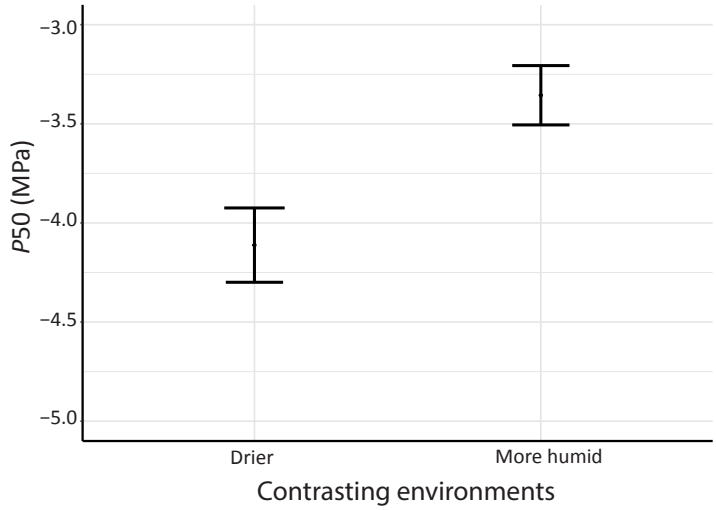


**Figure 3** • Intraspecific differences of mean stem $P_{50}$ between the two populations of the Brassicaceae *Hirschfeldia incana* and *Sisymbrium orientale* collected in contrasting environments (*H. incana*: mean annual precipitation = 311.8 mm; aridity index = 0.39 for the drier site, and mean annual precipitation = 526.9 mm; aridity index = 0.68 for the more humid site. *S. orientale*: mean precipitation = 264.3 mm; aridity index = 0.34 for the drier site, and mean annual precipitation = 396.3 mm; aridity index = 0.53 for the more humid site).

*Structure-function relationships in the herbaceous stems show correlation between embolism resistance and anatomy*

The stem anatomical variables that best explain the variation in $P_{50}$ are the proportion of lignified area per total stem area ($P_{LIG}$, which is a measure of stem woodiness) (Fig. 4) and the thickness of intervessel pit membrane ($T_{PM}$) (Fig. 5) ($P < 0.001$; $R^2 = 0.6783$) [Supplementary Information Tables S2, S4]. The $P_{50}$ - $P_{LIG}$ relationship remains significant for the separate datasets ($P < 0.001$; $R^2 = 0.58$ for Brassicaceae and $P < 0.01$; $R^2 = 0.48$ for Asteraceae), while the $P_{50}$ - $T_{PM}$ correlation disappears when analysing the Brassicaceae and Asteraceae datasets separately ($P = 0.2164$, $R^2 = 0.040$ vs $P = 0.6175$, $R^2 = -0.099$, respectively). In addition, $P_{LIG}$ is the main variable explaining 69% of the $P_{50}$ variation, while $T_{PM}$ explains the remaining 31% [Supplementary Information Tables S4].

The *S. orientale* population growing in the drier sampling site shows higher proportion of lignified area per total stem area ($P_{LIG}$), thicker intervessel pit membranes ($T_{PM}$) and thicker intervessel walls ($T_{VW}$) than the population growing in the more humid sampling site (Fig. 6; Table 1) [Supplementary Information Table S2]. No significant anatomical differences were found between the two populations of *H. incana* growing in contrasting environments.

All Brassicaceae observed have vestured pits (Fig. 5 B-D; Fig. 6 C-D), while these are absent in the Asteraceae species. No differences in the level of vesturing are observed amongst the embolism resistant vs vulnerable Brassicaceae species.

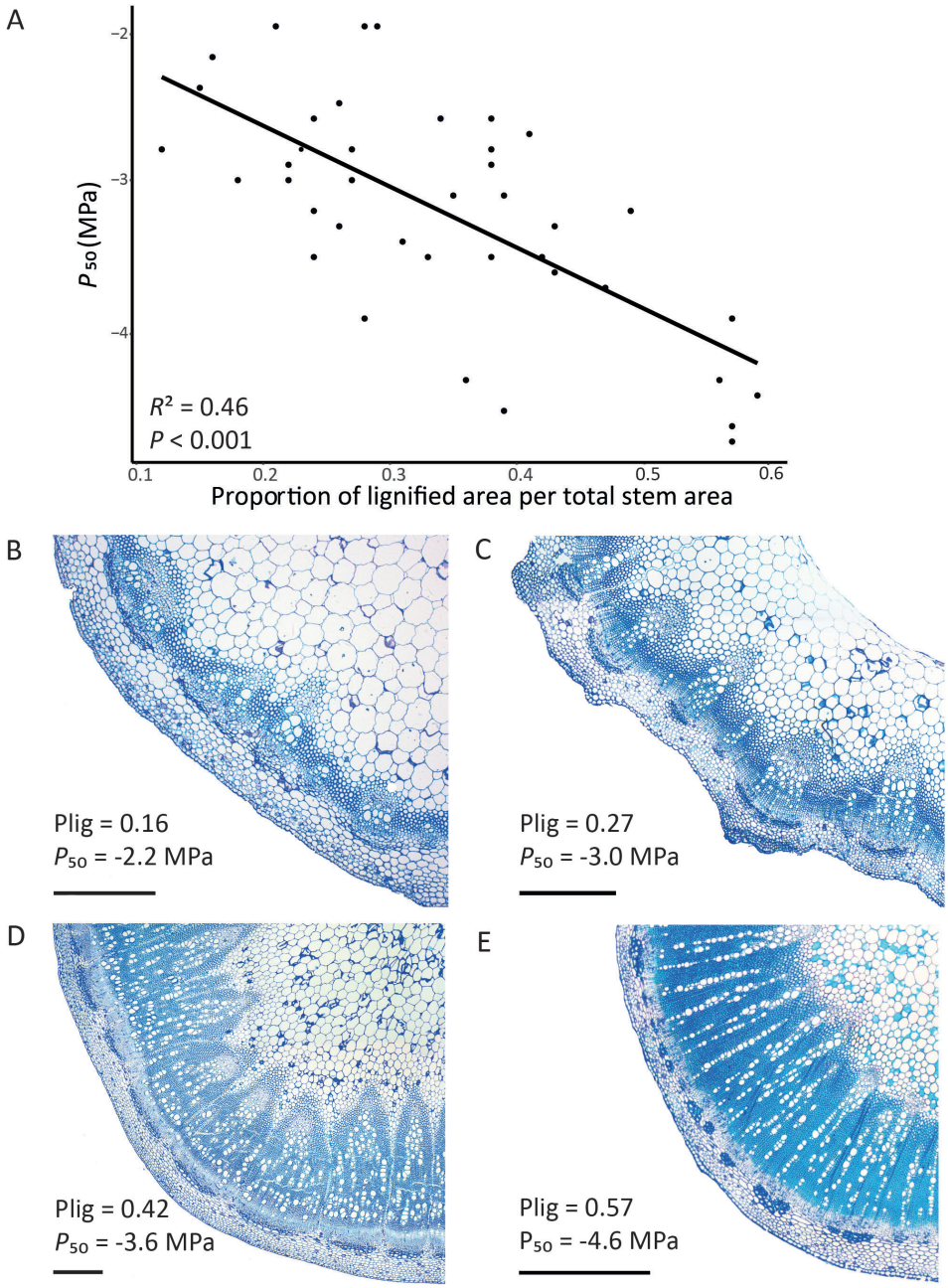


**Figure 4** • Relationships between stem $P_{50}$ and the proportion of lignified area per total stem area ($P_{LIG}$). (A) Linear regression between $P_{50}$ and $P_{LIG}$. The adjusted $R^2$ and the level of significance are given. Each dot represents one individual (on average 3 individuals per species). (B-E) Light microscope images of cross sections through the stem of Brassicaceae species showing an increase of $P_{LIG}$ matching with increasing in embolism resistance. (B) *Raphanus raphanistrum*. (C) *Sinapis alba*. (D) *Rapistrum rugosum*. (E) *Sisymbrium orientale* from the drier sampling site. The scale bars represent 500 µm.

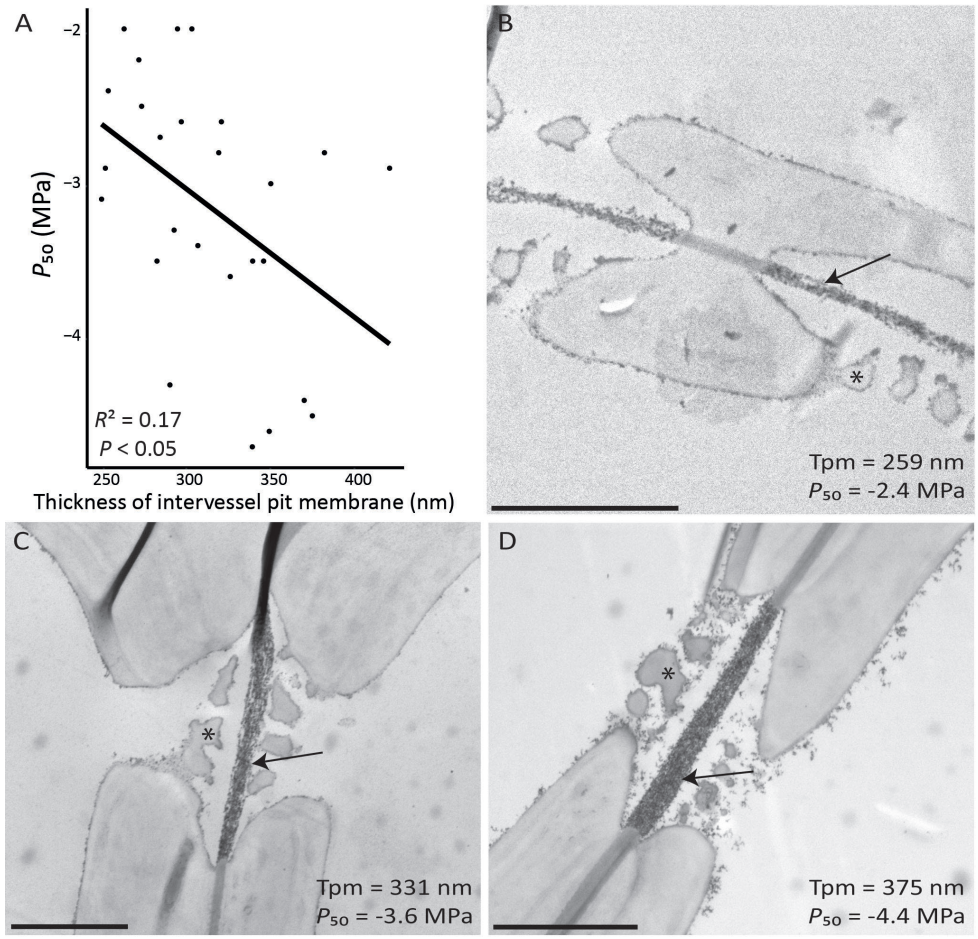


**Figure 5** • Relationships between stem $P_{50}$ and thickness of intervessel pit membrane ($T_{PM}$). (A) Linear regression between $P_{50}$ and $T_{PM}$. The adjusted $R^2$ and the level of significance are given. Each dot represents one individual (on average 2 individuals per species). (B-D) Transmission electron microscope images of intervessel pits of Brassicaceae species showing thicker pit membranes (arrows) in species that are more embolism resistant; all the herbaceous Brassicaceae species studied have vestures (asterisks). (B) *Raphanus raphanistrum*. (C) *Rapistrum rugosum*. (D) *Sisymbrium erysimoides*. Scale bars represent 2 μm.

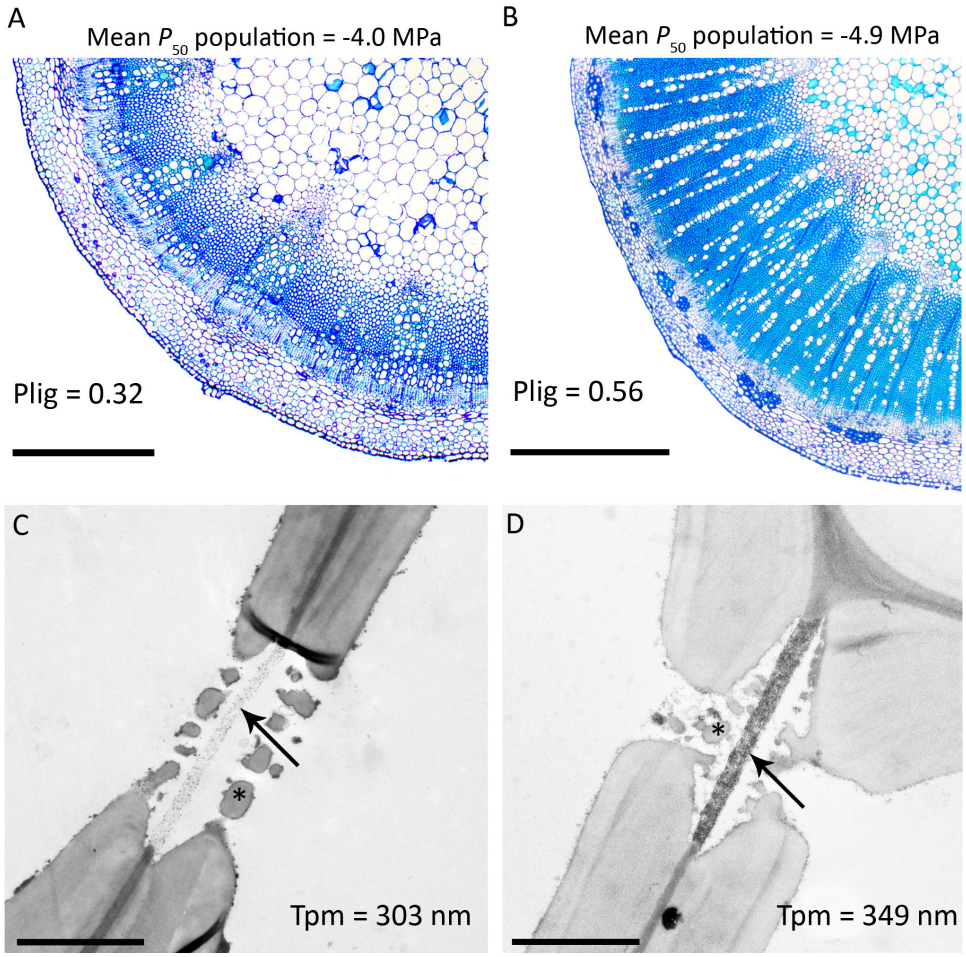


**Figure 6** • Intraspecific differences between two populations of *Sisymbrium orientale* growing in the more humid habitat (A,C) versus the drier sampling site (B,D). (A,B) Light microscope image of cross sections through the stems showing the population mean $P_{50}$ values and proportion of lignified area per total stem area ($P_{LIG}$). Scale bars represent 500 µm. (C,D) Transmission electron microscope images of intervessel pits showing the population mean of thickness of intervessel pit membrane ($T_{PM}$) (arrows). Vestures are marked with an asterisk. Scale bars represent 2 µm.

**Table 1** • Stem anatomical variables that showed significant t-test differences between the two populations of *Sisymbrium orientale* growing in contrasting environments (mean annual precipitation for the drier site is 264.3 mm, and 396.3 mm for the more humid site; the aridity indexes are 0.34, 0.53, respectively).

| Stem anatomical variable | Mean for *S. orientale* from the drier site | Mean for *S. orientale* from the more humid site | *t*-test (P value) |
|---|---|---|---|
| Proportion of lignified area per total stem area | 0.57 | 0.32 | 0.00763 |
| Thickness of intervessel pit membrane (nm) | 349.14 | 303.43 | 0.04231 |
| Thickness of intervessel wall (μm) | 3.70 | 3.31 | 0.01194 |

### *Relationship between mean precipitation ($P_R$), stem anatomy and $P_{50}$*

The PERMANOVA test shows that the mean annual precipitation explains the variation of both stem anatomical characters and $P_{50}$ ($F = 3.8098$, $R^2 = 0.14$, $P < 0.05$) [Supplementary Information Table S5].

When analyzing the association amongst stem anatomical characters, mean annual precipitation and $P_{50}$ using a principal component analysis (PCA), the first axis of the PCA explains 40% of the total variance observed, while the second axis explains 21%. The first principal component has large positive associations with $P_{50}$, and with mean annual precipitation ($P_R$), and negative associations with the proportion of lignified area per total stem area as observed in a cross section ($P_{LIG}$), the proportion of xylem fiber wall area per fiber area as observed in a cross section ($P_{FW}F_X$), and the thickness of intervessel pit membranes ($T_{PM}$) (Fig. 7). Along this first axis, the proportion of xylem fiber wall per fiber is correlated with $P_{50}$ ($P < 0.01$, $r = -0.45$). The second principal component has large positive association with the hydraulically weighted vessel diameter ($D_H$) and negative association with thickness-to-span ratio of vessels ($T_WD_V$). These two variables are negatively correlated with each other ($P < 0.01$, $r = -0.51$), but neither of them are correlated with embolism resistance ($P = 0.7608$, $r = -0.0525$; $P = 0.5662$, $r = -0.0988$). The thickness of the vessel is also not correlated with $T_WD_V$ ($P = 0.2811$, $r = 0.1846$). The individuals distributed at the right side of the multivariate PCA space are associated with less negative values of $P_{50}$ and higher mean annual precipitation. Some of these individuals present higher values of thickness-to-span ratio of vessels, while others have higher hydraulically weighted vessel diameters. Contrastingly, the individuals at the left side of the multivariate PCA space are associated with more negative values of $P_{50}$, more pronounced lignification characters, thicker intervessel pit membranes, and with lower mean annual precipitation (Fig. 7).

Individuals of the two Brassicaceae populations of *H. incana* (represented by circles) and *S. orientale* (represented by triangles) occupy different areas of the multivariate space (Fig. 7). The individuals collected in drier sites (empty circles for *H. incana* and empty triangles for *S. orientale*) are associated with higher degree of lignification characters, thicker intervessel pit membranes and lower values of mean annual precipitation (Fig. 7). The individuals collected in more humid sites (filled circles for *H. incana* and filled triangles for *S. orientale*) are associated with higher hydraulically weighted vessel diameter and higher values of thickness-to-span-ratio of vessels (Fig.7).

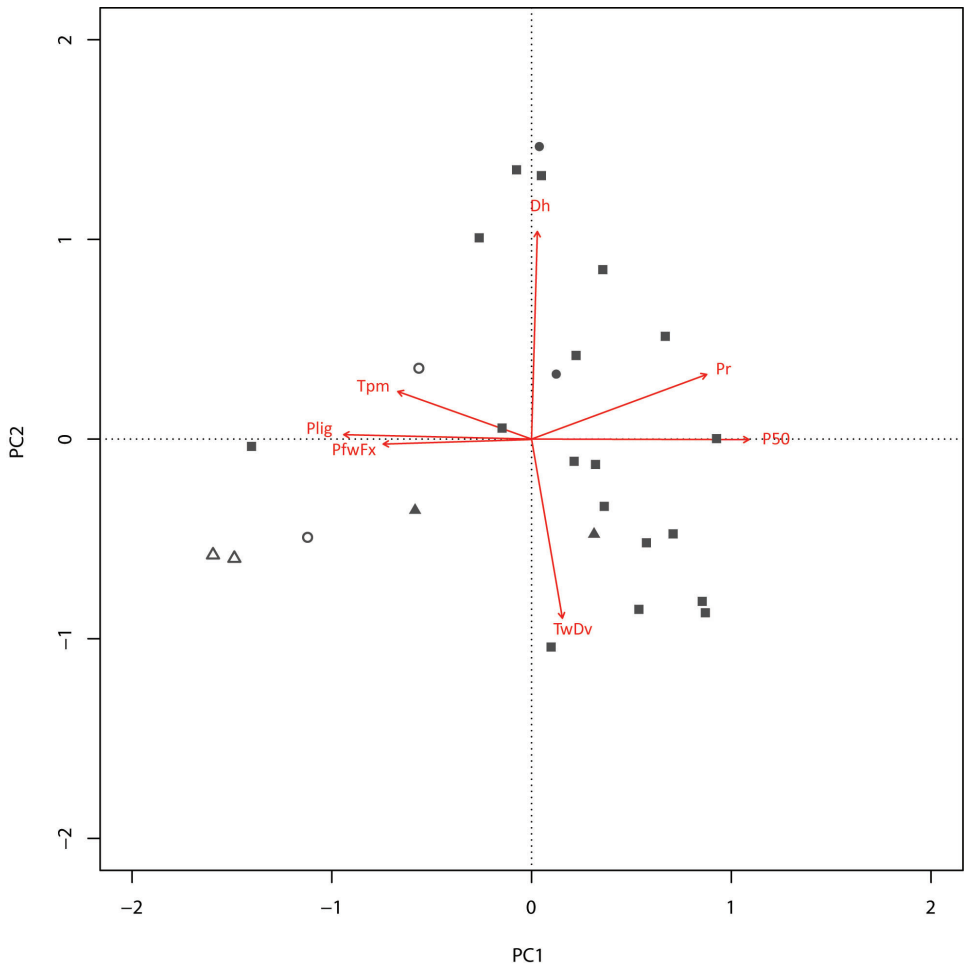


**Figure 7** • Principal component analysis of stem anatomical characters, mean annual precipitation and $P_{50}$ on the first two axes. $P_{LIG}$= proportion of lignified area per total stem area as observed in a cross section; $P_{FW}F_X$ = proportion of xylem fiber wall area per fiber area as observed in a cross section; $P_R$ = mean annual precipitation; $T_{IW}D_V$ = thickness-to-span ratio of vessels; $P_{50}$ = pressure inducing 50% loss of hydraulic conductivity ; $D_H$ = hydraulically weighted vessel diameter; $T_{PM}$ = thickness of intervessel pit membrane. Circles represent individuals of *H. incana* from humid (filled) and dry (open) sampling sites, while triangles refer to individuals of *S. orientale* from the humid (filled) and dry (open) sites. The squares represent the other individuals of Brassicaceae and Asteraceae studied.

# Discussion

### *Interspecific and intraspecific stem $P_{50}$ variation across herbaceous eudicots is strongly linked with precipitation*

Our dataset, including 11 herbaceous species of Brassicaceae and Asteraceae from five different habitats of Tenerife with a mean annual precipitation from 252 mm to 527 mm, shows a two-fold range of stem $P_{50}$ values that match the precipitation values of the sampling sites: the most vulnerable species ($P_{50}$: -2.1 MPa) was collected from wetter environments and the most resistant species ($P_{50}$: -4.9 MPa) was sampled from drier vegetation types (Fig. 1, 2). The explanatory power of mean annual precipitation towards stem $P_{50}$ supports the functional relevance of resistance to xylem embolism as an adaptive response to water deficit, as has been repeatedly demonstrated for woody trees (Maherali *et al.* 2004; Blackman *et al.* 2012; Choat *et al.* 2012) and to a lesser extent also herbs (mainly grasses, Lens *et al.* 2016). Likewise, the intraspecific (between-populations) differences in stem $P_{50}$ for both *Sisymbrium orientale* and *Hirschfeldia incana* (Fig. 3) are also explained by mean annual precipitation: for both species, the more embolism resistant populations occur in areas with less annual precipitation. This suggests that differences in habitat amongst herbaceous populations from the same species can increase the intraspecific plasticity in $P_{50}$.

### *Percentage of lignified area per total stem area ($P_{LIG}$) outcompetes intervessel pit membrane ($T_{PM}$) as explanatory variable explaining variation in stem $P_{50}$*

The percentage of lignified area per total stem area ($P_{LIG}$), which is mainly defined by the amount of woodiness in the herbaceous stems as observed in a cross section, is the character that best explains the variation of embolism resistance in stems, with more lignified stems being more resistant to embolism (Fig. 4). Since the germination time of the herbaceous species on Tenerife does more or less converge after the arrival of the rains in fall and winter, we believe that the differences in woodiness is species- and/or niche-specific rather than dependent on major differences in stem age between species. For example, the three species (*Raphanus raphanistrum*, *Sinapis arvensis* and the population of *Sisymbrium orientale* from more humid area) collected in Vilaflor village (sampling site 4 of Supplementary Information, Fig. S1) show a two-fold difference in the degree of woodiness matching nicely with stem $P_{50}$, despite the fact that these three populations occurred along the same road [Supplementary Information, Tables S1, S2]. The relationship between characters related to higher stem lignification and higher absolute values of $P_{50}$ has been recorded for different plant groups, both in woody (Jacobsen *et al.* 2005; Hacke *et al.* 2001a; Jansen *et al.* 2009; Pereira *et al.* 2017), and in her-

baceous lineages (Lens *et al.* 2012b; Tixier *et al.* 2013; Lens *et al.* 2013a, 2016) and in closely related woody lineages that are derived from herbaceous relatives (Dória *et al.* 2018). Differences in the proportion of the lignified area in the stem is also found at intraspecific level in this study, with the more resistant population of *S. orientale* showing thicker intervessel walls and higher $P_{LIG}$ values compared to those of the more vulnerable population (Fig. 6; Table 1). The higher $P_{LIG}$ values in the drier population could also be strengthened by the presumably earlier germination time in the area of El Escobonal (470 m asl), which is about 900 m lower than the colder (and wetter) site of Vilaflor (1400m asl), making the stems of the drier (and lower) site older, enabling them to lignify more.

It is challenging to functionally relate increased stem lignification with embolism resistance, since most lignification characters do not directly influence embolism formation and spread in the 3D network of angiosperm vessels. Indeed, the thickness of intervessel pit membranes ($T_{PM}$) is more likely to affect the length of the tortuous and irregularly shaped pores that air-water menisci need to cross before air-seeding may occur, explaining the spread of embolism through intervessel pit membranes into adjacent conduits (Jansen *et al.* 2009; Lens *et al.* 2011, 2013; Li *et al.* 2016). Although the $P_{50}$ - $T_{PM}$ relationship is confirmed in our herbaceous eudicot dataset (Fig. 5), $T_{PM}$ provides a much lower explanatory power to explain differences in $P_{50}$ compared to the degree of woodiness as observed in a cross section, calculated as the percentage of lignified area per total stem area ($P_{LIG}$). This may seem surprising, but studies investigating the relationship between stem $P_{50}$ and $T_{PM}$ amongst herbaceous species are scarce and the functional relevance of $T_{PM}$ in herbs might be less important compared to woody species. Few examples that suggest this poor $P_{50}$ -$T_{PM}$ relationship in herbs are: the $P_{50}$ - $T_{PM}$ relationship disappears in our study when only including the Brassicaceae species, no link between $P_{50}$ and $T_{PM}$ was found in a grass dataset based on four species with contrasting $P_{50}$ values (Lens *et al.* 2016), and a third study investigating closely related herbaceous and woody daisies showed that the $P_{50}$ - $T_{PM}$ relationship was retrieved only when the herbaceous dataset was combined with the woody dataset (Dória *et al.* 2018). Evidently, more work on stem $P_{50}$ and additional anatomical measurements based on the same - properly fixated - herbaceous stems are needed to shed more light into the functional relevance of $T_{PM}$ in herbs, which should in theory match the hydraulic importance of $T_{PM}$ as observed in shrubs and trees (Li *et al.* 2016).

Relationships between increased lignification and thicker intervessel pit membranes have been reported, which could explain the indirect correlation between higher lignification and higher embolism resistance (Jansen *et al.* 2009; Li *et al.* 2016; Dória *et al.* 2018). These findings are in accordance with our results for the two populations of *S. orientale* collected in contrasting environments (Table 1; Fig. 6): the more resistant population shows higher proportion of lignified area in the

stem, thicker intervessel walls, and thicker intervessel pit membranes. However, the $T_{PM}$ - lignification correlation disappears in our entire dataset (including Asteraceae and Brassicaceae species), showing that increased lignification characters are not necessarily linked to thicker intervessel pit membranes.

### *The mean precipitation explains both $P_{50}$ and anatomical variation in stems of herbaceous eudicots*

Mean annual precipitation explains both the variation in stem $P_{50}$ and the variation in stem anatomical characters across the herbaceous species studied. It has been well documented that environmental factors influence $P_{50}$ (Maherali *et al.* 2004; Choat *et al.* 2012; Trueba *et al.* 2017) as well as anatomical traits (Carlquist 1975; Baas *et al.* 1983; Lens *et al.* 2004; Dória *et al.* 2016; O'Brien *et al.* 2017). In our study, populations from drier sites show stems with more negative $P_{50}$ values and more pronounced lignification, such as the proportion of lignified area per total stem area (measure of amount of woodiness) and the proportion of xylem fiber wall area per fiber area as observed in a cross section. These characters are most associated with the first PCA axis (Fig. 7).

Our results show that the common pattern observed for woody species, i.e., shift in rainfall patterns associated with survival and distribution of trees and shrubs (Engelbrecht *et al.* 2007; Allen *et al.* 2010; Trueba *et al.* 2017), and drought-induced tree mortality associated with substantial loss of hydraulic conductivity across taxa and biomes (Adams *et al.* 2017), is also true for herbaceous species (see also first section of discussion). At the same time, different environment conditions also impact stem anatomical characters allowing plants to adapt to changing climates (Carlquist 1975; Baas *et al.* 1983; Martinez-Vilalta *et al.* 2010; Kattge *et al.* 2011).

Across woody trees, a lineage-specific subset of stem anatomical traits can be linked with drought-induced embolism resistance, such as increased wood density (linked to fiber wall thickness in angiosperms; Chave *et al.* 2009; Zieminska *et al.* 2013), increased thickness-to-span ratio of conduits (Hacke *et al.* 2001a; Bouche *et al.* 2014), thicker intervessel pit membranes (Jansen *et al.* 2009; Lens *et al.* 2011; Li *et al.* 2016; Dória *et al.* 2018) and narrower vessel diameters (Poorter *et al.* 2010; Hacke *et al.* 2016; Olson *et al.* 2018). Amongst herbaceous species, fragile stems also need to be reinforced by a suite of mechanical characters as shown in our study: individuals occurring in drier areas show higher degree of lignification/woodiness ($P_{LIG}$) and thicker intervessel pit membranes (Fig. 7) (see previous section). The increment of cellular support against implosion is often cited as the reason for this hydraulic-mechanical trade-off, which can result from either an increase in vessel wall to lumen ratio (Hacke *et al.* 2001a; Jacobsen *et al.* 2007; Cardoso *et al.* 2018) or an increase in fiber matrix support (more and thicker-walled xylem fibers) (Jacobsen *et al.* 2005, 2007; Pratt & Jacobsen 2017; Dória *et al.* 2018).

For the herbaceous species studied here, we found the latter relationship, demonstrated by the correlation between higher proportion of xylem fiber cell wall per fiber ($P_{FW}F_X$) and more negative $P_{50}$. Both kinds of cellular reinforcements, due to either vessel wall reinforcements or a more pronounced surrounding fiber matrix, would result in increasing xylem density offering support against implosion. In accordance with this hydraulic-mechanical trade-off, collapse of xylem conduits was only observed in cells that lack a robust support of fiber matrix, for instance in leaves (Cochard *et al.* 2004; Brodribb & Holbrook 2005; Zhang *et al.* 2016) and in low-lignin stems of poplar mutants (Kitin *et al.* 2010). Our study confirms that increasing the mechanical strength of fragile herbaceous stems using a suite of lignification characters may be highly relevant to require a higher level of embolism resistance.

Another aspect of the hydraulic-mechanical relationship in our dataset is highlighted by the negative correlation between the thickness-to-span ratio of vessels ($T_WD_V$), determining the resistance to implosion of the conduit, and the hydraulically weighted vessel diameter ($D_H$). Since there is a significant relationship between $T_WD_V$ and $D_H$, but not between $T_WD_V$ and the thickness of the vessel wall ($T_{VW}$), it can be concluded that vessel diameter impacts much more the variation of $T_WD_V$ than the thickness of vessel wall. It is known that larger vessel lumina increase hydraulic conductivity (Tyree & Zimmerman, 2002), and because in our dataset vessel wall thickness remains more or less the same, it gives rise to larger vessels that become mechanically weaker and potentially more vulnerable (Preston *et al.* 2006; Zanne *et al.* 2010; Pratt & Jacobsen 2017). However, in our dataset, $P_{50}$ is not correlated with $D_H$, not with $T_{VW}$, nor with $T_WD_V$, meaning that vessel diameter and thickness-to-span ratio of vessels do not impact embolism resistance in our herbaceous dataset.

In conclusion, this study investigated structure-function relationships in stems of seven herbaceous Brassicaceae occurring in different vegetation zones across the island of Tenerife and merged it with a similar dataset for herbaceous Asteraceae growing on the same island. The two-fold difference in embolism resistance found here shows that stems of herbaceous eudicots are able to deal with a range of negative pressures inside xylem conduits, although the $P_{50}$ range in woody trees remains considerably higher. In addition, mean annual precipitation is the major determinant influencing both embolism resistance and anatomical characters in the herbaceous stems, demonstrating the predictive value of both characters with respect to survival and distribution of herbs along environmental gradients. This improves our understanding of the evolutionary and ecological significance of embolism resistance in non-woody species. Our results also show that the degree of woodiness ($P_{LIG}$) outcompetes the thickness of intervessel pit membranes ($T_{PM}$) as the most powerful character determining embolism resistance in stems of herbaceous eudicots studied. This may question the hydraulic relevance of $T_{PM}$ in herbs,

although many more observations on embolism resistance and anatomical observations on herbaceous plants need to be carried out before a final conclusion can be reached.

## Funding

This work was supported by the CNPq - Conselho Nacional de Desenvolvimento Científico e Tecnológico, Brazil [PROC. N 206433/2014-0)], the Alberta Mennega Stichting, the Cluster of Excellence COTE (ANR-10-LABX-45, within the DEFI project) and the programme 'Investments for the Future' (ANR-10-EQPX-16, XYLOFOREST) funded by the French National Agency for Research.

## Acknowledgements

We thank the Cabildo de Tenerife (AFF 147/13 Nº Sigma: 2013-00748; AFF 429/13 Nº Sigma: 2013-02030; AFF 149/15 Nº Sigma: 2015-00925; AFF 85/16 Nº Sigma: 2016-00838) and Teide National Park (Nº 152587, REUS 27257, 2013; Nº 536556, REUS 83804, 2013; Res. Nº 222/2015) for the collection permits, and the AEMET - Agencia Estatal de Meteorología, Spanish Government, for providing meteorological data. We also acknowledge the technical support of R. Langelaan, W. Star and G. Capdeville.

# Supplementary Information

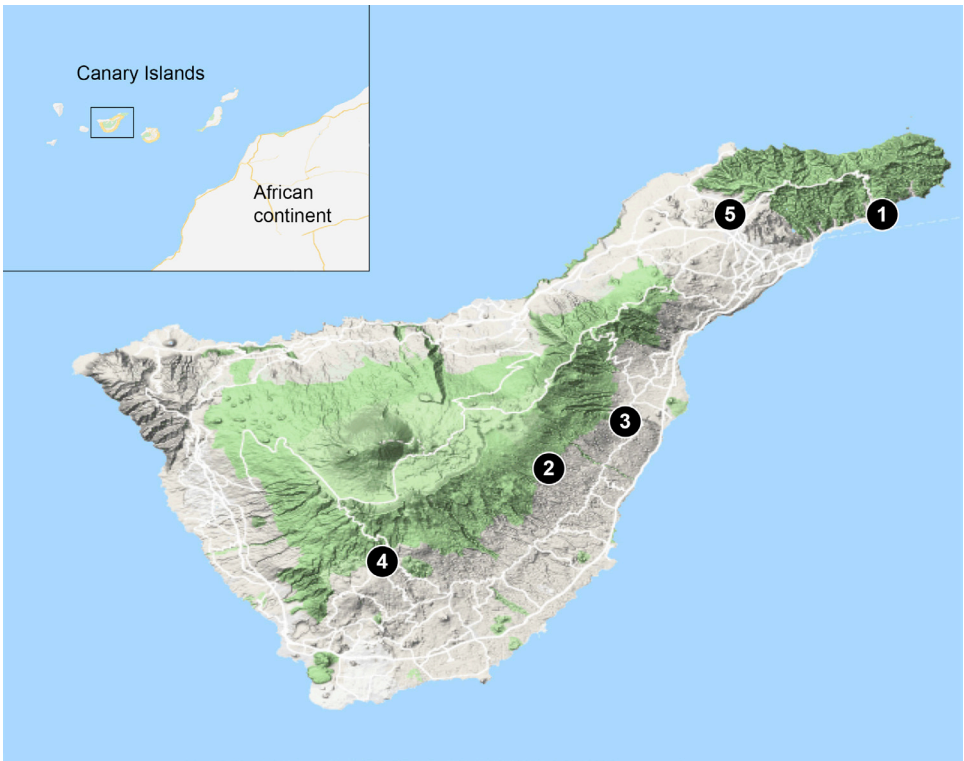


**Figure S1** • Map of Tenerife with the five sampling sites, each corresponding to unique aridity indices (AI). 1 – San Andrés village, sampling site of *Sisymbrium erysimoides* (AI = 0.27); 2 – El Escobonal region, sampling site of the drier population of *Sisymbrium orientale* (AI = 0.34); 3 – Guímar municipality, sampling site of the drier population of *Hirschfeldia incana* (AI = 0.39); 4 – Vilaflor village, sampling site of the more humid population of *Sisymbrium orientale*, *Raphanus raphanistrum* and *Sinapis arvensis* (AI = 0.53); 5 – La Laguna town, sampling site of the more humid population of *Hirschfeldia incana*, *Rapistrum rugosum*, *Sinapis alba* and the four Asteraceae species *Cladanthus mixtus, Coleostephus myconis, Glebionis coronaria* and *Glebionis segetum* (AI = 0.68).

**Table S1** • Hydraulic parameters of the herbaceous Brassicaceae species studied. Mean value and standard error are given. For the Asteraceae species, see Dória *et al.* (2018).

| Species | $P_{50}$ (MPa) | $P_{12}$ (MPa) | $P_{88}$ (MPa) | Slope (%MPa$^{-1}$) | $K_{MAX}$ (m$^2$MPa$^{-1}$s$^{-1}$) |
|---|---|---|---|---|---|
| *Hirschfeldia incana* (population from drier area) | -3.3±0.20 | -2.3±0.18 | -4.4±0.31 | 59.3±11.36 | 0.004062882±0.003005135 |
| Hirschfeldia incana (population from more humid area) | -2.7±0.10 | -1.6±0.16 | -3.8±0.14 | 49.3±5.68 | 0.008323244±0.005518186 |
| *Sinapis alba* | -3.1±0.15 | -1.1±0.20 | -5.2±0.28 | 25.2±2.50 | 0.036192619±0.015321967 |
| *Sisymbrium erysimoides* | -4.8±0.49 | -2.3±0.10 | -7.2±0.95 | 23.0±4.98 | 4.19464E-05±2.04684E-05 |
| *Raphanus raphanistrum* | -2.5±0.10 | -1.7±0.15 | -3.2±0.11 | 75.0±9.33 | 7.17684E-05±1.90366E-05 |
| *Sisymbrium orientale* (population from drier area) | -4.9±0.17 | -2.9±0.50 | -6.9±0.36 | 37.9±10.82 | 0.00022239±2.71079E-05 |
| *Sisymbrium orientale* (population from more humid area) | -4.0±0.20 | -2.4±0.34 | -5.6±0.13 | 32.6±3.73 | 0.00031542±4.08823E-05 |
| *Rapistrum rugosum* | -3.4±0.12 | -2.2±0.25 | -4.7±0.28 | 54.3±15.29 | 0.080916805±0.032345281 |
| *Sinapis arvensis* | -2.9±0.10 | -1.5±0.14 | -4.2±0.11 | 37.4±1.77 | 0.015427343±0.007817781 |

$P_{50}$ = pressure inducing 50% loss of hydraulic conductivity; $P_{12}$ = pressure inducing 12% loss of hydraulic conductivity; $P_{88}$ = pressure inducing 88% loss of hydraulic conductivity; Slope = indicator of the speed at which embolism affect the stem; $K_{MAX}$ = maximum hydraulic conductance measured under xylem pressure close to zero.

**Table S2** • Stem anatomical measurements of the herbaceous Brassicaceae species studied, along with the aridity indices and values for mean annual precipitation. Mean values and standard deviation are given. For the Asteraceae species, see Dória *et al.* (2018).

| Individuals | $P_{LIG}$ (µm) | $F_{AP}$ | $T_{PM}$ (nm) | $D_H$ (µm) | $P_{FW}F_X$ | $T_{VW}$ (µm) | $T_WD_V$ | AI | $P_R$ (mm) |
|---|---|---|---|---|---|---|---|---|---|
| *Hirschfeldia incana* 1 (Population from drier area) | 0.33 | 0.24±0.05 | 350.81±77.82 | 36.14 | 0.68±0.08 | 3.51±0.57 | 0.02±0.01 | 0.39 | 311.80 |
| *Hirschfeldia incana* 2 (Population from drier area) | 0.39 | 0.20±0.05 | 379.81±72.99 | 25.89 | 0.72±0.08 | 3.70±0.84 | 0.03±0.02 | 0.39 | 311.80 |
| *Hirschfeldia incana* 3 (Population from drier area) | 0.26 | 0.26±0.05 | - | 38.49 | 0.62±0.11 | 3.82±0.67 | 0.02±0.01 | 0.39 | 311.80 |
| *Hirschfeldia incana* 1 (Population from more humid area) | 0.27 | 0.27±0.04 | 386.98±70.91 | 43.58 | 0.67±0.09 | 4.37±0.83 | 0.01±0.006 | 0.68 | 526.90 |
| *Hirschfeldia incana* 2 (Population from more humid area) | 0.38 | 0.17±0.04 | 301.89±51.17 | 32.64 | 0.71±0.06 | 4.36±1.17 | 0.02±0.02 | 0.68 | 526.90 |
| *Hirschfeldia incana* 3 (Population from more humid area) | 0.35 | 0.20±0.03 | - | 37.42 | 0.84±0.07 | 4.06±0.82 | 0.02±0.02 | 0.68 | 526.90 |
| *Sinapis alba* 1 | 0.27 | 0.18±0.05 | 355.09±86.87 | 39.40 | 0.55±0.01 | 3.66±0.76 | 0.02±0.006 | 0.68 | 526.90 |
| *Sinapis alba* 2 | 0.38 | 0.16±0.04 | 344.31±58.05 | 42.45 | 0.54±0.11 | 3.80±0.60 | 0.01±0.004 | 0.68 | 526.90 |
| *Sinapis alba* 3 | 0.24 | 0.16±0.04 | - | 26.64 | 0.63±0.08 | 3.32±0.63 | 0.03±0.03 | 0.68 | 526.90 |
| *Sisymbrium erysimoides* 1 | 0.59 | 0.19±0.04 | 374.95±92.04 | 29.64 | 0.64±0.08 | 4.19±1.00 | 0.02±0.02 | 0.27 | 251.90 |
| *Sisymbrium erysimoides* 2 | 0.24 | 0.23±0.06 | - | 19.28 | 0.62±0.08 | 3.23±0.83 | 0.04±0.03 | 0.27 | 251.90 |
| *Sisymbrium erysimoides* 3 | 0.20 | 0.26±0.06 | 372.97±83.35 | 18.74 | 0.65±0.08 | 3.37±0.72 | 0.06±0.04 | 0.27 | 251.90 |
| *Raphanus raphanistrum* 1 | 0.15 | 0.25±0.07 | 258.46±56.18 | 18.27 | 0.52±0.10 | 2.51±0.44 | 0.02±0.01 | 0.53 | 396.30 |
| *Raphanus raphanistrum* 2 | 0.16 | 0.17±0.05 | 276.65±57.50 | 39.87 | 0.61±0.07 | 3.87±0.82 | 0.02±0.01 | 0.53 | 396.30 |
| *Raphanus raphanistrum* 3 | 0.18 | 0.28±0.06 | - | 25.39 | 0.47±0.01 | 2.72±0.52 | 0.03±0.02 | 0.53 | 396.30 |
| *Sisymbrium orientale* 1 (Population from drier area) | 0.57 | 0.17±0.03 | 354.17±68.21 | 26.25 | 0.78±0.12 | 3.75±0.66 | 0.03±0.02 | 0.34 | 264.30 |
| *Sisymbrium orientale* 2 (Population from drier area) | 0.57 | 0.18±0.03 | 344.11±54.05 | 26.29 | 0.73±0.08 | 3.63±0.66 | 0.03±0.02 | 0.34 | 264.30 |
| *Sisymbrium orientale* 3 (Population from drier area) | 0.56 | 0.18±0.04 | - | 23.51 | 0.76±0.07 | 3.73±0.75 | 0.03±0.01 | 0.34 | 264.30 |
| *Sisymbrium orientale* 1 (Population from more humid area) | 0.36 | 0.19±0.06 | 295.12±87.16 | 29.47 | 0.73±0.07 | 3.46±0.93 | 0.03±0.02 | 0.53 | 396.30 |
| *Sisymbrium orientale* 2 (Population from more humid area) | 0.31 | 0.21±0.05 | 311.74±67.95 | 21.59 | 0.42±0.11 | 3.18±0.57 | 0.02±0.007 | 0.53 | 396.30 |
| *Sisymbrium orientale* 3 (Population from more humid area) | 0.28 | 0.12±0.03 | - | 24.37 | 0.69±0.08 | 3.3±0.64 | 0.02±0.01 | 0.53 | 396.30 |
| *Rapistrum rugosum* 1 | 0.42 | 0.10±0.03 | 287.42±42.02 | 45.12 | 0.66±0.07 | 4.39±0.88 | 0.01±0.007 | 0.68 | 526.90 |
| *Rapistrum rugosum* 2 | 0.43 | 0.12±0.02 | 330.99±133.3 | 42.85 | 0.67±0.08 | 4.67±1.02 | 0.02±0.01 | 0.68 | 526.90 |
| *Rapistrum rugosum* 3 | 0.49 | 0.13±0.03 | - | 50.54 | 0.66±0.08 | 4.4±0.98 | 0.01±0.01 | 0.68 | 526.90 |
| *Sinapis arvensis* 1 | 0.22 | 0.20±0.06 | 425.72±84.18 | 26.54 | 0.61±0.07 | 3.43±0.60 | 0.02±0.01 | 0.53 | 396.30 |
| *Sinapis arvensis* 2 | 0.24 | 0.29±0.05 | 325.72±91.35 | 27.16 | 0.57±0.08 | 3.75±0.75 | 0.02±0.01 | 0.53 | 396.30 |
| *Sinapis arvensis* 3 | 0.22 | 0.19±0.04 | - | 25.17 | 0.58±0.08 | 3.66±0.67 | 0.02±0.01 | 0.53 | 396.30 |

$P_{LIG}$ = proportion of lignified area per total stem area; $F_{AP}$ = intervessel pit aperture fraction (pit aperture area / bordered pit area); $T_{PM}$ = thickness of the intervessel pit membrane; $D_H$ = hydraulically weighted vessel diameter; $P_{FW}F_X$ = proportion of xylem fiber wall area per fiber area as observed in a cross section; $T_{VW}$ = thickness of the vessel wall; $T_WD_V$ = thickness-to-span ratio of vessels; AI = aridity index; $P_R$ = mean annual precipitation.

**Table S3** • Analysis of covariance of species and mean precipitation explaining the variance in $P_{50}$ of the herbaceous Brassicaceae and Asteraceae species studied.

| Source of variation | Degrees of freedom | Sum of squares | Mean of Squares | F Value | P value | Hierarchical Partitioning |
|---|---|---|---|---|---|---|
| Species | 10 | 58.02 | 5.802 | 27.161 | <2e-16 | 70.15 |
| Precipitation | 1 | 3.56 | 3.565 | 16.689 | 0.000109 | 29.85 |
| Species: Precipitation | 1 | 0.63 | 0.630 | 2.948 | 0.090109 | --- |
| Residuals | 75 | 16.02 | 0.214 | --- | --- | --- |

**Table S4** • Multiple regression model of anatomical features explaining the variance in $P_{50}$ of the herbaceous Brassicaceae and Asteraceae species studied.

| Source of variation | Parameter estimate | SE | t-value | P value | Hierarchical Partitioning |
|---|---|---|---|---|---|
| Intercept | 0.3675 | 0.6893 | 0.533 | 0.5991 | --- |
| $P_{LIG}$ | -5.0281 | 0.8040 | -6.254 | 2.21e-06 | 69.2903 |
| $T_{PM}$ | -0.0056 | 0.0021 | -2.620 | 0.0153 | 30.7097 |

$P_{LIG}$ = the proportion of lignified area per total stem area; $T_{PM}$ = thickness of intervessel pit membranes.

**Table S5** • Permutational multivariate analysis of variance of mean annual precipitation explaining the variance in $P_{50}$ and in the main stem anatomical characters of the herbaceous Brassicaceae and Asteraceae species studied.

| Source of variation | Degrees of freedom | Sum of Squares | Mean of Squares | F Model | $R^2$ | P value |
|---|---|---|---|---|---|---|
| Precipitation | 1 | 0.2026 | 0.2026 | 3.8098 | 0.137 | 0.017 |
| Residuals | 24 | 1.2763 | 0.05318 | --- | 0.863 | --- |
| Total | 25 | 1.4789 | --- | --- | 1.000 | --- |

*Chapter 6*

# DISCUSSION AND GENERAL CONCLUSION

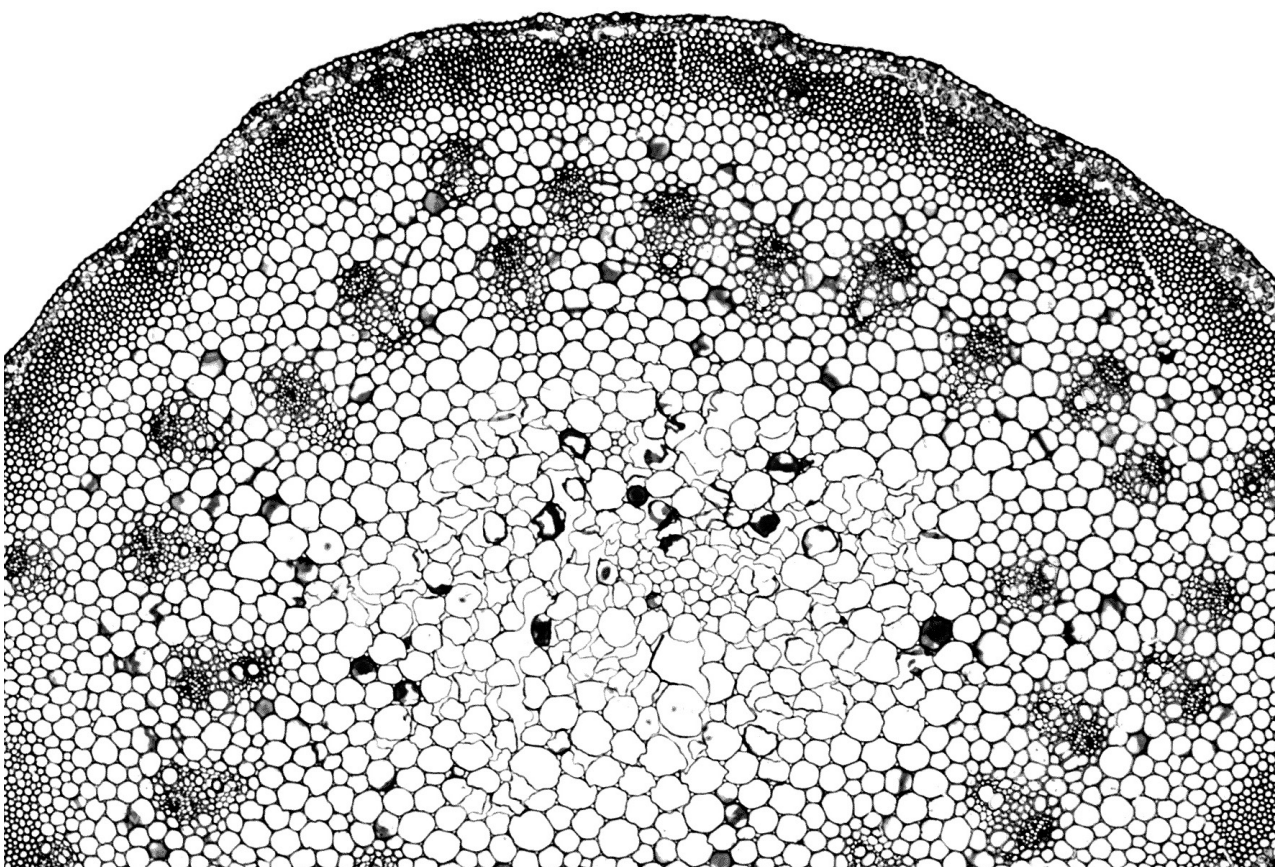

Frequent episodic droughts and heat waves due to the ongoing climate change are increasing drought-induced forest mortality in a vast range of forest ecosystems (Allen *et al.* 2010; Dai 2013). This also applies to grassland and crop productivity that will undergo severe yield loss under this climate scenario since water limitation is one of the most important constraints for agriculture (Ciais *et al.* 2005; Brookshire & Weaver 2015). Under these water limiting conditions, plant hydraulics and plant anatomy have become important traits to predict species' vulnerability and its impact on plant distribution and survival under increasing climatic stresses (Anderegg *et al.* 2013). Understanding how mortality mechanisms work in plant species is challenging, and approaches used so far to construct realistic mortality vegetation models vary in terms of species, life stage studied and variables measured (Anderegg *et al.* 2013; Anderegg 2015). Therefore, efforts on investigating plant mortality mechanisms still remain insufficient (McDowell *et al.* 2008; Choat *et al.* 2012; Urli *et al.* 2013; Adams *et al.* 2017).

Plants will respond to changes in availability of abiotic natural resources through environmentally-induced shifts in phenotype (phenotypic plasticity), thereby explaining that hydraulic and wood traits vary across different zones (O'Brien *et al.* 2017). Along this line, investigating plastic responses about structure-function relationships on drought-induced embolism is crucial for increasing the predictability of modeling climate impacts on vegetation (Soudzilovskaia *et al.* 2013).

The results of my PhD thesis contribute to the comprehension of the ecological significance of embolism resistance and the functional aspects of xylem anatomical traits related to water conductivity. An overview of the main findings of the thesis can be seen in Fig. 1. In chapter 2 I show that abiotic differences between the Brazilian cerrado and caatinga habitats are important to explain the variation in wood anatomical characters in the co-occurring species *Tabebuia aurea* and *Tocoyena formosa*, and that soil differences - especially high aluminum concentrations and low nutrients in cerrado soils - are likely to explain the intraspecific wood anatomical differences between individuals from different sites. In chapter 3, I investigate the intraspecific wood anatomical variation in the same population of the two co-occurring Brazilian species, demonstrating wood trait variation along the main stem to deal with constraints related to increasing tree height, especially increasing hydraulic resistance. This intraspecific variation along the vertical axis of the main trunk outcompetes site as predictor for wood trait variation. In chapter 4 I show the (indirect) link between embolism resistance and lignification via the thickness of intervessel pit membranes, reflected in higher embolism resistance of insular woody stems of the Canary Island *Argyranthemum* (Asteraceae) species compared to the stems of their herbaceous continental relatives. This result matches with the abundance of insular woody species in the drier areas of the Canary Islands (Lens *et al.* 2013b) and with the ongoing observation of the distribution of derived woody species in continental areas that experience a few consecutive months of

drought per year (F. Lens, global derived woodiness dataset, personal communication). Finally, in chapter 5 I investigate the often neglected field of embolism resistance in stems of herbaceous (Brassicaceae and Asteraceae) species occurring in different vegetation zones of Tenerife (Canary Islands, Spain). I demonstrate that also herbaceous eudicot stems can vary considerably in embolism resistance. Additionally, I emphasize that the difference in mean annual precipitation across the habitats of the herbaceous species is strongly linked to their ability to withstand embolism formation in stems as well as their ability of adapt specific anatomical features of their hydraulic system, both at inter and intraspecific level.

Below, I explain the main findings of the chapters 2-5 with their major implications in the integrated field of plant hydraulics and wood anatomy. I finalize the chapter with a personal view about future directions that have great potential to boost this research field.

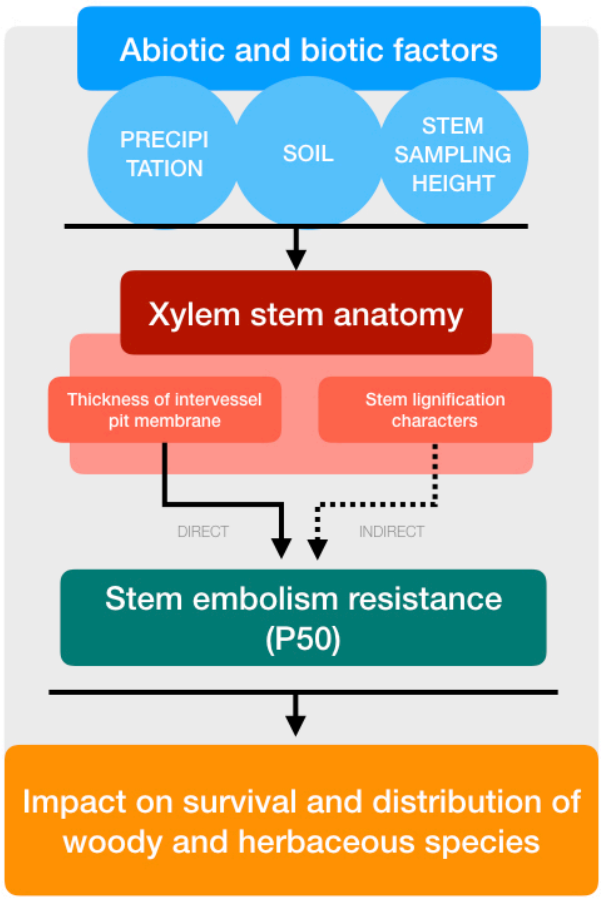


**Figure 1** • Schematic representation of the main findings of my thesis.

### *Site and tree sampling height as predictors of xylem anatomical plasticity and its functional adaptive meaning in water conductance, survival and distribution of species*

Xylem forms the bulk tissue in woody plants, and enables long distance water transport towards the tree canopy, where transpiration via stomata induces water loss and CO2 uptake to photosynthesis (Brodribb & Feild 2000). The different xylem functions are integrated to maximize plant fitness, but the environmental constraints have a major role in determining the different adaptive solutions to the structure/function demands (Ackerly 2004; Baas *et al.* 2004).

A remarkable example of how the environment plays an important role in the plasticity of wood anatomical characteristics was shown in chapter 2. The variation in xylem anatomical traits of two common co-occurring species (*Tabebuia aurea* and *Tocoyena formosa*) of the two main seasonally dry environments in Brazil, cerrado and caatinga, is explained by differences between sites. Since the two species belong to two unrelated families (Bignoniaceae and Rubiaceae, respectively), the factor species was found to be stronger than site to explain wood anatomical variation, and thereby emphasizing the importance of variation determined by evolutionary history. The impact of site (cerrado and caatinga) on the plasticity of wood anatomy was clearly demonstrated in the paired comparisons of each wood anatomical character between individuals from the same species growing in both sites, emphasizing the intraspecific species adaptation.

Rain seasonality is typical of both the cerrado and caatinga, although both biomes have unique rainfall patterns. In caatinga, the irregularity of rainfall is remarkable throughout the years and the mean precipitation is confined to only three months. The cerrado, despite its marked dry season, is not considered a xerophytic vegetation in contrast to caatinga (Oliveira & Marques 2002), especially due to certain general aspects of the vegetation. For instance, most of the cerrado plants develop large green leaves during the entire year and also flourish during the dry period (Rivera *et al.* 2002). Additionally, they also develop deep rooting systems enabling plants to access water deeply stored in the soil during the dry periods, maintaining transpiration and carbon fixation (Oliveira *et al.* 2005). However, the cerrado plants have to deal with edaphic adversities: the cerrado soils are nutrient-poor and aluminum-rich, which leads to toxic conditions that plants need to overcome (Coutinho 2002). Based on that, I suggested that the xeromorphic wood features associated with the individuals from cerrado in chapter 2 might be a response for the chronic low availability of edaphic mineral nutrients (oligotrophism) and the high aluminum concentration (aluminum toxicity). Accordingly, the oligotrophic and aluminum toxic soils have been reported as the main causes of xeromorphic features in cerrado plants, such as sclerophylly in leaves (Coutinho 1983; Oliveira *et al.* 2003; Souza *et al.* 2015), and it has been conceptualized as the

Theory of Oligotrophic Scleromorphism (Arens 1958; Arens *et al.* 1958; described in English in Salatino 1993), or peinomorphism (sensu Walter 1973). The results of chapter 2 corroborate the findings of higher lignification (higher sclerophylly) in cerrado plants, showing thicker fiber walls in individuals of *T. aurea* from cerrado. Additionally, the reduced size of individuals of *T. formosa* from cerrado might also be explained by the higher aluminum concentration as well as by the lower concentration of essential micronutrients, such as manganese in the cerrado soils. Aluminum is a strong plant growth reducing element in acid soils (Kochian 1995), and the deficiency of any essential micronutrient can cause disorders in physiological and biochemical processes, resulting in reduced plant growth (Kozlowski *et al.* 1991).

Besides the influence of environmental factors on the plasticity of wood anatomy, it is also known that plant height has an important effect due to necessary xylem adjustments to overcome increasing resistance in hydraulic conductance (Petit *et al.* 2010; Andofillo *et al.* 2013; Olson *et al.* 2018; Pfautsch *et al.* 2018). In chapter 3 I showed how sampling height influences the variation of wood traits along the main trunk of the same two species and sites described in chapter 2. The approach of using two species occurring in two different environments was important because it enabled us to test to which extent the factor site would also influence the axial trait variation in wood, since I had already studied the impact of site to explain species specific adaptation for each environment. I found that site was negligible to explain the variation of wood traits, since out of 13 wood traits assessed, only three had shown to be influenced by site and for only one species.

There was much variation in wood traits for the two species along the tree trunk in vessels, fibers as well as axial and ray parenchyma. Some of the variation can be functionally interpreted as a way of counterbalancing the increased resistance in water conductivity with increased tree height, such as the widening of vessels downwards and the increase in vessel density and vessel fraction upwards in both species. Additionally, both species showed that the largest vessels are linked to the thinnest intervessel pit membranes, which makes sense from a hydraulic point of view since more efficient, wider (and presumably also longer) vessels towards the trunk base of taller trees should have thinner intervessel pit membranes in order to synergistically reduce the resistance to long distance water transport (Hacke *et al.* 2006; Choat *et al.* 2008; Rosell *et al.* 2017).

Analogous to the particular adaptations of each species to deal with the adversities of the two environments shown in chapter 2, there were particular wood trait adaptations along the main trunk of the trees to deal with mechanical and hydraulic constraints between the two species in chapter 3. For instance, the axial variation of wood density in *T. aurea* is linked to fiber wall thickness, while in *T. formosa* wood density is related to vessel and ray characters. Likewise, rays seem to

have different functions for each species, linked to conductance in *T. aurea* and to mechanics in *T. Formosa*, and this could be related to contrasting ray compositions in both species. In summarize, the two first chapters of my thesis showed that the two species have species-specific trade-offs to deal with environment constraints and with trade-offs associated with axial variation.

### *The functional significance of $P_{50}$ as an adaptive trait to plant survival and distribution*

The functional significance of stem $P_{50}$ as an adaptive trait responding to environmental changes and plant distribution is shown in chapters 4 and 5. In chapter 4, this relationship was observed at the genus level, amongst five species of the insular woody *Argyranthemum* on Tenerife, Canary Islands. The most vulnerable species was the evergreen A. broussonetii from the wet laurel forests of Tenerife. Accordingly, all the other species studied of *Argyranthemum* are more resistant to embolism and native to drier areas of Tenerife. The functional significance of these findings are supported by the observations of chapter 5, where I showed that the difference in mean annual precipitation along different vegetations zones of Tenerife explains the variation in stem anatomy and embolism resistance amongst herbaceous species of Brassicaceae and Asteraceae. The data proved that the most vulnerable species were collected in wetter environments while the most resistant ones were sampled in drier vegetation types, thereby emphasizing the ecological value of $P_{50}$ in the distribution and survival of herbaceous species. Additionally, I also showed this same functional relevance of stem $P_{50}$ at the intraspecific level within both *Sisymbrium orientale* and *Hirschfeldia incana* (Brassicaceae) occurring in different areas with contrasting mean annual precipitation. While the majority of studies assess interspecific differences in $P_{50}$ (Oliveira *et al.* in press; Zhang *et al.* 2018), the intraspecific variation is less understood, and only studied in a few woody and herbaceous species showing no variation in some species and considerable variation in others (Choat *et al.* 2007; Martínez-Vilalta *et al.* 2009; Lamy *et al.* 2014; Cardoso *et al.* 2018; Volaire *et al.* 2018). In chapter 5, a significant intraspecific difference in stems of the two Brassicaceae species was observed and was found to be explained by precipitation: for both species, the more embolism resistant populations occur in drier areas. This positive correlation between drought and embolism resistance in stems has been demonstrated in the literature for woody trees (Maherali *et al.* 2004; Bouche *et al.* 2014; Blackman *et al.* 2012; Trueba *et al.* 2017), and it also seems to be valid for herbaceous species (Lens *et al.* 2016).

*The thickness of intervessel pit membrane in angiosperms is a major anatomical character explaining variation in embolism resistance*

As expected from the air-seeding hypothesis, the intervessel pit membrane has a key role in avoiding the spread of embolism between adjacent conduits, since the thickness of the pit membrane corresponds to the size and shape of the pit pores through which the air-water menisci cross during the air-seeding process (Choat *et al.* 2008; Lens *et al.* 2013a; Li *et al.* 2016). In chapter 4, the thickness of intervessel pit membrane ($T_{PM}$) was found to be the most important anatomical trait explaining stem $P_{50}$ variation of the insular woody species of *Argyranthemum* and their five herbaceous relatives. The more resistant, woody species have thicker intervessel pit membranes compared to the herbaceous, less resistant relatives, occurring on the European continent. Another noteworthy finding of this study is that $T_{PM}$ was positively linked with the degree of lignification in stems. This leads us to the main conclusion of our chapter 4: the increase in woodiness of insular woody species explains indirectly the increase in embolism resistance via the thickness of intervessel pit membrane.

Despite all the strong evidence that $T_{PM}$ plays a major role in explaining embolism resistance, in chapter 5 the degree of woodiness ($P_{LIG}$) provided a higher explanatory power for differences in embolism resistance amongst herbaceous Brassicaceae and Asteraceae. It might be that the functional relevance of $T_{PM}$ in herbs is less important compared to woody species, for a reason that is not known. A previous study investigating the $P_{50}$ - $T_{PM}$ relationship in grasses also did not find any relationship (Lens *et al.* 2016). Moreover, in my study of chapter 5, the $P_{50} - T_{PM}$ relationship disappeared when only assessing the Brassicaceae species dataset, and in chapter 4, the $P_{50} - T_{PM}$ relationship was true only when the herbaceous data set was combined with the woody data set. Nevertheless, studies investigating the relationship between stem $P_{50} - T_{PM}$ amongst herbaceous species remain very scarce, so it is too soon to make any conclusion about the functional relevance of $T_{PM}$ in herbs. That being said, when analysing the two populations of *Sisymbrium orientale*, a significant difference in $P_{50}$ was observed, matching the significant difference in $T_{PM}$, with the more embolism resistant population having thicker intervessel pit membranes.

*The strong but indirect link between lignification and embolism resistance*

Water transport in plants is driven by a gradient in negative pressures inside the water conducting cells, which generates an inner xylem mechanical stress (Bittencourt *et al.* 2016). The tensions inside conduits generate imploding forces and therefore cell walls, or even entire stems (Lens *et al.* 2016) need to be reinforced to avoid a potential collapse of conduits (Hacke *et al.* 2001a). In this line, collapse of xylem conduits has only been observed in cells that lack a robust support of the

fibre matrix, for instance in leaves (Cochard *et al.* 2004; Brodribb & Holbrook 2005; Zhang *et al.* 2016) and in low-lignin stems of poplar mutants (Kitin *et al.* 2010). Additional to imploding forces, positive pressures can also occur inside embolized conduits (Pereira *et al.* 2017). The interaction between these opposite forces requires the presence of a mechanical system in wood that would mitigate the costs associated with high tensions (Hacke *et al.* 2001a). In this context, a stronger mechanical system due to thicker-walled conduits or fibers leads to higher wood density and is linked to water transport safety rather than water transport efficiency (Jacobsen *et al.* 2005, 2007; Chave *et al.* 2009). In addition, more lignified stems are interpreted as a mechanism to avoid the formation of microcracks through which embolism nucleation may occur or air could be sucked in (Jacobsen *et al.* 2005; Zwieniecki & Secci 2015). Accordingly, the formation of cracks in wood does occur during the drying process of wood material (Hanhijarvi *et al.* 2003) and the likelihood of cracks formation decreases with wood density (Ilic 1999). Therefore, numerous studies have reported the relationship between higher wood density (which could also be linked with higher stem lignification) and higher absolute values of $P_{50}$, both in woody (Hacke *et al.* 2001a; Jacobsen *et al.* 2005; Jansen *et al.* 2009; Pereira *et al.* 2017) and in herbaceous lineages (Lens *et al.* 2012b, 2013, 2016; Tixier *et al.* 2013).

In my study, I corroborated these findings in chapter 4 showing that the insular woody stems of *Argyranthemum* species are more embolism resistant than those of their herbaceous relatives. The proportion of lignified area per total stem area ($P_{LIG}$) as well as the proportion of xylem fiber wall per fiber ($P_{FW}F_X$) explained the variation in embolism resistance in this clade of daisies. The increment of a xylem mechanical support against implosion is the reason for the hydraulic-mechanical trade-off, which can result from either an increase in vessel wall to lumen ratio (Hacke *et al.* 2001a; Jacobsen *et al.* 2007; Cardoso *et al.* 2018) or an increase in fibre matrix support (more and thicker walled xylem fibres) (Jacobsen *et al.* 2005, 2007; Pratt & Jacobsen 2017; Dória *et al.* 2018). Interestingly, we also found a positive correlation between lignification and increasing embolism resistance amongst the different individuals of *Cladanthus mixtus* (Asteraceae). This species showed the highest range in the degree of stem lignification amongst the individuals studied, coupled to the highest degree in embolism resistance.

Besides the hydraulic-mechanical trade-off, the link between increased wood formation and embolism resistance in the daisy lineage matches the observation that the majority of insular woody species native to the Canary Islands are often distributed in the dry coastal areas (Lens *et al.* 2013b). Additionally, it also agrees with an ongoing global derived woodiness database at the flowering plant level, comprising almost 7,000 species of which most of them are native to regions with a marked drought period such as (semi-)deserts, savannas, steppes and Mediterranean-type habitats (F. Lens, global derived woodiness dataset, personal com-

munication). The abundance of derived woody species in (periodically) dry areas supports the hypothesis that drought might have driven wood formation in many derived woody lineages (Dória *et al.* 2018).

Also amongst the herbaceous Brassicaceae and Asteraceae species studied (chapter 5), the link between lignification and embolism resistance was retrieved. Surprisingly, the proportion of lignified area per total stem area ($P_{LIG}$), which is mainly defined by the amount of woodiness, was the character that best explained the variation in embolism resistance in stems: the higher the stem lignification, the more resistant to embolism formation the species is. The same trend was found between the two populations of *Sisymbrium orientale*: the more resistant population showed thicker intervessel walls and higher $P_{LIG}$ compared to the more vulnerable population.

Despite the overwhelming evidence for the mechanical-hydraulic link, it is hard to functionally explain why more lignified species are better adapted to drought. At first sight, there seems to be no evidence for a direct functional link between increased wood formation and increased embolism resistance. As commented above, the embolism spreading via air-seeding occurs at the intervessel pit membrane level, which is more likely to affect the existence of high levels of embolisms. Therefore, the reported correlations between higher lignification and thicker intervessel pit membranes, such as thicker vessel walls and thicker membranes (Jansen *et al.* 2009; Li *et al.* 2016), might indicate that mechanically reinforced stems are indirectly correlated with embolism resistance via air-seeding. This hypothesis was highlighted in chapter 4, where intervessel pit membrane thickness ($T_{PM}$) was found to be the functional missing link explaining the correlation between stem lignification and embolism resistance in the daisy clade. In chapter 5, the link $T_{PM}$ - lignification was also found at the intraspecific level in the herbaceous *Sisymbrium orientale* collected in contrasting environments: the more resistant population showed a higher proportion of lignified area in the stem, thicker intervessel wall, and thicker intervessel pit membranes. However, the $T_{PM}$ – lignification correlation disappeared in our entire data set (including all the herbaceous Asteraceae and Brassicaceae species), showing that increased lignification characters are not necessarily linked to thicker intervessel pit membranes.

## Future perspectives

Our understanding about relationships between xylem structure and long-distance water transport has made great progress during the last decades. This progress is particularly due to novel non-invasive techniques available to examine water flow and air bubble formation in xylem conduits, such as nuclear magnetic resonance imaging, high-resolution computed tomography and the optical technique (Brodersen *et al.* 2013, 2018; Knipfer *et al.* 2015; Torres-Ruiz *et al.* 2015; Brodribb *et al.* 2016). Likewise, progress in identification of artefacts during hydraulic measurements (long vessels generating r-shaped curves) and artefacts due to incorrect lab protocols (proper fixation of fresh samples to preserve the pit membranes), has led to more reliable measurements (Plavcová *et al.* 2013; Li *et al.* 2016).

As a result of this progress, the direct functional link between embolism formation and pit structure has been demonstrated in several studies, although the chemical composition of the pit membranes and the 3D structures of their micropores remain poorly known. Likewise, detecting the presence of hydrophobic surfaces at the pit membrane area, which would affect the contact angle between air bubbles and the pit membrane micropores, would help to elucidate how the first embolisms are formed and the detailed mechanisms behind drought-induced embolism formation and spread via air-seeding. Moreover, a better understanding about the presence and variety of chemical components in living xylem parenchyma and dead water conducting cells would increase our knowledge about the effect of sap flow content on surface tension and pit membrane function, which is important specially under the light of new discoveries of stable, surfactants-coated nanobubbles (Jansen & Schenk 2015; Schenk *et al.* 2015, 2017, 2018). Furthermore, these fine-scale observations in pits and xylem sap should be carried out in different organs, along different height positions within the tree, and throughout different time periods in the year to better understand the importance of interconduit pits in long-distance water transport of plants.

Given the importance of $P_{50}$ as an ecological trait influencing the distribution of species and a potential driver for plant diversification and species coexistence (Larter *et al.* 2017; Oliveira *et al.* in press), a promising venue for future studies is investigating whether generalists exhibit higher phenotypic plasticity in $P_{50}$ than specialists in their stems, roots and leaves. Additionally, integrating hydraulic traits with molecular phylogenies will be relevant to better understand evolution of the hydraulic system, especially in these lineages that show low morphological variation, but clear habitat and soil preferences. Furthermore, considering that embolism resistance is linked to drought-induced mortality, using hydraulic data in models for predicting tree mortality during climate extremes will help to better

elucidate the physiological processes and mechanisms underlying drought mortality. In this line, gathering data from underrepresented forests, such as rainforest species - represented by only 59 tree species out of 226 species from 81 sites worldwide in a meta-analysis of Choat *et al.* 2012 - would be of utmost importance to accurately predict which trees/forests are more vulnerable to climate change. Consistent with a better prediction of plant response to climate change, assessing plant height in relationship with hydraulic traits across species and environments will also be valuable to understand the distribution of tree species across different biomes, since plant height is the main driver for vessel diameter (Olson *et al.* 2018).

In conclusion, it is clear that the boundary between plant hydraulics and wood anatomy has great potential to generate crucial information about plant survival and adaptation, geographic distribution, and evolution. However, xylem hydraulic and anatomical traits represent only one element of an entire range of adaptive strategies that plants employ to survive and compete. Therefore, these hydraulic and anatomical observations in stems should be combined with leaf and root measurements in order to obtain a global plant approach. Features of special interest are (1) stomata sensitivity, which determine transpiration rate and xylem pressure, (2) sapwood to leaf area ratios, which have an influence in the safety and efficiency of water conductance, (3) root distribution and depth, which influence the access to water source, and (4) and xylem capacitance, helping to maintain the integrity of the water transport. This more integrative approach will definitely help us to understand inter and intraspecific variation in hydraulic and anatomical traits with respect to drought tolerance across diverse plant lineages.

# SUMMARIES

## Summary

The combination of increasing heat waves and decreasing precipitation frequency has led to multiple large-scale tree mortality events in different plant ecosystems. Xylem vulnerability to embolism has been associated with drought-induced tree mortality. Additionally, the plasticity of wood anatomy, as a result of adaptation over long-term responses, plays a central role in plant hydraulic strategies. Therefore, understanding how plants cope with drought-induced embolism will help us to predict species distribution and model climate impact on vegetation.

With this thesis, I investigated the ecological significance of embolism resistance, and explored the plasticity and functional aspects of xylem anatomical traits in stems of woody and herbaceous species. Chapters 2 and 3 emphasized the effect of biotic and abiotic constraints to assess different adaptive solutions to the wood structure/function demands. In chapter 2, environmental constraints related to temperature, precipitation and soil conditions explained the wood anatomical variation amongst individuals of the same species occurring in two seasonally dry environments in Brazil, i.e. cerrado and caatinga. In addition to the remarkable dry season in both vegetation types, I highlighted the role of the edaphic toxicity of cerrado soils (high aluminum concentration and low nutrient availability) on the variation in wood anatomy plasticity, resulting in xeromorphic features in cerrado individuals. In addition to abiotic factors, plant height has also appeared as a source for wood trait variation along the main trunk in chapter 3. I showed that compared to axial sampling height, the effect of site was negligible for explaining the variation of wood traits: out of 13 wood traits assessed, only three were influenced by site differences including only in one of both species. Some of the axial variation can be functionally interpreted as a way of counterbalancing the increased resistance in water conductivity with increased tree height, such as the widening of vessels downwards and the increase in vessel density and vessel fraction upwards in both species.

The functional ecological significance of the pressure inducing 50% of loss hydraulic conductance ($P_{50}$) as an adaptive trait responding to environmental chang-

es and plant distribution is shown in chapters 4 and 5. Amongst the five insular woody *Argyranthemum* species studied in chapter 4, the most vulnerable was the evergreen *A. broussonetii* from the wet laurel forests of Tenerife, Canary Islands, while the other four species were native to drier areas of the island and expressed a higher resistance to embolism in their stems. In chapter 5, the difference in mean annual precipitation along different vegetations zones of Tenerife explains the variation in both stem anatomy and embolism resistance amongst herbaceous species of Brassicaceae and Asteraceae, emphasizing the importance of $P_{50}$ as a predictor of ecological distribution between and within species.

The spread of embolism in the vessel network occurs via air-seeding, a mechanism that has been shown to be mediated by the thickness of intervessel pit membranes ($T_{PM}$). This functionally explains the correlation between $T_{PM}$ and $P_{50}$ in several studies. Likewise, in chapter 4, $T_{PM}$ was the best predictor for the variation of embolism resistance amongst the insular woody *Argyranthemum* species and their continental herbaceous counterparts. Similarly, $T_{PM}$ appeared as an important trait explaining the variation of embolism resistance amongst the herbaceous Brassicaceae and Asteraceae species studied in chapter 5. However, in these herbaceous species, the degree of woodiness provided a higher explanatory power for the variation of embolism resistance than $T_{PM}$. The link between higher lignification (woodiness) and higher embolism resistance, which is associated with the ability of plants to withstand more negative pressures in their xylem, was also demonstrated in chapter 4 where stems of the insular woody species were more embolism resistant than those of their herbaceous continental relatives. This result matches with the reported abundance of insular woody species in the drier areas of the Canary Islands and with the ongoing observation of the distribution of phylogenetically derived woody species that thrive in continental areas experiencing a few consecutive dry months per year. The positive relationship between higher lignification and higher embolism resistance was also reported at the intraspecific level in chapter 4, amongst herbaceous individuals of *Cladanthus mixtus* (Asteraceae), as well as in chapter 5 between populations of *Sysimbrium orientale* and *Hirschfeldia incana* (Brassicaceae) growing in contrasting environments. Despite the stunning evidence for the mechanical-hydraulic trade-off, this relationship is often reported as indirect. The missing functional link was found to be $T_{PM}$ that seems to co-evolve with increased woodiness in the Asteraceae and Brassicaceae studied, both at the interspecies and intraspecies level.

For future studies, I emphasized the importance of gathering more plant hydraulic data from the poorly studied environments, such as tropical rainforests. When filling these gaps, we will be better able to predict which trees/forests are more vulnerable to embolism, allowing us to further optimize tree mortality models. Additionally, I highlighted the need to assess the fine-scale anatomical observations in pits in different organs and along different height positions within a tree

across many species. Finally, a more integrative approach, combining embolism resistance across organs with other measurements such as stomata response, xylem capacitance, and root depth will definitely increase our understanding with respect to plant drought tolerance and mortality across diverse plant lineages.

## Samenvatting

De combinatie van toenemende hittegolven en droogte heeft geleid tot grootschalige boomsterfte in verscheidene plantenecosystemen. De kwetsbaarheid van het xyleem met betrekking tot embolievorming is geassocieerd met droogte-geïnduceerde boomsterfte. Daarnaast speelt ook de plasticiteit in houtanatomie – als resultaat van adaptatie over een evolutionaire tijdspanne – een centrale rol in hydraulische plantenstrategieën. Daarom is het belangrijk te begrijpen hoe planten omgaan met droogte-geïnduceerde embolievorming voor het voorspellen van plantenverspreiding en het modelleren van de klimaatimpact op de vegetatie.

In deze thesis, heb ik de ecologische relevantie van embolieresistentie bij planten bestudeerd, en heb ik de plasticiteit en functionele aspecten van xyleemanatomische kenmerken in stengels van houtige en kruidachtige soorten onderzocht. Hoofdstukken 2 en 3 leggen de nadruk op het effect van biotische en abiotische omstandigheden voor adaptieve oplossingen met betrekking tot structurele-functionele benodigdheden. In hoofdstuk 2, heb ik gevonden dat omgevingsfactoren – die gerelateerd zijn aan temperatuur, precipitatie en bodemcondities – de houtanatomische variatie verklaren tussen individuen van dezelfde soort die in twee seizoensgebonden droge vegetatietypes in Brazilië voorkomen, namelijk cerrado en caatinga. Naast het overduidelijke droge seizoen in beide vegetatietypes, heb ik de rol van bodemtoxiciteit benadrukt in de cerrado (hoge aluminiumconcentratie en lage beschikbaarheid in nutriënten) om de variatie in houtanatomische plasticiteit te na te gaan. Deze typische bodemcondities resulteren in allerlei xeromorfe eigenschappen in de cerrado-individuen. Naast de abiotische condities, bleek ook de plantenhoogte gerelateerd te zijn met houtanatomische variatie over de ganse lengte van de stam in hoofdstuk 3. Ik heb aangetoond dat het effect van vindplaats verwaarloosbaar was in vergelijking met de axiale verzamelhoogte in de stam om de variatie in houtkenmerken te verklaren: van de 13 geobserveerde houtkenmerken waren er slechts drie die beïnvloed worden door de vindplaats, waarbij maar één kenmerk met een correlatie voor beide soorten. Een deel van de axiale variatie kan functioneel geïnterpreteerd worden als een compensatie voor de verhoogde resistentie in watertransport omwille van de grotere boomhoogte.

Een voorbeeld hiervan is de verbreding van vaten naar lager gelegen delen in de stam en de toename in vatdensiteit hogerop in de takken in beide soorten.

De functionele ecologische significantie van de druk ('pressure') die 50% verlies aan hydraulische conductiviteit veroorzaakt ($P_{50}$) is aangetoond als een voorname aanpassing in de strijd tegen de klimaatswijziging en is sterk gelinkt aan plantenverspreiding (hoofdstukken 4 en 5). De immergroene verhoute eilandsoort *Argyranthemum* broussonetii, inheems in de natte laurierbossen op Tenerife (Canarische Eilanden), was de meest kwetsbare *Argyranthemum* soort die ik heb onderzocht. De andere vier onderzochte *Argyranthemum* soorten, inheems in veel drogere gebieden van het eiland, hadden stengels die veel beter bestand waren tegen droogte-geïnduceerde embolievorming (hoofstuk 4). In hoofdstuk 5, heb ik gevonden dat het verschil in de gemiddelde jaarlijks precipitatie tussen de verschillende vegetatietypes in Tenerife sterk gelinkt is aan de variatie in stengelanatomie en embolieresistentie tussen de onderzochte kruidachtige Brassicaceae en Asteraceae soorten. Dit benadrukt nogmaals hoe belangrijk $P_{50}$ is om de ecologische verspreiding tussen en binnen soorten te begrijpen.

De verspreiding van embolieën in het vatnetwerk gebeurt via 'air-seeding', volgens een mechanisme dat door de dikte van de vat-vat stippelmembranen (VSM) wordt beïnvloed. Dit air-seeding mechanisme verklaart dus de functionele correlatie tussen VSM en $P_{50}$ in verscheidene publicaties. Ook in hoofdstuk 4, vond ik dat VSM de hoogste voorspellende waarde had om de variatie in $P_{50}$ te verklaren tussen de verhoute *Argyranthemum* soorten op de Canarische Eilanden en hun kruidachtige, continentale verwante soorten. VSM bleek ook een belangrijk kenmerk te zijn om de variatie in embolieresistentie in de stengels van de kruidachtige Asteraceae en Brassicaceae soorten te begrijpen (hoofdstuk 5). Echter, in dezelfde groep van kruidachtige soorten, vond ik dat de mate van houtvorming in de stengels beter de variatie in $P_{50}$ verklaarde dan VSM. De correlatie tussen $P_{50}$ en VSM, die kan gelinkt worden aan het vermogen van planten om beter de meer negatieve drukken in het xyleem te weerstaan, werd ook aangetoond in hoofdstuk 4 waar de stengels van de verhoute eilandsoorten meer resistent waren dan de stengels van de kruidachtige verwanten. Dit resultaat komt overeen met het veelvuldige voorkomen van verhoute eilandsoorten in drogere gebieden op de Canarische Eilanden, en ondersteunt ook de observatie dat verhoute continentale soorten die geëvolueerd zijn vanuit kruidachtige voorouders frequent groeien in gebieden met een jaarlijks wederkerende droogteperiode die minstens een paar maanden duurt. De positieve relatie tussen hogere lignificatie en verhoogde embolieresistentie in stengels was ook aangetoond binnen eenzelfde soort tussen populaties van *Cladanthus mixtus* (Asteraceae, hoofdstuk 4), en tussen populaties van Sysimbrium orientale en *Hirschfeldia incana* (Brassicaceae, hoofdstuk 5) die in contrasterende habitats verzameld werden. Ondanks het overduidelijke bewijs voor deze mechanische-hydraulische link, wordt deze correlatie vaak aangeduid als

indirect. De verborgen functionele schakel om de lignificatie-$P_{50}$ link te begrijpen, is VSM vermits dit kenmerk co-evolueert met verhoogde verhouting in de stengel in de bestudeerde Asteraceae en Brassicaceae, zowel tussen als binnen soorten.

Voor toekomstige studies is het belangrijk om meer hydraulische gegevens te verzamelen voor gebieden die nog onderbestudeerd zijn, zoals tropische regenwouden. Wanneer we deze hiaten in onze kennis opvullen, zullen we beter in staat zijn om te voorspellen welke bomen/bossen meer kwetsbaar zijn voor droogte-geïnduceerde embolievorming, wat ons dan weer helpt om modellen over boomsterfte verder te optimaliseren. Bijkomend, heb ik benadrukt dat het noodzakelijk is om fijnschalige anatomische observaties in stippels te blijven uitvoeren, zowel in verschillende organen van dezelfde plant als in verschillende delen over de ganse lengte van de plant voor vele soorten. Tot slot, een meer integratieve benadering, die verschillende functionele aspecten van de plant combineert, zoals embolieresistentie, respons van huidmondjes, xyleem 'capacitance', en diepte van wortelstelsel zullen zonder twijfel onze kennis verhogen met betrekking tot droogtetolerantie bij planten en plantensterfte over een brede fylogenetische waaier van taxa.

# REFERENCES


Ackerly D. 2004. Functional strategies of chaparral shrubs in relation to seasonal water deficit and disturbance. Ecological Monographs 74: 25 - 44.

Adams HD, Zeppel MJB, Anderegg WRL, Hartmann H, Landhausser SM, Tissue DT, *et al.* 2017. A multi-species synthesis of physiological mechanisms in drought-induced tree mortality. Nature, Ecology & Evolution 1: 1285 - 1291.

Ahmad HB, Lens F, Capdeville G, Burlett R, Lamarque LJ, Delzon S. 2018. Intraspecific variation in embolism resistance and stem anatomy across four sunflower (*Helianthus annuus* L.) accessions. Physiologia Plantarum 163: 59 - 72.

Allen CD, Macalady AK, Chenchouni H, Bachelet D, McDowell N, Vennetier M, *et al.* 2010. A global overview of drought and heat- induced tree mortality reveals emerging climate change risks for forests. Forest Ecology and Management 259: 660 - 684.

Aloni R, Zimmermann MH. 1983. The control of vessel size and density along the plant axis. Differentiation 24: 203 - 208.

Aloni R. 2015. Ecophysiological implications of vascular differentiation and plant evolution. Trees-Structure and Function 29: 1 - 16.

Alves ES, Angyalossy-Alfonso V. 2000. Ecological trends in the wood anatomy of some Brazilian species. 1. Growth rings and vessels. IAWA Journal 21: 3 - 30.

Alves ES, Angyalossy-Alfonso V. 2002. Ecological trends in the wood anatomy of some Brazilian species. 2 Axial parenchyma, rays and fibers. IAWA Journal 23: 391 - 418.

Anderegg WRL, Berry JA, Smith DD, Sperry JS, Anderegg LDL, Field C. 2012. The roles of hydraulic and carbon stress in a wodespread climate-induced forest die-off. Proceedings of the National Academy of Science USA 109: 233-237.

Anderegg LDL, Anderegg WRL, Berry JA. 2013. Not all droughts are created equal: translating meteorological drought into woody plant mortality. Tree Physiology 33: 701 - 712.

Anderegg WRL. 2015. Spatial and temporal variation in plant hydraulic traits and their relevance for climate change impacts on vegetation. New Phytologist 205: 1008 - 1014.

Anderegg WRL, Meinzer FC. 2015. Wood anatomy and plant hydraulics in a changing climate. In: Hacke U (Ed.), Functional and Ecological Xylem Anatomy. Springer International Publishing Switzerland, pp: 235 - 253.

Anderegg WRL, Klein T, Bartlett M, Sack L, Pellegrini AFA, Choat B, *et al.* 2016. Meta-analysis reveals that hydraulic traits explain cross-species patterns of drought-induced tree mortality across the globe. Proceedings of the National Academy of Science USA 113: 5024 - 5029.

Andrade-Lima D. 1981. The Caatingas dominium. Brazilian Journal of Botany 4: 149 - 163.

Anfodillo T, Petit G, Crivellaro A. 2013. Axial conduit widening in woody species: a still neglected anatomical pattern. IAWA Journal 34: 352 - 364.

Arechavaleta M, Rodriguez S, Zurita N García A. 2010. Lista de especies silvestres de Canarias: hongos, plantas y animales terrestres. Gobierno de Canarias, Tenerife, pp. 579

Arens K. 1958. Consideracoes sobre as causas do xeromorfismo foliar. Boletim da Faculdade de Filosofia Ciências e Letras da USP 224: 25 - 56.

Arens K, Ferri MG, Coutinho LM. 1958. Papel do fator nutricional na economia d'água de plantas do cerrado. Revista de Biologia 1: 313 - 324.

Awad H, Herbette S, Brunel N, Tixier A, Pilate G, Cochard H, *et al.* 2012. No trade-off between hydraulic and mechanical properties in several transgenic poplars modified for lignin metabolism. Environmental and Experimental Botany 77: 185 - 195.

Baas P. 1976. Some functional and adaptive aspects of vessel member morphology. Leiden Botanical Series 3: 157 - 181.

Baas P, Werker E, Fahn A. 1983. Some ecological trends in vessel characters. IAWA Bulletin 4: 141 - 159.

Baas P, Carlquist S. 1985. A comparison of the ecological wood anatomy of the floras of Southern California and Israel. Iawa Journal 6: 349 - 353.

Baas P, Schweingruber FH. 1987. Ecological trends in the wood anatomy of trees, shrubs and climbers from Europe. IAWA Bulletin New Series. 8: 245 - 274.

Baas P, Ewers FW, Davis SD, Wheeler EA. 2004. Evolution of xylem physiology. In: Hemsley AR, Poole I. (Eds.), The Evolution of Plant Physiology: From Whole Plant to Ecosystems. Elsevier Academic, Amsterdam, pp: 273 - 295.

Bailey IW, Tupper WW. 1918. Size variation in tracheary cells: a comparison between the secondary xylems of vascular cryptogams, gymnosperms and angiosperms. Proceedings of the American Academy of Arts and Sciences 54: 149 - 204.

Baldwin BG, Sanderson MJ. 1998. Age and rate of diversification of the Hawaiian silversword alliance (Compositae). Proceedings of the National Academy of Science USA 95: 9402 - 9406.

Barigah TS, Charrier O, Douris M, Bonhomme M, Herbette S, Améglio T, *et al.* 2013. Water stress-induced xylem hydraulic failure is a causal factor of tree mortality in beech and poplar. Annals of Botany 112: 1431 - 1437.

Barnard DM, Meinzer FC, Lachenbruch B, McCulloh KA, Johnson DM, Woodruff DR. 2011. Climate-related trends in sapwood biophysical properties in two conifers: avoidance of hydraulic dysfunction through coordinated adjustments in xylem efficiency, safety and capacitance. Plant, Cell & Environment 34: 643 - 654.

Bittencourt PRL, Pereira L, Oliveira RS. 2016. On xylem hydraulic efficiencies, wood space-use and the safety - efficiency tradeoff. New Phytologist 211: 1152 - 1155.

Blackman CJ, Brodribb TJ, Jordan GJ. 2012. Leaf hydraulic vulnerability influences species' bioclimatic limits in a diverse group of woody angiosperms. Oecologia 168: 1 - 10.

Böhle UR, Hilger HH, Martin WF. 1996. Island colonization and evolution of the insular woody habit in Echium L. (Boraginaceae). Proceedings of the National Academy of Sciences of the United States of America 93: 11740 - 11745.

Borchert R, Pockman WT. 2005. Water storage capacitance and xylem tension in isolated branches of temperate and tropical trees. Tree Physiology 25: 457 - 466.

Bosio F, Soffiatti P, Torres-Boeger MR. 2010. Ecological wood anatomy of Miconia sellowiana (Melastomataceae) in three vegetation types of Paraná State, Brazil. IAWA Journal 31: 179 - 190.

Bouche PF, Larter M, Domec JC, Burlett R, Gasson P, Jansen S, *et al.* 2014. A broad survey of xylem hydraulic safety and efficiency in conifers. Journal of Experimental Botany 65: 4419 - 4431.

Brodersen C, Mcelrone A, Choat B, Matthews M, Shackel K. 2010. The dynamics of embolism repair in xylem: in vivo visualizations using high-resolution computed tomography. Plant Physiology 154: 1088 - 1095.

Brodersen CR, McElrone AJ. 2013. Maintenance of xylem network transport capacity: a review of embolism repair in vascular plants. Frontiers in Plant Science 108: 1 - 11.

Brodersen CR, McElrone AJ, Choat B, Lee EF, Shackel KA, Matthews MA. 2013. In vivo visualizations of drought-induced embolism spread in Vitis vinifera. Plant Physiology 161: 1820 - 1829.

Brodersen CR, Knipfer T, McElrone A. 2018. In vivo visualization of the final stages of xylem vessel refilling in grapevine (*Vitis vinifera*) stems. New Phytologist 217: 117 - 126.

Brodribb TJ, Field TS. 2000. Stem hydraulic supply is linked to leaf photosynthetic capacity: evidence from New Caledonian and Tasmanian rainforests. Plant, Cell & Environment 23: 1381 - 1388.

Brodribb TJ, Hill RS. 2000. Increases in water potential gradient reduce xylem conductivity in whole plants. Evidence from a low-pressure conductivity method. Plant Physiology 123: 1021 - 1028.

Brodribb TJ, Holbrook NM. 2005. Water stress deforms tracheids peripheral to the leaf vein of a tropical conifer. Plant Physiology 173: 1139 - 1146.

Brodribb TJ. 2009. Xylem hydraulic physiology: the functional backbone of terrestrial plant productivity. Plant Science 177: 245 -251.

Brodribb TJ, Cochard H. 2009. Hydraulic failure defines the recovery and point of death in water-stressed conifers. Plant Physiology 149: 575 - 584.

Brodribb TJ, Bowman D, Nichols S, Delzon S, Burlett R. 2010. Xylem function and growth rate interact to determine recovery rates after exposure to extreme water deficit. New Phytologist 188: 533 - 542.

Brodribb TJ, Pittermann J, Coomes DA. 2012. Elegance versus speed: examining the competition between conifer and angiosperm trees. International Journal of Plant Sciences 173: 673 - 694.

Brodribb TJ, Skelton RP, McAdam SAM, Bienaimé D, Lucani CJ, Marmottant P. 2016. Visual quantification of embolism reveals leaf vulnerability to hydraulic failure. New Phytologist 209: 1403 - 1409.

Brodribb TJ. 2017. Progressing from 'functional' to mechanistic traits. New Phytologist 215: 9 - 11.

Brookshire ENJ, Weaver T. 2015. Long-term decline in grassland productivity driven by increasing dryness. Nature communications 6: 7148.

Bucci SJ, Scholz FG, Goldstein G, Meinzer FC, Sternberg LDSL. 2003. Dynamic changes in hydraulic conductivity in petioles of two savanna tree species: factors and mechanisms contributing to the refilling of embolized vessels. Plant, Cell & Environment 26: 1633 - 1645.

Burgert I, Bernasconi A, Eckstein D. 1999. Evidence for the strength function of rays in living trees. Holz als Roh-und Werkstoff 57: 397 - 399.

Burgert I, Eckstein D. 2001. The tensile strength of isolated wood rays of beech (*Fagus sylvatica* L.) and its significance for the biomechanics of living trees. Trees 15: 168 - 170.

Burgess SO, Pittermann J, Dawson TE. 2006. Hydraulic efficiency and safety of branch xylem increases with height in *Sequoia sempervirens* (D.Don) crowns. Plant, Cell & Environment 29: 229 - 239.

Cardoso AA, Brodribb TJ, Lucani CJ, DaMatta FM, McAdam SAM. 2018. Coordinated plasticity maintains hydraulic safety in sunflower leaves. Plant, Cell & Environment 41: 2567 - 2576.

Carlquist S. 1966. Wood anatomy of Compositae: a summary, with comments on factors controlling wood evolution. Aliso 6: 25 - 44.

Carlquist S. 1974. Insular woodiness. In: Island Biology, Columbia University Press, New York, pp: 350 - 428.

Carlquist S. 1975. Ecological strategies of xylem evolution. University of California Press, Berkeley.

Carlquist S. 1977. Ecological factors in wood evolution, a floristic approach. American Journal of Botany 6: 887 - 896.

Carlquist S. 1980. Further concepts in ecological wood anatomy, with comments on recent work in wood anatomy and evolution. Aliso 9: 499 - 553.

Carlquist S. 1982. Wood anatomy of *Illicium* (Illiciaceae). Phylogenetical, ecological and functional interpretations. American Journal of Botany 69: 1587 - 1598.

Carlquist S. 1984. Vessel grouping in Dicotyledon wood: significance and relationship to imperforate tracheary elements. Aliso 10: 505 - 525.

Carlquist S. 1985. Vasicentric tracheids as a drought survival mechanism in the woody flora of southern California and similar regions; review of vasicentric tracheids. Aliso 11: 37 - 68.

Carlquist S, Hoekman DA. 1985. Ecological wood anatomy of the woody southern Californian flora. IAWA Bulletin 6: 319 - 347.

Carlquist S. 1988. Tracheids dimorphism: a new pathway in evolution of imperforate tracheary elements. Aliso 12: 103 - 118.

Carlquist S. 2001. Comparative Wood Anatomy. Systematic, Ecological and Evolutionary Aspects of Dicotyledon Wood, 2nd ed. Springer, Santa Barbara.

Carlquist S. 2012. How wood evolves: a new synthesis. Botany 90: 901 - 940.

Challinor AJ, Ewert F, Arnold S, Simelton E, Fraser E. 2009. Crops and climate change: progress, trends, and challenges in simulating impacts and informing adaptation. Journal of Experimental Botany 60: 2775 - 2789.

Chave J, Muller-Landau HC, Baker TR, Easdale TA, Steege H ter, Webb CO. 2006. Regional and phylogenetic variation of wood density across 2456 neotropical tree species. Ecology Application 16: 2356 - 2367.

Chave J, Coomes D, Jansen S, Lewis SL, Swenson NG, Zanne AE. 2009. Towards a worldwide wood economics spectrum. Ecology Letters 12: 351 - 366.

Chevan A, Sutherland M. 1991. Hierarchical partitioning. American Statistical Association 45: 90 - 96.

Choat B, Ball MC, Luly JG, Holtum JAM. 2005. Hydraulic architecture of deciduous and evergreen dry rainforest tree species from north-eastern Australia. Trees 19: 305 - 311.

Choat B, Brodie Tw, Cobb AR, Zwieniecki MA, Holbrook NM. 2006. Direct measurements of intervessel pit membrane hydraulic resistance in two angiosperm tree species. American Journal of Botany 93: 993 - 1000.

Choat B, Sack L, Holbrook NM. 2007. Diversity of hydraulic traits in nine *Cordia* species growing in tropical forests with contrasting precipitation. New Phytologist 175: 686 - 698.

Choat B, Cobb AR, Jansen S. 2008. Structure and function of bordered pits: new discoveries and impacts on whole-plant hydraulic function. New Phytologist 177: 608 - 626.

Choat B, Drayton WM, Brodersen C, Matthews MA, Shackel KA, Wada H. *et al.* 2010. Measurement of vulnerability to water stress-induced cavitation in grapevine: a comparison of four techniques applied to a long-vesseled species. Plant, Cell & Environment 33: 1502 - 1412.

Choat B, Jansen S, Brodribb TJ, Cochard H, Delzon S, Bhaskar R, *et al.* 2012. Global convergence in the vulnerability of forests to drought. Nature 491: 752 - 755.

Ciais O, Reichstein M, Viovy N, Granier A, Ogée J, Allard V, *et al.* 2005. Europe-wide reduction in primary productivity caused by the heat and drought in 2003. Nature 437: 529 - 533.

Cochard H. 2002. A technique for measuring xylem hydraulic conductance under high negative pressures. Plant, Cell & Environment 25: 815-819.

Cochard H, Nardini A, Coll L. 2004. Hydraulic architecture of the leaf blades: where is the main resistance? Plant, Cell & Environment 27: 1257 - 1267.

Cochard H, Gaelle D, Bodet C, Tharwat I, Poirier M, Ameglio T. 2005. Evaluation of a new centrifuge technique for rapid generation of xylem vulnerability curves. Physiologia Plantarum 124: 410 - 418.

Cochard H. 2006. Cavitation in trees. Comptes Rendus Physique 7: 1018 - 1026.

Cochard H, Barigah T, Kleinhentz M, Eshel A. 2008. Is xylem cavitation resistance a relevant criterion for screening drought resistance among *Prunus* species? Journal of Plant Physiology 165: 976 - 982.

Cochard H, Herbette S, Barigah T, Badel E, Ennajeh M, Vilagrosa A. 2010. Does sample length influence the shape of xylem embolism vulnerability curves? A test with the Cavitron spinning technique. Plant, Cell & Environment 33: 1543 - 1552.

Cochard H, Badel E, Herbette S, Delzon S, Choat B, Jansen S. 2013. Methods for measuring plant vulnerability to cavitation: a critical review. Journal of Experimental Botany 64: 4779 - 4791.

Corcuera L, Cochard H, Gil-Pelegrin E, Notivol E. 2011. Phenotypic plasticity in mesic populations of Pinus pinaster improves resistance to xylem embolism ($P_{50}$) under severe drought. Trees 25: 1033 - 1042.

Coutinho LM. 1983. Aspectos ecológicos da saúva no cerrado – a saúva, as queimadas, e sua possível relacão na ciclagem de nutrientes. Boletim de Zoologia 8: 1 - 9.

Coutinho LM. 2002. O bioma do cerrado. In: Klein AL (Ed.), Eugen Warming e o Cerrado Brasileiro. UNESP, Imprensa Oficial do Estado, São Paulo, pp: 77 - 92.

Crawley MJ. 2007. The R Book. Chichester: John Wiley & Sons Ltd.

Dai AG. 2013. Increasing drought under global warming in observations and models. Nature Climate Change 3: 52 - 58.

Darwin C. 1859. On the origin of species by means of natural selection (reprint of 1st ed. 1950). J. Murray, London.

Davis SD, Sperry JS, Hacke UG. 1999. The relationship between xylem conduit diameter and cavitation caused by freezing. American Journal of Botany 86: 1367 - 1372.

del-Arco M, Pérez-de-Paz PL, Acebes JR, Gonzáles-Mancebo JM, Reyes-Betancort J, Bermejo JA, *et al.* 2006. Bioclimatology and climatophilous vegetation of Tenerife (Canary Islands). Annales Botanici Fennici 43: 167 - 192.

Delzon S, Cochard H. 2014. Recent advances in tree hydraulics highlight the ecological significance of the hydraulic safety margin. New Phytologist 203: 355 - 358.

Dixon HH, Joly J. 1894. On the ascent of sap. Philosophical Transactions of the Royal Society London 186: 563-576.

Dixon HH. 1914. Transpiration and the Ascent of Sap. Macmillan and Co. Ltd., London.

Domec J-C, Lachenbruch B, Meinzer FC, Woodruff DR, Warren JM, McCulloh KA. 2008. Maximum height in a conifer is associated with conflicting requirements for xylem design. Proceedings of National Academic Science USA 33: 12069 - 12074.

Dória LC, Podadera DS, Batalha, MA, Lima, RS, Marcati, CR. 2016. Do woody plants of the Caatinga show a higher degree of xeromorphism than in the Cerrado? Flora 224: 244 - 251.

Dória LC, Podadera DS, del Arco M, Chauvin T, Smets E, Delzon S, *et al.* 2018. Insular woody daisies (*Argyranthemum*, Asteraceae) are more resistant to drought-induced hydraulic failure than their herbaceous relatives. Functional Ecology 32: 1467 - 1478.

Dória LC, Meijs C, Podadera DS, del Arco M, Smets E, Delzon S, *et al.* 2019. Embolism resistance in stems of herbaceous Brassicaceae and Asteraceae is linked with differences in woodiness and precipitation. Annals of Botany 124: 1 - 14.

Doyle JA. 2012. Molecular and fossil evidence on the origin of angiosperms. Annual Review of Earth and Planetary Sciences 40: 301 - 326.

Dulin, MW, Kirchoff BK. 2010. Paedomorphosis, secondary woodiness and insular woodiness in plants. Botanical review 76: 405 - 490.

Eckblad JW. 1991. How many samples should be taken. Journal of Biological Sciences 41: 346 - 348.

Engelbrecht BMJ, Comita LS, Condit R, Kursar TA, Tyree MT, Turner BL, *et al.* 2007. Drought sensitivity shapes species distribution patterns in tropical forests. Nature 447: 80 - 82.

Esau K. 1965. Plant Anatomy. 2nd Edition, John Wiley, New York.

Evert RF. 2006. Esau's Plant Anatomy: Meristems, Cells, and Tissues of the Plant Body: Their Structure, Function, and Development. 3rd Edition. John Wiley & Sons, Inc.

Ewers FW, Fisher JB, Chiu S. 1990. A survey of vessel dimensions in stems of tropical lianas and other growth forms. Bauhinia 84: 544 - 552.

Fan ZX, Cao KF, Becker P. 2009. Axial and radial variations in xylem anatomy of angiosperm and conifer trees in Yunnan, China. IAWA Journal 30: 1 - 13.

Fichot R, Barigah TS, Chamaillard S, LE Thiec D, Laurans F, Cochard H, *et al.* 2010. Common trade-offs between xylem resistance to cavitation and other physiological traits do not hold among unrelated *Populus deltoids* × *Populus nigra* hybrids. Plant, Cell & Environment 33: 1553 - 1568.

Francisco-Ortega J, Crawford DJ, Santos-Guerra A, Jansen RK. 1997. Origin and evolution of *Argyranthemum* (Asteraceae: Anthemidae) in Macaronesia. In Givnish TJ, Sytsma KJ (Eds.), Molecular evolution and adaptive radiation. Cambridge University Press, Cambridge, pp: 407 - 431.

Franklin GL. 1945. Preparation of thin sections of synthetic resins and wood-resins composites, and a new macerating method for wood. Nature 155: 51.

Freese F. 1967. Elementary Statistical Methods for Foresters, USDA Forest Service, Agriculture Handbook 317, Washington.

Givnish TJ. 1998. Adaptive plant evolution on islands: classical patterns, molecular data, new insights. In: Grant PR (Ed.), Evolution on Islands, Oxford University Press, Oxford, pp: 281-304.

Gleason SM, Butler DW, Zieminska K, Waryszak P, Westby M. 2012. Stem xylem conductivity is key to plant water balance across Australian angiosperm species. Functional ecology 26: 343 - 356.

Gleason SM, Westoby M, Jansen S. Choat B, Hacke UG, Pratt RB, *et al.* 2016a. Weak tradeoff between xylem safety and xylem-specific hydraulic efficiency across the world's woody plant species. New Phytologist 209: 123 - 136.

Gleason SM, Westoby M, Jansen S, Choat B, Brodribb TJ, Chochard H, *et al.* 2016b. On research priorities to advance understanding of the safety-efficiency trade off in xylem. New Phytologist 211: 1156 - 1158.

Hacke UG, Sperry JS, Pockman WT, Davis SD, McCulloh KA. 2001a. Trends in wood density and structure are linked to prevention of xylem implosion by negative pressure. Oecologia 126: 457 - 461.

Hacke UG, Stiller V, Sperry JS, Pittermann J, McCulloh KA. 2001b. Cavitation fatigue. Embolism and refilling cycles can weaken the cavitation resistance of xylem. Plant Physiology 125: 779 - 786.

Hacke UG, Sperry JS. 2003. Limits to xylem refilling under negative pressure in *Laurus nobilis* and *Acer negundo*. Plant, Cell & Environment 26: 303 - 311.

Hacke UG, Sperry JS, Pitterman J. 2004. Analysis of circular bordered pit function. II. Gymnosperm tracheids with torus-margo pit membranes. American Journal of Botany 91: 386 - 400.

Hacke UG, Sperry JS, Wheeler JK, Castro L. 2006. Scaling of angiosperm xylem structure with safety and efficiency. Tree Physiology 26: 689 - 701.

Hacke UG, Jansen S. 2009. Embolism resistance of three boreal conifer species varies with pit structure. New Phytologist 182: 675 - 686.

Hacke UG, Spicer R, Schreiber SG, Plavcová L. 2017. An ecophysiological and developmental perspective on variation in vessel diameter. Plant Cell & Environment 40: 831 - 845.

Hamann TD, Smets E, Lens F. 2011. A comparison of paraffin and resin-based techniques used in bark anatomy. Taxon 60: 841 - 851.

Hanhijarvi A, Wahl P, Rasanen J, Silvennoinen R. 2003. Observation of development of microcracks on wood surface caused by drying stresses. Holzforschung 57: 561 - 565.

Hartmann H. 2011. Will a 385 million year-struggle for light become a struggle for water and for carbon? – How trees may cope with more frequent climate change-type drought events. Global Change Biology 17: 642 - 655.

Hoffman WA, Marchin RM, Abit P, Lau LO. 2011. Hydraulic failure and tree dieback are associated with high wood density in a temperate forest under extreme drought. Global Change Biology 17: 2731 - 2742.

Holbrook MN. 1995. Stem water storage. In: Gardner BL (Ed.), Plant stems. Academic Press, New York, pp: 151 - 174.

Holste EK, Jerke MJ, Matzner SL. 2006. Long-term acclimatization of hydraulic properties, xylem conduit size, wall strength and cavitation resistance in *Phaseolus vulgaris* in response to different environmental effects. Plant, Cell & Environment 29: 836 - 843.

Höltta T, Vesala T, Perämäki M, Nikinmaa E. 2006. Refilling of embolised conduits as a consequence of 'Münch water' circulation. Functional Plant Biology 33: 949 - 959.

Höltta T, Mencuccini, M, Nikinmaa, E. 2011. A carbon cost-gain model explains the observed patterns of xylem safety and efficiency. Plant, Cell & Environment 34: 1819 - 1834.

Humphries CJ. 1976. A revision of the Macaronesian genus *Argyranthemum* Webb ex Schultz-Bip. (Compositae-Anthemideae). Bulletin of the British Museum (Natural History) Botany 5: 147 - 240.

IAWA Committee. 1989. IAWA list of microscopic features for hardwood identification. IAWA Bulletin 10: 219 - 332.

IBGE [Instituto Brasileiro de Geografia e Estatística]. 2012. Manual técnico da vegetação brasileira. IBGE, Rio de Janeiro.

Ilic J. 1999. Shrinkage-related degrade and its association with some physical properties in *Eucalyptus regnans* F. Muell. Wood Science and Technology 33: 425 - 437.

Iqbal M. 1995. The cambial derivatives. Schweizerbart Science Publishers, Stuttgart.

Jacobsen AL, Ewers FW, Pratt RB, Paddock WA, Davis D. 2005. Do xylem fibers affect vessel cavitation resistance? Plant Physiology 139: 546 - 556.

Jacobsen AL, Pratt RB, Davis SD, Ewers FW. 2007. Cavitation resistance and seasonal hydraulics differ among three arid Californian plant communities. Plant, Cell & Environment 30: 1599 - 1609.

Jacobsen AL, Pratt RB, Tobin MF, Hacke UG, Ewers FW. 2012. A global analysis of xylem vessel length in woody plants. American Journal of Botany 99: 1583 - 1591.

Jacobsen AL, Pratt RB. 2018. Going with the flow: structural determinants of vascular tissue transport efficiency and safety. Plant, Cell & Environment 41: 2715 - 2717.

James S, Meinzer F, Goldstein G, *et al.* 2003. Axial and radial water transport and internal water storage in tropical forest canopy trees. Oecologia 134: 37 - 45.

Jansen J, Baas P, Gasson P, Lens F, Smets E. 2004. Variation in xylem structure from tropics to tundra: evidence from vestured pits. Proceedings of the National Academy Sciences USA 101: 8833 - 8837.

Jansen S, Choat B, Pletsers A. 2009. Morphological variation of intervessel pit membranes and implications to xylem function in angiosperms. American Journal of Botany 96: 409 - 419.

Jansen S, Schenk HJ. 2015. On the ascent of sap in the presence of bubbles. American Journal of Botany 102: 1561 - 1563.

Johansen DA. 1940. Plant Microtechique. McGraw Hill, New York.

Johnson DM, Mcculloh KA, Woodruff DR, Meinzer FC. 2012. Hydraulic safety margins and embolism reversal in stems and leaves: why are conifers and angiosperms so different? Plant Sciences 195: 48 - 53.

Karnovsky MJ. 1965. A formaldehyde - glutaraldehyde fixative of high osmolality for use in electron microscopy. Journal of Cell Biology 27: 137 - 138.

Kattge J, Diaz S, Lavorel S, Prentices IC, Leadley P, Bonisch G, *et al.* 2011. TRY – a global database of plant traits. Global Change Biology 17: 2905 - 2935.

Kidner C, Groover A, Thomas D, Emelianova K, Soliz-Gamboa C, Lens F. 2016. First steps in studying the origins of secondary woodiness in *Begonia* (Begoniaceae): combining anatomy, phylogenetics, and stem transcriptomics. Biological Journal of the Linnean Society 117: 121 - 138.

Kitin P, Voelker SL, Meinzer FC, Beeckman H, Strauss SH, Lachenbruch B. 2010. Tyloses and phenolic deposits in xylem vessels impede water transport in low-lignin transgenic poplars: A study by cryo-fluorescence microscopy. Plant Physiology 154: 887 - 898.

Knipfer T, Brodersen CR, Zedan A, Kluepfel DA, McElrone AJ. 2015. Patterns of drought-induced embolism formation and spread in living walnut saplings visualized using X-ray microtomography. Tree Physiology 35: 744 - 755.

Kochian LV. 1995. Cellular mechanisms of aluminum toxicity and resistance in plants. Annual Review of Plant Physiology and Plant Molecular Biology 46: 237 - 260.

Kokacinar F, Sage RF. 2003. Photosynthetic pathway alters xylem structure and hydraulic function in herbaceous plants. Plant, Cell & Environment 26: 2015 - 2026.

Kolb KJ, Sperry JS. 1999. Differences in drought adaptation between subspecies of Sagebrush (*Artemisia tridentata*). Ecology 7: 2373 - 2384.

Koch GW, Sillett SC, Jennings GM, Davis SD. 2004. The limits to tree height. Nature 428: 851 - 854.

Kollmann F, Cote WA. 1968. Principles of wood science and technology I - Solid wood. Springer Verlag.

Kord B, Kialashaki A, Kord B. 2010. The within-tree variation in wood density and shrinkage, and their relationship in Populus euramericana. Turkish Journal of Agriculture and Forestry 34: 121 - 126.

Kozlowski TT, Kramer PJ, Pallardy SG. 1991. The Physiological Ecology of Woody Plants. Academic Press, San Diego.

Kraus JE, Arduin M. 1997. Manual básico de métodos em morfologia vegetal. Seropédica, Rio de Janeiro.

Lachenbruch B, McCulloh KA. 2014. Traits, properties, and performance: how woody plants combine hydraulic and mechanical functions in a cell, tissue, or whole plant. New Phytologist 204: 747 - 764.

Lamy J, Delzon S, Bouche PS, Alia R, Vendramin GG, Cochard H, *et al.* 2014. Limited genetic variability and phenotypic plasticity detected for cavitation resistance in a Mediterranean pine. New Phytologist 201: 874 - 886.

Larter M, Brodribb TJ, Pfautsch S, Burlett R, Cochard H, Delzon S. 2015. Extreme aridity pushes trees to their physical limits. Plant Physiology 168: 804 - 807.

Larter M, Pfautsch S, Domec J-C, Trueba S, Nagalingum N, Delzon S. 2017. Aridity drove the evolution of extreme embolism resistance and the radiation of conifer genus *Callitris*. New Phytologist 215: 97 - 112.

Lazzarin M, Crivellaro A, Williams CB, Dawson TE, Mozzi G, Anfodillo T. 2016. Tracheid and pit anatomy vary in tandem in a tall *Sequoiadendron giganteum* tree. IAWA Journal 37: 172 - 185.

Lefcheck JS. 2015. piecewiseSEM: Piecewise structural equation modelling in R for ecology, evolution, and systematics. Methods in Ecology and Evolution 7: 573 - 579.

Lens F, Luteyn JL, Smets E, Jansen S. 2004. Ecological trends in the wood anatomy of Vaccinioideae (Ericaceae s.l.). Flora 199: 309 - 319.

Lens F, Sperry JS, Christman MA, Choat B, Rabaey D, Jansen S. 2011. Testing hypotheses that link wood anatomy to cavitation resistance and hydraulic conductivity in the genus *Acer*. New Phytologist 190: 709 - 723.

Lens F, Eeckhout S, Zwartjes R, Smets E, Janssens S. 2012a. The multiple fuzzy origins of woodiness within Balsaminaceae using an integrated approach. Where do we draw the line? Annals of Botany 109: 783 - 799.

Lens F, Smets E, Melzer S. 2012b. Stem anatomy supports *Arabidopsis thaliana* as a model for insular woodiness. New Phytologist 193: 12 - 17.

Lens F, Tixier A, Cochard H, Sperry JS, Jansen S, Herbette S. 2013a. Embolism resistance as a key mechanism to understand adaptive plant strategies. Current Opinion in Plant Biology 16: 287 - 292.

Lens F, Davin N, Smets E, del Arco M. 2013b. Insular woodiness on the Canary Islands: remarkable case of convergent evolution. International Journal of Plant Sciences 174: 992 - 1013.

Lens F, Picon-Cochard C, Delmas CEL, Signarbieux C, Buttler A, Cochard H, *et al.* 2016. Herbaceous angiosperms are not more vulnerable to drought-induced embolism than angiosperm trees. Plant Physiology 172: 661 - 667.

Li S, Lens F, Espino S, Karimi Z, Klepsch M, Schenk HJ, *et al.* 2016. Intervessel pit membrane thickness as a key determinant of embolism resistance in angiosperm xylem. IAWA Journal 37: 152 - 171.

Ligrone R, Duckett JG, Renzaglia KS. 2012. Major transitions in the evolution of early land plants: a bryological perspective. Annals of Botany 109: 851 - 871.

Loepfe L, Martínez-Vilalta J, Pinol J, Mencuccini M. 2007. The relevance of xylem network structure for plant hydraulic efficiency and safety. Journal of Theoretical Biology 247: 788 - 803.

Lucas JW, Groover A, Lichtenberger R, Furuta K, Yadav S, Helariutta Y, *et al.* 2013. The plant vascular system: evolution, development and functions. Journal of Integrative Plant Biology 55: 294 - 388.

Lupi C, Morin H, Deslauriers A, Rossi S, Houle D. 2012. Increasing nitrogen availability and soil temperature: effects on xylem phenology and anatomy of mature black spruce. Canadian Journal of Forest Research 42: 1277 - 1288.

Maherali H, Pockman WT, Jackson RB. 2004. Adaptive variation in the vulnerability of woody plants to xylem cavitation. Ecology 85: 2184 - 2199.

Maherali H, Walden AE, Husband BC. 2009. Genome duplication and the evolution of physiological responses to water stress. New Phytologist 184: 721 - 731.

Marcati CR, Angyalossy-Alfonso V, Benetati L. 2001. Anatomia comparada do lenho de *Copaifera langsdorffii* Desf. (Leguminosae-Caesalpinoideae) de floresta e cerradão. Revista Brasileira de Botânica 24: 311 - 320.

Martin-St Paul N, Longepierre D, Huc R, Delzon S, Burlett R, Joffre R, *et al.* 2014. How reliable are methods to assess xylem vulnerability to cavitation? The issue of 'open vessel' artifact in oaks. Tree Physiology 34: 894 - 905.

Martinez-Cabrera HI, Jones CS, Espino S, Schenk HJ. 2009. Wood anatomy and wood density in shrubs: responses to varying aridity along transcontinental transects. American Journal of Botany 96: 1388 - 1398.

Martinez-Vilalta J, Cochard H, Mencuccini M, Sterck F, Herrero A, Korhonen JFJ, *et al.* 2009. Hydraulic adjustment of Scots pine across Europe. New Phytologist 184: 353 - 364.

Martinez-Vilalta J, Muncuccini M, Vayreda J, Retana J. 2010. Interspecific variation in functional traits, not climatic differences among species ranges, determines demographic rates across 44 temperate and Mediterranean tree species. Journal of Ecology 98: 1462 - 1475.

Mattheck C, Kubler H. 1995. Wood – the internal optimization of trees. Springer-Verlag, Berlin.

Mattos BD, Gatto DA, Stangerlin DM, Calegari L, Melo RR, Santini EJ. 2011. Variação axial da densidade básica da madeira de três espécies de gimnospermas. Brazilian Journal of Agricultural Sciences 6: 121 -126.

McCulloh KA, Sperry JS. 2005. Patterns in hydraulic architecture and their implications for transport efficiency. Tree Physiology 25: 257 - 267.

McDowell NG, Phillips N, Lunch C, Bond BJ, Ryan MG. 2002. An investigation of hydraulic limitation and compensation in large, old Douglas-fir trees. Tree Physiology 22: 763 - 774.

McDowell NG, Pockman WT, Allen CD, Breshears DD, Cobb N, Kolb T, *et al.* 2008. Mechanisms of plant survival and mortality during drought: why do some plants survive while others succumb to drought? New Phytologist 178: 719 - 739.

Meinzer FC, Woodruff DR, Domec J-C, Goldstein G, Campanello PI, Gatti MG, *et al.* 2008. Coordination of leaf and stem water transport properties in tropical forest trees. Oecologia 156: 31 - 41.

Meinzer FC, McCulloh KA, Lachenbruch B, Woodruff DR, Johnson DM. 2010. The blind men and the elephant: the impact of context and scale in evaluating conflicts between plant hydraulic safety and efficiency. Oecologia 164: 287 - 296.

Mencuccini M, Comstock J. 1999. Variability in hydraulic architecture and gas exchange of common bean (*Phaseolus vulgaris*) cultivars under well-watered conditions: interactions with leaf size. Australian Journal of Plant Physiology 26: 115 - 124.

Mendiburu F. 2017. Agricolae: Statistical Procedures for Agricultural Research. R package version 1.2-8. https://CRAN.R-project.org/package=agricolae.

Metcalfe CR, Chalk L. 1950. Anatomy of the Dicotyledons. Vol. 1, Clarendon Press, Oxford.

Metcalfe CR. 1973. Metcalfe and Chalk's anatomy of the dicotyledons and its revision. Taxon 22: 659 - 668.

Metzner R, Thorpe MR, Breuer U, Blumler P, Schurr U, Schneider H, *et al.* 2010. Contrasting dynamics of water and mineral nutrients in stems shown by stable isotope tracers and cryo-SIMS. Plant, Cell & Environment 33: 1393 - 1407.

Meyra AG, Kuz VA, Zarragoicohea GJ. 2007. Geometrical and physicochemical considerations of the pit membrane in relation to air seeding: the pit membrane as a capillary valve. Tree Physiology 27: 1401 - 1405.

Mrad A, Domec J-C, Huang C-W, Lens F, Katul G. 2018. A network model links wood anatomy to xylem tissue hydraulic behaviour and vulnerability to cavitation. Plant, Cell & Environment 41: 2718 - 2730.

Monfreda C, Ramankutty N, Foley JA. 2008. Farming the planet: 2. Geographic distribution of crop areas, yields, physiological types, and net primary production in the year 2000. Global Biogeochemical Cycles 22: Gb1022

Morretes BL, Ferri MG. 1959. Contribuição ao estudo da anatomia das folhas de plantas do cerrado. Boletim da Faculdade de Filosofia Ciências e Letras 243: 7–70.

Morris H, Plavcová L, Gorai M, Klepsch MM, Kotowska M, Schenk HJ, *et al.* 2018. Vessel-associated cells in angiosperm xylem: highly specialized living cells at the symplast–apoplast boundary. American Journal of Botany 105: 151 - 160.

Moro MF, Lughada EN, Filer DL, Araújo FS, Martins FR. 2014. A catalogue of the vascular plants of the Caatinga Phytogeographical Domain: a synthesis of floristic and phytosociological surveys. Phytotaxa 160: 1 - 118.

Moro MF, Lughadha EN, Araújo FS, Martins FR. 2016. A phytogeographical meta-analysis of the semiarid Caatinga domain in Brazil. Botanical Review 82: 91 - 148.

Moya R, Perez LD, Arce V. 2003. Wood density of *Tectona grandis* at two plantation spacings in Costa Rica. Journal of Tropical Forest Products 9: 153 - 161.

Nakagawa S, Schielzeth H. 2013. A general and simple method for obtaining $R^2$ from generalized linear mixed-effect models. Methods in Ecology and Evolution 4: 133 - 142.

Nardini A, Lo Gullo MA, Salleo S. 2011. Refilling embolized xylem conduits: is it a matter of phloem unloading? Plant Sciences 180: 604 - 611.

Nolf M, Pagitz K, Mayr S. 2014. Physiological acclimation to drought stress in *Solidago canadensis*. Physiologia Plantarum 150: 529 - 539.

Nolf M, Rosani A, Ganthaler A, Beikircher B, Mayr, S. 2016. Hydraulic variation in three *Ranunculus* species. Plant Physiology 170: 2085 - 2094.

Nimer E. 1972. Climatologia da Região Nordeste do Brasil. Revista Brasileira de Geografia 34: 3 - 51.

O'Brien MJ, Leuzinger S, Philipson CD, Tay J, Hector A. 2014. Drought survival of tropical tree seedlings enhanced by non-structural carbohydrate levels. Nature climate change 4: 710 - 714.

O' Brien MJ, Engelbrecht BMJ, Joswig J, Pereyra G, Schuldt B, Jansen S, *et al.* 2017. A synthesis of tree functional traits related to drought induced mortality in forests across climatic zones. Journal of Applied Ecology 54: 1669 - 1686.

Oberprieler C, Himmelreich S, Källersjö M, Vallès J, Watson LE, Vogt R. 2009. Anthemidae. In: Funk VA, Susanna A, Stuessy TF, Bayer RJ (Eds.), Systematics, evolution, and biogeography of Compositae. International Association for Plant Taxonomy, Vienna, pp: 631 - 666.

Ogasa M, Miki NH, Murakami Y, Yoshikawa K. 2013. Recovery performance in xylem hydraulic conductivity is correlated with cavitation resistance for temperate deciduous tree species. Tree Physiology 33: 335 - 344.

Oksanen J, Blanchet FG, Kindt R, Legendre P, Minchin PR, O'Hara RB. *et al.* 2015. Vegan: Community Ecology, Available online at: http://CRAN.R-project. org/package=vegan.

Oliveira PS, Marques RJ. 2002. The Cerrado of Brazil: Ecology and Natural History of a Neotropical Savanna. Columbia University Press, New York.

Oliveira AFM, Meirelles ST, Salatino A. 2003. Epicuticular waxes from caatinga and cerrado species and their efficiency against water loss. Anais da Academia Brasileira de Ciências 75: 431 - 439.

Oliveira RS, Bezerra L, Davidson EA, Pinto F, Klink CA, Nepstad DC, *et al.* 2005. Deep root function in soil water dynamics in cerrado savannas of central Brazil. Functional Ecology 19: 574 - 581.

Oliveira RS, Costa FRC, van Baalen E, Jonge A, Bittencourt PR, Almanza Y, *et al.* In press. Embolism resistance drives the distribution of Amazonian rainforest tree species along hydro-typographic gradients. New Phytologist. doi: 10.1111/nph.15463

Olson ME. 2012. Linear trends in botanical systematics and the major trends of xylem evolution. Botanical Review 78: 154 - 183.

Olson ME, Rosell J. 2013. Vessel diameter–stem diameter scaling across woody angiosperm and the ecological causes of xylem vessel diameter variation. New Phytologist 197: 1204 - 1213.

Olson ME, Rosell J, Léon C, Zamora S, Weeks A, Alvarado-Cárdenas LO, *et al.* 2013. Convergent vessel diameter–stem diameter scaling across five clades of new and old world eudicots from desert to rain forest. International Journal of Plant Sciences 174: 1062 - 1078.

Olson ME. 2014. Xylem hydraulic evolution, I.W. Bailey, and Nardini & Jansen (2013): Pattern and process. New Phytologist 203: 7 - 11.

Olson ME, Anfodillo T, Rosell J, Petit G, Crivellaro A, Isnard S, *et al.* 2014. Universal hydraulics of the flowering plants: vessel diameter scales with stem length across angiosperm lineages, habits and climates. Ecology Letters 17: 988 - 997.

Olson ME, Soriano D, Rosell JA, Anfodillo T, Donoghue MJ, Edwards EJ, *et al.* 2018. Plant height and hydraulic vulnerability to drought and cold. Proceedings of the National Academy of Sciences USA 115: 7551 - 7556.

Onoda Y, Richards AE, Westoby M. 2010. The relationship between stem biomechanics and wood density is modified by rainfall in 32 Australian woody plant species. New Phytologist 185: 493 - 501.

Pammenter NW, Van der Willigen C. 1998. A mathematical and statistical analysis of the curves illustrating vulnerability of xylem to cavitation. Tree Physiology 18: 589 - 593.

Pennington, T.R., Prado, D.E., Pendry, C.A., 2000. Neotropical seasonally dry forests and Quaternary vegetation changes. Journal of Biogeography 27: 261 - 273.

Pereira L, Bittencourt PRL, Oliveira RS, Junior MBM, Barros FV, Ribeiro RV, *et al.* 2016. Plant pneumatics: stem air flow is related to embolism – new perspectives on methods in plant hydraulics. New Phytologist 211: 357 - 370.

Pereira L, Domingues-Junior AP, Jansen S, Choat B, Mazzafera P. 2017. Is embolism resistance in plant xylem associated with quantity and characteristics of lignin? Trees 32: 349 - 358.

Petit G, Pfautsch S, Anfodillo T, Adams MA. 2010. The challenge of tree height in *Eucalyptus regnans*: when xylem tapering overcomes hydraulic resistance. New Phytologist 187: 1146 - 1153.

Pfautsch S, Keitel C, Turnbull TL, Braimbridge MJ, Wright TE, Simpson RR, *et al.* 2011. Diurnal patterns of water use in *Eucalyptus victrix* indicate pronounced desiccation-rehydration cycles despite unlimited water supply. Tree Physiology 31: 1041 - 1051.

Pfautsch S, Renard J, Tjoelker MG, Salih A. 2015a. Phloem as capacitor: radial transfer of water into xylem of tree stems occurs via symplastic transport in ray parenchyma. Plant Physiology 167: 963 - 971

Pfautsch S, Holtta T, Mencuccini M. 2015b. Hydraulic functioning of tree stems: fusing ray anatomy, radial transfer and capacitance. Tree Physiology 35: 706 -722.

Pfautsch S, Aspinwall MJ, Drake JE, Chacon-Doria L, Langelaan RJA, Tissue DT, *et al.* 2018. Traits and trade-offs in whole-tree hydraulic architecture along the vertical axis of *Eucalyptus grandis*. Annals of Botany 121: 129 - 141.

Pinheiro J, Bates D, DebRoy S, Sarkar D, R Core Team. 2016. nlme: linear and nonlinear mixed effects models. R package version 3.1-126. http://CRAN.R-project.org/package=nlme.

Pinheiro J, Bates D, DebRoy S, Sarkar D, R Core Team. 2018. nlme: Linear and Nonlinear Mixed Effects Models. R package version 3.1-137. https://CRAN.R-project.org/package=nlme.

Pittermann J, Sperry JS. 2003. Tracheid diameter is the key trait determining the extent of freezing-induced embolism in conifers. Tree Physiology 23: 907 - 914.

Pittermann J. 2010. The evolution of water transport in plants: an integrated approach. Geobiology 8: 112 - 139.

Pittermann J, Choat B, Jansen S, Stuart SA, Lynn L, Dawson TE. 2010. The Relationships between xylem safety and hydraulic efficiency in the Cupressaceae: the evolution of pit membrane form and function. Plant Physiology 153: 1919 - 1931.

Pivovaroff AL, Pasquini SC, Guzman ME, Alstad KP, Stemke JS, Santiago LS. 2015. Multiple strategies for drought survival among woody plant species. Functional Ecology 30: 517 - 526.

Plavcová L, Jansen S, Klepsch M, Hacke UG. 2013. Nobody's perfect: can irregularities in pit structure influence vulnerability to cavitation? Frontiers in Plant Science 4: 1 - 6.

Plavcová L, Jansen S. 2015. The role of xylem parenchyma in the storage and utilization of nonstructural carbohydrates. In: Hacke UW (Ed.), Functional and ecological xylem anatomy. Springer International Publishing, Switzerland, pp: 209 - 234.

Pockman WT, Sperry JS, O'Leary JW. 1995. Sustained and significant negative water pressure in xylem. Nature 378: 715 - 716.

Pockman WT, Sperry JS. 2000. Vulnerability to xylem cavitation and the distribution of Sonoran Desert vegetation. American Journal of Botany 87: 1287 - 1299.

Poorter L, Bongers L, Bongers F. 2006. Architecture of 54 moist forest tree species: traits, trade-offs, and functional groups. Ecology 87: 1289 - 1301.

Poorter L, McDonald I, Alarcón A, Fichtler E, Licona J-C, Peña-Claros M. 2010. The importance of wood traits and hydraulic conductance for the performance and life history strategies of 42 rainforest tree species. New Phytologist 185: 481 - 492.

Pratt RB, Jacobsen AL, Golgotiu KA, Sperry JS, Ewers FW, Davis SD. 2007. Life history type and water stress tolerance in nine California chaparral species (Rhamnaceae). Ecology Monographs 77: 239 - 253.

Pratt RB, Jacobsen AL. 2017. Conflicting demands on angiosperm xylem: tradeoffs among storage, transport and biomechanics. Plant, Cell & Environment 40: 897 - 913.

Preston KA, Cornwell WK, DeNoyer JL. 2006. Wood density and vessel traits as distinct correlates of ecological strategy in 51 California coast range angiosperms. New Phytologist 170: 807 - 818.

R Core Team, 2014. R: A Language and Environment for Statistical Computing. R Foundation for Statistical Computing, Vienna, Austria, URL http://www.R- project.org/.</doc ref.

R Core Team. 2016. R: A Language and Environment for Statistical Computing. R Foundation for Statistical Computing, Vienna. URL http://www.R-project.org/.</doc ref.

R Core Team. 2017. R: A Language and Environment for Statistical Computing. R Foundation for Statistical Computing, Vienna. http://www.R-project.org.

R Studio Team. 2016. RStudio: Integrated Development for R. RStudio, Inc., Boston. http://www.rstudio.com/

Raij B, van Andrade JC, Cantarella H, Quaggio JA. 2001. Análise química para avaliacão da fertilidade do solo. Instituto Agronômico, Campinas.

Rahmstorf S, Coumou D. 2012. A decade of weather extremes. Nature Climate Change 2: 491 - 496.

Ratter JA, Bridgewater S, Ribeiro JF. 2003. Analysis of the floristic composition of the Brazilian cerrado vegetation III: comparison of the woody vegetation of 376 areas. Edinburgh Journal of Botany 60: 57 - 109.

Reiterer A, Burgert I, Sinn G, Tschegg S. 2002. The radial reinforcement of the wood structure and its implication on mechanical and fracture mechanical properties -- a comparison between two tree species. Journal of Materials Sciences 37: 935 - 940.

Rivera G, Elliot S, Caldas LS, Nicolossi G, Coradin VTR, Borchert R. 2002. Increasing day length induces spring flushing in tropical dry forest trees in the absence of rain. Trees 16: 445 - 456.

Rosell JA, Olson ME, Anfodillo T. 2017. Scaling of xylem vessel diameter with plant size: causes, predictions, and outstanding questions. Current Forestry Reports 3: 46 - 59.

Rosenthal DM, Stiller V, Sperry JS, Donovan LA. 2010. Contrasting drought tolerance strategies in two desert annuals of hybrid origin. Journal of experimental botany 61: 2769 - 2778.

Rosner S. 2017. Wood density as a proxy for vulnerability to cavitation: size matters. Journal of Plant Hydraulics 4: 1 - 10.

Salatino A. 1993. Chemical ecology and the theory of oligotrophic scleromorphism. Anais da Academia Brasileira de Ciências 65: 1 - 13.

Salleo S, Lo Gullo MA, Trifilo P, Nardini A. 2004. New evidence for a role of vessel-associated cells and phloem in the rapid xylem refilling of cavitated stems of *Laurus nobilis* L. Plant, Cell & Environment 27: 1065 - 1076.

Salleo S, Trifilò P, Lo Gullo MA. 2006. Phloem as a possible major determinant of rapid cavitation reversal in stems of *Laurus nobilis* (laurel). Functional Plant Biology 33: 1063 - 1074.

Salleo S, Trifiló P, Lo Gullo MA. 2008. Vessel wall vibrations: trigger for embolism repair. Functional Plant Biology 35: 289 - 297.

Salleo S, Trifiló P, Esposito S, Nardini A, Lo Gullo MA. 2009. Starch-to-sugar conversion in wood parenchyma of field-growing *Laurus nobilis* plants: a component of the signal pathway for embolism repair? Functional Plant Biology 36: 815 - 825.

Sass JE. 1951. Botanical Microtechinique, 20 ed. The Iowa State College Press, Ames.

Scholz FG, Bucci SJ, Goldstein G, Meinzer FC, Franco AC, Miralles-Wilhelm F. 2007. Biophysical properties and functional significance of stem water storage tissues in Neotropical savannah trees. Plant, Cell & Environment 30: 236 - 248.

Scholz A, Klepsch M, Karimi Z, Jansen S. 2013. How to quantify conduits in wood? Frontiers in Plant Sciences 56: 1 - 11.

Scholz FG, Phillips NG, Bucci SJ, Meinzer FC, Goldstein G. 2011. Hydraulic capacitance: biophysics and functional significance of internal water sources on relation to tree size. In: Meinzer FC, Phillips NG, Bucci SJ, Meinzer FC, Goldstein G (Eds.), Size-and age-related changes in tree structure. Springer Science Business Media, pp: 341 - 361.

Schenk HJ, Steppe K, Jansen S. 2015. Nanobubbles: a new paradigm for air-seeding in xylem. Trends in Plant Science 20: 199-205.

Schenk HJ, Espino S, Romo DM, Nima N, Do AYT, Michaud JM, *et al.* 2017. Xylem surfactants introduce a new element to the cohesion-tension theory. Plant Physiology 173: 1177 - 1196.

Schenk HJ, Espino S, Rich-Cavazos SM, Jansen S. 2018. From the sap's perspective: the nature of vessel surfaces in angiosperm xylem. American Journal of Botany 105: 172 - 185.

Schindelin J, Carreras A, Frise E, Kaynig V, Longair M, Pietzsch T, *et al.* 2012. Fiji - an Open Source platform for biological image analysis. Nature Methods 9: 676 - 682.

Schreiber S, Hacke UG, Hamann A. 2015. Variation of xylem vessel diameters across a climate gradient: insight from a reciprocal transplant experiment with a widespread boreal tree. Functional Ecology 29: 1392 - 1401.

Schweingruber FH. 2007. Wood structure and environment. Springer-Verlag, Berlin.

Schweingruber FH, Borner A, Schulze ED. 2011. Atlas of stem anatomy in herbs, shrubs and trees. Vol. 1. Springer, Heidelberg.

Shoemaker HE, McLean EO, Pratt PF. 1961. Buffer methods for determining the lime requirement of soils with appreciable amounts of extractable aluminum. Soil Science Society of Ameica Proceedings 25: 274 -277.

Silva FAM, Assad ED, Evangelista BA. 2008. Caracterização climática do bioma cerrado. In: Sano, S.M., Almeida, S.P., Ribeiro, J.F. (Eds.), Cerrado: Ecologia e Flora. Embrapa, Brasília, pp: 71 - 88.

Skelton RP, Brodribb TJ, Choat B. 2017. Casting light on xylem vulnerability in an herbaceous species reveals a lack of segmentation. New Phytologist 214: 561 - 569.

Solereder H. 1908. Systematic anatomy of the Dicotyledons: a handbook for laboratories of pure and applied botany. Vol. 2, Clarendon Press, Scott, Oxford.

Sonsin JO, Gasson GE, Barros CF, Marcati CR. 2012. A comparison of the wood anatomy of 11 species from two cerrado habitats (cerado s.s and adjacent gallery forest). Botanical Journal of the Linnean Society 170: 257 - 276.

Soudzilovskaia NA, Elumeeva TG, Onipchenko VG, Shidakov II, Salpagarova FS, Khubiev AB, *et al.* 2013. Functional traits predict relationship between plant abundance dynamic and long-term climate warming. Proceedings of the National Academy of Science USA 110: 18180 - 18184.

Souza MC, Franco AC, Haridasan M, Rossatto DR, Araújo JF, Morellato LPC, *et al.* 2015. The length of the dry season may be associated with leaf scleromorphism in cerrado plants. Anais da Academia Brasileira de Ciências 87: 1691 - 1699.

Sperry JS, Donnelly JR, Tyree MT. 1988. Seasonal occurrence of xylem embolism in sugar maple (*Acer saccharum*). American Journal of Botany 75: 1212 - 1218.

Sperry JS, Tyree MT. 1988. Mechanism of water stress-induced xylem embolism. Plant Physiology 88: 581 - 587.

Sperry J, Sullivan EM. 1992. Xylem embolism in response to freeze-thaw cycles and water stress in ring-porous, diffuse-porous, and conifer species. Plant Physiology 100: 605 - 613.

Sperry JS, Nichols KL, Sullivan JEM. 1994. Xylem embolism in ring-porous, diffuse-porous, and coniferous trees of Northern Utah and Interior Alaska. Ecology 75: 1736 – 1752.

Sperry J, Hacke U. 2002. Desert shrub water relations with respect to soil characteristics and plant functional type. Functional Ecology 16: 367 - 378.

Sperry JS. 2003. Evolution of water transport and xylem structure. International Journal of Plant Sciences 164: 115 - 127.

Sperry JS, Hacke UG, Wheeler JK. 2005. Comparative analysis of end wall resistivity in xylem conduits. Plant, Cell & Environment 28: 456 - 465.

Sperry JS, Hacke UG, Pittermann J. 2006. Size and function in conifer tracheids and angiosperm vessels. American Journal of Botany 93: 1490 - 1500.

Sperry JS, Meinzer FC, McCulloh KA. 2008. Safety and efficiency conflicts in hydraulic architecture: scaling from tissues to trees. Plant, Cell & Environment 31: 632 - 645.

Spicer R. 2014. Symplasmic networks in secondary vascular tissues: parenchyma distribution and activity supporting long-distance transport. Journal of Experimental Botany 65: 1829 - 1848.

Spicer R. 2016. Variation in angiosperm wood structure and its physiological and evolutionary significance. In: Groover A, Cronk Q (eds.), Comparative and Evolutionary Genomics of Angiosperm Trees. Springer, Switzerland, pp:19 - 60.

Stiller V, Sperry JS. 2002. Cavitation fatigue and its reversal in sunflower (*Helianthus annuus* L.). Journal of Experimental Botany 53: 1155 - 1161.

Thornthwaite CW. 1948. An approach toward a rational classification of climate. Geographical Review 38: 55 - 94.

Tixier A, Cochard H, Badel E, Dusotoit-Coucaud A, Jansen S, Herbette S. 2013. *Arabidopsis thaliana* as a model species for xylem hydraulics: does size matter? Journal of Experimental Botany 64: 2295 - 2305.

Tng DYP, Apgaua DMG, Ishida YF, Mencuccini M, Lloyd J, Laurance WF, *et al.* In press. Rainforest trees respond to drought by modifying their hydraulic architecture. Ecology and Evolution 1 - 13.

Torres-Ruiz JM, Cochard H, Mayr S, Beikircher B, Diaz-Espejo A, Rodriguez-Dominguez CM, *et al.* 2014. Vulnerability to cavitation in Olea europea current-year shoots: further evidence of an open-vessel artifact with centrifuge and air-injection techniques. Physiologia Plantarum 152: 465 - 474.

Torres-Ruiz JM, Jansen S, Choat B, McElrone AJ, Cochard H, Brodribb TJ, *et al.* 2015. Direct micro-CT observation confirms the induction of embolism upon xylem cutting under tension. Plant Physiology 167: 40 - 43.

Trifiló P, Barbera PM, Raimondo F, Nardini A, Lo Gullo MA. 2014. Coping with drought-induced xylem cavitation: coordination of embolism repair and ionic effects in three Mediterranean evergreens. Tree Physiology 34: 109 - 122.

Trueba S, Pouteau R, Lens F, Field TS, Isnard S, Olson ME, *et al.* 2017. Vulnerability to xylem embolism as a major correlate of the environmental distribution of rainforest species on a tropical island. Plant, Cell & Environment 40: 277 - 289.

Tyree MT, Sperry JS. 1989. Vulnerability of xylem to cavitation and embolism. Annual Review of Plant Physiology and Plant Molecular Biology 40: 19 - 38.

Tyree MT, Alexander J, Machado JL. 1992. Loss of hydraulic conductivity due to water stress in intact juveniles of *Quercus rubra* and *Populus deltoides*. Tree Physiology 10: 411 - 415.

Tyree MT, Davis SD, Cochard H. 1994. Biophysical perspectives of xylem evolution – is there a tradeoff of hydraulic efficiency for vulnerability to dysfunction. IAWA Journal 15: 335 - 360.

Tyree MT, Zimmermann MH. 2002. Xylem Structure and the Ascent of Sap. Springer, Berlin.

Tyree MT. 2003. Hydraulics limits on tree performance: transpiration, carbon gain and growth of trees. Trees – Structure and Function 17: 95 - 100.

UNEP. 1997. World Atlas of Desertification. United nations Environmental Program. Nairobi, Kenya.

Urli M, Porté AJ, Cochard H, Guengant Y, Burlett R, Delzon S. 2013. Xylem embolism threshold for catastrophic hydraulic failure in angiosperm trees. Tree Physiology 33: 672 - 683.

Van Bell AJE. 1990. Xylem-phloem exchange via the rays: the undervalued route of transport. Journal of Experimental Botany 41: 631 - 644.

Van den Oever L, Baas P, Zandee M. 1981. Comparative wood anatomy of *Symplocos* and latitude and altitude of provenance. IAWA Bulletin 2: 3 - 24.

Venturas MD, Sperry JS, Hacke UG. 2017. Plant xylem hydraulics: what we understand, current research, and future challenges. Journal of Integrative Plant Biology 59: 356 - 389.

Volaire F, Lens F, Cochard H, Xu H, Chacon-Dória L, Bristiel P, *et al.* 2018. Embolism and mechanical resistances play a key role in dehydration tolerance of a perennial grass *Dactylis glomerata* L. Annals of Botany 22: 325 - 336.

Wallace AR. 1878. Tropical nature and other essays. Macmillan Press, London.

Walkley A, Black IA. 1934. An examination of Degtjareff method for determining soil organic matter and a proposed modification of the chromic acid titration method. Soil Science (Baltimore) 37: 29 - 38.

Walter H. 1973. Vegetation of the Earth. Springer, New York.

Wang R, Zhang L, Zhang S, Cai J, Tyree MT. 2014. Water relations of *Robinia pseudoacacia* L.: Do vessels cavitate and refill diurnally or are R-shaped curves invalid in Robinia? Plant, Cell & Environment 37: 2667 - 2678.

West GB, Brown JH, Enquist BJ. 1999. A general model for the structure and allometry of plant vascular systems. Nature 400: 664.

Wheeler JK, Sperry JS, Hacke UG, Hoang N. 2005. Intervessel pitting and cavitation in woody Rosaceae and other vessel vesselled plants: a basis for a safety versus efficiency trade-off in xylem transport. Plant, Cell & Environment 28: 800 - 812.

Whittaker RJ, Fernandez-Palacios JM. 2007. Island biogeography: ecology, evolution, and conservation, 2nd ed. Oxford University Press, Oxford.

Williamson GB, Wiemann MC. 2010. Measuring wood specific gravity...correctly. American Journal of Botany 97: 519 - 524.

Woodruff DR, Meinzer FC, McCulloh KA. 2016. Forest canopy hydraulics. In: Hikosaka K, Niinemets U, Anten NPR (Eds.), Canopy Photosynthesis: from Basics to Applications. Springer Dordrecht, New York London, pp: 187 - 218.

Woodrum CL, Ewers FW, Telewski FW. 2003. Hydraulic, biomechanical, and anatomical interactions of xylem from five species of *Acer* (Aceraceae). American Journal of Botany 90: 693 - 699.

Wortemann R, Herbette S, Barigah TS, *et al.* 2011. Genotypic variability and phenotypic plasticity of cavitation resistance in *Fagus sylvatica* L. across Europe. Tree Physiology 31: 1175 - 1182.

Zanne AE, Westoby M, Falster DS, Ackerly DD, Loarie SR, Arnold SEJ, *et al.* 2010. Angiosperm wood structure: global patterns in vessel anatomy and their relation to wood density and potential conductivity. American Journal of Botany 97: 207 - 215.

Zhang YJ, Rockwell FE, Graham AC, Alexander T, Holbrook M. 2016. Reversible leaf collapse: a potential "circuit breaker" against cavitation. Plant Physiology 172: 2261 - 2274.

Zhang Y, Lamarque LJ, Torres-Ruiz JM, Schuldt B, Karimi Z, Li S, *et al.* 2018. Testing the plant pneumatic method to estimate xylem embolism resistance in stems of temperate trees. Tree Physiology 38: 1016 - 1025.

Zheng J, Martínez-Cabrera HI. 2013. Wood anatomical correlates with theoretical conductivity and wood density across China: evolutionary evidence of the functional differentiation of axial and radial parenchyma. Annals of Botany 112: 927 - 935.

Zieminska K, Butler DW, Gleason SM, Wright IJ, Westoby M. 2013. Fibre wall and lumen fractions drive wood density variation across 24 Australian angiosperms. Annals of Botany 5: 1 - 14.

Zieminska K, Westoby M, Wright IJ. 2015. Broad anatomical variation within a narrow wood density range – A study of twig wood across 69 Australian angiosperms. PLoS One 10: 1 - 25.

Zimmermann MH, Brown CL. 1977. Trees: structure and function. Springer Verlag, New York.

Zimmermann MH. 1983. Xylem Structure and the Ascent of Sap. Springer, Berlin, Heidelberg, New York.

Zobel BJ, Sprague JR. 1998. Juvenile wood in forest trees. Springer, New York.

Zuur AF, Ieno EN, Walker N, Saveliev AA, Smith GM. 2009. Mixed effects models and extensions in ecology with R. Springer, New York.

Zuur AF, Ieno EN, Smith GM. 2007. Analysing ecological data, 1st edn. Springer Science, New York.

Zuur AF, Ieno EN, Elphick CS. 2010. A protocol for data exploration to avoid common statistical problems. Methods in Ecology and Evolution 1: 3 – 14.

Zwieniecki MA, Secci F. 2015. Threats to xylem hydraulic function of trees under 'new climate normal' conditions. New Phytologist 38: 1713 - 1724.

# ACKNOWLEDGMENTS

*My PhD journey started in May 2015, when I moved from Brazil to the Netherlands. Pursuing a PhD in Botany was an old life goal, and I can honestly say that it was more challenging than I could ever expected. Though, I am grateful for the lessons that life has brought me, and for all the beautiful people that crossed my path, and helped me to complete this important step in my career.*

*I am grateful for all the researchers who directly collaborated on this PhD project. I thank the time and invaluable contributions of my coauthors, Diego Podadera, Prof. dr. Marcelino del Arco, Cynthia Meijs, and Thibaud Chauvin. A special thanks to Dr. Sylvain Delzon for helping me with the vulnerability curves, for his direct and accurate scientific contribution, and for his cheerful life-approach. I also thank the researches and technicians from the physiology lab of Dr. S. Delzon in the University of Bordeaux for always receiving me in a positive and pleasant atmosphere, especially Gaelle Capdeville, for all the support during my visits. Thanks to the technicians from Naturalis Biodiversity Center, Bertie Joan, Rob Langelaan and Wim Star, for teaching me good techniques and helping me to process several samples with perfect results. I also thank my previous supervisors, Prof. Dr. Rivete S. Lima and Prof. Dr. Carmen R. Marcati, for the trust, the support (even from many kilometers away), and for the lovely way they introduced me to the world of wood anatomy.*

*Thanks to Understanding Evolution group, for the exchanging of scientific ideas during our Tuesday meetings, with a special thanks for the support and empathy of my group leader Vincent Merckx. I also want to thank the support of Naturalis researchers, Jorinde Nuytinck, Renato Lima, Hans ter Steege (especially for the cookies and paçoquitas), and Prof. Dr. Pieter Baas for his kindness and for continuously inspiring students in the field of wood anatomy. A very special thanks for Sylvia Mota de Oliveira, for the friendship, the emotional and scientific support, the countless beers, laughs, and sharing; thanks for reminding me every day the goodness of the Brazilian energy.*

*A big thanks to all Naturalis fellow PhDs. We were in the same boat, and the company and support from you all were invaluable. A special thanks to the PhDs 'from the 3rd floor' - Ajaree, Bob, Deyi, Leon, Merhdad, Nieke, Saroj and Sofia - for making my everyday work a bit smoother, always bringing a smile, a cup of tea and*

*a lot of laughs. Also, for those PhDs with whom I had the opportunity to be closer and share nice moments: Andres, Dewi, Eka, Irene, Kevin, Marina, Renato, Richa, and Roderick. I heartily thank my old and good friends from Brazil, with whom I have shared years of life achievements, always celebrating together. Thanks for the support and love, either from a distance or in the warm hug in our reencounters. I am also grateful for the friends that the Netherlands has brought me - thanks for making this cold part of the world a bit warmer. Without citing names (to not forget anyone), you all know the big importance in my life, and the support in the exact moment!*

*This journey would never be possible without the support of my family. For the unconditional love, I thank my parents, Girlan and Helenita, and my sisters Leila and Luciana. Obrigada por me encorajarem e por estarem sempre tão orgulhosos com as minhas conquistas, por menor que seja, isso me motiva. Obrigada, ainda, por me darem o conforto da certeza que terei sempre um local e pessoas com quem posso contar e celebrar a vida! A very special thanks to Fabio, my partner, who was by my side since the beginning of this journey, holding together all the troubles of constructing a life in the Netherlands. Obrigada pelo suporte emocional de todos os dias, por me encorajar e, especialmente, por tantas vezes me emprestar a sua visão da vida.*

# CURRICULUM VITAE

**Larissa Chacon Dória** was born on January 13th, 1988, in João Pessoa, Paraíba, Brazil. She completed her 4 years bachelor's degree in Biological Sciences in 2011 at Universidade Federal da Paraíba, Brazil. During her undergraduate course, she received scholarships from the Brazilian Government funding agency Conselho Nacional de Desenvolvimento Científico e Tecnológico (CNPq) for developing research on ecological wood anatomy of plants from the caatinga of Paraiba state, Brazil. She continued her interest in this scientific field performing a Master's degree in Botany, investigating wood anatomy strategies of plants in two seasonally dry Brazilian vegetations, cerrado and caatinga, at the Universidade Estadual Paulista, São Paulo, Brazil. During her Master's period she received funding from the Fundação de Amparo à Pesquisa do Estado de São Paulo (FAPESP), and graduated in 2014. All over the period of her bachelor's and master's degree, she presented the results of her research in several scientific meetings, mainly organized by the Botanical Society of Brazil. She was awarded for the best undergraduate poster presentation during the meeting of the International Association of Wood Anatomists (IAWA), in Recife, Brazil, in 2012. Later, in 2015, she was selected by the CNPq funding agency to carry out her 4 year PhD at Leiden University and Naturalis Biodiversity Center, in the Netherlands. The PhD project was focused on functional xylem anatomy of herbaceous and woody species, under the supervision of Dr. Frederic Lens and Prof. Dr. Erik Smets. During the PhD, the candidate performed field work on Tenerife, Canary Islands, as well as in the cerrado (São Paulo state) and in the caatinga (Paraíba state) of Brazil. Additionally, she visited several times the lab of Dr. Sylvain Delzon, in the University of Bordeaux (France) to perform hydraulic measurements in stems of herbaceous and woody species. She also attended several international scientific meetings to present the results of her research, such as the Island Biology Meeting in the Azores, the Xylem International Meeting in France and the Botanical Society of America Meeting in the United States. The scientific findings of her PhD project are compiled in this thesis, and resulted in 4 scientific papers as first authors in renowned peer-reviewed scientific journals. Additionally, scientific collaborations during her PhD resulted in 4 co-authorship papers .

# List of publications

## Articles in peer-reviewed journals

**Dória LC**, Podadera DS, Batalha, MA, Lima, RS, Marcati, CR. 2016. Do woody plants of the Caatinga show a higher degree of xeromorphism than in the Cerrado? Flora 224: 244 - 251.

Lens F, Vos RA, Charrier G, van der Niet T, Merckx V, Baas P, Gutierrez JA, Jacobs B, **Dória LC**, Smets E, Delzon S, Janssens SB. 2016. Scalariform-to-simple transition in vessel perforation plates triggered by differences in climate during the evolution of Adoxaceae. Annals of Botany 118: 1043 - 1056.

Lens F, Picon-Cochard C, Delmas CEL, Signarbieux C, Buttler A, Cochard H, Jansen S, Chauvin T, **Dória LC**, del Arco M, Delzon S. 2016. Herbaceous angiosperms are not more vulnerable to drought-induced embolism than angiosperm trees. Plant Physiology 172: 661 - 667.

Pfautsch S, Aspinwall MJ, Drake JE, **Dória LC**, Langelaan RJA, Tissue DT, Tjoelker MG, Lens F. 2018. Traits and trade-offs in whole-tree hydraulic architecture along the vertical axis of *Eucalyptus grandis*. Annals of Botany 121: 129 - 141.

**Dória LC**, Podadera DS, del Arco M, Chauvin T, Smets E, Delzon S, Lens F. 2018. Insular woody daisies (*Argyranthemum*, Asteraceae) are more resistant to drought-induced hydraulic failure than their herbaceous relatives. Functional Ecology 32: 1467 - 1478.

Volaire F, Lens F, Cochard H, Xu H, **Dória LC**, Bristiel P, Balachowski J, Rowe N, Violle C, Picon-Cochard C. 2018. Embolism and mechanical resistances play a key role in dehydration tolerance of a perennial grass *Dactylis glomerata* L. Annals of Botany 22: 325 - 336.

**Dória LC**, Meijs C, Podadera DS, del Arco M, Smets E, Delzon S, Lens F. 2019. Embolism resistance in stems of herbaceous Brassicaceae and Asteraceae is linked with differences in woodiness and precipitation. Annals of Botany 124: 1 - 14.

**Dória LC**, Podadera DS, Lima RS, Lens F, Marcati CR. 2019. Axial sampling height outperforms site as predictor of wood trait variation. IAWA Journal 40: 191 - 214.

## Abstracts

**Dória LC**, Motta NA, Lima RS. 2010 Tendências ecológicas do lenho de espécies da caatinga. XXXIII Reunião Nordestina de Botânica, Aracaju, SE, Brazil, 30 June - 03 July 2010. (poster presentation)

**Dória LC**, Bo DD, Cop JG, Motta NA, Lima RS. 2010. Anatomia comparada do lenho de espécies da caatinga e da restinga com relação à condução de água. 61° Congresso Nacional de Botânica, Manaus, AM, Brazil, 05-10 September 2010. (poster presentation)

**Dória LC**, Diniz EL, Pellegrino NS, Cop JG, Lima RS. 2011. Estudo da anatomia ecológica da folha e do lenho de *Aspidosperma pyrifolium* Mart. (Apocynaceae) ocorrente na caatinga paraibana. 62° Congresso Nacional de Botânica, Fortaleza, CE, Brazil, 7-12 Agosto 2011. (poster presentation)

**Dória LC**, Diniz EL, Lima RS. 2012. Wood anatomy of nine species of Fabaceae from caatinga of Paraíba State. IAWA Pan-American Meeting, Recife, PE, Brazil, 01-05 October 2012. (poster presentation)

**Dória LC**, Lima RS, Marcati CR. 2013. Alguns aspectos da estrutura e da anatomia caulinar de *Tabebuia aurea* (Bignoniaceae) ocorrente no cerrado e na caatinga. 64° Congresso Nacional de Botânica, Belo Horizonte, MG, Brazil, 10-15 November 2013. (poster presentation)

**Dória LC**, del Arco M, Delzon S, Lens F. 2016. Is insular woodiness in the genus *Argyranthemum* (Asteraceae) driven by drought? Island Biology Meeting. Terceira Island, the Azores, Portugal, 18-22 July 2016. (oral presentation)

**Dória LC**, Delzon S, Lens F. 2017. Insular woody daisies (*Argyranthemum*, Asteraceae) are more embolism resistant than their herbaceous continental relatives. Xylem International Meeting. Bordeaux, France, 27-29 September 2017. (oral presentation)

**Dória LC**, Delzon S, Lens F. 2018. Insular woody daisies (*Argyranthemum*, Asteraceae) are more embolism resistant than their herbaceous continental relatives. Botanical Society of America Meeting, Rochester, MN, United States, 21-25 July 2018. (oral presentation)